Aus dem Institut für Molekularbiologie und Tumorforschung
Geschäftsführender Direktor: Prof. Dr. Rolf Müller
des Fachbereichs Medizin der Philipps-Universität Marburg

Function of the ATP-dependent chromatin remodeler Mi-2 in the regulation of ecdysone dependent genes in *Drosophila melanogaster*

Inaugural-Dissertation
zur Erlangung des Doktorgrades der Naturwissenschaften
(Dr. rer. nat.)

dem Fachbereich Medizin der Philipps-Universität Marburg
vorgelegt von

Judith Kreher

aus Gera, Deutschland

Marburg, 2014

Angenommen vom Fachbereich Medizin der Philipps-Universität Marburg am: 29.09.2014

Gedruckt mit Genehmigung des Fachbereichs.

Dekan: Prof. Dr. Helmut Schäfer

Referent: Prof. Dr. Alexander Brehm

1. Korreferent: Prof. Dr. Rainer Renkawitz

“It is not the critic who counts; not the man who points out how the strong man stumbles, or where the doer of deeds could have done them better. The credit belongs to the man who is actually in the arena, whose face is marred by dust and sweat and blood; who strives valiantly; who errs, who comes short again and again, because there is no effort without error and shortcoming; but who does actually strive to do the deeds; who knows great enthusiasms, the great devotions; who spends himself in a worthy cause; who at the best knows in the end the triumph of high achievement, and who at the worst, if he fails, at least fails while daring greatly, so that his place shall never be with those cold and timid souls who neither know victory nor defeat.”

Theodor Roosevelt, Paris 1910

Table of contents

1 Summary 9

1.1 Abstract 9

1.2 Zusammenfassung 11

2 Introduction 13

2.1 Chromatin 14

2.1.1 Chromatin organization 14

2.1.2 Histone variants 16

2.1.3 Histone modifications 17

2.1.3.1 Histone acetylation 18

2.1.3.2 Histone methylation 19

2.1.3.3 Histone phosphorylation 20

2.1.3.4 Genome-wide mapping of histone modifications 20

2.1.4 Chromatin-remodeling enzymes 21

2.1.4.1 SWI/SNF family 22

2.1.4.2 INO80 family 23

2.1.4.3 ISWI family 23

2.1.4.4 CHD family 24

2.2 Nuclear hormone receptors 27

2.2.1 Nuclear receptor superfamily 27

2.2.2 Chromatin architecture at hormone inducible promoters 29

2.2.3 Ashburner model of the ecdysone cascade 31

2.2.4 Regulation of gene expression by EcR 34

2.2.4.1 EcR co-activators 35

2.2.4.2 EcR co-repressors 37

2.3 Objectives 38

3 Material and Methods 39

3.1 Material 39

3.1.1 Material sources 39

3.1.1.1 Enzymes 39

3.1.1.2 Enzyme Inhibitors 40

3.1.1.3 Bioactive molecules 40

3.1.1.4 Affinity purification material 40

3.1.1.5 Dialysis and filtration material 40

3.1.1.6 SDS-PAGE and Western blotting 40

3.1.1.7 Agarose gel electrophoresis 41

3.1.1.8 Other consumables 41

3.1.1.9 Kits 41

3.1.2 Standard solutions and buffers 42

3.1.3 Bacteria strains and culture media 42

3.1.3.1 Antibiotics and selection marker 43

3.1.3.2 Culture media 43

3.1.4 Insect cell lines and tissue culture 43

3.1.5 Plasmids 44

3.1.6 Oligonucleotides 47

3.1.6.1 Oligonucleotides for PCR cloning 47

3.1.6.2 Oligonucleotides for sequencing 50

3.1.6.3 Oligonucleotides for generation of dsRNA by *in vitro* transcription 50

3.1.6.4 Oligonucleotides for gene expression analysis by RT-qPCR 51

3.1.6.5 Oligonucleotides for ChIP analysis by qPCR 52

3.1.6.6 Oligonucleotides for MNase analysis by qPCR 53

3.1.7 Antibodies and antisera 55

3.1.7.1 Primary antibodies 55

3.1.7.2 Secondary antibodies 56

3.2 Methods 56

3.2.1 Cell biological methods 56

3.2.1.1 Standard cell culture procedures 56

3.2.1.2 Freezing and thawing of cells 56

3.2.2 Molecular biological methods 57

3.2.2.1 Isolation of total RNA 57

3.2.2.2 Complementary DNA (cDNA) synthesis 58

3.2.2.3 Synthesis of double-strand RNA (dsRNA) by *in vitro* transcription (*iv*T) 58

3.2.2.4 RNAi mediated knockdown 59

3.2.2.5 Polymerase chain reaction (PCR) 59

3.2.2.6 PCR for site-directed mutagenesis 60

3.2.2.7 Quantitative PCR (qPCR) 60

3.2.3 Biochemical methods 62

3.2.3.1 Determination of protein concentration 63

3.2.3.2 SDS-polyacrylamide gel electrophoresis (SDS-PAGE) 63

3.2.3.3 Coomassie staining of SDS polyacrylamide gel 64

3.2.3.4 Western blot 64

3.2.3.5 Nuclear extract preparation 65

3.2.3.6 Immunoprecipitation of endogenous Mi-2 66

3.2.3.7 Whole cell extract preparation from Sf9 cells 67

3.2.3.8 FLAG affinity purification 67

3.2.3.9 Chromatin immunoprecipitation (ChIP) 68

3.2.3.10 ChIPSeq 70

3.2.3.11 Micrococcal nuclease (MNase) protection assay 70

3.2.3.12 Recombinant protein expression using the baculovirus system 72

3.2.3.13 GST protein expression 75

3.2.3.14 GST pulldown with radioactively labelled proteins 76

4 Results 77

4.1 Identification of genome-wide Mi-2 binding sites in S2 cells 77

4.1.1 Induction of ecdysone cascade in S2 cells 77

4.1.2 Mi-2 expression is not dependent on 20-hydroxyecdysone 78

4.1.3 Mi-2 ChIP Seq analysis in S2 cells 79

4.1.4 Mi-2 bound genes are ecdysone inducible 82

4.1.5 Validation of Mi-2 ChIPSeq data at the *broad* and *vrille* gene 84

4.1.6 Lint-1 is not recruited to ecdysone dependent genes upon 20HE treatment 90

4.1.7 Depletion of Mi-2 leads to a reduction of 20HE induced Mi-2 ChIP signals.. 90

4.2 Function of Mi-2 at ecdysone dependent genes 92

4.2.1 Mi-2 functions as a transcriptional repressor at ecdysone induced genes ... 92

4.2.2. Depletion of Iswi does not lead to superactivation of ecdysone dependent genes 94

4.2.3 Mi-2 regulates transcription of two non-coding RNAs 95

4.3 Interaction studies on Mi-2 and EcR 96

4.3.1 Mi-2 and EcR interact *in vitro* 96

4.3.2 Interaction of Mi-2 and EcR is independent of 20HE 98

4.3.3 Mi-2 and EcR form a stable complex *in vitro* 98

4.3.4 EcR and Mi-2 interact *in vivo* 99

4.3.5 The ATPase domain of Mi-2 directly interacts with EcR 100

4.3.6 ATPase domains of several chromatin remodelers interact with EcR 104

4.3.7 The activation function 2 (AF2) of EcR interacts with Mi-2 105

4.3.8 Mi-2 ATPase domain and AF2 domain of EcR are sufficient for interaction 107

4.4 Recruitment of Mi-2 to ecdysone dependent genes 108

4.4.1 Inhibition of transcription elongation does not affect Mi-2 recruitment 108

4.4.2 Mi-2 binding on chromatin correlates with EcR binding sites 109

4.4.3 Depletion of EcR decreases recruitment of Mi-2 to *broad* and *vrille* in 20HE treated cells 114

4.5 Regulation of chromatin structure by Mi-2 at the *vrille* gene 115

4.5.1 Mi-2 maintains chromatin structure at the *vrille* gene 115

5 Discussion 120

5.1 Mi-2 is recruited to ecdysone dependent loci 120

5.2 Mi-2 is a regulator of ecdysone dependent transcription 122

5.3 Mi-2 interacts with EcR *in vivo* 125

5.4 The ATPase domain of Mi-2 interacts with the AF2 domain of EcR 126

5.5 Recruitment of Mi-2 is mediated by EcR 128

5.6 Several ATP-dependent chromatin remodeler can interact with EcR 131

5.7 Mi-2 maintains a closed chromatin structure at ecdysone regulated genes 133

5.8 A recruitment model for Mi-2 134

5.9 Conservation of cooperation between Mi-2 and NRs 136

6 References 139

7 Appendix 157

ChIPSeq results: Mi-2 binding sites that are increased and decreased upon 20HE treatment 157

List of abbreviations and acronyms 164

Curriculum vitae 169

List of academic teachers 170

Acknowledgements 171

Ehrenwörtliche Erklärung 173

1 Summary

1.1 Abstract

The development of the fruitfly *Drosophila melanogaster* is regulated by the steroid hormone ecdysone. Ecdysone is released at the onset of metamorphosis and initiates a cascade of transcriptional events. First, it leads to the heterodimerisation of the Ecdysone receptor (EcR) with its binding partner ultraspiracle. This complex recruits the transcription machinery to ecdysone inducible genes and thereby initiates transcription of genes that contribute to pupariation and metamorphosis. ATP-dependent chromatin remodelers regulate transcription by altering DNA accessibility and often reside in multimeric protein complexes. Mi-2 is a member of the CHD family of ATP-dependent chromatin remodelers and can function both as co-repressor and co-activator in transcription regulation. The results described in this thesis investigate the function of the chromatin remodeler Mi-2 in the regulation of ecdysone dependent genes. Further, they provide a model by which Mi-2 is targeted to and influences transcription of ecdysone dependent genes.

In the first part of this thesis, genome-wide Mi-2 binding sites were mapped by chromatin immunoprecipitation followed by DNA-Sequencing (ChIPSeq) in untreated and ecdysone treated Drosophila S2 cells. This led to the identification of 103 Mi-2 binding sites that show increased binding of Mi-2 upon hormonal stimulation. Further analyses showed that a significant proportion of these binding sites resides in the close proximity of ecdysone inducible genes, implicating that Mi-2 functions in the regulation of these loci. Six ecdysone induced Mi-2 binding sites at two ecdysone dependent genes, the *vrille* and the *broad* loci were investigated in more detail. Here, depletion of Mi-2 resulted in a strong increase in expression of these genes in untreated and ecdysone treated cells. However, depletion of a different ATP-dependent chromatin remodeler, Iswi, did not result in derepression of *broad* and *vrille*, indicating that Mi-2 function is specific at the *broad* and *vrille* genes.

In the second part of this thesis, interaction studies revealed that Mi-2 can bind to EcR. This interaction was found to be independent of the hormone ecdysone. Further, the interaction between Mi-2 and EcR was mapped to the ATPase domain of Mi-2. These results demonstrated the first described interaction between the catalytic domain of Mi-2 and a nuclear receptor. In addition, the activation function 2 (AF2 domain) of EcR was found to be important for the interaction with Mi-2. The finding that Mi-2 and EcR

can physically interact led to the hypothesis that EcR can recruit Mi-2 to specific sites in the genome. Indeed, a significant overlap between EcR and Mi-2 binding sites was found in both untreated and ecdysone treated cells. In agreement with this hypothesis, depletion of EcR led to decreased ecdysone induced Mi-2 recruitment to the *vrille* and *broad* genes. These findings established a new recruitment model for Mi-2 by EcR to chromatin. Finally, Micrococcal nuclease (MNase) mapping demonstrated that Mi-2 functions at the *vrille* gene by maintaining a closed chromatin structure at this locus. Here, depletion of Mi-2 resulted in a more open chromatin structure, which correlated with an increase in expression of *vrille*.

In summary, the results of this thesis support a model, which suggests that Mi-2 recruitment to ecdysone dependent genes is mediated by EcR. At these genes Mi-2 functions as a repressive modulator of transcription by maintaining a closed chromatin structure at relevant genomic regions. Thereby this thesis contributes to a better understanding into the co-operation of transcription factors and chromatin remodelers on chromatin. Further it gives a mechanistic insight into the function of ATP-dependent chromatin remodelers in the regulation of developmentally transcribed genes.

1.2 Zusammenfassung

Die Entwicklung der Fruchtfliege *Drosophila melanogaster* wird durch das Steroidhormon Ecdyson reguliert. Ecdyson wird zu Beginn der Metamorphose sekretiert und initiiert eine Kaskade von transkriptionellen Ereignissen. Zunächst führt es zur Heterodimerisierung des Ecdyson Rezeptors (EcR) mit seinem Bindungspartner ultraspiracle. Dieser Komplex rekrutiert die Transkriptionsmaschinerie an Ecdyson induzierbare Gene und initiiert dadurch die Transkription von Genen, welche direkt zur Verpuppung und Metamorphose beitragen. ATP-abhängige Chromatinremodeler regulieren die Transkription in dem sie die Zugänglichkeit der DNA ändern und befinden sich in multimeren Proteinkomplexen befinden. Mi-2 ist ein Mitglied der CHD Familie der ATP-abhängigen Chromatin Remodeler und fungiert als Korepressor und Koaktivator in der transkriptionellen Regulation. Die in dieser Arbeit beschriebenen Resultate untersuchen die Funktion des Chromatin Remodelers Mi-2 in der Regulation von ecdysonabhängigen Genen. Diese Ergebniss führten zu einem Modell welches beschreibt, wie Mi-2 an hormonregulierte Gene bindet und die Transkription von ecdysonabhängigen Genen beeinflußt.

Im ersten Teil dieser Arbeit wurden genomweite Mi-2 Bindungsstellen durch Chromatin-Immunopräzipitation gefolgt von DNA-Sequenzierung (ChIPSeq) in unbehandelten und ecdysonbehandelten Drosophila S2 Zellen kartiert. Dies führte zur Identifizierung von 103 Mi-2 Bindestellen, die verstärkte Bindung von Mi-2 nach hormoneller Stimulation zeigen. Weitere Analysen zeigten, dass ein signifikanter Anteil dieser Bindungsstellen in der Umgebung von ecdysoninduzierbaren Genen liegt, was eine Funktion von Mi-2 in der Regulation dieser Loci impliziert. Sechs ecdysoninduzierte Mi-2 Bindungsstellen an zwei ecdysonabhängigen Genen, *broad* und *vrille*, wurden eingehender untersucht. Hier führte Depletierung von Mi-2 zu einem starken Anstieg dieser Gene in unbehandelten und ecdysonbehandelten Zellen. Die Depletierung eines anderen ATP-abhängigen Chromatin Remodelers, Iswi, führte hingegen nicht zu einer Dereprimierung von *broad* und *vrille*. Dies deutet darauf hin, dass die Funktion von Mi-2 an den Genen *broad* und *vrille* spezifisch ist.

Interaktionsstudien im zweiten Teil dieser Arbeit machten deutlich, dass Mi-2 an den EcR binden kann. Es wurde gezeigt, dass diese Interaktion unabhängig von dem Hormon Ecdyson ist. Desweiteren wurde die Interaktion zwischen Mi-2 und EcR auf die ATPase Domäne von Mi-2 kartiert. Diese Ergebnisse weisen zum ersten mal eine Interaktion zwischen der katalytischen Domäne von Mi-2 und einem Kernrezeptor

nach. Zusätzlich dazu wurde beobachtet, dass die Aktivierungsfunktion 2 (AF2 Domäne) des EcR wichtig für die Interaktion mit Mi-2 ist. Die Erkenntnis, dass Mi-2 und EcR physisch interagieren können, führte zu der Hypothese, dass EcR Mi-2 an spezifische Stellen im Genom rekrutieren kann. In der Tat wurde ein signifikanter Überlapp zwischen Mi-2 und EcR Bindungsstellen, sowohl in unbehandelten als auch in ecdysonbehandelten Zellen, gefunden. In Übereinstimmung mit dieser Hypothese, führte eine Depletierung von EcR zu einer verminderten, ecdysoninduzierten Rekrutierung von Mi-2 an die Gene *broad* und *vrille*. Diese Ergebnisse etablierten ein neues Modell für die Rekrutierung von Mi-2 durch den EcR an das Chromatin. Schließlich zeigten MNase Kartierungsstudien mit Mikrokokkus-Nuklease (MNase), dass Mi-2 durch die Aufrechterhaltung einer geschlossenen Chromatinsstruktur am *vrille* Gen fungiert. Hier führte eine Depletierung von Mi-2 zu einer geöffneten Chromatinstruktur, welche mit einer verstärkten Expression von *vrille* korrelierte.

Zusammenfassend führten die Ergebnisse zu einem Model das nahelegt, dass die Rekrutierung von Mi-2 an ecdysoninduzierte Gene durch den EcR vermittelt wird. An diesen Genen fungiert Mi-2 als repressiver Modulator der Transkription durch die Aufrechterhaltung einer geschlossenen Chromatinstruktur an relevante genomischen Regionen. Dadurch trägt diese Arbeit zu einem besseren Verständnis der Kooperation von Transkriptionsfaktoren und Chromatin Remodeler am Chromatin bei. Des Weiteren gewährt sie einen Einblick in den funktionellen Mechanismus ATP-abhängiger Chromatin Remodeler in der Regulation von Genen, die in der Entwicklung transkribiert werden.

2 Introduction

The discovery that living organisms inherit characteristic traits from their ancestors by Gregor Johann Mendel, is perceived as the birth of the research field of modern genetics. Mendel studied seven independently inherited traits in pea such as seed shape and flower colour, elegantly demonstrating the action of invisible “factors” that provide phenotypic characteristics in predictable ways (Mendel and Tschermak, 1901). These days it is known that these “factors” refer to genes, the hereditary unit of a living organism that is encoded in the DNA. The sum of all genes of one organism is also referred to as the genome. Further experiments by Thomas Hunt Morgan and colleagues in *Drosophila melanogaster* (Drosophila) revealed that genes are arranged on chromosomes, thereby formulating the mechanistic explanation for heredity (Morgan, 1915). This theory allowed to predict the outcome of a genetic cross with the help of a crossing scheme and simple probability computation. However, there were phenotypical exceptions that could not be explained by genetics. For example, a phenomenon called position-effect variegation (PEV) caught the attention of geneticists (Elgin and Reuter, 2013). PEV occurs when an otherwise actively transcribed gene is placed in the close vicinity of a transcriptionally inactive, chromosomal region. This results in somatic inactivation of the gene in some cells and variegating phenotypes such as the red and white mosaic eye pattern of Drosophila carrying the w^{m4} (white-mottled-4) allele (Figure 2.1A). Another example of phenotypical variation in the same genetic background is the Agouti (A^{vy}) mouse model that displays coat colours ranging from yellow to brown depending on the degree of DNA methylation at a specific gene promoter (Figure 2.1B) (Rosenfeld, 2010).

Figure 2.1: Epigenetic phenomena – Position effect variegation (PEV) in Drosophila and the Agouti mouse model. (A) Genomic rearrangement of the *white* gene in the wm^4 mutant changes the wildtype eye (red) into a variegating phenotype (white mottled). Adapted from (Elgin and Reuter, 2013) (B) Spectrum of mice carrying the A^{vy} allele with phenotypes ranging from yellow to agouti. Adapted from (Cropley et al., 2006).

These observations forced scientists to question the traditional genetic paradigm as the sole explanation for inheritance mechanisms and to reach out for additional explanations of phenotypical variation. In 1996, Arthur Riggs and colleagues defined the term “epigenetics” as “the study of mitotically and/or meiotically heritable changes in gene function that cannot be explained by changes in DNA sequence” . Epigenetic mechanisms are studied on the basis of chromatin biology that involves a multitude of mechanisms such as chemical modifications of histones and the DNA, the effects of RNA interference and the formation of the higher order structure of chromosomes within the nucleus (Li and Reinberg, 2011; Rinn and Chang, 2012; Zentner and Henikoff, 2013).

2.1 Chromatin

2.1.1 Chromatin organization

Chromatin was first described by Walther Flemming as a cellular structure that strongly absorbed basophilic dyes (Flemming, 1882). It consists of contiguous DNA molecules that associate with octamers of core histone proteins (Figure 2.2). In detail, 147 base pairs (bp) of DNA are wrapped 1.65 times around the histone octamer. This structure is referred to as the nucleosome and represents the first degree of chromosomal packaging (Luger et al., 1997).

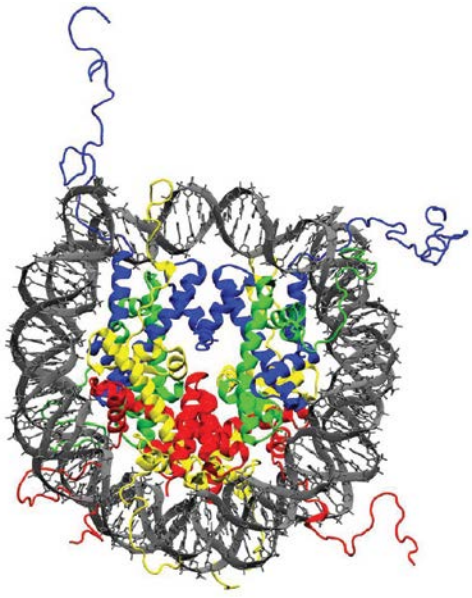

Figure 2.2: The nucleosome as the basic subunit of chromatin. Crystal structure of the nucleosome at 1.9Å resolution. Ribbon traces for the DNA phosphodiester backbone (grey) and eight histone proteins (blue: H3; green: H4; yellow: H2A; red: H2B). Adapted from (Davey et al., 2002).

The highly basic nature of the histone octamer primarily favours contacts with the DNA helix via the phosphodiester backbone, allowing interaction in a largely sequence independent manner. Depending on species and cell type, nucleosomes are spaced by 10 to 60 bp of linker DNA, assembling into a 10nm “beads on a string” array (Szerlong and Hansen, 2011). Chromatin can be further compacted by binding of the linker histone H1 to the entry and exit region of linker DNA. It was hypothesised that association of H1 with the nucleosomal array contributes to a higher order chromatin fiber with a diameter of 30nm (Finch and Klug, 1976). However, this idea was challenged by recent cryo electron-microscopy studies that could not confirm the existence of the 30nm fiber in human mitotic chromosomes (Nishino et al., 2012). It has been proposed that intermolecular interactions within the 30nm fiber can form even higher order chromatin structures during interphase and a 200-300nm chromonema in mitotic chromosomes (Horn and Peterson, 2002). However, the compaction of nucleosomal arrays into these tertiary structures remains elusive and subject to ongoing research (Luger et al., 2012). During the metaphase of cell cycle, chromatin is visible as highly condensed chromosomes that align in an equatorial plane of the cell in order to be distributed to the dividing daughter cells. However, during interphase, chromatin is a more loose structure that arranges into two different subtypes: eu- and heterochromatin (Lamond and Earnshaw, 1998). Heterochromatin remains mostly condensed during interphase as it consists of tightly arranged nucleosomes and is therefore transcriptionally silent. In contrast, euchromatin is defined by a more open chromatin structure and a high density of actively transcribed genes.

The histone octamer consists of two copies of each core histone H2A, H2B, H3 and H4. Expression of these canonical histones occurs during S-phase from a large histone gene cluster and is tightly regulated (DeLisle et al., 1983). Histones are subsequently incorporated into chromatin during DNA replication. The core histones are highly conserved within eukaryotes and share a very similar structure (Malik and Henikoff, 2003). All histones harbor a common structural motif, the histone fold, that is involved in the pairwise association of the dimerisation partners H2A/H2B and H3/H4 also described as the “handshake motif” (Arents et al., 1991). Additionally, all four histones contain an N-terminal tail that appears as a disordered structure and protrudes from the nucleosomal core (Luger et al., 1997). The fundamental nucleosome unit can be modified by the incorporation of variant or “replacement” histone subspecies as well as the attachment of posttranslational modifications (PTMs). These mechanisms contribute to the dynamic nature of chromatin.

2.1.2 Histone variants

Histone variants differ in sequence, genome-wide localisation, deposition mechanism and most importantly, their function from canonical histones(Biterge and Schneider, 2014). In contrast to canonical histones, histone variants are usually coded as single genes in the genome and are incorporated into chromatin throughout the cell cycle in a replication-independent manner (Skene and Henikoff, 2013).

With respect to histone H3, two canonical isoforms, H3.1 and H3.2, as well as two variants, H3.3 and cenH3 have been described in detail. H3.3 differs in its sequence only in five amino acid positions from H3.1 and H3.2. It has been shown to localise to transcriptionally active loci such as the rDNA cluster, where it is incorporated as a consequence of transcription (Ahmad and Henikoff, 2002). However, H3.3 was also shown to be deposited at telomeric and pericentric repeats, where it contributes to the repression of telomeric repeat containing RNA (Goldberg et al., 2010). The presence of the H3 variant cenH3 (CENP-A in mammals, cid in Drosophila) marks specifically centromeres (Verdaasdonk and Bloom, 2011). Interestingly, overexpression of cenH3 leads to its spreading across the chromosome and to the formation of neocentromeres (Mendiburo et al., 2011; Van Hooser et al., 2001).
For core histone H2A, four different variants (H2AX, H2AZ, macroH2A and H2AB) have been reported that exert distinct nuclear functions. H2AZ has been demonstrated to localise to actively described loci that are in close vicinity to heterochromatic regions, where it functions to limit spreading of repressive chromatin (Meneghini et al., 2003). In addition, H2A.Z was shown to flank the nucleosome free region (NFR) at the transcriptional start site (TSS) of nearly all genes (Raisner et al., 2005). Here, incorporation of H2A.Z was shown to promote rapid induction of gene expression as H2A.Z containing nucleosomes are less stable than nucleosomes containing canonical histones (Zhang et al., 2005). The histone variant H2AX is an essential component in the repair of DNA double strand breaks. In response to DNA damage it is rapidly phosphorylated to yH2AX that marks foci thereby recruiting the DNA repair machinery (Scully and Xie, 2013). Deletion of H2AX in mice is viable, but results in genomic instability due to failed DNA repair (Celeste et al., 2002). MacroH2A is a variant specific to mammals and contains a globular, C-terminal (macro-) domain that is not present in any other histone isoform (Gamble and Kraus, 2010). It is specifically enriched on the inactive X chromosome of female cells where it contributes to X inactivation (Costanzi and Pehrson, 1998). H2AB (bar body-deficient) shares only ~50% identity with canonical H2A and is enriched on transcriptionally active loci on the

active X and the autosomes, but completely absent from the inactive X in mammals (Chadwick and Willard, 2001; Tolstorukov et al., 2012). Both, H2B and H4 are markedly deficient in variants. The few existing H2B variants are highly stage specific and their precise function is unknown. For example, the sperm-specific variant in sea urchin (Green et al., 1995). Histone H4 is one of the slowest evolving proteins, the reason for this lack of sequence variability is not known.

2.1.3 Histone modifications

As described above, the histones contain N-terminal tails that protrude from the nucleosome core. Interestingly, both the globular domains of the histones as well as the histone tails are subject to post-translational, covalent modification (PTM). The best studied modifications include acetylation, methylation, phosphorylation and ubiquitination (Figure 2.3). However, also more rare modifications such as SUMOylation, ADP-ribosylation, proline-isomerisation, propionylation, butyrylation and glycosylation are of great interest to the scientific community (Kouzarides, 2007; Sakabe et al., 2010; Zhang et al., 2009).

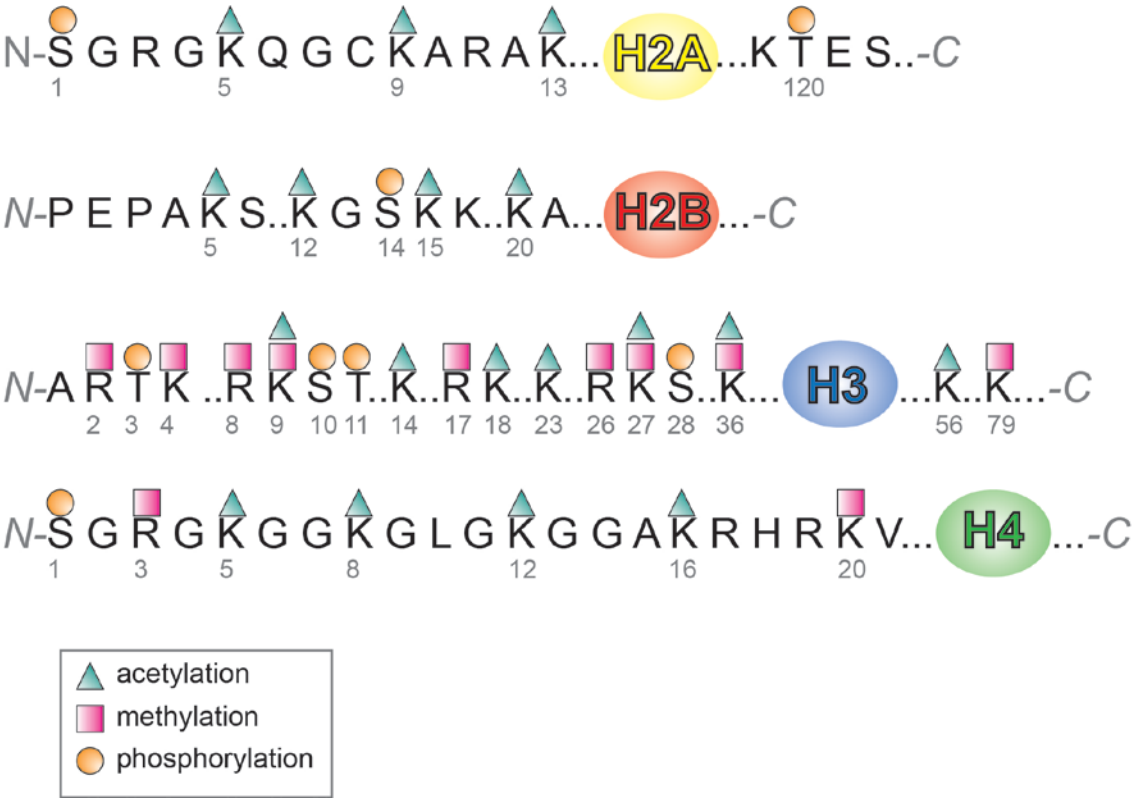

Figure 2.3: Covalent, posttranslational modification of histones. Histones can be acetylated, methylated and phosphorylated at specific residues. Position of modified residues is depicted by the number below the amino acid sequence. Adapted from (Bhaumik et al., 2007).

Histone modifications contribute to the higher order chromatin structure by influencing intra- and inter-nucleosomal DNA-histone contacts. Further, they provide direct binding surfaces for chromatin associated factors. Proteins that bind PTMs are referred to as histone “readers” and can further recruit protein complexes acting on chromatin (Ruthenburg et al., 2007). Protein complexes that catalyse the attachment of histone modifications are termed “writers” whereas the removal of PTMs is conducted by “eraser” proteins. Histone modifications have been demonstrated to be specifically localised at certain chromatin regions such as active genes and heterochromatin, but also to mark biological processes on chromatin such as transcription, DNA repair and replication. Therefore, they play a key role in a majority of biological processes and their understanding forms the foundation of studying chromatin related processes.

2.1.3.1 Histone acetylation

Histone acetylation is accomplished by histone acetyltransferases (HATs) that use acetyl coenzyme A (acetyl-CoA) to catalyse the transfer of an acetyl residue onto the ε-amino group of a lysine residue (Marmorstein and Zhou, 2014). Newly translated, cytoplasmic histones are acetylated upon synthesis. For example, histone H4 is acetylated at lysine residues 5 and 12 (H4K5 and K12) (Ruiz-Carrillo et al., 1975; Sobel et al., 1995). Following their integration during replication, histones are rapidly deacetylated (Jackson et al., 1976). Generally speaking, histone acetylation neutralises the electrostatic interaction between histones and DNA and thereby leads to less compaction and a more open chromatin structure (Shahbazian and Grunstein, 2007). Therefore, histone acetylation is crucial to permit binding of the transcriptional machinery and the initiation of gene transcription. This hypothesis has been supported by genome-wide studies demonstrating that acetylation of histone H3 and H4 positively correlates with active gene transcription in yeast (Pokholok et al., 2005). The removal of acetyl moieties is performed by proteins with histone deacetylase activity (HDACs). HDACs are classified into two subgroups; the family of NAD-dependent Sir proteins and the classical HDAC family. Reader proteins of histone acetylation are characterised by the presence of a Bromo domain or the tandem Plant Homeo Domain (PHD)(Sanchez and Zhou, 2011). The Bromo domain was originally described by Tamkun and colleagues as a module of the Drosophila protein brahma that binds to acetylated lysines (Dhalluin et al., 1999; Tamkun et al., 1992). Several chromatin regulators possess a Bromo domain, including the chromatin remodeling factor Snf2 and several histone acetyltransferases such as CBP/p300 and Gcn5 (Goodwin, 1997; Mujtaba et al., 2004; Ornaghi et al., 1999).

2.1.3.2 Histone methylation

The methylation of histones is catalysed by histone methyltransferases (HMTs) that transfer one, two or three methyl-groups from S-Adenosylmethionine (SAM) onto a lysine or arginine residue (Trievel et al., 2002). The exact location of the methyl-group within the histone as well as the degree of methylation determines its specific function and distribution within the genome (Black et al., 2012). For example, when histone H3 is methylated at lysine 4 or 36 (H3K4me and H3K36me) it is associated with active genes whereas methylation of H3K9 and H3K27 is a mark for heterochromatic, transcriptionally inactive chromatin regions (Bernstein et al., 2002; Ebert et al., 2006; Krogan et al., 2003; Ng et al., 2003; Peters et al., 2003). Further, methylation of the lysine residue 4 of histone H3 can occur as mono-, di- or trimethylated state (H3K4me1, me2 or me3). H3K4me3 is localised at TSS of active and poised genes, and plays an important role in the initiation of transcription. In contrast, H3K4me1 is crucial to establish enhancers, gene regulatory elements that are located in cis up to one megabase away from the gene they regulate (Heintzman et al., 2007; Santos-Rosa et al., 2002; Schneider et al., 2004). An additional layer of complexity is added by the methylation of arginine residues within the histone tails. This modification can be present as mono- as well as symmetric and asymmetric di-methylation. Also methylation of arginine residues can have both, a positive (e.g. H3R17me2a) or negative (e.g. H3R2me2a) effect on transcriptional activation (Bauer et al., 2002; Guccione et al., 2007; Hyllus et al., 2007).

For several years, it was believed that methylation of histones is a thermodynamically highly stable modification that cannot be reversed. This hypothesis had to be revised when the first histone demethylase LSD1 was discovered (Shi et al., 2004). LSD1 catalyses the demethylation of mono- and di-methylated histone H3K4 and K9 in a flavin adenine dinucleotide (FAD)-dependent amine oxidase reaction (Forneris et al., 2005). Further, a protein family containing the JmjC domain that was first discovered in Jarid2, is capable of demethylating trimethylated histones (Tsukada et al., 2006).

Histone reader proteins that recognise methylated histone possess a domain from the so-called Royal family of domains (Maurer-Stroh et al., 2003). This Royal family is a group of structurally related protein folds and includes the Tudor, PWWP, MBT and chromodomain. The chromodomain (chromatin organisation modifier domain) was first discovered as a module within the Drosophila heterochromatin protein 1 (HP1) that is crucial of heterochromatic silencing. HP1 has a high affinity for methylated lysine 9 of

histone H3 (Bannister et al., 2001). The crystal structure of its chromodomain revealed that the methylated histone tail is caged by three aromatic side chains thereby explaining a specific targeting mechanism of chromatin associated proteins with histones (Jacobs and Khorasanizadeh, 2002).

2.1.3.3 Histone phosphorylation

Phosphorylation of histones can occur on serine, threonine and tyrosine residues. These residues are modified by several kinases that transfer a phosphate-group from a high-energy donor, such as ATP onto their substrate (Rossetto et al., 2012). The best characterised phosphorylation site within a histone is serine 10 of histone H3. This mark is set by the kinase AuroraB and first visible during late G2 phase in pericentric heterochromatin from where it further spreads across the whole chromosome arm (Hsu et al., 2000). Phosphorylation of H3S10 has been demonstrated to directly correlate with chromatin compaction during mitosis and meiosis, and is therefore commonly used as a mark for these cellular processes (Hans and Dimitrov, 2001). Dephosphorylation of H3S10 by protein phosphatase 1 (PP1) starts during anaphase and is critical for proper chromosome segregation (Hsu et al., 2000). In addition, studies on histone phosphorylation have demonstrated a link to transcriptional activation. Data suggest that H3S10, T11 and S28 phosphorylation promote histone acetylation of H3K14 by the acetyltransferase Gcn5 thereby demonstrating a cross talk between different histone modifications (Lo et al., 2000).

2.1.3.4 Genome-wide mapping of histone modifications

The finding that histones can be modified on several residues and that these modifications are interdependent creates a complex diversity of possible combinations, each of which potentially implies a different functional consequence. Therefore, a multitude of genome-wide analyses of histone modifications and chromatin associated proteins have led to the definition of “chromatin states” (Ernst et al., 2011; Filion et al., 2010). Kharchenko and colleagues defined nine combinatorial patterns of histone marks as well as reader and writer proteins within the Drosophila genome (Kharchenko et al., 2011). For example, chromatin stage 1 includes active gene promoters and TSS that are marked by an enrichment of H3K4me2/3, H3K9ac and the presence of the RNA Pol II complex whereas chromatin stage 7 is characterised by high levels of H3K9me2/3, HP1 and therefore represents constitutive heterochromatin. This

annotation allowed a systematic characterisation of the Drosophila genome as well as the prediction of functional elements within newly sequenced genomes.

2.1.4 Chromatin-remodeling enzymes

The organisation of DNA into regularly spaced nucleosomes allows the condensation of this large molecule and therefore its packaging into the nucleus. However, it also makes DNA sequences essential for gene transcription, DNA replication and repair inaccessible to the binding of regulatory protein complexes. In order to overcome the nucleosomal barrier the cell contains a set of specific proteins named ATP-dependent chromatin remodeler that enable dynamic access to DNA (Narlikar et al., 2013). These enzymes use the energy derived from the hydrolysis of ATP to reposition, reconstitute or eject the histone octamer within chromatin in order to expose or mask specific DNA regions.

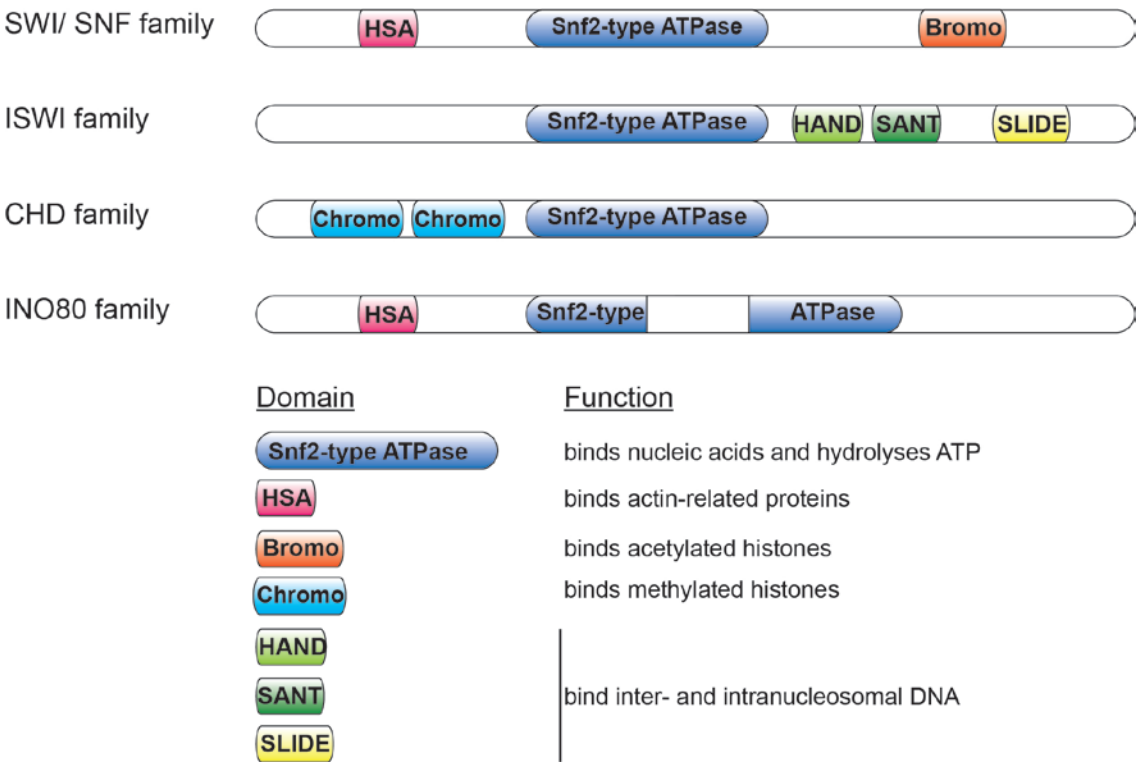

Figure 2.4: Families of ATP dependent chromatin remodeler. Schematic representation of the domain structure of the four different families of ATP-dependent chromatin remodeler. Function of the depicted domains is explained in the legend. Adapted from (Manelyte and Längst, 2013).

There are four main families of ATP-dependent chromatin remodelers: SWI/SNF, INO80, ISWI and CHD (Figure 2.4) (Durr et al., 2006). All members of these families share common features such as a general affinity to nucleosomes as well as the

presence of an DEAD/H-Box containing, SNF2-type ATPase domain. However, they differ from each other in the composition of adjacent domains, which provide specificity for the recognition of modified histones and the interaction with various proteins in large multimeric complexes (Manelyte and Längst, 2013). The following paragraphs describe the four different families of ATP-dependent chromatin remodelers in Drosophila as the main focus of this study is the function of the chromatin remodeler Mi-2 in Drosophila.

2.1.4.1 SWI/SNF family

The SWI/SNF (SWItch/ Sucrose Non Fermenting) family of ATP-dependent chromatin remodelers was first discovered in a genetic screen for *S.cerevisiae* mutants with defects in the fermentation of sucrose (Neigeborn and Carlson, 1984). This effect was later explained by the finding that snf2Δ mutants fail to eliminate promoter-bound nucleosomes resulting in repression of the *SUC2* gene due to blocked transcription factor binding (Wu and Winston, 1997). SWI/SNF complexes are highly evolutionary conserved from yeast to man. However, other than *S.cerevisiae* and mammals that contain two distinct SWI/SNF enzymes, Drosophila possesses only a single SWI/SNF-type ATPase that is encoded in the gene *brahma*. Loss-of-function of *brahma* causes peripheral neural system defects, homeotic transformation and decreased cell viability in the fly (Elfring et al., 1998; Tamkun et al., 1992). Purification of brahma associated proteins identified six subunits that differ between two kinds of complexes: BAP and PBAP (Mohrmann et al., 2004; Papoulas et al., 1998). In brief, these complexes can be distinguished as BAP contains OSA, whereas PBAP encompasses Polybromo and BAP170. Studies on human SWI/SNF containing complexes identified 29 subunits that show differential combinatorial assembly and have diverse biological functions in various tissues (Ho and Crabtree, 2010) The catalytic ATPase brahma contains an N-terminal HAS (helicase-SANT) and an C-terminal bromo domain. The bromo domain is thought to target SWI/SNF complexes to transcriptionally active chromatin via its interaction with acetylated histones. This hypothesis is underlined by the finding that brahma co-localises with RNA PolII and marks nearly all transcriptionally active loci on Drosophila polytene chromosomes (Armstrong et al., 2002; Mohrmann et al., 2004).. Further, the loss or inactivation of SWI/SNF complex subunits is frequently observed in cancer and the mammalian homolog of brahma, BRG1 has been shown to be a key tumour suppressor (Hargreaves and Crabtree, 2011).

2.1.4.2 INO80 family

INO80 complexes were initially identified as transcriptional regulators of inositol responsive genes in yeast (Ebbert et al., 1999). Purification of the complex revealed the presence of five specific subunits: Reptin, Pontin, Actin and two actin-related protein Arp5 and 8. Reptin and Pontin represent homologs of the yeast Rvb1 and 2 AAA-ATPases, constituting a helicase function in the INO80 complex (Klymenko et al., 2006). The ATPase domain of the INO80 family is characterised by the presence of a linker region that splits this conserved domain and most likely presents a binding platform for complex subunits such as RuvB-like AAA-ATPases (Wu et al., 2005). In addition, Klymenko *et al.* revealed the association of the transcription factor Pho (Pleiohomeotic) with the INO80 complex (Klymenko et al., 2006). Pho recognises Polycomb repressive elements (PRE) and recruits INO80 complexes to participate in the regulation of homeotic genes (Bhatia et al., 2010). Furthermore, the Drosophila ortholog Domino/p400 of the yeast SWR1 complex has been described to harbor Ino80 as a subunit and to be specifically required for H2AZ deposition at DNA double strand breaks in both species (Kobor et al., 2004; Kusch et al., 2004).

2.1.4.3 ISWI family

ISWI (Imitation SWItch) was identified based on the sequence similarity to Drosophila brahma (Elfring et al., 1994). The chromatin remodeler is a subunit of three well-studied protein complexes in Drosophila: NURF (nucleosome remodeling factor), ACF (ATP-dependent chromatin assembly and remodeling factor) and CHRAC (chromatin accessibility complex) (Ito et al., 1997; Tsukiyama et al., 1995; Tsukiyama and Wu, 1995; Varga-Weisz et al., 1997). NURF consists of four subunits: ISWI, NURF301, NURF55 and NURF38. The complex has been purified from Drosophila embryonic extracts and demonstrated to enable GAGA factor binding to the *hsp70* promoter by establishing a DNase I hypersensitive site (Tsukiyama and Wu, 1995). Further, NURF is a regulator of ecdysone and STAT responsive genes, as it can directly interact with the ecdysone receptor (EcR) and Ken, a negative regulator of STAT signalling (Badenhorst et al., 2005; Kwon et al., 2008). In addition to the interaction with sequence specific transcription factors, NURF contains two well characterized domains that can bind PTMs on histones. The PHD finger can bind to H3K4me2/3, whereas the neighbouring bromodomain can interact with H4K16ac thereby enabling NURF recruitment to specific chromatin regions (Kwon et al., 2009; Wysocka et al., 2006). In comparison, ACF is a heterodimer of ISWI and its binding partner ACF1, whereas the

CHRAC complex contains ISWI, ACF1 and two additional subunits CHRAC14 and 16. Both complexes are capable of assembling nucleosomes from free DNA and histones in the presence of ATP *in vitro* (Ito et al., 1997; Varga-Weisz et al., 1997).

2.1.4.4 CHD family

The CHD (Chromodomain-Helicase-DNA-binding protein) family of ATP-dependent chromatin remodelers is distinguished from other ATPases by the presence of two N-terminally located chromodomains. According to the presence of additional domains three subfamilies of CHD proteins have been designated in Drosophila: Chd1, Mi-2/Chd3 and kismet.

Chd1 exists predominantly as a monomer in the cell and its chromodomains bind specifically to H3K4me3 (Lusser et al., 2005; Morettini et al., 2011). In addition, immunofluorescence analysis in Drosophila polytene chromosomes visualised Chd1 localisation to interbands (Stokes et al., 1996). These findings suggest a role of the ATP-dependent chromatin remodeler in the activation of transcription. Another interesting function of Chd1 has been demonstrated in the deposition of histone H3.3 in the developing sperm of Drosophila (Konev et al., 2007). It was shown that *Chd1* mutants fail to incorporate the histone variant H3.3 in the paternal pronucleus. Further, Chd1 interacts with the histone chaperone HIRA that delivers the histones at the sites of incorporation, indicating that Chd1 is essential for nucleosome assembly during sperm condensation.

In order to understand how the nucleosomal substrate is recognized by the ATP-dependent chromatin remodeler and how the catalytic activity of the ATPase motor is regulated, the Bowman laboratory solved the crystal structure of yeast Chd1. (Hauk et al., 2010). It was previously shown that activation ATP dependent chromatin remodelers requires the N-terminus of histone H4 to stabilise the ATPase domain on the nucleosomal substrate (Clapier et al., 2001; Gangaraju et al., 2009). This was thought to enable the remodeler to distinguish between naked and nucleosomal DNA. The crystal structure of Chd1 showed that the chromodomains contact both ATPase lobes, thereby inhibiting their catalytic activity. The so-called chromo-wedge domain packs against a DNA binding surface of the ATPase domain interfering with DNA binding to the ATPase motor. A conformational switch in the presence of nucleosomes releases the chromodomains from the ATPase, allowing efficient ATP hydrolysis and

remodeling activity. Hence, this model explains the discrimination between naked DNA and nucleosomes and may apply to other ATP-dependent chromatin remodelers.

The second subfamily of CHD proteins includes the two Drosophila proteins Mi-2 and Chd3. The mammalian homolog of Mi-2 was initially identified in and named after an antibody serum of a dermatomyositis patient by the name Mitchell (Seelig et al., 1995). Identification of factors involved in Polycomb-mediated gene repression classified Drosophila Mi-2 as a hunchback interacting protein (Kehle et al., 1998). This study also showed that homozygous deletion of Mi-2 resulted in developmental arrest during first and second instar larva stages. Several studies have purified Mi-2 as a subunit of the highly conserved protein complex NuRD (nucleosome remodeling and deacetylase) that contributes to the repression of gene expression. NuRD integrates the nucleosome remodeling activity of Mi-2 and the deacetylation of histones by a specific HDAC subunit (Tong et al., 1998; Wade et al., 1998; Xue et al., 1998; Zhang et al., 1998). In Drosophila the complex is composed of Mi-2, the histone deacetylase Rpd3, MTA, MBD2/3, p55 and p66 and functions as a transcriptional repressor at its target genes (Brehm et al., 2000; Marhold et al., 2004). In addition to the NuRD complex, a second Mi-2 containing complex has been purified from Drosophila embryos (Kunert et al., 2009). The dMec (Mep1-containing) complex consists of Mi-2 and the newly identified dMep1 protein. It functions in the repression of proneural genes of the *achaete-scute* locus in an HDAC-independent manner.

Several mechanisms for targeting of Mi-2 to chromatin have been proposed. First, Mi-2 possesses two tandemly arranged PHD (plant homeodomain) fingers and a double chromodomain that was shown to preferentially bind unmodified H3K4 as well as methylated H3K9 in the human homolog Chd4 (Mansfield et al., 2011). Second, the MBD2/3 (methyl-CpG binding domain) subunit of the NuRD complex enables recruitment by binding to methylated DNA (Roder et al., 2000). Further, NuRD has been demonstrated to interact with sequence-specific transcription factors such as Tramtrack69 (Murawsky et al., 2001; Reddy et al., 2010). Interestingly, Mi-2 and Mep1 have been identified as transcriptional repressors of SUMO (small ubiquitin-related modifier)-mediated repression of a reporter gene in a genome-wide RNAi screen (Stielow et al., 2008). Both proteins can bind the SUMO-modified transcription factor Sp3 and are thereby recruited to mediate HDAC-independent gene silencing *in vivo*. Also, Mi-2 has been demonstrated to be recruited to active heat shock loci promoting proper induction upon heat shock. Association with highly inducible genes is mediated by an interaction with poly-(ADP)ribose, enabling Mi-2 to spread over the entire heat

shock locus and participate in proper RNA processing of heat shock transcripts (Mathieu et al., 2012; Murawska et al., 2011). The finding that Mi-2 colocalises with RNA PolII at transcriptionally active loci on polytene chromosomes is in contrast to the well-established function of Mi-2 as a transcriptional repressor. In addition to the function of Mi-2/NuRD in the regulation of gene expression, evidence has accumulated that the complex also plays an important role in the regulation of DNA damage response (DDR) (O'Shaughnessy and Hendrich, 2013). The mammalian homolog of Mi-2, CHD4 was shown to be a phosphorylation target of the DDR kinases ATR and ATM and that its expression is induced upon UV irradiation (Burd et al., 2008; Matsuoka et al., 2007; Mu et al., 2007). Further studies established that CHD4 can be recruited to sites of DDR by interaction with PARylated proteins and the ubiquitin ligase RNF (RING finger protein) 8 (Polo et al., 2010). The recruitment of CHD4 allows the remodeler to decondense the chromatin at the damaged DNA site and stimulates the formation of ubiquitin conjugates by RNF8 (Luijsterburg et al., 2012). This amplifies the DNA-damage repair pathway and recruits downstream acting proteins for DNA break repair (Smeenk et al., 2010).

The remodeler Chd3 is highly related to Mi-2 as it shares one PHD finger, the chromodomains and the ATPase domain with Mi-2. Purification of Chd3 from Drosophila embryonic extracts revealed its presence as a monomer in these early developmental stages (Murawska et al., 2008). Furthermore, Chd3 co-localises with Mi-2 to a multitude of interbands on polytene chromosomes. Since Chd3 is not part of a multisubunit complex and lacks parts of the N-terminal domain that is relevant for specific recruitment of Mi-2, recruitment mechanisms of Chd3 to chromatin are subject to ongoing experiments (S. Awe, personal communication).

Finally, the CHD-domain containing protein kismet has been identified as a strong suppressor of homeotic transformation in several Polycomb mutants (Daubresse et al., 1999). Molecular analysis defined the BRK-domain (BRM and KIS) in the C-terminus of kismet, a region also conserved in brahma. Staining of polytene chromosomes with an antibody recognising kismet revealed its association with actively transcribed loci and colocalisation with RNA PolII. Strikingly, loss of kismet results in dramatic reduction of elongating RNA PolII and the transcription elongation factors Spt5 and Chd1 (Srinivasan et al., 2005). In line with these findings kismet was also shown to establish binding of the H3K4 methyltransferase TRX and ASH1 and to antagonise H3K27 methylation on chromatin (Dorighi and Tamkun, 2013; Srinivasan et al., 2008).

Therefore, it has been suggested that kismet contributes to initial steps of transcriptional activation.

In conclusion the family of ATP-dependent chromatin remodeler contains highly related proteins that can function in transcriptional activation and/or establishment of repressive chromatin. Therefore, their function is highly dependent on the interacting proteins within a complex and the chromatin environment to which they are recruited.

2.2 Nuclear hormone receptors

2.2.1 Nuclear receptor superfamily

The nuclear receptor (NR) superfamily is a group of eukaryotic transcription factors that bind specific biologically active substances (ligands), which leads to a conformational change within the protein that can result in alterations in gene expression of a particular cell (Bain et al., 2007). Nuclear receptors have a significant importance in development, differentiation, metabolism and physiology of an organism. Members of this family include receptors that bind thyroid and steroid hormones, retinoids and vitamin D, as well as “orphan” receptors that have no defined endogenous ligand. Over the past decades scientists have identified more than 300 members of the NR superfamily that are characterised by structural homology between several domains (Figure 2.5) (Nuclear Receptors Nomenclature, 1999). Even though the letters A/B, C, D, E and F have been traditionally designated to different regions within the protein, they do not necessarily correspond to structural domains. All family members harbour a centrally located DNA-binding domain (DBD, region C) containing two zinc fingers and a C-terminally located ligand binding domain (LBD, region E).

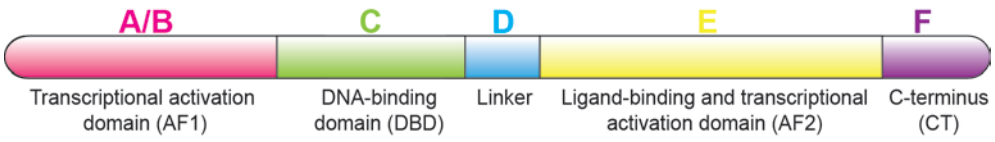

Figure 2.5: Domain organisation of the nuclear receptor superfamily. Adapted from (Hill et al., 2013).

Interestingly, it was found that a receptor lacking the LBD is constitutively active, suggesting that neither the hormone, nor the hormone-binding region is necessary for DNA-binding. Therefore, it was proposed that the LBD prevents the DBD from interaction with the DNA. This inhibition is relieved upon ligand binding (Godowski et al., 1987). In contrast to the highly conserved DBD, the N-terminus (AF1, region A/B)

of nuclear hormone receptors contains a region that is hypervariable in size and amino acid composition. It was shown that the N-terminus contributes to receptor function as deletion mutants show a 10- to 20-fold reduced activity in reporter gene activation (Hollenberg et al., 1987). In addition to the three structural domains described above, nuclear receptors contain a flexible hinge region between the DBD and LBD (region D) that harbours nuclear localisation signals. This region was also shown to further modulate receptor activity (Guiochon-Mantel et al., 1992; Jackson et al., 1997).

Nuclear receptors conduct their function by making base-specific contacts with the major groove of the DNA via the zinc finger motif in the DNA binding domain (Helsen et al., 2012). Gene transfer studies with the mouse mammary tumour virus (MMTV) promoter demonstrated that short sequences, acting in cis, are necessary for transcriptional activation by hormones. If these elements are cloned in front of an otherwise hormone-nonresponsive gene, its transcription is induced upon hormonal stimulation (Robins et al., 1982). Functionality of these hormone response elements (HREs) is independent of their orientation and position with respect to the gene (Chandler et al., 1983). Therefore, these sequences act as transcriptional enhancers to which the hormone receptor binds in a ligand dependent fashion. In most cases, NRs recognise a purine base followed by the sequence GGTCA (Chalepakis et al., 1988; De Vos et al., 1993). This HRE is often present in two copies, which can occur in a head-to-head (palindrom), head-to-tail (direct repeats) or tail-to-tail (inverted repeats) orientation (Gronemeyer and Moras, 1995). Furthermore, two HREs within a repeat can be separated by variable linker sequences. Due to the dyad symmetry of the DNA motif, nuclear receptors bind as dimers to their specific sequence (Beato et al., 1995; Germain and Bourguet, 2013). In addition to a homology-based classification, the nuclear receptor superfamily can be broadly divided into four groups based on their dimerisation and DNA-binding properties (Olefsky, 2001). Class I receptors, such as the glucocorticoid and estrogen receptor, bind as ligand-induced homodimers to inverted repeats, whereas Class II receptors, like thyroid hormone receptor (TR), heterodimerise with their retinoid X receptor (RXR) binding partner and bind to direct repeats. Class III composes a group of nuclear receptors that bind as homodimers primarily to direct repeats. Receptors belonging to Class IV typically interact with a single PuGGTCA sites as monomers. Class III and IV include most orphan receptors (Mangelsdorf et al., 1995; Stunnenberg, 1993).

Recent advances in sequencing technologies allowed scientists to dissect NR action on a genome-wide scale (Mendoza-Parra and Gronemeyer, 2013). Surprisingly,

ChIPSeq results revealed that most of the identified NR binding sites were situated within intronic or promoter-distal, intergenic regions and not, as expected, at promoters. In addition, the correlation between receptor occupancy and gene regulation was found to be very small (Carroll et al., 2006; Delacroix et al., 2010; Wang et al., 2007). These unexpected findings prompted scientists to question the simple promoter recruitment model and to investigate the cross-talk between nuclear receptors and chromatin associated proteins in detail.

2.2.2 Chromatin architecture at hormone inducible promoters

Nuclear receptors regulate transcription by binding specific DNA sequences and recruiting enzymes that establish a repressive or active chromatin state (Figure 2.6). Various co-activator complexes associate with the receptor in the presence of hormone in a sequential and combinatorial manner to potentiate NR activity. Direct interaction with the AF-2 of NRs is mediated by the presence of leucine-rich motifs of the consensus sequence LXXLL, where L represents leucine and X any amino acid (Heery et al., 1997). In contrast, co-repressor complexes bind to NRs in a ligand-independent fashion to limit or abolish transcription of target genes.

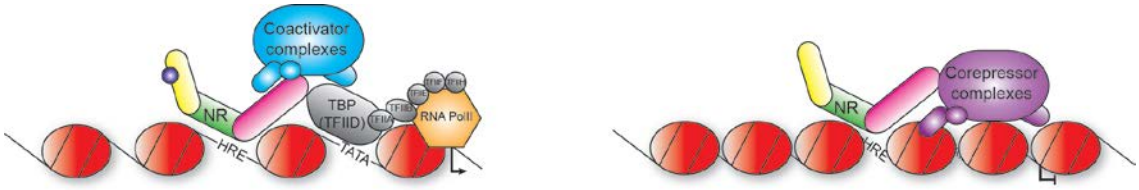

Figure 2.6: Transcriptional regulation by nuclear receptors. NRs interact with co-activator complexes in the presence of hormonal substances and recruit the transcription machinery (grey circles and RNA PolII) to the transcriptional start site. In the absence of hormone, co-repressor complexes bind to the nuclear receptor to establish a repressive chromatin environment and inhibit transcription. Adapted from (Nettles and Greene, 2005). TATA – TATA-box, HRE – hormone responsive element., NR-nuclear receptor.

The estrogen-dependent gene *pS2* (trefoil factor 1; TFF1) has been used extensively as a model promoter to explore the processes by which nuclear receptors influence chromatin remodeling and thereby transcription. The *pS2* promoter is a target of estrogen-receptor mediated transcriptional activation. It harbours a single consensus estrogen response element positioned 400 bp upstream of the TSS (Figure 2.7). Further, it is occupied by two nucleosomes positioned such that they encompass the TATA box (nucT) and the ERE (nucE) at their edge (Sewack and Hansen, 1997).

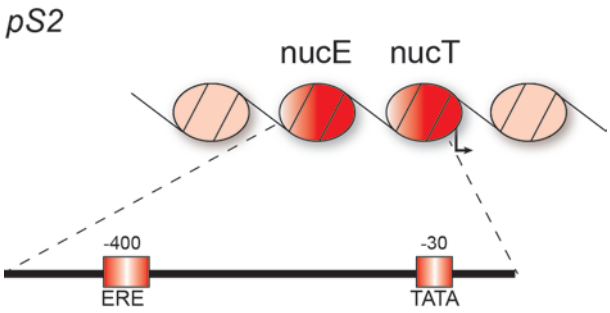

Figure 2.7: Chromatin architecture at the *pS2* promoter. The positioning of specific nucleosomes (nuc) over relevant DNA sequences is illustrated. HRE-hormone responsive element, TATA-TATA box, ERE-estrogen responsive element. Adapted from (Sewack and Hansen, 1997).

Detailed ChIP analyses provide a comprehensive picture of the timing of events at this locus and introduced the concept of a “transcriptional clock” (Burakov et al., 2002; Metivier et al., 2003; Reid et al., 2003; Shang et al., 2000). Metivier *et al.* describes the subsequent binding of 30 different proteins upon treatment of MCF-7 cells with 17b-estradiol (E2) using re-ChIP assays, hereby identifying the combinations of factors engaged at the *pS2* promoter. This showed that transcription factors, histone modifying enzymes and chromatin remodeler occupy the promoter in oscillatory waves of association. In detail, productive transcription is preceded by a non-productive cycle in which ER binds to the pS2 promoter and recruits co-activator complexes such as p160, p300 and PRMT1. That contribute to acetylation of H3K14 and dimethylation of H4R3 (Shang et al., 2000). This first cycle is followed by two alternating, transcriptionally productive cycles. The factors to be recruited in the productive cycles are the SWI/SNF complex followed by CARM1 and p300/CBP, which promote additional covalent histone modifications such as H4K16ac and H3R17me2 (Chen et al., 1999; DiRenzo et al., 2000). This creates a chromatin environment that enables recruitment of the basal transcription machinery by binding of TBP, TFIIA and TAF130 and RNA PolII. The recruitment of Mediator and elongation promoting complexes facilitates separation of the DNA double strand, release of RNA PolII from the promoter and eventually mRNA synthesis.

Termination of the hormonal response due to a decrease in hormone titer requires the removal of ER and its co-activators from the promoter in order to establish a repressive state. This is achieved by removal of active histone marks by HDAC1 and 7 that are recruited via NCoR/SMRT. Additionally, the NuRD complex was demonstrated to localise to the methylated CpGs in the promoter via MBD2/3 (Kangaspeska et al., 2008; Metivier et al., 2008). The NuRD complex contributes to promoter clearance by shifting the nucT nucleosome over the TATA box, thereby excluding TBP binding. As

demonstrated by ChIP, cycling of the *pS2* promoter occurs with a periodicity of around 50 min. The mode of action of ER on a genome-wide scale has been established using ChIA-PET (Fullwood et al., 2009). This study demonstrated that ER is bound to promoter-distal regions and upon chromosomal loop formation it associates with RNA PolII at promoter-proximal regions. It was hypothesised that this three-dimensional architecture establishes “transcription factories” with a high concentration of factors important for transcription, which allows for efficient cycling of the involved complexes described above (Osborne et al., 2004).

2.2.3 Ashburner model of the ecdysone cascade

The development of holometabolous invertebrates requires the moulting of the cuticula, a process termed ecdysis (Aguinaldo et al., 1997). In insects, this process is initiated by hormones in response to environmental and physiological cues such as the photoperiod and the weight of the animal (Heming, 2003; Truman, 2005). Ecdysone is the master regulator of development of Drosophila. It is a steroid hormone that is mainly produced in the prothoracic gland (Kopeć, 1922). Upon release into the hemolymph, ecdysone is converted to the biologically active substance 20-hydroxyecdysone (20HE) that regulates the transition from larval to pupal stage (Petryk et al., 2003). The ecdysteroid titer rises rapidly at the end of the Drosophila third instar larva development, triggering puparium formation and the onset of metamorphosis (Handler, 1982; Richards, 1981). Subsequently, 20HE levels drop in mid prepupae and peak again 10- to 12-hours later, triggering head eversion and pupation (Handler, 1982; Sliter and Gilbert, 1992).

Through a series of detailed studies, Ashburner and colleagues postulated a model to explain the genetic regulation of polytene chromosome puffing by 20HE (Figure 2.8A) (Hill et al., 2013). Puffing of polytene chromosomes reflects the immense alteration of chromatin structure upon transcriptional activation by 20HE at specific loci. According to this model, the 20HE receptor complex directly induces a small set of “early genes” that are represented by a few polytene puffs visible immediately after the first pulse of hormone (most prominently 2B, 23E, 63F, 74EF, and 75B) (Ashburner, 1972a; Ashburner, 1972b; Ashburner, 1973). The protein products of early transcribed genes are transcription factors that directly contribute to activation of “late genes” as visualised by approximately 100 late puffs on the polytene chromosomes. Treatment with protein synthesis inhibitors, such as puromycin or cycloheximide, did not restrain

induction of early puffs. However, it did indicate that late-puff induction was dependent on new protein synthesis (Ashburner, 1974; Clever, 1964).

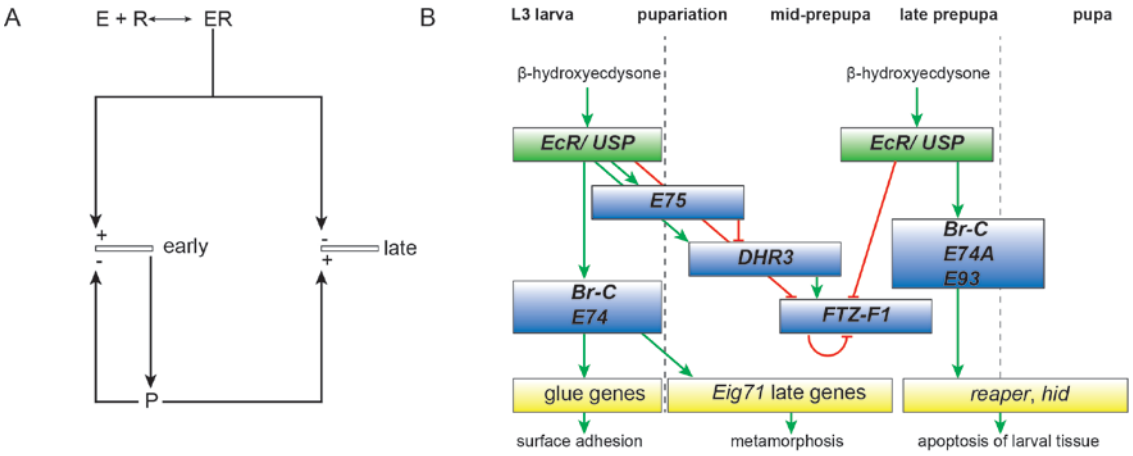

Figure 2.8: Ashburner Model in comparison to a more complex ecdysone cascade. Adapted from (Ashburner, 1990; Thummel, 1995).

In the past decades, molecular characterisation of early gene puffs and cloning of the related genes involved in the ecdysone cascade, lead to the isolation of the transcription factors *broad* (*Br-C*), *E74* and *E75*. Genetic studies implied that the *broad* gene (residing within the 2B puff), is required for transcription of genes in the *Eig71* late puff. Also, mutations in *broad* were shown to prevent metamorphosis (Guay and Guild, 1991; Kiss et al., 1988). In order to identify the gene associated with the polytene puff at 75B, chromosomal walks were conducted and confirmed the gene product E75 to be a member of the nuclear receptor superfamily (Feigl et al., 1989; Segraves and Hogness, 1990). The sequence of the putative DNA-binding domain of E75 was subsequently used as a hybridisation probe in a cDNA library screen and allowed the isolation of the *EcR* gene (Koelle et al., 1991). Later, the functional ecdysone sensing receptor was shown to be generally a heterodimer consisting of the nuclear proteins EcR and ultraspiracle (USP). (Thomas et al., 1993; Yao et al., 1993; Yao et al., 1992). USP is the Drosophila homolog of the mammalian nuclear hormone receptor heterodimeric partner RXR (Oro et al., 1990). These results confirmed the basic concept of the Ashburner Model and lead to a better understanding of the sequential regulation of the ecdysone network (Figure 2.8B).

The Ashburner model is an oversimplification of a direct response to a single ecdysone pulse. Therefore, it can not clarify how diverse tissues can respond differently to the same ecdysone pulse or how a specific tissue reacts to several independent ecdysone pulses (Rewitz et al., 2013). This can be in part explained by varying sensitivity to

20HE, the expression of different EcR isoforms and the availability of a distinct set of co-activator and –repressor complexes (discussed below) (Karim and Thummel, 1992; Talbot et al., 1993). The finding that the transcription factor/ nuclear receptor FTZ-F1 is differentially expressed in subsequent developmental stages and represses its own transcription added more complexity to the network (Lavorgna et al., 1993; Woodard et al., 1994). FTZ-F1 expression requires a high concentration of 20HE followed by ecdysone withdrawal, as is observed three to eight hours after pupariation (Handler, 1982; Richards, 1976). Therefore, it acts as a competence factor to reset the system during the mid-prepupal period to allow both, the reinduction of the early puffs and the initial induction of the prepupal-specific early puffs by ecdysone (Broadus et al., 1999; Woodard et al., 1994).

The tight regulation and expression of the transcription factors described above translates the hormonal signal into the expression of secondary-response effector genes such as the glue genes and apoptosis promoting genes (Yamanaka et al., 2013). The expression of glue-genes is limited to the late third instar larva. Secretion of glue proteins at this stage allows the larva to adhere to a solid surface for the duration of the pupal period (Beckendorf and Kafatos, 1976; Kodani, 1948). Also, the late larval ecdysone pulse triggers a set of metamorphic responses such as larval tissue histolysis and eversion of the imaginal discs that will later form the adult appendages. The degradation of larval tissue is coordinated by the process of programmed cell death, for which the 20HE-induced expression of “death activator” genes like *reaper* (*rpr*) and *head involution defective* (*hid*) is essential (Denton et al., 2013a; Jiang et al., 1997; Yin and Thummel, 2005). Approximately ten hours after puparium formation, this is followed by a second hormonal pulse that leads to growth and differentiation of adult tissues such as head eversion and gut formation (Bate and Martinez Arias, 1993).

In order to identify all genes involved in the ecdysone response, several studies examined the genome-wide expression pattern upon an ecdysone pulse in cell culture or by analysing subsequent stages of the metamorphosis in the fly (Beckstead et al., 2005; Gonsalves et al., 2011; White et al., 1999). Microarray analysis of whole staged animals showed approximately four times more genes were regulated during metamorphosis than Ashburner proposed by the appearance of puffs on polytene chromosomes (White et al., 1999).

More recent studies demonstrated that the ecdysone response cascade is not only crucial for larval to pupal transition, but is already activated in the extraembryonic

amnioserosa during early embryo development. Here, ecdysone activation influences shaping events for the first instar larva, such as germ band retraction and head involution (Kozlova and Thummel, 2003). Additionally, ecdysone has been shown to be crucial for ovary development in the adult fly, as germline clones of EcR null mutants arrest during oogenesis resulting in female sterility (Buszczak et al., 1999). Further, EcR was shown to influence follicle development, border cell migration and to promote self-renewal of germline stem cells in the Drosophila ovary (Ables and Drummond-Barbosa, 2010; Carney and Bender, 2000; Jang et al., 2009). In conclusion, ecdysone and its corresponding receptor complex is involved in a multitude of gene regulatory functions and is considered to be a master regulator of insect development.

2.2.4 Regulation of gene expression by EcR

In Drosophila, the EcR gene encodes for three different isoforms (EcR-A, -B1, -B2), of which each isoform has a distinct expression and trans-activation function during insect development (Davis et al., 2005). Mutations in a common exon of all isoforms, leads to embryonic lethality. In contrast, depletion of only the EcR-B1 isoform results in lethality at the onset of metamorphosis (Bender et al., 1997; Schubiger et al., 1998). The functional ecdysone receptor is a heterodimer between the nuclear receptors EcR and USP, and this heterodimer is required for binding both ecdysone response element DNA (EcRE) and ecdysteroids (Koelle et al., 1991; Thomas et al., 1993; Yao et al., 1993). The LBD of EcR (activation function 2, AF-2) and USP both display a canonical nuclear receptor LBD tertiary structure, which consists of 12 α-helices (H1 to H12). These pack together in three antiparallel layers, which encloses the steroid hormone in a conserved position in the ligand binding pocket (Billas et al., 2003; Billas et al., 2001). Crystal structure analysis of the DBD of EcR and USP bound to the *hsp27* promoter showed that important sequence specific base-contacts with the major groove are mediated by residues of the so called DNA-recognition α-helix. These contacts are formed such that the EcR DBD makes seven and the USP DBD ten specific interactions with the palindromic sequence (Figure 2.9) (Devarakonda et al., 2003; Jakob et al., 2007).

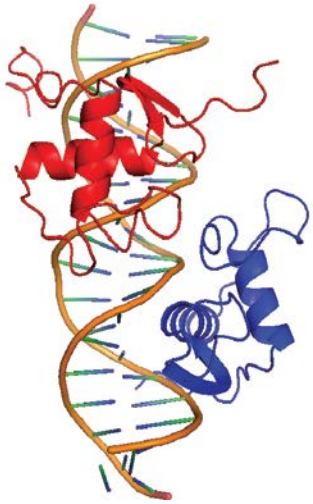

Figure 2.9: Crystal structure of DNA-binding domains of USP (blue) and EcR (red) bound to the *hsp27* EcRE. Adapted from (Jakob et al., 2007).

The cellular distribution of EcR is subject to debate. In some cells it exclusively localises to the nucleus, yet in others it is evenly distributed between the cytoplasm and the nucleus (Smagghe, 2009). However, a recent study shows that in the absence of the hormone, both EcR subunits localise to the cytoplasm, and the heme-binding nuclear receptor E75A replaces EcR/USP at common target sequences in several genes (Johnston et al., 2011). Upon hormone release, the receptor complex shifts into the nucleus. Subsequent binding of the EcR/USP heterodimer to its DNA recognition sequence causes the release of associated co-repressor proteins. This allows receptor association with co-activator proteins that function to either modify chromatin structure or link the nuclear receptors to the transcription machinery.

2.2.4.1 EcR co-activators

Initiation of the ecdysone cascade can be observed in Drosophila instar larva as puffing of the underlying chromatin structure. Tulin and Spradling showed that puff formation requires ADP-ribosylation of histone and non-histone proteins by the poly(ADP)-ribose polymerase (PARP) (Tulin and Spradling, 2003). *Parp* mutants fail to form puffs and display a developmental arrest at the onset of ecdysis (Tulin et al., 2002). Examination of the functional relationship between EcR and PARP revealed that PARP interacts with EcR and is recruited to the *hsp27* promoter in a ligand-dependent manner (Sawatsubashi et al., 2004). Adding to the concept of chromosomal puffing in response to 20HE, the Nasmyth laboratory demonstrated that Cohesin, a multisubunit complex that functions in sister chromatid segregation during mitosis, is also implicated in transcriptional regulation of ecdysone dependent genes. Depletion of

the Cohesin subunit Rad21 resulted in misregulation of 20HE inducible genes, which resulted in dramatic reduction of puff size at the *Eip74* and *Eip75* loci (Pauli et al., 2010).

Another EcR co-activator is the SET-domain containing protein TRR (trithorax related) that can methylate H3K4. It contains a C-terminal LXXLL motif that mediates interaction with both, USP and EcR and accordingly co-localises with the nuclear receptor complex to 20HE target genes on polytene chromosomes. Further, the presence of TRR at the promoter region of *Br-C* coincides with an increase in H3K4me3 upon hormonal stimulation demonstrated by ChIP analysis (Sedkov et al., 2003). In comparison to its mammalian homolog, MLL2 and 3, TRR lacks the N-terminal PHD and HMG domains that contribute to chromatin binding. Interestingly, the protein encoded by *cmi* (*cara mitad*) was identified as the N-terminal half of MLL2 present in Drosophila. Cmi has been demonstrated to bind to mono- and di-methylated H3K4. This prevents demethylation and stabilises TRR for hormone-stimulated histone methylation (Chauhan et al., 2012). A subsequent study reported that ASH2 (absent, small or homeotic discs 2), a protein found to be a core subunit of methyltransferase complexes in mammals, also stabilises TRR at ecdysone response genes. Therefore, it also acts as a co-activator for EcR dependent transcription (Carbonell et al., 2013; Dou et al., 2006). Activation of transcription does not only require the establishment of active histone marks such as H3K4me3, but also removal of repressive marks like H3K27me3. The H3K27 demethylase UTX was studied in the regulation of apoptosis and autophagy genes during ecdysone-mediated programmed cell death of salivary glands. Here, UTX interacts with EcR and induces expression of apoptotic genes such as *reaper*, *dark* and *dronc* (Denton et al., 2013b).

Badenhorst and colleagues identified the ISWI-containing chromatin remodeling complex NURF to physically associate with EcR (Badenhorst et al., 2005). Loss-of-function mutation for NURF lead to a strong down-regulation of several genes of the ecdysone cascade. This resulted in pupariation defects highlighting the critical function of NURF in EcR-mediated gene activation. Comparable results have been reported for the Drosophila SWI/SNF complex. Overexpression of dominant negative *brahma* renders the chromatin remodeler catalytically inactive, but does not disrupt incorporation into the complex. These mutants showed a decreased expression of the late-induced *Eig71* (ecdysone induced gene) cluster on chromosome 3 (Zraly et al., 2006). This data was further supported by the finding that SAYP (supporter of activation of yellow protein) interacts with the orphan nuclear receptor DHR38 and is

recruited to ecdysone dependent genes (Vorobyeva et al., 2011). SAYP was found to form a super-complex connecting TFIID and the brahma-containing PBAP complex. and may thus tether brahma to DHR38 regulated loci where it contributes to transcriptional activation of second response genes in the ecdysone cascade (Soshnikova et al., 2009).

A genetic screen for proteins that regulate chromosomal puffing in Drosophila 3rd instar larva identified the histone chaperone dDEK. DEK is a histone chaperone that interacts with EcR in an ecdysone dependent manner in S2 cells. It is suggested to function as a co-activator by incorporating H3.3 at transcriptionally active chromatin within EcR target gene promoters (Sawatsubashi et al., 2010).

2.2.4.2 EcR co-repressors

Studies on the mode of action of nuclear receptors in mammals demonstrated that repression of basal transcription by the thyroid receptor occurs via association with the co-repressor proteins N-CoR and SMRT (Chen et al., 1996). The homolog of N-CoR and SMRT was identified as the Drosophila protein SMRTER that contains two domains which bind with high affinity to the EcR/USP heterodimer (Tsai et al., 1999). Further, SMRTER is suggested to contribute to transcriptional repression by interaction with the histone deacetylase Sin3a (Nagy et al., 1997). However, in the presence of hormone the interaction with the nuclear receptor is lost, characterising SMRTER as an EcR ligand-dependent co-repressor. In addition to histone deacetylation, histone methylation plays a crucial role in the establishment of a repressive chromatin environment. The arginine methyltransferase DART1 interacts with EcR in the absence and presence of hormone. Knockdown of DART1 slightly enhanced 20HE-dependent EcR activation in a Luciferase reporter assay (Kimura et al., 2008). As described above, regulation of hormone induced genes is also accomplished by long-range promoter-enhancer interactions that are controlled by the presence of insulator elements. Insulators are DNA sequences that are bound by insulator proteins such as CTCF and Cp190 (Bartkuhn et al., 2009). Ecdysone treatment of Drosophila Kc cells resulted in new or increased binding of Cp190 to 306 DNA loci. In depth analysis of Cp190 binding to the *Eip75B* locus revealed that hormonal induction alters the 3D structure of the locus. Furthermore, it was demonstrated that depletion of Cp190 resulted in misexpression of *Eip75B* neighbouring genes. Thus, Cp190 may create a chromatin environment that blocks the spread of 20HE-induced transcription to surrounding loci (Wood et al., 2011).

2.3 Objectives

Previous studies of the ATP-dependent chromatin remodeler Mi-2 demonstrated its recruitment to active heat shock loci on third instar larva polytene chromosome of Drosophila. Here, Mi-2 is crucial for efficient transcription and co-transcriptional processing of the nascent *hsp* transcripts (Mathieu et al., 2012; Murawska et al., 2011). These findings were opposing to several studies that identified Mi-2 as a member of the repressive NuRD complex (Marhold et al., 2004; Wade et al., 1998; Zhang et al., 1998).

Interestingly, in addition to heat shock loci, Mi-2 was shown to localise to the ecdysone induced puff of the *broad* gene in third instar larvae (Murawska, 2011) (Figure 2.10). This locus is highly transcribed upon 20HE release. Therefore, Mi-2 may be involved in the regulation of ecdysone dependent genes. Involvement of various ATP-dependent chromatin remodelers in the regulation of 20HE dependent genes has been studied, however so far Mi-2 function has not been connected to the ecdysone cascade (Badenhorst et al., 2005; Zraly et al., 2006). This study aims to understand the function of Mi-2 at ecdysone dependent genes. Further, it investigates the underlying recruitment mechanism that leads to binding of the chromatin remodeler to 20HE inducible loci in Drosophila S2 cells. Finally, it examines an additional role of Mi-2 in the regulation of transcriptional activation.

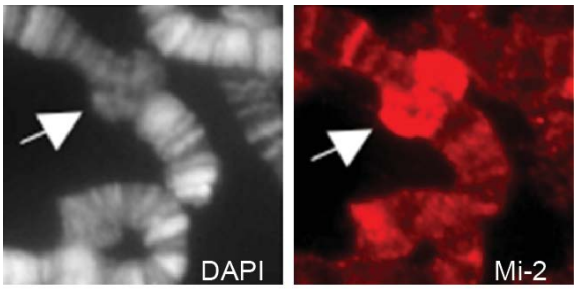

Figure 2.10: Mi-2 localises to the ecdysone induced puff of the *broad* gene on third instar larva polytene chromosomes. DNA is visualised by DAPI staining (left). Immunofluorescence with anti-Mi-2 antibody (right). Experiment performed by Magdalena Murawska.

3 Material and Methods

3.1 Material

3.1.1 Material sources

The instruments, materials, chemicals and reagents used in this study were purchased from the following companies and trademarks:

5 Prime, Abcam, Abgene Ltd., Agilent Technologies Inc., Alexis Biochemicals, Biosciences, AppliChem GmbH, Bayer AG, B. Braun Melsungen AG, Beckman Coulter Inc., Biometra, Bio-Rad Laboratories Inc., Biozym Scientific GmbH, Boehringer Ingelheim, Calbiochem, Camag, Covance Inc., Diagenode, Eppendorf, Fermentas, Fisher Scientific, Fujifilm, GE Healthcare, Gibco, Gilson Inc., G. Kisker, Greiner Bio-one, Hartmann Analytic GmbH, Heraeus, HMC Europe GmbH, Julabo Labortechnik GmbH, Otto E. Kobe AG, Kodak, Labnet International, Lauda Dr. R. Wobser GmbH & Co. KG, Leica Microsystems GmbH, Life Technologies Corporation, Merck Chemicals, Millipore, MWG Biotech, New England Biolabd, PAA Biolaboratories GmbH, PeqLab Biotechnologie GmbH, Perbio, Pierce, Polysciences Inc., Promega, Qiagen, Roche, Roth, Santa Cruz Biotechnology, Sarstedt AG & Co, Sartorius AG, Scientific Industries, Serva Electrophoretics GmbH, Sigma-Aldrich, Stratagene, Thermo Scientific Inc., Upstate, VWR International, Whatman and Zeiss.

3.1.1.1 Enzymes

Calf intestine alkaline phosphatase	Thermo Scientific
DNase I (RNase-free)	Peqlab
Fast AP Thermosensitive Alkaline	Thermo Scientific
Phosphatase	Thermo Scientific
Micrococcal Nuclease	Sigma
M-MLV Reverse Transcriptase	Life Technologies
Proteinase K	Roth
Restriction endonucleases	Thermo Scientific, NEB
RNase A (DNase-free)	Qiagen
Taq DNA Polymerase	Thermo Scientific
T4 DNA ligase	Thermo Scientific

3.1.1.2 Enzyme Inhibitors

Aprotinin	Roth
Leupeptin	Roth
Pepstatin	Roth
PMSF (phenyl-methane-sulfonyl-flouride)	Roth
RiboLock RNase Inhibitor	Thermo Scientific

3.1.1.3 Bioactive molecules

20-Hydroxyecdysone	Sigma-Aldrich
^{35}S-Methionine	Hartmann Analytic

3.1.1.4 Affinity purification material

Anti-FLAG M2 Affinity Gel	Sigma-Aldrich
Glutathione Sepharose	GE Healthcare
Protein A Sepharose FF	GE Healthcare
Protein G Sepharose FF	GE Healthcare

3.1.1.5 Dialysis and filtration material

Filtropur bottle top filters	Sarstedt
Slide-A-Lyzer Dialysis Cassettes	Thermo Scientific
Sterile syringe filters	VWR

3.1.1.6 SDS-PAGE and Western blotting

APS (ammonium persulfate)	Serva Electrophoresis
Immobilon Western Chemiluminescent HRP Substrate	Millipore
PageBlue Protein Staining Solution	Thermo Scientific
PageRuler Prestained Protein Ladder	Thermo Scientific
Protein Assay (Bradford solution)	Bio-Rad
Rotiphorese Gel 30 (Acrylamide-Bisacrylamide 37,5:1)	Roth
Roti-PVDF membrane	Roth

SuperRX Fuji Medical X-ray film	Fujifilm
TEMED (tetramethyl-ethylene-diamine)	Roth
Whatman 3MM paper	Whatman

3.1.1.7 Agarose gel electrophoresis

Ethidium bromide	AppliChem
GeneRuler 1kb DNA Ladder Plus	Thermo Scientific

3.1.1.8 Other consumables

Amicon Ultra-4 Centrifugal Filter Units	Millipore
Amplify Flourographic Reagent	GE Healthcare
Fish skin gelatin	Sigma
Poly-prep column	Biorad
Phenol/ Chloroform/ Isoamylalcohol (25:24:1)	Roth

3.1.1.9 Kits

Table 3.1: List of application and supplier of the kits used in this study.

Kit	Application	Supplier
ABsolute SYBR Green Mix	qPCR	Thermo Scientific
Bac-N-Blue Baculovirus Expression System	Sf9 cell transfection for baculovirus generation	Life Technologies
Bac-to-Bac Baculovirus Expression System	Sf9 cell transfection for baculovirus generation	Life Technologies
Expand High Fidelity^{PLUS} PCR System	PCR	Roche
Immobilon Western Chemiluminescent HRP	Detection of Western blot	Millipore
Megascript T7 Kit	*In vitro* transcription	Life Technologies
peqGOLD Total RNA Kit	RNA isolation	Peqlab
QIAGEN Plasmid Maxi Kit	DNA isolation	Qiagen

QIAquick Gel Extraction Kit	DNA isolation from agarose gels	Qiagen
QIAquick PCR Purification kit	DNA isolation after ChIP	Qiagen
TNT SP6 Coupled Reticulocyte Lysate System	Coupled *in vitro* transcription and translation	Promega

3.1.2 Standard solutions and buffers

Standard solutions and buffers were prepared according to standard protocols. Stock solutions were freshly diluted before use. Additional buffers are listed in the individual subsections of section 3.2 Methods.

Phosphate Buffered Saline (PBS)	140 mM NaCl 2.7 mM KCl 8.1 mM Na_2HPO_4 1.5 mM KH_2PO_4 pH adjusted to 7.4 with HCl
TAE Buffer	40 mM Tris-Acetate, pH 8.0 1 mM EDTA, pH 8.0

3.1.3 Bacteria strains and culture media

The *Escherichia coli* (*E.coli*) strain XL1-Blue [endA1 gyrA96(nal^R) thi-1 recA1 relA1 lac glnV44 F'[::Tn10 proAB$^+$ lacI^q Δ(lacZ)M15] hsdR17(r_K^- m_K^+)] was used for cloning and propagation of plasmid DNA.

The *E.coli* strain BL21 [(F- *dcm ompT hsdS*(r_B- m_B-) gal [malB$^+$]$_{K-12}$(λ^S)] was used for recombinant expression of GST fusion proteins.

The *E.coli* strain DH10Bac [F– *mcr*A Δ(*mrr-hsd*RMS-*mcr*BC) φ80*lac*ZΔM15 ΔlacX74 *rec*A1 *end*A1 *ara*D139 Δ(*ara*, *leu*)7697 *gal*U *gal*K κ– *rps*L*nup*G/bMON14272/ pMON7124] was used for recombination of plasmid DNA into a bacmid.

The E.coli strain XL10-Gold [TetR ∆(mcrA)183 ∆(mcrCB-hsdSMR-mrr)173 endA1 supE44 thi-1 recA1 gyrA96 relA1 lac Hte (F´ proAB lacI^q Z∆M15 Tn10 (Tet^R) Amy

Cam^{R})[a]] was used for transformation of plasmids generated by site-directed mutagenesis.a

Transformed bacteria were selected on agar plates with the according antibiotic resistance and/ or selection marker encoded on the plasmid.

3.1.3.1 Antibiotics and selection marker

Table 3.2: Antibiotics and selection marker and their corresponding concentration.

Antibiotic/ Selection marker	Concentration
Ampicillin	100 µg/ml
Gentamicin	7 µg/ml
Kanamycin	50 µg/ml
Tetracycline	10 µg/ml
5-bromo-4-chloro-3-indolyl-β-D-galactopyranoside (X-gal)	100 µg/ml

3.1.3.2 Culture media

Lysogeny Broth (LB) medium	1% (w/v) Peptone 0.5% (w/v) Yeast extract 1% (w/v) NaCl
Agar plates medium	1.5% (w/v) Agar-agar in LB
SOC medium	2% (w/v) tryptone 0.5% (w/v) yeast extract 10 mM NaCl 2.5 mM KCl 10 mM $MgCl_2$ 10 mM $MgSO_4$ 20 mM glucose

3.1.4 Insect cell lines and tissue culture

S2: Male aneuploidy *Drosophila melanogaster cell* line derived from a primary culture of 20 to 24 hrs old embryos (Schneider, 1972). S2 cells were cultured in Schneider's Drosophila Medium (Life Technologies), supplemented with 10% (v/v) fetal bovine serum (FBS; Gibco) and 1% (v/v) Penicillin-Streptomycin (10mg/ml; PAA).

Sf9: Female cell line established from pupal ovaries of *Spodoptera frugiperda (Vaughn et al., 1977)*. Sf9 cells were cultured in Sf-900 II SFM medium (Life Technologies), supplemented with 10% (v/v) FBS and 0.1% (v/v) Gentamicin (10mg/ml; PAA).

3.1.5 Plasmids

Table 3.3: Plasmids used in this study.

Plasmid	Description	Source/ Reference
ER33854	cDNA encoding for full length *EcR*-RB in the pFlc-1 vector.	DGRC BDGP Gold collection
pGex4T1	Vector for IPTG-inducible expression of N-terminal GST-tagged proteins in *E.coli*.	GE Healthcare
pGex4T1 dMi-2 aa 2-690	Vector for IPTG-inducible expression of N-terminal GST-tagged dMi-2 amino acids 2-690 in *E.coli*.	(Murawska, 2011)
pGex4T1 dLint1 aa 1-301	Vector for IPTG-inducible expression of N-terminal GST-tagged C-terminus of dLint-1 in *E.coli*.	(Meier, 2012)
pING14A	Vector for *in vitro* transcription containing an SP6 promoter.	(Hagemeier et al., 1993)
pING14A-EcR	Encodes full length EcR under the control of an SP6 promoter for *in vitro* transcription.	(Amrhein, 2012)
pFastBac1	Baculovirus transfer vector for recombinant protein expression in Sf9 cells. (Bac-to-Bac Baculovirus Expression System)	Life Technologies
pVL1392	Baculovirus transfer vector for recombinant protein expression in Sf9 cells. (Bac-N-Blue Baculovirus Expression System)	Life Technologies

pFastBacDual Mi2-FLAG	Encodes full length Mi-2 C-terminally FLAG tagged, for generation of recombinant baculovirus.	Ulla Kopiniak

Table 3.4: Plasmids generated in this study.

Plasmid	Description
pING14A EcR aa 1-227	Encodes the activation function 1 (AF1) of EcR under the control of an SP6 promoter for *in vitro* transcription, cloned with *Xba*I and *Sma*I using oligos EcR-AF1-Xba_fwd and EcR-AF1-Sma_rev
pING14A EcR aa 228-431	Encodes the DNA-binding domain (DBD) of EcR under the control of an SP6 promoter for *in vitro* transcription, cloned with *Xba*I and *Sma*I using oligos EcR-DBD-Xba_fwd and EcR-DBD-Sma_rev.
pING14A EcR aa 432-655	Encodes the activation function 2 (AF2) of EcR under the control of an SP6 promoter for *in vitro* transcription, cloned with *Xba*I and *Sma*I using oligos EcR-AF2-Xba_fwd and EcR-AF2-Sma_rev.
pING14A EcR aa 656-878	Encodes the C-terminus of EcR under the control of an SP6 promoter for in *vitro* transcription, cloned with *Xba*I and *Sma*I using oligos EcR-CTerm-Xba_fwd and EcR-CTerm-Sma_rev.
pVL1392 EcR	Encodes the full length EcR for generation of recombinant baculovirus, cloned with NotI and *Xba*I using oligos EcR_NotI_fwd and EcR_Xba_rev.
pFastBac FLAG-EcR	Encodes the full length EcR, N-terminally FLAG-tagged, for generation of recombinant baculovirus, derived from pFastBac by site directed mutagenesis using oligos FastBac_EcR_FLAG_fwd and FastBac_EcR_FLAG_rev.
pFastBac FLAG-EcR aa 1-227	Encodes the activation function 1 (AF1) of EcR, N-terminally FLAG-tagged, for generation of recombinant baculovirus, cloned with BamHI and NotI using oligos EcRAF1_FLAG_fwd and EcRAF1_rev.
pFastBac FLAG-EcR aa 228-431	Encodes the DNA-binding domain (DBD) of EcR, N-terminally FLAG-tagged, for generation of recombinant baculovirus, cloned with BamHI and NotI using oligos EcRDBD_FLAG_fwd and EcRDBD_rev.

pFastBac FLAG-EcR aa 432-655	Encodes the activation function 2 (AF2) of EcR, N-terminally FLAG-tagged, for generation of recombinant baculovirus, cloned with BamHI and NotI using oligos EcRAF2_FLAG_fwd and EcRAF2_rev.
pFastBac FLAG-EcR aa 656-878	Encodes the C-terminus of EcR, N-terminally FLAG-tagged, for generation of recombinant baculovirus, cloned with BamHI and NotI using oligos EcRCT_FLAG_fwd and EcRCT_rev.
pFastBac HA-EcR aa 1-227	Encodes the activation function 1 (AF1) of EcR, N-terminally HA-tagged, for generation of recombinant baculovirus, cloned with BamHI and NotI using oligos EcRAF1_HA_fwd and EcRAF1_rev.
pFastBac HA-EcR aa 432-655	Encodes the activation function 2 (AF2) of EcR, N-terminally HA-tagged, for generation of recombinant baculovirus, cloned with BamHI and NotI using oligos EcRAF2_HA_fwd and EcRAF2_rev.
pGex4T1 Mi-2 aa 691-1271	Contains N-terminal GST fusion of Mi-2 ATPase domain for IPTG-inducible expression in *E.coli*, cloned with *Sma*I and NotI using oligos ATPase_Sma_fwd and ATPase_Not_rev.
pGex4T1 Mi-2 aa 691-1271 LFHAA	Contains N-terminal GST fusion of Mi-2 ATPase domain with a mutation of the LFHLL motif to LFHAA for IPTG-inducible expression in *E.coli,* derived from pGex4T1 Mi-2 aa 691-1271 by site-directed mutagenesis using oligos LXXAA_ATPase_fwd and LXXAA_ATPase_rev
pGex4T1 Mi-2 aa 691-965	Contains N-terminal GST fusion of Mi-2 ATPase domain Fragment 1 for IPTG-inducible expression in *E.coli*, cloned with BamHI and NotI using oligos ATPase_F1_Bam_fwd and ATPase_F1_Not_rev
pGex4T1 Mi-2 aa 966-1183	Contains N-terminal GST fusion of Mi-2 ATPase domain Fragment 2 for IPTG-inducible expression in *E.coli*, cloned with BamHI and NotI using oligos ATPase_F2_Bam_fwd and ATPase_F2_Not_rev
pGex4T1 Mi-2 aa 1184-1271	Contains N-terminal GST fusion of Mi-2 ATPase domain Fragment 3 for IPTG-inducible expression in *E.coli*, cloned with BamHI and NotI using oligos ATPase_F3_Bam_fwd and ATPase_F3_Not_rev

pGex4T1 Mi-2 aa 1272-1982	Contains N-terminal GST fusion of Mi-2 C-terminal domain for IPTG-inducible expression in *E.coli*, cloned with *Sma*I and NotI using Cterm_Sma_fwd and Cterm_Not_rev.
pGex4T1 Chd1 aa 505-1067	Contains N-terminal GST fusion of Chd1 ATPase domain for IPTG-inducible expression in *E.coli,* cloned with XhoI and NotI using oligos Chd1_Xho_fwd and Chd1_Not_rev.
pGex4T1 Chd3 aa 232-804	Contains N-terminal GST fusion of Chd3 ATPase domain for IPTG-inducible expression in *E.coli*, cloned with EcoRI and NotI using oligos Chd3_Eco_fwd and Chd3_Not_rev.
pGex4T1 ISWI aa 99-611	Contains N-terminal GST fusion of ISWI ATPase domain for IPTG-inducible expression in *E.coli*, cloned with BamHI and NotI using oligos ISWI_Bam_fwd and ISWI_Not_rev.
pFastBacDual Mi2-FLAG LFHAA	Encodes full length Mi-2, C-terminally FLAG-tagged with a mutation of the LFHLL motif to LFHAA, for generation of recombinant baculovirus. Derived from pFastBacDual Mi-2-FLAG by site directed mutagenesis using oligos LXXAA_ATPase_fwd and LXXAA_ATPase_rev.

3.1.6 Oligonucleotides

Unmodified DNA oligonucleotides were purchased from Eurofins MWG Operon. The stock solutions were dissolved in double distilled water (ddH_20) to a concentration of 100 pmol/ µl and stored at -20°C.

3.1.6.1 Oligonucleotides for PCR cloning

Table 3.5: Oligonucleotides used for PCR cloning. Recognition sites of restriction endonucleases are underlined and HA/FLAG-tag sequences are depicted in bold.

Oligo name	Sequence
EcR-AF1-Sma_rev	AGGTCTAGAAAGCGGCGCTGGTCGAAC
EcR-AF1-Xba_fwd	TCTCCCGGGTAACCTGAAGATATAGAATTC

EcR-DBD-Xba_fwd	AGGTCTAGACGCGATGATCTCTCGCCTTCG
EcR-DBD-Sma_rev	TCTCCCGGGTTACATCCTGGTACCAAATTAACT
EcR-AF2-Xba_fwd	AGGTCTAGATACCAGGATGGCTATGAG
EcR-AF2-Sma_rev	TCTCCCGGGTTAATGAACGTCCCAGATCTCC
EcR-CTerm-Xba_fwd	AGGTCTAGAGCCATCCCGCCATCGGTCCAG
EcR-CTerm-Sma_rev	TCTCCCGGGCTATGCAGTCGTCGAGTGCTCCG
EcR_NotI_fwd	GAAGCGGCCGCATGAAGCGGCGCTTGTCG
EcR_XbaI_rev	TCTAGACTATGCAGTCGTCGAGTGCTCCGA
FastBac_EcR_FLAG_fwd	CCGCTTTCGAATCTAGGATG**GATTACAAGGATGACGACGATAAG**AAGCGGCGCTGGTCGAAC
FastBac_EcR_FLAG_rev	GTTCGACCAGCGCCGCTTCTTATCGTCGTCATCCTTGTAATCCATCCTAGATTCGAAAGCGG
EcRAF1_FLAG_fwd	AGAGGATCCATG**GATTACAAGGATGACGACGATAAG**AAGCGGCGCTGGTCGAAC
EcRAF1_rev	TCTGCGGCCGCGTAACCTGAAGATATAGAATTC
EcRDBD_FLAG_fwd	AGAGGATCCATG**GATTACAAGGATGACGACGATAAG**CGCGATGATCTCTCGCCTTCG
EcRDBD_rev	TCTGCGGCCGCTTACATCCTGGTACCAAATTAACT
EcRAF2_FLAG_fwd	AGAGGATCCATG**GATTACAAGGATGACGACGATAAG**TACCAGGATGGCTATGAG
EcRAF2_rev	TCTGCGGCCGCGTTAATGAACGTCCCAGATCTCC
EcRCT_FLAG_fwd	AGAGGATCCATG**GATTACAAGGATGACGACGATAAG**GCCATCCCGCCATCGGTCCAG
EcRCT_rev	TCTGCGGCCGCCTATGCAGTCGTCGAGTGCTCCG

EcRAF1_HA_fwd	AGAGGATCCATG**TACCCATACGACGTCCCAGACTACGCT**AAGCGGCGCTGGTCGAAC
EcRAF1_rev	TCTGCGGCCGCGTAACCTGAAGATATAGAATTC
EcRAF2_HA_fwd	AGAGGATCCATG**TACCCATACGACGTCCCAGACTACGCT**TACCAGGATGGCTATGAG
EcRAF2_rev	TCTGCGGCCGCGTTAATGAACGTCCCAGATCTCC
ATPase_Sma_fwd	AGACCCGGGGACGACGAGGATCGCC
ATPase_Not_rev	AGAGCGGCCGCCTTAAACGAGGACAGATACTCGTTGG
LXXAA_ATPase_fwd	GAGGAGCTGTTCCATGCGGCAAACTTCTTGAGCCGC
LXXAA_ATPase_rev	GCGGCTCAAGAAGTTTGCCGCATGGAACAGCTCCTC
ATPase_F1_Bam_fwd	GAAGGATCCGACGACGAGGATCGCCCG
ATPase_F1_Not_rev	TTCGCGGCCGCTCCTTCAGCACATCCGTCTT
ATPase_F2_Bam_fwd	GAAGGATCCAACATGCCGTCCAAGTCT
ATPase_F2_Not_rev	TTCGCGGCCGCTCCTCCTCCACAGAATT
ATPase_F3_Bam_fwd	GAAGGATCCCGCGTTACCCAGGTGGCC
ATPase_F2_Not_rev	TTCGCGGCCGCTCCTTAAACGAGGACAGATA
Cterm_Sma_fwd	AGACCCGGGGTGGCTTCGTACGCCACTAA
Cterm_Not_rev	AGAGCGGCCGCCGAAAGTTGGCAAAGTTGCCA
Chd1_Xho_fwd	AGGCTCGAGGTGATCAAGTATCGCCCCAA
Chd1_Not_rev	TCTGCGGCCGCTTATTTGAAGGCGGACAACAAGT

Chd3_Eco_fwd	AGAGAATTCCGTCAAAGAGATAGACCTGC
Chd3_Not_rev	TCTGCGGCCGCTCACTTAAAGGACGAAAGATACT
ISWI_Bam_fwd	AGAGGATCCGAGGATGAGGAGTTGCTGGC
ISWI_Not_rev	TCTGCGGCCGCTCAGCTGAACACTTGGTTAGCTC

3.1.6.2 Oligonucleotides for sequencing

Table 3.6: Oligonucleotides used for sequencing.

Oligo name	Sequence
EcRseq1_fwd	AGTCCAGGCAGCGTGCCCAGC
EcRseq2_fwd	ATGACCACTTCGCCGAGCTC
EcRseq3_fwd	ACCACAGCTCGGACTCAATA
GEX-F	CTTTGCAGGGCTGGCAAG
GEX-R	GAGCTGCATGGTGCAGAGG
pFastBacF	ATTAAAATGATAACCATCTCTGC
pFastBacR	TCAGGTTCAGGGGGAGGT
pVL1392seq_fwd	AAAATGATAACCATCTCGC
pVL1392seq_rev	GTCCAAGTTTCCCTG

3.1.6.3 Oligonucleotides for generation of dsRNA by *in vitro* transcription

Oligonucleotides used to generate gene-specific dsRNA by in vitro transcription contain a T7 promoter sequence at the 5' and 3' end. dsRNA probes were used for RNA interference (RNAi) experimens to specifically knock down proteins in S2 cells. RNAi amplicons were designed using the E-RNAi database of the German Cancer Research Center (DKFZ, Heidelberg) available at http://www.dkfz.de/signaling/e-rnai3/.

Table 3.7: Oligonucleotides for dsRNA synthesis by *in vitro* transcription. T7 promoter sequences are depicted in lowercase letters, whereas the gene-specific DNA sequence is shown in uppercase letters.

Oligo name	Sequence
5’-T7-EcR	taatacgactcactatagggTACTCGCAGCGTTACGAAG
3’-T7-EcR	taatacgactcactatagggTACTCAACTGGACCGTGAG
5'-T7-EGFP	gaattaatacgactcactatagggaGAGCTGGACGGCGACGTAA
3'-T7-EGFP	gaattaatacgactcactatagggagACTTGTACAGCTCGTCCATG
5'-T7-Mi-2(2)	taatacgactcactatagggTTAACTCGCTGACCAAGGCT
3'-T7-Mi-2(2)	taatacgactcactatagggATATCGTTGTGGGGATTCCA

3.1.6.4 Oligonucleotides for gene expression analysis by RT-qPCR

For reverse transcription of polyA mRNA into cDNA an Oligo-dT primer, containing 17 dT nucleotides, was used. Oligonucleotides for RT-qPCR were designed using the Universal Probe Library Assay Desgin Center (Roche) available at http://www.roche-applied-science.com/webapp/wcs/stores/servlet/CategoryDisplay?catalogId=10001&tab=Assay+Design+Center&identifier=Universal+Probe+Library&langId=-1

Table 3.8: Oligonucleotides for RT-qPCR gene expression analysis.

Oligo name	Sequence
broad(RB)_fwd	TACAACCGCACCATCCAGT
broad(RB)_rev	ATGCGTTACGATGCGATG
CG12535_fwd	GCTAATGCTTATTTACGGAATCG
CG12535_rev	GGAAGCACTCCATCGTTAGG
Cpr49Ac_fwd	ATGAGGGTCGCCACAAGAT
Cpr49Ac_rev	CGCCATAGATTCCATTCTCAG
CR44742_fw	CAATGACACTTGGGCATGG
CR44742_rev	TGTGGACGTGGAATTGGAT
CR44743_fw	TTTTGTAAAAACCTTAAATGCCACT
CR44743_rev	TTGTGCTAACTAATCTGCGTACAGT
E23_fwd	GCTCATGCTCCTGGATGAA
E23_rev	CGCTGATCACGATGGTCTT
Glut4EF_fwd	GATCTTGAAAAATACGCTAAAAGGA
Glut4EF_rev	GTCGCGATTCCAGCAGAC
Hr4_fwd	TGCTCTCCCACATACCAGAGA
Hr4_rev	CACGAAGGGCACATAGAACA

Iswi_fwd	AAAGGATGTGGCCGATCA
Iswi_rev	AGGCATCGAAGCGAAAGAT
let-7_fwd	AGGTGCGATCTAGTGTGCCGTCTC
let-7_rev	TTAGGGCAAGCTCTGTTGTCCGAA
Mi-2_fwd	CGATTCTCTCCCGACTGG
Mi-2_rev	CAATGTTGTGCCCTGGAAT
Rh5_fwd	TGCTGCCATTGTTCCAGAT
Rh5_rev	GTCCGTGTTGGTCAGGTAATC
Rp49_fwd	TGTCCTTCCAGCTTCAAGATGACCATC
Rp49_rev	CTTGGGCTTGCGCCATTTGTG
vrille_fwd	ATGAACAACGTCCGGCTATC
vrille_rev	CATATTTGCCCAGACTGTCG

3.1.6.5 Oligonucleotides for ChIP analysis by qPCR

Oligonucleotides for ChIP analysis by qPCR were designed using www.flybase.org.

Table 3.9: Oligonucleotides for ChIP analysis by qPCR

Oligo name	Sequence
Broad_ChIP1_fwd	GCCGGCAATATTAGAAGTTCG
Broad_ChIP1_rev	ATTGGATTGGATGGTGCAG
Broad_ChIP2_fwd	AACTTTAGAGGCAGCCCACA
Broad_ChIP2_rev	AGGTAGCAGGGGTACAGTGG
Broad_ChIP3_fwd	TGCCCACACAGACACACAG
Broad_ChIP3_rev	GCCAACTGTGCCTAACTGGT
Broad_ChIP4_fwd	TTCGCAGTCGCTGTTTTCT
Broad_ChIP4_rev	AACAACCTGACGGCGTAGAC
Broad_ChIP5_fwd	CACAGAAGGAAGAAGCAGCA
Broad_ChIP5_rev	CGGGACTGGCAAATTTCTT
Broad_ChIP6_fwd	GCCAGCTGGAGAAAGGTG
Broad_ChIP6_rev	GATTCCCATTCCCACTGATACT
Broad_ChIP7_fwd	GCGCGTCTCTGGACTCAC
Broad_ChIP7_rev	TGGCCAATACTCACGCTGT
Broad_ChIP8_fwd	CAATGATGAAAGCGCAAGC
Broad_ChIP8_rev	CACAGTTTTTCCATTTGCCTAA

Broad_ChIP9_fwd	GGGGCGTTTTGGTAGAACTAA
Broad_ChIP9_rev	TGGTTAGGCATAGACGTGTCC
intergenic2R_fwd	TGCTGACTGCCATCAAATTC
intergenic2R_rev	TACTTGCTGTGACGGCTTTG
vrille_ChIP1_fwd	GATTTAAAAGCCGCCAACTG
vrille_ChIP1_rev	GAGCTGTTATCACAACTGCAAAG
vrille_ChIP2_fwd	TGTGGACGTGGAATTGGAT
vrille_ChIP2_rev	CAATGACACTTGGGCATGG
vrille_ChIP3_fwd	GCCGCTTGTCGCTTATGTA
vrille_ChIP3_rev	TTCTGAGACTGCTTCCTTTGC
vrille_ChIP4_fwd	GGGTTTTATCGCTGTTGCAT
vrille_ChIP4_rev	CATACGCCCCATGGGTTA
vrille_ChIP5_fwd	TCTCTTTGGCTCCCACTCTG
vrille_ChIP5_rev	AAGCGGTAATAGCCAGCAAA
vrille_ChIP6_fwd	GTTTCTTCTGCCCCAATGC
vrille_ChIP6_rev	CCTCTTTGGCCGAAAAATCT
vrille_ChIP7_fwd	TGTGTGTGTGTGATTGTGCTG
vrille_ChIP7_rev	AGAGGGAGCGAGAATTAGACG
vrille_ChIP8_fwd	AGGCCAATGTGGTAACCAGT
vrille_ChIP8_rev	TGGCCACCTCGGACTCTA
vrille_ChIP9_fwd	TTGTAGGGTATCCTGTCCGAAT
vrille_ChIP9_rev	GAAGATTTAGCATTTTGATGGATTT

3.1.6.6 Oligonucleotides for MNase analysis by qPCR

Oligonucleotides for MNase analysis by qPCR were designed using www.flybase.org. For each theoretical nucleosome, three overlapping oligo pairs were designed. Oligo pairs depicted in bold (Table 3.10) were selected as they showed to be protected from MNase digest according to qPCR results.

Table 3.10: Oligonucleotides for MNase analysis by qPCR

Oligo name	Sequence
vrille2_MN1_fw	**GGAATTGGATGTTGCTTCTGGT**
vrille2_MN1_re	**AAGTCTTTGGCTGGCGTCGC**
vrille2_MN2_fw	CGCGGGCCCGTTCTGCCCAT

vrille2_MN2_rev	TTACCGCACGTCCTTTATG
vrille2_MN3_fw	TAACCTTGAAAAGTTTAACTT
vrille2_MN3_rev	CACATGATCCGAGTACATCG
vrilleRE_MN1_fw	AAGCAATTGCGTCGACTGAGC
vrilleRE_MN1_re	GGGTTGTTGTTGGGGATGATGTTG
vrilleRE_MN2_fw	**GTGAAATTTCTGTGCGGCGGC**
vrilleRE_MN2_re	**TAACGACCAACGGCCGCGCCT**
vrilleRE_MN3_fw	GGCAAAAGATCGAGAATTTC
vrilleRE_MN3_re	TGTGAGCAATTGCATATTTC
vrilleRC_MN1_fw	**ACCGCTTATGTTAAGTGATT**
vrilleRC_MN1_re	**ACTTAGCCGTATTTATGACTC**
vrilleRC_MN2_fw	GGATTTCTCAGCCGTTCTGA
vrilleRC_MN2_re	ATTTGATTTTGGGGTCTATTG
vrilleRC_MN3_fw	TATGTGTCATAAGGTGAAAC
vrilleRC_MN3_re	CGACACTATGAAGCCCAGTT
vrille6_MN1_fw	GTACAAAATTTCGGTTTCGT
vrille6_MN1_re	GGTTTTGGAAGAACCCCCAA
vrille6_MN2_fw	**GAATTGCCCGGGTGGCGGGG**
vrille6_MN2_re	**GCTTACAACTTTCACACCGCA**
vrille6_MN3_fw	TGTGCTAGACGTTTCGATGTTG
vrille6_MN3_re	CAACAAGCATTGGGGCAGAAG
vrilleRA_MN1_fw	**AATGCTTTTACAAATTCAATTG**
vrilleRA_MN1_re	**AACCCGATCGGCTGTATATTA**
vrilleRA_MN2_fw	GACTATACTACCAAACCATATA
vrilleRA_MN2_re	CTGCGCTTGATGCACTTGGCC
vrilleRA_MN3_fw	TCGAGCCGTTAAAAGCATTT
vrilleRA_MN3_re	GAAAATTGTTTTTCAAACACTTG
vrilleEx_MN1_fw	**CTATCGCGTCGGGCCTGCTCACC**
vrilleEx_MN1_re	**TCGTGCTCCTGCTCATCATC**
vrilleEx_MN2_fw	CATCGGGAGCTGTTTCCGGCG
vrilleEx_MN2_re	GCTTGAGGGGCAGACAGTTGT
vrilleEx_MN3_fw	AGTCCGCAGCAGGGCAGCGAT
vrilleEx_MN3_re	TGAGAGTAGCGCCGTGGC
vrille3'_MN1_fw	CCAGCAAAGGTCTTTTACTGCC
vrille3'_MN1_re	TGTGTAATAGATTAACTTGC

vrille3'_MN2_fw	ATACACAATTATTGTATATCAGC
vrille3'_MN2_re	TAACTCATTCTGCAATATGCGAT
vrille3'_MN3_fw	**CACCATCATCGCACGAGCTTA**
vrille3'_MN3_re	**TAATCTCTTTACCACTCGACG**

3.1.7 Antibodies and antisera

3.1.7.1 Primary antibodies

Table 3.11: Primary antibodies and antisera used in this study. Antibodies are listed with their name, clone number (if available) and order number (for commercial antibodies). Depending on the type of experiment, amounts (in µl) or dilutions are depicted. ChIP: Chromatin immunoprecipitation, WB: Western blot, DSHB: Developmental Studies Hybridoma Bank.

Antibody	Host origin	Experiment	Amount or dilution	Source/ Reference
αEcR (DDA2.7)	Mouse, monoclonal	WB	1:1000	DSHB
αFLAG M2 (F3165)	Mouse, monoclonal	WB	1:4000	Sigma-Aldrich
αFLAG (F7425)	Rabbit, polyclonal	WB	1:2000	Sigma-Aldrich
αMi-2	Rabbit, polyclonal	WB ChIP	1:10000 2 µl	(Kehle et al., 1998)
αMi-2 (4D8)	Rat monoclonal	IP	200 µl	E. Kremmer
Normal rabbit IgG #2729	Rabbit, polyclonal	ChIP	2 µl	Cell Signaling
Normal Rat IgG	Rat	IP	16 µl	Sigma Aldrich
αp53 (7A7)	Rat monoclonal	IP	200 µl	E. Kremmer
αβ-Tubulin (KMX-1)	Mouse, monoclonal	WB	1:5000	Millipore
αUsp (ab106341)	Rabbit, polyclonal	ChIP	5 µl	Abcam

3.1.7.2 Secondary antibodies

Table 3.12: Secondary antibodies used for Western blot analysis.

Antibody	Host origin	Dilution	Source
ECL αrabbit	Donkey, polyclonal	1:30000	GE Healthcare
ECL αmouse	Sheep, polyclonal	1:30000	GE Healthcare

3.2 Methods

If not stated otherwise reactions were performed at RT.

3.2.1 Cell biological methods

3.2.1.1 Standard cell culture procedures

S2 and Sf9 cells were propagated in 75 cm² flasks (Greiner) at 26°C in their respective media with supplements (see 3.1.3.2). Every three to four days cells were removed from the flask using a cell scraper and re-seeded to a new flask with a density of 1.5-2·10^6 cells/ ml. Cell number was determined using a hemocytometer. Collection of cells for experiments and freezing was achieved by spinning the cells down at 1200 rpm for 5 min (Heraeus Megafuge 1.0).

3.2.1.2 Freezing and thawing of cells

For freezing, cells from a dense flask were collected and resuspended in 0.5 ml freezing medium A. Afterwards 0.5 ml of freezing medium B was added dropwise. 1 ml of this cell suspension was transferred into a cryovial and frozen in a 50 ml Falcon with isopropanol at -80°C. For long term storage, vials were transferred to liquid nitrogen.

Freezing medium A	Schneider's insect or Sf-900 SFM medium 40% (v/v) FBS 1% (v/v) Penicillin-Streptomycin or 0.1% (v/v) Gentamicin

Freezing medium B	Schneider's insect or Sf-900 SFM medium 40% (v/v) dimethyl-sulfoxide (DMSO) 1% (v/v) Penicillin-Streptomycin or 0.1% (v/v) Gentamicin

For thawing, cryovials with cells were transferred to RT and resuspended in 15 ml of Schneider's insect medium or Sf-900 SFM medium. In order to remove the DMSO, cells were spun down and the supernatant was removed. Afterwards, the cell pellet was resuspended in fresh Schneider's insect or Sf-900 SFM medium and cells were transferred into a 75 cm² flask.

3.2.2 Molecular biological methods

Standard molecular biology protocols such as plasmid DNA transformation into chemically-competent *E.coli,* amplification and purification of plasmid DNA from *E.coli*, digestion of plasmid DNA using specific restriction endonucleases, dephosphorylation of digested plasmid DNA using alkaline phosphatase, ligation of DNA fragments, determination of DNA concentration and analysis of DNA on TAE agarose gels were carried out according to standard protocols and manufacturer's recommendation (Thermo Scientific)(Sambrook and Russell, 2001). Large scale plasmid DNA purification was done using the QIAGEN Plasmid Midi Kit (Qiagen). Purification of PCR products and digested plasmid DNA was conducted using the QIAquick Gel Extraction Kit.

3.2.2.1 Isolation of total RNA

Due to the sensitivity of RNA towards degradation by RNases, certain precautions were considered before working with RNA. Nuclease-free pipet tips and reaction tubes were used for all preparations. Additionally, working space and pipets were treated with RNaseZap (Ambion). For elution of RNA from columns and all further reaction steps nuclease-free water (Ambion) was used. Total RNA was purified from Drosophila S2 cells to determine expression levels of genes of interest using the peqGOLD Total RNA Kit (Peqlab). One well (6-well plate) of adherently growing cells was lysed in 400 µl of RNA lysis buffer. Further RNA isolation steps were conducted according to the manufacturer's instructions, including on-column DNase

I digest using the peqGOLD DNase I Digest Kit (Peqlab). RNA concentration was determined at an absorption of 260 nm using the Nanodrop 2000c (Thermo Scientific).

3.2.2.2 Complementary DNA (cDNA) synthesis

In order to quantify the amount of specific RNA in the total RNA sample, cDNA was synthesized using an oligo $(dT)_{17}$ for polyA-mRNA or random hexamer primer for non-coding RNAs. cDNA synthesis was conducted using the M-MLV Reverse Transcriptase kit (Life Technologies) according to the manual's instructions. dNTPs were purchased from Thermo Scientfic and oligo $(dT)_{17}$ were synthesized by MWG Biotech. Generally, 1µg of total RNA was transcribed, cDNA was further diluted 1:10 in ddH_2O and used as template for qPCR.

3.2.2.3 Synthesis of double-strand RNA (dsRNA) by *in vitro* transcription (*iv*T)

In order to generate a gene-specific template for dsRNA synthesis, PCR was used to amplify a DNA product with a length of 300-600 bp from plasmid DNA containing the gene of interest. The specific oligos contained both a minimal T7 polymerase recognition site (TAATACGACTCACTATAGGG) at their 5'-end. Upon gel purification of the PCR product, an *iv*T reaction was performed using the MEGAscript T7 Kit (Ambion). To 500 ng of DNA template, 2 µl of each rNTP, reaction buffer and T7 enzyme were added in a total volume of 20 µl. The reaction was incubated for 16 hrs at 37°C. Upon addition of stop solution (5 M ammonium acetate, 100 mM EDTA) in a 1:1 ratio, RNA was precipitated with 2.5 volume of 100% ethanol at -20°C for one hour. The sample was centrifuged for 30 min at 13000 rpm (Heraeus BIOFUGE pico). The resulting RNA pellet was washed by 5 min of centrifugation in 70% ethanol. The supernatant was carefully removed and the pellet was dried at room temperature. Upon dissolving the RNA in 40 µl of nuclease-free H_2O, the sample was incubated in a thermoshaker at 65°C for 30 min and allowed to cool down to RT by turning off the thermoshaker. This slow temperature decrease allows for proper alignment of complementary RNA strands. RNA concentration was subsequently determined at an absorption of 260 nm and integrity was judged by electrophoretic separation on an 1.5% TAE agarose gel.

3.2.2.4 RNAi mediated knockdown

For RNAi mediated knockdown, 0.8-1.2x10^6 S2 cells were incubated with 15 µg of the relevant dsRNA per well of a 6-well plate. The amount of cells required for each experiment was spun down at 1200 rpm and resuspended in medium without any supplements. dsRNA was added to 1 ml of cell suspension and incubated at 26°C for one hour. Subsequently 1 ml of medium containing 20% FBS (v/v), 2% Pen/Strep (v/v) was added. For ChIP experiments the amount of cells and dsRNA was scaled up accordingly for use in 75 cm^2 flasks. Transfections were incubated for five to six days at 26°C and further processed for nuclear extracts, RNA isolation or ChIP experiments. For each knockdown experiment, successful depletion of the protein of interest was determined by Western blot or changes in mRNA levels quantified by RTqPCR.

3.2.2.5 Polymerase chain reaction (PCR)

PCR allows the amplification of a specific DNA sequence based on a template and sequence specific oligos.(Saiki et al., 1985) All DNA fragments synthesized for cloning or *in vitro* transcription were amplified using the Expand High Fidelity^{PLUS} PCR System (Roche). In accordance with the manufacturer's instruction, PCR reactions were set up as follows:

10 µl	5x	Expand HiFi^{PLUS} Reaction Buffer
1 µl	10 mM	dNTPs
2 µl	10 pmol/ µl	forward primer
2 µl	10 pmol/ µl	reverse primer
2 µl	50 ng	plasmid DNA
0.5 µl	5U/ µl	Expand HiFi^{PLUS} polymerase
32.5 µl		ddH_2O

The PCR reaction was incubated in a T3000 Thermocycler (Biometra) with the following program:

Initial denaturation	94°C	2 min	
Denaturation	94°C	20 sec	35 cycles
Annealing	55-60°C	30 sec	
Elongation	72°C	1 min/ kb	
Final elongation	72°C	7 min	

3.2.2.6 PCR for site-directed mutagenesis

Introduction of specific changes in DNA sequence (mutagenesis) of a plasmid was conducted using the Quick Change II XL Site Directed Mutagenesis Kit (Stratagene) according to the manufacturer's instructions. The PCR reaction was set up as follows:

5 µl	10x	reaction buffer
1 µl		dNTP mix
2 µl		forward primer (125ng)
2 µl		reverse primer (125ng)
2 µl		plasmid DNA (10ng)
3 µl		Quick Solution
1 µl		PfuUltra HF DNA polymerase
34 µl		ddH_2O

The PCR reaction was incubated in a T3000 Thermocycler (Biometra) with the following program:

Initial denaturation	95°C	1 min	
Denaturation	95°C	50 sec	18 cycles
Annealing	60°C	50 sec	
Elongation	68°C	1 min/ kb	
Final elongation	68°C	7 min	

3.2.2.7 Quantitative PCR (qPCR)

In order to ascertain the amount of a specific cDNA, obtained from total mRNA or DNA fragment within a sample, isolated samples were subjected to qPCR. cDNA was usually diluted 1:10, whereas DNA precipitated from ChIP experiments was used in a 1:6 dilution. A total volume of 6 µl was provided in one well of a Thermo-Fast 96 non-skirted PCR plate (Thermo Scientific). Thereafter, 19 µl of a PCR mix containing all necessary reagents as well as gene or locus specific oligos was added. The PCR mix consisted of 1 µl oligo (1:1 mixture of forward and reverse primers in a 1:10 dilution), 12 µl Absolute SYBR Green Mix (Thermo Scientific) and 8 µl ddH_2O. The PCR reaction and fluorescent measurement of SYBR Green were carried out according to the following program:

Initial denaturation	95°C	15 min	
Denaturation	95°C	15 sec	45 cycles
Annealing	58°C	30 sec	
Elongation	72°C	20 sec	
Denaturation	95°C	1 min	
Dissociation curve	55°C	30 sec	
	55°C → 95°C	gradually	
	95°C	30 sec	

The Cycle threshold (Ct) for each reaction is calculated automatically by the MxPro Software. Ct is defined as the number of cycles required for the fluorescent signal to cross a detection threshold exceeding the background fluorescence. As all samples were measured in triplicates, the Ct is the mean of three values.

For a comparative analysis of gene expression between two samples (e.g. untreated vs. 20HE treated), both samples were first normalized to *Rp49* as a reference gene. The normalized value is referred to as ΔCt:

$$\Delta Ct = Ct_{sample} - Ct_{reference}.$$

The subtraction of the ΔCt of two samples results in the ΔΔCt:

$$\Delta\Delta Ct = \Delta Ct_{sample1} - \Delta Ct_{sample2}.$$

The fluorescent signal increases per amplification in an exponential manner, therefore the difference in expression (x) is calculated as

$$x = 2^{-\Delta\Delta Ct}.$$

To show relative changes in gene expression, the control sample (i.e. “untreated”) was set to 1 and all other samples (i.e. “20HE treated”) were displayed normalized to the control.

The standard deviation of each set of triplicate Ct values were used to calculate a standard deviation $s_{\Delta Ct}$ of Ct:

$$s_{\Delta Ct} = \sqrt{{s_{reference}}^2 + {s_{sample}}^2}$$

and further a standard deviation s_{norm} for the normalized fold expression:

$$s_{norm} = \sqrt{(x_{norm} \cdot \ln(2))^2 \cdot {s_{ct}}^2}.$$

For the analysis of chromatin immunoprecipitation samples, all values were normalized to the corresponding input sample before precipitation:

$$\Delta Ct = Ct_{input} - Ct_{sample}$$

and further displayed as percentage of the input:

$$\%input = 2^{\Delta Ct_{sample}}.$$

The standard deviation was calculated from the error of triplicate measurements as follows:

$$s_{input} = \ln(2) \cdot \%\text{input} \cdot \sqrt{{s_{input}}^2 + {s_{sample}}^2}.$$

For the analysis of MNase digested chromatin samples, all values were normalized to the corresponding undigested sample:

$$\Delta Ct = 2^{-(Ct_{digested} - Ct_{undigested})}.$$

and further normalized to 1 by dividing all ΔCt of one locus by the highest ΔCt in the primer set.

The standard deviation was calculated from the error of triplicate measurements as described above, replacing “input” by “undigested” and “sample” by “digested”.

3.2.3 Biochemical methods

When working with proteins, all buffers and samples were kept on ice and supplemented with fresh protease inhibitors (Leupeptin, Pepstatin, Aprotinin at a

concentration of 1µg/ml; 0.2 mM PMSF and 0.5 mM DTT). Critical steps were performed in the cold room and vortexing of protein samples was avoided whenever possible.

3.2.3.1 Determination of protein concentration

Protein concentration was determined using the Bio-Rad Protein Assay (Bio-Rad), which is based on the colorimetric method described by Bradford in 1976, according to the manufacturer's instructions (Bradford, 1976). In order to estimate the protein concentration of purified GST proteins, a protein standard (bovine serum albumin) was loaded on the same SDS-PAGE as the protein of unknown concentration and subsequently stained with PageBlue Protein Staining Solution (Thermo Scientific). The protein concentration was calculated using Image J Gel Analyzer tool (Ferreira, 2010 - 2012).

3.2.3.2 SDS-polyacrylamide gel electrophoresis (SDS-PAGE)

SDS-PAGE is used to separate proteins according to their electrophoretic mobility that is a function of length, conformation and charge of the molecule. Preparation of SDS-polyacrylamide gels (SDS-PAGE) and subsequent electrophoresis was conducted using disposable gel cassettes and the XCell SureLock mini-Cell system (Life Technologies). Gel solutions were prepared according to standard protocols using a ready-to-use acrylamide/bisacrylamide mixture (Rotiphoresegel 30, 37.5:1; Roth). The stacking gel contained 4% and the resolving gel 7.5, 10 or 15% of polyacrylamide depending on the protein of interest. Protein samples were supplemented with 1x SDS-PAGE loading buffer(Laemmli, 1970). In order to visualize the running behavior of known proteins, PageRuler Prestained Protein Ladder (Fermentas) was loaded onto the same SDS polyacrylamide gel. Electrophoresis was performed with 1x SDS-PAGE running buffer at a voltage of 100V for proteins in the stacking gel and at 150V in the resolving gel. Subsequently gels were further processed by Western blot or Coomassie blue staining.

1x SDS running buffer	25 mM Tris
	192 mM Glycine
	0.1% SDS (w/v)

SDS-PAGE loading buffer	375 mM Tris HCl, pH 6.8 9% (w/v) SDS 50% (v/v) Glycerol 9% (v/v) β-mercaptoethanol 0.5% (w/v) Bromophenol blue

3.2.3.3 Coomassie staining of SDS polyacrylamide gel

In order to visualize purified recombinant proteins after separation by SDS-PAGE, gels were washed in ddH_2O for 15 min and incubated with PageBlue Protein Staining Solution (Fermentas) over night. The next day, gels were destained with ddH_2O until the protein bands were clearly distinguishable from the background staining.

3.2.3.4 Western blot

Western blotting is the transfer of proteins onto a membrane, enabling the detection by specific antibodies against the protein of interest. All Western blots were conducted using the Biorad Wet Blot Module (Biorad). Proteins were generally transferred to a polyvinylidene fluoride (PVDF) membrane, upon equilibration in methanol. Subsequently, the gel and the membrane were placed between two layers of buffer-soaked Whatman paper and sponges provided with the Wet Blot Module. Transfer was carried out for 1 hr 15 min at 400 mA in the presence of an ice block inside the blotting chamber and further cooling from the outside. After successful transfer, the membrane was incubated for at least 30 min in blocking milk (5% milk powder in PBST) at RT to reduce background signals.

PBST	1x PBS supplemented with 0.1% (v/v) Tween
Transfer buffer	25 mM Tris 192 mM Glycine 20%(v/v) Methanol 0.02% (v/v) SDS

All further antibody incubation and washing steps were carried out on a rocking platform. Antibodies were diluted in blocking milk at an appropriate concentration.

Incubation with primary antibody was performed overnight in the cold room, followed by three washes for 5 min at RT. Subsequently, the membrane was incubated with the relevant HRP-labelled secondary antibody for two hours at RT. After another 3 washes of 5 min at RT, antigen-antibody complexes were detected by chemiluminescence using the Immobilon Western Chemiluminescent HRP Substrate Kit (Millipore) and SuperRX Fuji Medical X-ray films. Exposure times were estimated by empirical determination.

For re-probing of Western blot membranes with a different primary antibody, membranes were incubated in 50 ml of stripping buffer for 30 min at 50°C in a water bath and subsequently washed in PBST three times for 10 min. Afterwards, membranes were blocked and incubated with antibody as described above.

Stripping buffer	62.5 mM Tris HCl, pH 6.8
	10% (v/v) β-mercaptoethanol
	2% (w/v) SDS

3.2.3.5 Nuclear extract preparation

In order to prepare nuclear extracts, S2 cell were harvested, washed twice in 1x PBS and resuspended in an appropriate volume of low salt buffer (one well of a 6 well plate: 200 µl; 75 cm^2 flask: 1000 µl, 175 cm^2 flask: 2500 µl). After incubation on ice for 10 min, cells were collected by centrifugation at 13000 rpm for 1 minute at 4°C. The supernatant was removed and the remaining nuclear fraction was resuspended in an appropriate volume of high salt buffer (one well of a 6 well plate: 50 µl; 75 cm^2 flask: 200 µl, 175 cm^2 flask: 750 µl). The suspension was further incubated for 20 min on ice and subsequently centrifuged at 13000 rpm for 30 min at 4°C. The supernatant contained the nuclear extract and was further processed for Western blot or frozen in liquid nitrogen and stored at -80°C.

Low salt buffer:	10 mM Hepes KOH, pH 7.6
	1.5 mM $MgCl_2$
	10 mM KCl
	DTT, protease inhibitors
High salt buffer:	20 mM Hepes KOH, pH 7.6
	1.5 mM $MgCl_2$

420 mM NaCl
0.2 mM EDTA
20% (v/v) Glycerol
DTT, protease inhibitors

3.2.3.6 Immunoprecipitation of endogenous Mi-2

For endogenous IP of Mi2, nuclear extract was prepared from S2 cells as follows. All steps were performed in the cold room with cold buffers. S2 cells were washed with 1x PBS on the plate and harvested by scraping in 1x PBS with protease inhibitors and centrifugation. The cell pellet volume (PV) was determined and gently dissolved in 5 PVs of buffer A. The cell suspension was left to incubate on ice for 10 min. Cells were collected by centrifugation for 10 min at 3000 rpm and dissolved in 2 PVs of low salt buffer. The cell suspension was transferred to a glass dounce homogenizer and dounced ten times with the loose pestle A. The released nuclei were collected by centrifugation for 10 min at 3000rpm and dissolved in 1.5 PV of high salt buffer. The suspension was transferred to the glass dounce homogenizer and dounced ten times with the tight pestle B. The nuclear suspension was transferred to a falcon and incubated for 30 min on a rotating wheel at 4°C. The suspension was transferred to Eppendorf tubes and centrifuged for 15 min at 13000 rpm to pellet nuclear debris. The nuclear extract was transferred to a dialysis bag (MWCO 6-8kDa) and dialyzed in buffer D for two times 2 hrs. After dialysis, the nuclear extract was transferred to Eppendorf tubes and centrifuged for 15 min at 13000 rpm to remove precipitates. The nuclear extract was flash frozen and stored at -80°C.

For immunoprecipitation (IP) of endogenous Mi-2, Protein G Sepharose was incubated for 1hr by rotation with 1% fish skin gelatine and 0.2 mg/mL BSA in buffer D +0.02% NP40 at room temperature. Subsequently, antibodies against Mi-2, p53 and normal IgG were incubated for 1 hr at 4°C with pre-blocked Protein G sepharose. After antibody/Protein G Sepharose incubation, beads were washed twice with buffer D +0.02% NP40 and transferred to protein low-binding tubes. For each IP, 30ul of Protein G Sepharose were incubated with 200ul of dialyzed nuclear extract by rotation for 3hrs at 4°C. The precipitated protein/antibody complexes were washed five times with buffer D +0.02% NP40 and subsequently eluted by addition of 40ul 2x SDS Loading Buffer and boiling at 95°C for 5 min.

Buffer D	20 mM Hepes KOH, pH 7.6 100 mM KCl 1.5 mM $MgCl_2$ 0.2 mM EDTA 20% (v/v) Glycerol DTT, PMSF, protease inhibitors

3.2.3.7 Whole cell extract preparation from Sf9 cells

Whole cell extracts from Sf9 cells where prepared 48 to 72 hours post infection. For this purpose, cells were harvested, washed twice in ice cold 1x PBS and resuspended in LyBu200 buffer. Upon two subsequent cycles of freeze-thaw in liquid nitrogen, cell extracts were collected by centrifugation at 13000rpm for 20 min at 4°C and further used for Western blot or interaction assays.

LyBux buffer	20 mM Hepes KOH, pH 7.6 x mM KCl 10% (v/v) Glycerol 0.1% (v/v) NP40 DTT, protease inhibitors

3.2.3.8 FLAG affinity purification

For interaction assays using the FLAG affinity protocol, whole cell extracts from Sf9 cells were prepared as described in 3.2.3.6. FLAG beads were equilibrated by washing three times 10 min in LyBu200 on a rotating wheel. 100 mg of total protein was incubated with 50 µl 1:1 slurry α-FLAG M2 agarose (FLAG beads, Sigma Aldrich) at 4°C for three hours on a rotating wheel. Beads were collected by centrifugation at 3500 rpm for 4 min at 4°C and washed three times for 10 min with 1 ml of LyBu200 to remove unbound proteins. Precipitated proteins were eluted by boiling the beads in 1x SDS-PAGE loading buffer and further subjected to Western blot analyses.

3.2.3.9 Chromatin immunoprecipitation (ChIP)

Chromatin immunoprecipitation allows the identification of genomic regions that are bound by a protein of interest. In short, $1 \cdot 10^8$ S2 cells in culture medium were fixed with 1% (v/v) formaldehyde (10% methanol free stock, Polysciences) for 10 min at RT. Fixation was quenched with a final concentration of 240 mM glycine. Cells were harvested, washed twice in ice cold 1x PBS and resuspended in 1 ml ChIP lysis buffer. After an incubation of 10 min on ice, samples were sonicated with a Bioruptor (Diagenode) twice for 10 min with 30 seconds on-off cycles at high power. In order to properly cool the samples during sonication, the Bioruptor was filled with an appropriate amount of ice. Afterwards samples were centrifuged at 13000 rpm for 15 min at 4°C. The supernatant containing the chromatin was further used for ChIP experiments. To quality check for proper sonication of all samples with a favored DNA length of about 500bp, 10 µl of chromatin was incubated with 5 µl of 5M NaCl for 4 hrs at 65°C. Upon RNase digest for 1 hr at 37°C, samples were subjected to agarose gel electrophoresis on a 1.5% TAE agarose gel. For further preparation Protein A beads (GE Healthcare) were washed twice in ddH_2O and twice in TE Buffer and blocked over night with 1mg/ml BSA in TE buffer. Furthermore, 130 µl of chromatin were diluted 1:10 in ChIP IP buffer and precleared by the addition of 80 µl Protein A beads (GE Healthcare) for 30 min at 4°C on a rotating wheel. The supernatant was collected and 13 µl were taken out and stored at 4°C as “input” sample. The antibody against the protein of interest was added in an appropriate amount and samples were incubated overnight at 4°C on a rotating wheel. As controls, ChIPs using normal rabbit IgG antibody were performed. The next day, 35 µl of 1:1 slurry Protein A beads was added to each sample and further incubated for 2 hrs at 4°C on a rotating wheel. Next, samples were washed for each 10 min on a rotating wheel and subsequently collected by centrifugation at 3500rpm for 4 min: three times with low salt buffer, three times with high salt buffer, once with LiCl and twice with TE buffer. With the last TE buffer wash, beads were transferred into fresh reaction tubes for elution. Elution took place twice with 250 µl ChIP elution buffer for each 20 min at RT. Accordingly, 500 µl of ChIP elution buffer was added to input samples and all further steps were performed identically. Reversal of cross-links was done by the addition of 20 µl 5M NaCl and incubation at 65°C overnight. The next day, proteins were digested by the presence of 2 µl 10 mg/ml Proteinase K in 20 µl 1 M Tris/ HCl, pH 6.5 for 1 hr a 45°C. The precipitated DNA was purified using the QIAquick PCR purification Kit (Qiagen) according to the manufacturer’s instructions.

ChIP lysis buffer	50 mM Tris/ HCl, pH 8.0 10 mM EDTA 1% (w/v) SDS protease inhibitors
ChIP IP buffer	16.7 mM Tris/ HCl, pH 8.0 16.7 mM NaCl 1.2 mM EDTA 0.01% (w/v) SDS 1.1% (v/v) Triton X-100 protease inhibitors
Low salt buffer	20 mM Tris/ HCl, pH 8.0 150 mM NaCl 2 mM EDTA 0.1% (w/v) SDS 1% (v/v) Triton X-100
High salt buffer	20 mM Tris/ HCl, pH 8.0 500 mM NaCl 2 mM EDTA 0.1% (w/v) SDS 1% (v/v) Triton X-100
LiCl buffer	10 mM Tris/ HCl, pH 8.0 250 mM LiCl 1 mM EDTA 1% (v/v) NP-40 1% (w/v) sodium deoxycholate
ChIP elution buffer	1% (w/v) SDS 0.1 M $NaHCO_3$
TE buffer	10 mM Tris/ HCl pH8.0 1 mM EDTA

3.2.3.10 ChIPSeq

ChIP samples were prepared as described above. Three ChIP experiments were combined in the last step and eluted in 30 µl TE buffer. DNA concentration was determined using the Nanodrop 2000c (Thermo Scientific) and 15 ng total DNA were sent and further processed by Maren Scharfe, Genome analytics unit, Helmholtz Centre for Infection Research, Braunschweig. ChIPSeq reads for each sample were generated in duplicate on an Illumina GaIIx instrument according to the manufacturer's instructions. Raw reads were aligned to the Ensembl import of FlyBase, revision 64 using Bowtie 0.12.7. Two of the lanes were aligned with a maximum of three mismatches in the seed, and a mismatch quality score sum of 110 to compensate for a large number of 'N' base calls in this sequencing run. The other two lanes were aligned with Bowtie defaults (2 mismatches in the seed, maximum mismatch quality score sum of 70). The aligned data was deduplicated to a maximum of 8 reads at a given starting position and direction to avoid PCR artefacts, leading to 9.686.701 usable reads for the "+20HE" sample and 15.464.273 "untreated" sample. Peak calling was performed with MACS 1.4.0rc2, modified to directly read BAM files. Parameters were m-fold=(6,36) and keep-dup=all. Peaks were annotated with distance to the next transcript and their genomic location (intra-/intergenic, close to a transcription start site, intron / exon, close to the end of a gene), again using Ensembl revision 64. Peaks from all 4 assays were pooled, and tag counts within each peak were normalized to a total of 1 million tags per assay. Peaks were classified as differentialy, if they had a +20HE / untreated tag ratio of at least 2.3x or untreated/ +20HE tag ratio of at least 2.3x.

3.2.3.11 Micrococcal nuclease (MNase) protection assay

Micrococcal nuclease is a nuclease derived from *Staphylococcus aureus* that induces double strand breaks in nucleosome linker regions but only single-stranded nicks within the nucleosome itself (Heins et al., 1967). Therefore, it is very useful to determine whether a DNA fragment is within a nucleosome, and protected from MNase digestion, or not. The protocol was based on a study published by Petesch *et al.* with minor changes as described below (Petesch and Lis, 2008).

Cells were harvested, counted and cross-linked by the addition of 10x MNase cross-linking buffer to a final concentration of 1x for 1 min at RT. Cross-linking was quenched by the addition of glycine to a final concentration of 125 mM. Cells were

collected by centrifugation at 1200 rpm for 5 min at 4°C. Afterwards, $1 \cdot 10^8$ cells were resuspended in 1 ml MNase buffer A. Samples were incubated on ice for 5 min and subsequently lysed by douncing 25 times rigorously using a small plastic pestle. The released nuclei were collected by centrifugation at 3500 rpm for 5 min at 4°C. Further they were washed twice with 1 ml MNase buffer A and twice with 1 ml MNase Buffer D. Finally nuclei were resuspended in 1 ml MNase buffer MN and allowed to warm up at room temperature for 5 min. For each MNase digest, 240 µl of isolated nuclei were incubated with a certain amount of MNase. The amount of MNase necessary to digest most of the chromatin to mononucleosomes was determined empirically for each new batch of MNase by titration. At the same time, one sample was kept aside as “undigested” reaction without the addition of MNase. All reactions were incubated for 1 hr at 28°C with moderate shaking at 300 rpm. The digest was stopped by the addition of 10x MNase Stop to a final concentration of 1x. De-cross-linking was performed by adding NaCl to a final concentration of 200 mM to each sample and incubation at 65°C in a horizontal shaker at 300 rpm overnight. The undigested and digested samples were treated with RNase A at a final concentration of 0.1 mg/ml for 30 min at 37°C. Further on proteins were digested by the addition of Proteinase K to a final concentration of 0.1 mg/ml and incubation at 45°C in a horizontal shaker at 300 rpm.DNA purification was carried out by phenol-chloroform extraction according to standard procedures. Samples were filled up with MNase buffer MN to a total volume of 500 µl, mixed with 500 µl Roti-Phenol/Chloroform-Isoamylalcohol (25:24:1; Roth) by vortexing for 1 min at maximum speed. All liquid was transferred to Phase Lock Gel Heavy tubes (5 Prime) under a fume hood and vials were centrifuged at 10000 rpm for 5 min at RT to achieve separation of aqueous and organic phase. The upper, aqueous phase was transferred to a fresh vial and supplemented with 500 µl ice cold isopropanol. Samples were incubated at -20°C for 2 hrs and subsequently centrifuged for 30 min at 13000 rpm at 4°C. The supernatant was aspirated, DNA precipitate was washed with 70% Ethanol and dried at RT. The pellet was resuspended in 200 µl of nuclease free ddH_2O and stored at -20°C until use for qPCR.

10x MNase cross-linking buffer	50 mM Tris/ HCl, pH 8.0 100 mM NaCl 1 mM EDTA 0.5 mM EGTA 3.3% (v/v) Methanol-free formaldehyde

MNase buffer A	10 mM Tris/ HCl, pH 8.0 300 mM Sucrose 3 mM $CaCl_2$ 2 mM Mg-acetate 0.1 % (v/v) Triton X-100 protease inhibitors, DTT
MNase buffer D	50 mM Tris/ HCl, pH 8.0 5 mM Mg-acetate 0.1 mM EDTA 25% (v/v) Glycerol DTT
MNase buffer MN	15 mM Tris/ HCl, pH 7.4 60 mM KCl 15 mM NaCl 250 mM Sucrose 1 mM $CaCl_2$
10x MNase STOP	125 mM EDTA 5% (v/v) SDS

3.2.3.12 Recombinant protein expression using the baculovirus system

Expression of proteins using the baculovirus system is highly useful for the purification of recombinantly expressed, eukaryotic proteins. Coding sequences of the protein of interest were cloned into the pVL1392 (Bac-N-Blue Baculovirus Expression System, Life Technologies) or pFastBac1/pFastBacDual (Bac-to-Bac Baculovirus Expression System, Life Technologies) vector.

3.2.3.12.1 Bac-N-Blue Baculovirus Expression System

pVL1392 constructs were transfected into Sf9 cells using the Bac-N-Blue Linear Transfection Kit (Life Technologies). 10^6 Sf9 cells were plated in one well of a 6-well plate and left to settle for 20 min at 26°C. In the meantime, the transfection mix was prepared: 4 µg of DNA, 1 ml of Sf-900 II SFM medium (without supplements) and 20 µl of Cellfectin Reagent were added to 0.5µg of Bac-N-Blue DNA, vortexed and

incubated for 20 min. The supernatant was removed from the attached Sf9 cells and replaced for 2 ml of unsupplemented medium. The transfection mix was added drop wise to the cells and incubated for 4 hr at RT on a rocking platform. 1 ml of supplemented Sf-900 II SFM medium was added and cells were incubated for 5 days at 26°C. The supernatant containing the first viral stock (V_A0) was transferred to 15 ml vials and stored at 4°C.

3.2.3.12.2 Bac-to-Bac Baculovirus Expression System

As Life Technologies replaced the Bac-N-Blue Baculovirus Expression System for the Bac-to-Bac Baculovirus Expression System, several of the viruses used in this thesis were produced using the Bac-to-Bac Baculovirus Expression System.

pFastBac1/ pFastBacDual constructs were transformed into DH10Bac *E.coli* and successful recombination into the bacmid was verified by PCR according to the manufacturer's instructions. $8 \cdot 10^5$ Sf9 cells were seeded in one well of a 6-well plate and left to settle for 20 min at 26°C. In the meantime, the transfection mix was prepared: 5 µl of bacmid DNA was diluted in 100 µl of unsupplemented Sf-900 II SFM medium. Next to it, 8 µl of Cellfectin were added to 100 µl of unsupplemented Sf-900 II SFM medium. Both mixtures were combined and incubated for 20 min at RT. The supernatant was removed from the attached Sf9 cells and replaced with 2 ml of plating medium (mixture of 1.5 ml supplemented Sf-900 II SFM medium and 8.5 ml unsupplemented Sf-900 II SFM medium). The transfection mix was added drop wise to the cells and incubated for 24 hrs at 26°C. The next day, the medium was aspirated and replaced by supplemented Sf-900 II SFM. 6-well plates were wrapped in parafilm and incubated for 5 days at 26°C. The supernatant containing the first viral stock (V_A0) was transferred to 15 ml vials and stored at 4°C.

3.2.3.12.3 Viral stock amplification

Virus amplification was carried out by infecting another two rounds of Sf9 cells. For the first viral amplification, $7.5 \cdot 10^6$ Sf9 cells in a volume of 3 ml supplemented Sf-900 II SFM medium were plated into a 10 cm dish and incubated with 500 µl of the first vial stock for 45 min on a rocking platform. After addition of 7 ml medium, cells were incubated for 6 days at 26°C. The supernatant containing the first viral amplification (V_A1) was transferred to 15 ml vials and stored at 4°C. For the first viral amplification $12 \cdot 10^6$ Sf9 cells in a volume of 5 ml supplemented Sf-900 II SFM

medium were plated into a 15 cm dish and incubated with 500 µl of the first vial stock for 45 min on a rocking platform. After addition of 10 ml medium, cells were incubated for 6 days at 26°C. The supernatant containing the second viral amplification (V_A2) was transferred to 15 ml vials and stored at 4°C.

3.2.3.12.4 Protein expression

For protein expression the supernatant of the second viral amplification was used to infect Sf9 cells as described for the preparation of the second viral amplification. Cells were harvested after 48 to 72 hours to prepare whole cell extracts as described in 3.2.3.6. In order to investigate interactions between two proteins, Sf9 cells were transfected with two different viral stocks. The amount of virus needed was titrated separately for each viral stock to achieve optimal levels of protein expression.

Table 3.13: Amounts of virus used for Sf9 infection.

Virus	Amount
EcR	400 µl
FLAG-EcR	400 µl
FLAG-EcR AF1	200 µl
FLAG-EcR DBD	200 µl
FLAG-EcR AF2	800 µl
FLAG-EcR C-terminus	200 µl
HA-EcR AF1	200 µl
HA-EcR AF2	800 µl
Mi-2 untagged	400 µl
Mi-2-FLAG	400 µl
Mi-2 LFHAA-FLAG	300 µl
Mi-2 ATPase-FLAG	200 µl
Lint-1-FLAG	300 µl

3.2.3.12.5 Large scale purification of FLAG-tagged proteins

For large scale expression of FLAG-tagged proteins, 30 dishes of 15 cm with Sf9 cells were infected and harvested as described above. The whole cell extract was incubated for 4 hours with 1ml 1:1 slurry of anti-FLAG M2 affinity gel at 4°C on a

rotating wheel. Subsequently the mixture was transferred onto a conical poly-prep plastic column (Biorad). Flow-through was collected and reapplied onto the column. FLAG beads were washed with two column volumes of LyBu200, 500 and 1000 followed by two more washing steps with LyBu500 and 200. Finally, FLAG beads were washed with FLAG elution buffer. Bound proteins were eluted from the FLAG beads by incubation with 0.25 mg/ml FLAG peptide in FLAG elution buffer twice for 15 min. Eluates were combined and concentrated using a Amicon Ultra-4 centrifugal filter unit (MWCO30kDa). Concentrated proteins were aliquoted, flash frozen in liquid nitrogen and stored at -80°C.

FLAG elution buffer	20mM Tris/ HCl, pH 8.0 150mM KCl 10% (v/v) Glycerol 1mM ß-mercaptoethanol protease inhibitors

3.2.3.13 GST protein expression

cDNA of the protein of interest was cloned into the pGEX4T1 expression vector in frame with a N-terminal GST-tag. This DNA construct was transformed into *E.coli* BL21 and further expressed according to standard procedures. In short, 500 ml of LB medium was inoculated with 5 ml of *E.coli* BL21 overnight culture and further incubated at 37°C to an OD_{600} of 0.6-0.7. Subsequently, the temperature of the incubator was set to 18°C and cells were induced with 0.1 mM IPTG overnight. The next day, cells were harvested by centrifugation at 4000 rpm (Heraeus Cryofuge 5000) and resuspended in 30 ml 1x PBS/ 1% (v/v) Triton X-100 supplemented with protease inhibitors. After sonication (10x12 sec, 25% output), the suspension was centrifuged for 30 min at 15000 rpm at 4°C (Sorvall RC-5B, SS34 rotor) to remove cell debris. The supernatant containing the GST fusion protein was bound to 500 µl of pre-washed Glutathione Sepharose 4 Fast Flow (GE Healthcare) for 2 hours on a rotating wheel. Afterwards, beads were washed five times with 10 ml 1x PBS/1% (v/v) Triton-X-100. GST-bound proteins were resuspended in 1x PBS/ 40% (v/v) Glycerol and stored at -20°C. Estimation of protein concentration and titration between different samples was monitored by Coomassie stained SDS-PAGE (see 3.2.3.3).

3.2.3.14 GST pulldown with radioactively labelled proteins

In order to investigate the interaction between two proteins, a GST pulldown with radioactively labelled protein was performed. For the synthesis of ^{35}S-labelled EcR the TNT Quick Coupled Reticulocyte Transcription/ Translation System (Promega) was used according to the manufacturer's instructions. Full-length EcR and EcR fragments were cloned into the pING14A vector under the control of a T7 RNA polymerase promoter. As a control, DNA encoding the *luciferase* gene, delivered with the kit, was used. Radioactively labelled ^{35}S-methionine was purchased from Hartmann Analytic GmbH. The reaction was assembled as depicted below and incubated at 30°C for 90 min.

12.5 µl	Rabbit reticulocyte lysate
1 µl	Reaction buffer
0.5 µl	T7 RNA Polymerase
0.5 µl	Amino acid mixture without Met
1 µl	^{35}S methionine (>1000 Ci/mmol at 10mCi/ml)
0.5 µl	RiboLock RNase Inhibitor (Thermo Scientific)
2 µl	DNA template pING14A (0.5 µg/ µl)
7 µl	Nuclease-free ddH_2O (Ambion)

Labelled proteins were further diluted in GST pulldown buffer. An input sample was taken and stored at -20°C. The ^{35}S-labeled sample was incubated with 2 µg of GST-fusion protein bound to GST-beads for 2 hours on a rotating wheel at 4°C. Beads were collected by centrifugation at 4000 rpm for 5 min at 4°C and washed 5 times with 1 ml of GST pulldown buffer for 5 min at 4°C. Proteins were eluted by boiling in 1x SDS-PAGE loading buffer and subjected to SDS-PAGE. The gels were fixed with fixing solution (25% (v/v) isopropanol, 10% (v/v) acetic acid) and treated with Amplify (GE Healthcare) for 30 min at RT. After drying the gel, radioactively labeled proteins were exposed to a SuperRX Fuji Medical X-ray film.

GST pulldown buffer	25 mM Hepes/ KOH, pH 7.6
	150 mM KCl
	12.5 mM $MgCl_2$
	0.1% (v/v) NP-40
	DTT, protease inhibitors

4 Results

Immunofluorescence with specific antibodies against Mi-2 on third instar larvae polytene chromosomes indicated that Mi-2 localises to the ecdysone induced puff of the *broad* gene (Figure 2.10) (Murawska, 2011). Transcription of the *broad* gene is strongly upregulated in the presence of ecdysone, suggesting a role for Mi-2 in the regulation of hormone inducible genes in *Drosophila melanogaster* (Drosophila). Previously it was shown that the ecdysone cascade can be induced in S2 cell culture. These cells were derived from a primary culture of late stage Drosophila embryos (Schneider, 1972). S2 cells can be easily cultured in high quantity and efficiently manipulated. Also, in contrast to multiple cell types that can be found within a tissue, S2 cells represent a uniform cell type. Therefore, these cells were used to conduct the majority of *in vivo* experiments described in this thesis.

This study aimed to investigate the functions of Mi-2 in the regulation of ecdysone dependent genes. Therefore, I examined the mechanism by which Mi-2 contributes to hormone regulated gene expression in Drosophila.

4.1 Identification of genome-wide Mi-2 binding sites in S2 cells

4.1.1 Induction of ecdysone cascade in S2 cells

In order to optimise the induction of the ecdysone cascade in S2 cells, different concentrations of the biologically active substance 20-hydroxecdysone (20HE) were applied to adherently growing S2 cells. A broad range of concentrations from 0.1 µM to 10 µM was tested for its ability to induce the ecdysone cascade. Cells were harvested after six hours of 20HE induction, since this time point was shown to induce expression of both, early and late genes of the ecdysone cascade and was in accordance with previous studies (Gauhar et al., 2009). Induction was measured by RTqPCR as increase in *broad* mRNA transcripts normalised to *Rp49*, whose mRNA expression is not altered upon ecdysone treatment (Figure 4.1) (Kilpatrick et al., 2005; King-Jones et al., 2005).

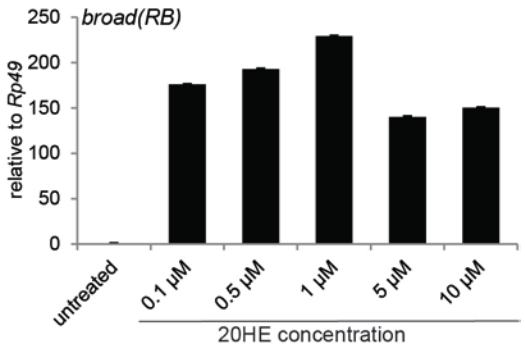

Figure 4.1: Induction of the *broad* gene in S2 cells. Expression of *broad(RB)* mRNA upon treatment of S2 cells with increasing amounts of 20-hydroxyecdysone (20HE) was determined by RTqPCR. mRNA levels were calculated relative to the housekeeping gene *Rp49* and mRNA levels in untreated cells were set to 1. Error bars denote standard deviation of technical triplicates of technical triplicates. Experiment was performed as biological triplicates and one representative experiment is shown here.

The *broad* locus contains several alternative transcripts that show differences in spatio-temporal expression in larvae, but were upregulated to a comparable extent in S2 cells (data not shown). Therefore, the change in transcript levels of the transcript *broad(RB)* was considered to be representative for all mRNAs produced at the *broad* locus upon 20HE treatment of S2 cells. In untreated cells, *broad(RB)* was described at very low levels as demonstrated by RTqPCR. Upon treatment of S2 cells with 0.1 µM 20HE for six hours, *broad(RB)* was upregulated 170-fold compared to untreated cells. Higher transcript levels were achieved by treating cells with up to 1 µM 20HE, allowing the detection of 200-fold more *broad(RB)* mRNA as compared to untreated cells. Further increase in 20HE concentration did not lead to higher expression, but resulted only in a 140-fold gene activation at 10µM 20HE. This effect was probably due to inhibition of cell proliferation and cellular aggregation that can result from treatment of insect cell lines with ecdysteroids (Mosallanejad et al., 2008; Smagghe et al., 2009). In accordance with the results shown here, the conditions for S2 cell incubation for all experiments were set to six hours treatment with 1µM 20HE.

4.1.2 Mi-2 expression is not dependent on 20-hydroxyecdysone

After optimisation of ecdysone induction, a possible effect of 20HE on Mi-2 expression and protein stability was analysed. This experiment was performed in order to exclude that changes in Mi-2 binding to chromatin in the following experiments were not due to alterations in Mi-2 expression levels. Therefore, mRNA as well as protein levels were investigated upon 20HE treatment of S2 cells.

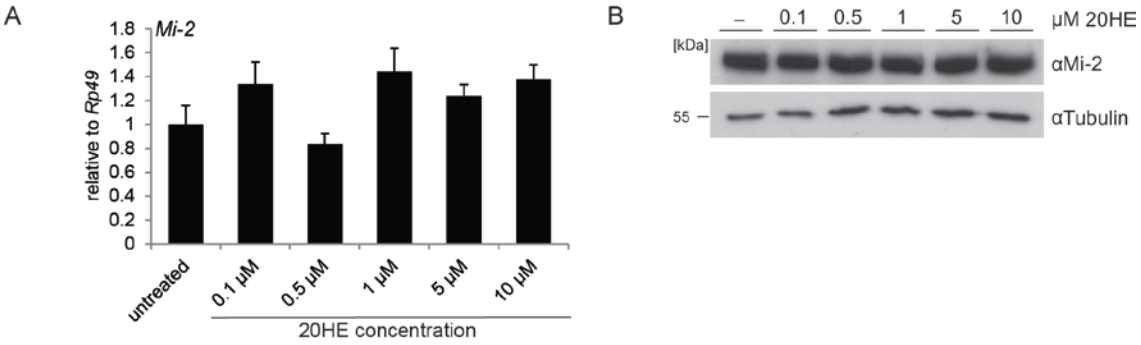

Figure 4.2: Expression of Mi-2 upon 20HE induction. (A) Expression of Mi-2 upon treatment of S2 cells with increasing amounts of 20HE was determined by RTqPCR. mRNA levels were calculated relative to the housekeeping gene *Rp49* and mRNA levels in untreated cells were set to 1. Error bars denote standard deviation of technical triplicates of technical triplicates. Experiment was performed as biological triplicates and one representative experiment is shown here. (B) Mi-2 protein levels were analysed upon 20HE treatment. Nuclear extracts from untreated and 20HE treated S2 cells were compared by Western blot using antibodies indicated on the right. Detection of tubulin served as a loading control. Molecular weight in kDa is depicted on the left.

Transcript levels of Mi-2 were examined by RTqPCR after 20HE treatment with concentrations between 0.1 to 10 µm. Under these conditions mRNA levels ranged between 0.8 to 1.4-fold as compared to untreated cells (Figure 4.2A). These differences were very small compared to the changes in *broad(RB)* expression and did not follow the concentration dependent trend detected for *broad(RB)*. Therefore, I concluded that Mi-2 transcription was not significantly altered upon 20HE treatment within six hours. Effects of 20HE treatment on Mi-2 protein stability levels were analysed by Western blot (Figure 4.2B). Tubulin was used to demonstrate equal loading of samples. No significant difference in Mi-2 protein levels was detected between untreated and 20HE treated cells. Taking together the results from the RTqPCR and the Western blot, I concluded that Mi-2 expression and protein stability was not influenced by the presence of ecdysone within six hours of 20HE treatment. This further supports that the findings described in the following sections were not due to changes in Mi-2 expression levels, but can be referred to changes in Mi-2 binding to chromatin detected by ChIPSeq.

4.1.3 Mi-2 ChIP Seq analysis in S2 cells

As described above, Mi-2 has been shown to bind to a single locus, the ecdysone induced puff of the *broad* gene (Magdalena Murawska, Figure 2.9). However, activation of the ecdysone cascade does influence the expression of several hundred genes (Ashburner, 1990). Therefore, I aimed to identify all sites of Mi-2 recruitment upon ecdysone induction. The identification of genome-wide binding sites of Mi-2 on

polytene chromosomes is limited due to the resolution of immunofluorescence. In order to identify Mi-2 binding sites across the Drosophila genome upon ecdysone treatment, chromatin immunoprecipitation followed by genome-wide sequencing (ChIPSeq) was performed in S2 cells. ChIP experiments using an antibody against an N-terminal Mi-2 fragment were established before on heat shock inducible (*hsp*) genes (Mathieu, 2013; Murawska, 2011). For this thesis, ChIP was performed from S2 cells that were either untreated or induced with 1µM 20HE.As a proof of principle for a successful ChIP experiment, two regions in the *broad* gene were compared to an unrelated, intergenic region (Figure 4.3A and B). This intergenic region was previously shown to exhibit only low Mi-2 binding in untreated cells (Mathieu et al., 2012; Murawska et al., 2011).

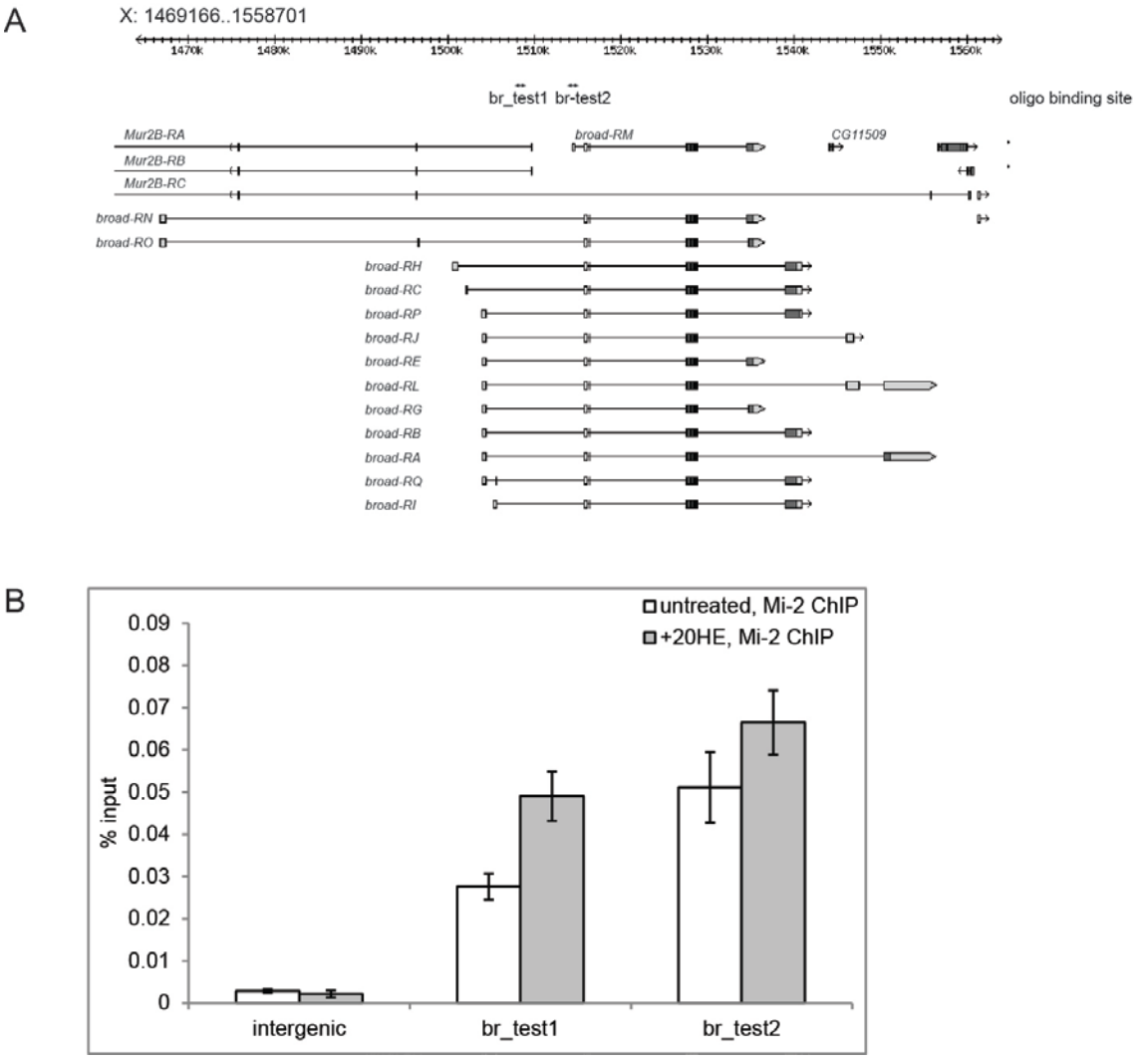

Figure 4.3: Test of Mi-2 binding to the *broad* gene by ChIP. (A) Detailed schematic representation of all transcripts at the *broad* locus and position of oligo binding sites tested in (B). (B) Chromatin was prepared from untreated and 20HE treated S2 cells. ChIP was performed using an antibody against Mi-2. Values are expressed as %input. Purified DNA was quantified by qPCR at binding sites indicated in (A). “Intergenic” refers to an unrelated intergenic region on chromosome arm 2R (see Material and Methods). Error bars denote standard deviation of technical triplicates.

Precipitated DNA from both ChIPs was detected by qPCR with specific oligos binding in a genomic region of interest (Figure 4.3A). Indeed, Mi-2 binding at the intergenic region was less than 0.01% of input as expected from previous studies (Mathieu et al., 2012) (Figure 4.3B). In comparison, Mi-2 binding in untreated S2 cells was about tenfold higher (0.03% input) at the genomic region broad_test1 and about 17-fold higher (0.05%) at broad_test2. The %input enriched in Mi-2 ChIP were comparable to specific ChIP signals that have been described before at the *hsp* genes . Upon treatment of cells with 20HE the ChIP signal at both test regions was even higher, with an 1.8-fold increase at region broad_test1 and a small increase at region broad_test2, compared to untreated cells. These results indicate that Mi-2 ChIP in untreated and 20HE treated cells was efficient. Moreover, it lead to the hypothesis that Mi-2 binds to the *broad* gene and that binding is increased upon 20HE treatment as it was observed on polytene chromosomes (Murawska, 2011).

From the remaining precipitated ChIP DNA a library was prepared and sequenced using the Illumina GaIIx platform under the supervision of Maren Scharfe, Helmholtz Centre for Infection Research. The resulting reads were analysed as described in the Material and Methods section of this thesis by Florian Finkernagel, IMT Marburg. A peak is defined as enrichment of sequence read tag density over a certain region relative to the estimated background tag density (Pepke et al., 2009). This enrichment is an indication for the binding of the analysed protein to the sequenced DNA region. Bioinformatic analysis of the ChIP for Mi-2 identified 15425 peaks in untreated cells and 14161 peaks in 20HE treated. The comparison of ChIPSeq reads in untreated and 20HE treated cells enabled the investigation of Mi-2 ChIPSeq peaks that are significantly increased or decreased upon hormonal induction. Mi-2 ChIP signals were considered increased or decreased when the region exhibited a 2.3-fold or more change in sequencing reads compared to untreated S2 cells. 103 Mi-2 binding sites that were enriched more than 2.3-fold upon 20HE treatment (Appendix, Table 7.1) were identified. ChIPSeq for Mi-2 verified the recruitment to the *broad* gene, as four 20HE induced Mi-2 binding sites were located within the gene, one of which was demonstrated by RTqPCR (Figure 4.3B). Also 76 binding sites where Mi-2 binding was decreased more than 2.3-fold upon 20HE treatment were found (Appendix, Table 7.2). However, I focused my further analysis on binding sites that were enriched upon hormonal induction.

4.1.4 Mi-2 bound genes are ecdysone inducible

In order to investigate regions where Mi-2 binding was induced upon 20HE treatment, a set of 12 strongly enriched (more than threefold) binding sites was selected (Table 4.1). Mi-2 ChIPSeq reads mapped to “Uextra” (Appendix, Table 7.1) were excluded from this list as these reads could not be precisely aligned when the Drosophila genome was assembled (Hoskins et al., 2007). Further, I excluded the first two Mi-2 binding sites that showed highest enrichment in 20HE treated cells (Appendix, Table 7.1) since these peaks were located within the *mRps5* gene, a locus that codes for a mitochondrial ribosomal protein. Ribosomal proteins are ubiquitously expressed and therefore I expected this gene to not be regulated by 20HE (Marygold et al., 2007). The selection of 12 strongly enriched Mi-2 ChIPSeq peaks shown in Table 4.1 demonstrated that the size of these peaks ranged between 556 bp to 3132 bp, with an average of 1352 bps. In order to correlate the identified binding sites to a potentially regulated gene, all peaks were assigned to the closest transcriptional start site (TSS) (Next transcript, Table 4.1) and the two genes in the closest proximity (Primary and Secondary gene). This means that an assigned gene can be the next transcript and the primary gene (e.g. peak at X:1843508..1846640). Further, if another gene is closer to the identified Mi-2 binding site the assigned primary gene can differ from the next transcript (e.g. peak at X:1503765..1504886). However, by visual inspection of the ChIPSeq tracks in the genome browser it became clear, that the peak at chromosomal location X:3302484..3302942 was actually located within the gene *CG12535*. Similarly, the peak at chromosomal location 3R:5789105..5790032 resided within the gene *Glut4EF*. Both genes were not assigned by the bioinformatic algorithm described above, but since 20HE induced Mi-2 binding was detected within their coding region, they were considered for further analysis. Interestingly, the peak at chromosomal location 2L:5287818..5288374 was assigned to the genes *Bub1* and *Bsg25D*. However, this peak was also in close proximity to the *vrille* (*vri*) gene promoter (570 bp from the TSS of *vrille(RE)*), a gene known to be induced by ecdysone. Therefore, this identified peak was assigned to the *vrille* gene. A literature search revealed that transcription of five of the 20 protein-coding genes close to ecdysone-induced Mi-2 peaks are induced upon ecdysone treatment of Drosophila cells (Table 4.1, printed in bold). Two of the selected genes are expressed at the beginning of the ecdysone cascade. The so called “early genes” *broad* and *Hr4* function as transcription factors to induce late genes. Late genes, such as *vrille* and *let-7*, directly contribute to the metamorphosis of the organism. I concluded that the identified Mi-2 binding sites were located within close vicinity of several genes with functions in the ecdysone cascade.

Table 4.1: Mi-2 binding sites induced upon 20HE treatment. Depicted is the exact chromosomal location within the Drosophila genome and the size of Mi-2 peaks in base pairs (bp). The next transcript as well as the two genes in the closest proximity (Primary and Secondary gene) of an identified Mi-2 binding site are given. Tag-count ratio of +20HE/ untreated represents the enrichment of tag counts of Mi-2 ChIPSeq in 20HE versus untreated S2 cells.

chromosomal location	Peak size		Next transcript	Primary gene	Secondary gene	Tag-count ratio +20HE/untreated
X:3302484..3302942	458 bp	a)	*CG14269*	*CR32493*	*CG14269*	5.4689555
X:1843508..1846640	3132 bp		***Hr4***	***Hr4***	*CG3587*	4.5522299
X:1503765..1504886	1121 bp		***br***	*Mur2B*	***br***	4.4419439
3R:5789105..5790032	927 bp	b)	*Art4*	*Art4*	*Gr85a*	4.0371862
2L:5300104..5300770	666 bp		***vri***	***vri***	*CG14024*	3.6915450
X:1504917..1507842	2925 bp		***br***	*Mur2B*	***br***	3.4217047
2L:5287818..5288374	556 bp	c)	*Bub1*	*Bub1*	*Bsg25D*	3.4067035
2L:12013199..12014424	1225 bp		*Rh5*	*Rh5*	*CG6734*	3.2973584
2L:3338014..3339943	1929 bp		***E23***	*CG15408*	*CG3285*	3.2752513
2R:8276716..8277539	823 bp		*Cpr49Ad*	*Cpr49Ad*	*Cpr49Ac*	3.2398497
2R:8274002..8275419	1417 bp		*Cpr49Ac*	*Cpr49Ac*	*CG8501*	3.2058114
2L:18466593..18467235	642 bp		*Ntf-2r*	*mir-100*	***let-7***	3.1695083

[a)] located within *CG12535*; [b)] located within *Glut4EF*; [c)] upstream of *vri* promoter

In order to test if genes that are associated with Mi-2 recruitment upon ecdysone treatment are also 20HE inducible in S2 cells, expression levels of nine of the 12 genes was examined by RTqPCR (Figure 4.4). Seven of the nine tested genes were highly induced upon ecdysone treatment. Interestingly, the genes *Glu4EF* and *Cpr49Ac* had not been described to be upregulated upon 20HE treatment in the literature. These results showed for the first time that *Glut4EF* and *Cpr49Ac* are expressed upon 20HE induction in S2 cells. However, the level of increased expression varied greatly between approximately tenfold for *vrille*, *let-7-C* and *Glut4EF* and several hundredfold for *Cpr49Ac*, *broad* and *Hr4*. For two of the tested genes, *Rh5* and *CG12535*, no significant change of RNA expression upon 20HE treatment was detected. These findings demonstrate that 10 of the 12 peaks that showed strong 20HE induced Mi-2 binding were located within the close proximity of ecdysone inducible genes.

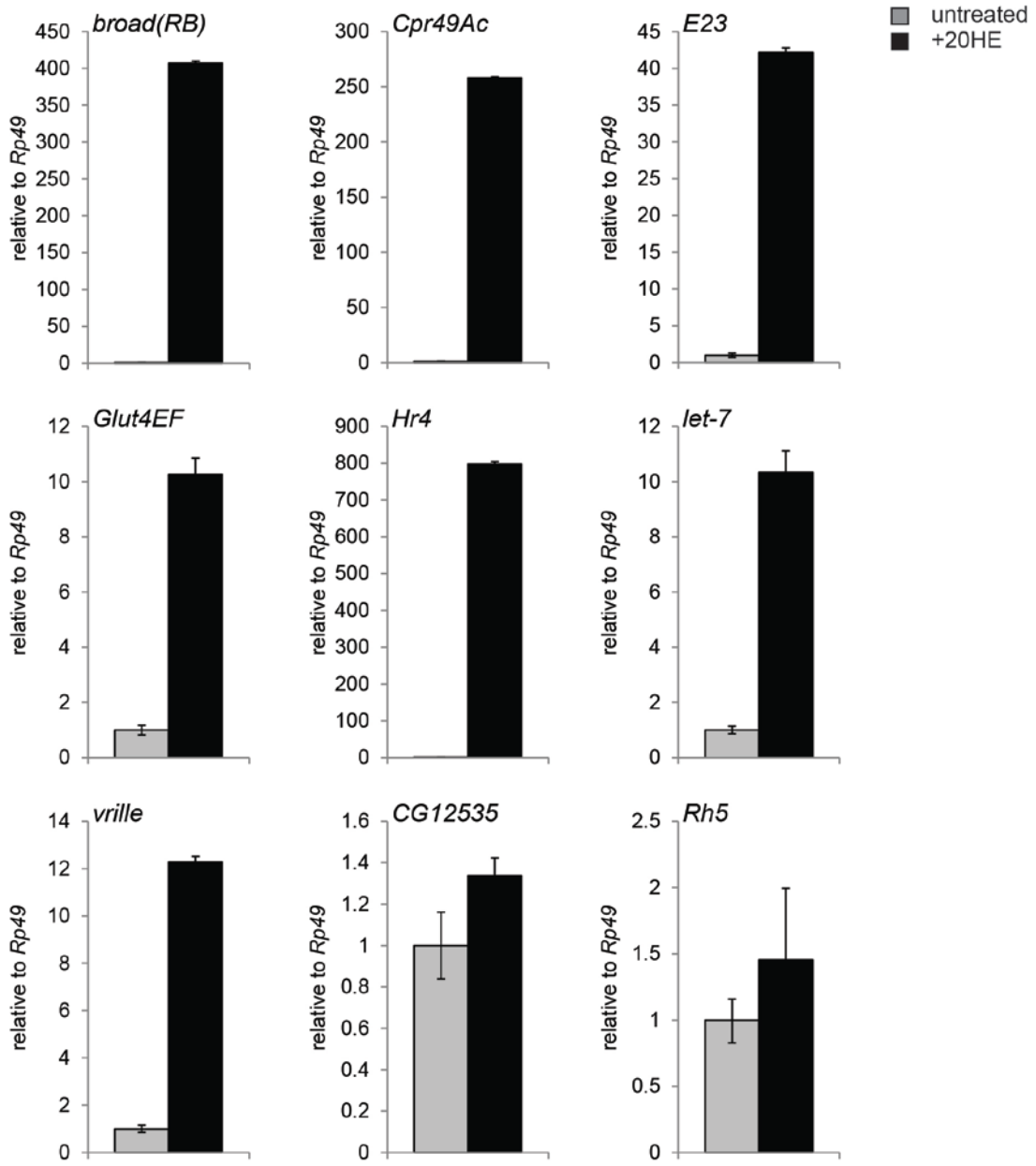

Figure 4.4: Expression of genes associated with Mi-2 binding upon 20HE treatment in S2 cells. Expression of mRNA of nine genes associated with 20HE induced Mi-2 ChIPSeq signals (Table 4.1) was determined by RTqPCR in untreated and 20HE treated S2 cells. mRNA levels were calculated relative to the housekeeping gene *Rp49* and mRNA levels in untreated cells were set to 1. Error bars denote standard deviation of technical triplicates. Experiments were performed as biological triplicates and one representative experiment is shown here.

4.1.5 Validation of Mi-2 ChIPSeq data at the *broad* and *vrille* gene

To confirm Mi-2 binding sites identified by the ChIPSeq experiment described above, I performed several control experiments. Six identified 20HE induced Mi-2 binding sites, two located within the *vrille* locus and four within the *broad* locus, were chosen for further investigation. This selection was made since *broad* was identified as an Mi-2 binding region by immunofluorescence on polytene chromosomes. Further, *vrille* and

broad are expressed at different time points of the ecdysone cascade, with *broad* being an early and *vrille* being a late induced gene. In addition, both loci allowed the analysis of several 20HE induced Mi-2 peaks within the same genomic region. In order to gain more insight into induced Mi-2 binding sites, the surrounding genomic landscape was analysed. The *broad* gene is encoded on the X chromosome and spans a genomic region of almost 100kb, which is about ninefold larger than the average Drosophila gene with 11.3 kb (Lewin, 1994). It codes for 14 alternative transcripts and contains an extended first intron. In addition, it overlaps with the *Mur2B* gene in the 5' region and contains three nested genes towards the 3' end (Figure 4.5). *Broad* encodes a family of related zinc-finger containing transcription factors that are major regulators in a multitude of developmental processes (Guay and Guild, 1991). When analysing the Mi-2 binding pattern in untreated S2 cells, it was observed that strong Mi-2 binding occurred at two regions (Figure 4.5). A small Mi-2 peak that spans approximately 1kb was found in the first intron shortly after the 5' untranslated region of the *broad(RN)* and *–(RO)* transcripts (Figure 4.5, region A). A rather broad Mi-2 binding region that contained several peaks with a width of 8kb was situated within the first intron of most of the transcripts. Other regions of the *broad* locus such as the second and third intron, the exons and the 3' UTR showed less Mi-2 ChIP signal. A region within the second intron did not contain any Mi-2 reads, which was most probable due to the fact that ChIPSeq reads could not be precisely mapped to this region. Sequence analysis revealed that this region indeed contained sequences that exist more than once within the Drosophila genome. These repetitive sequences are excluded from the bioinformatic analysis. When comparing the binding profile of Mi-2 in untreated and 20HE treated cells it was observed that the majority of ChIPSeq peaks was not significantly altered. However, bioinformatic analysis found four regions where Mi-2 binding was enriched up to 4.4-fold (Figure 4.5, red boxes). First, the peak in the 5' untranslated region showed 2.3-fold more Mi-2 binding upon 20HE treatment (X:147165..1473414, Fig 4.5 region A). Second, two peaks with a 4.4-fold (X:1503765..1504886, Fig 4.5 region B) and 3.4-fold (X:1504917..1507842, Fig 4.5 region C) Mi-2 enrichment were identified. These sites of enrichment were close to the major TSS of the *broad* gene. Finally, 2.3-fold stronger binding of Mi-2 within a region containing an exon within the *broad* gene was detected (X:1529697..1531480, Fig 4.5 region D). In conclusion, these findings suggest that Mi-2 bound to several regions in the *broad* gene in untreated S2 cells and was further recruited to specific genomic sites upon induction of the ecdysone cascade.

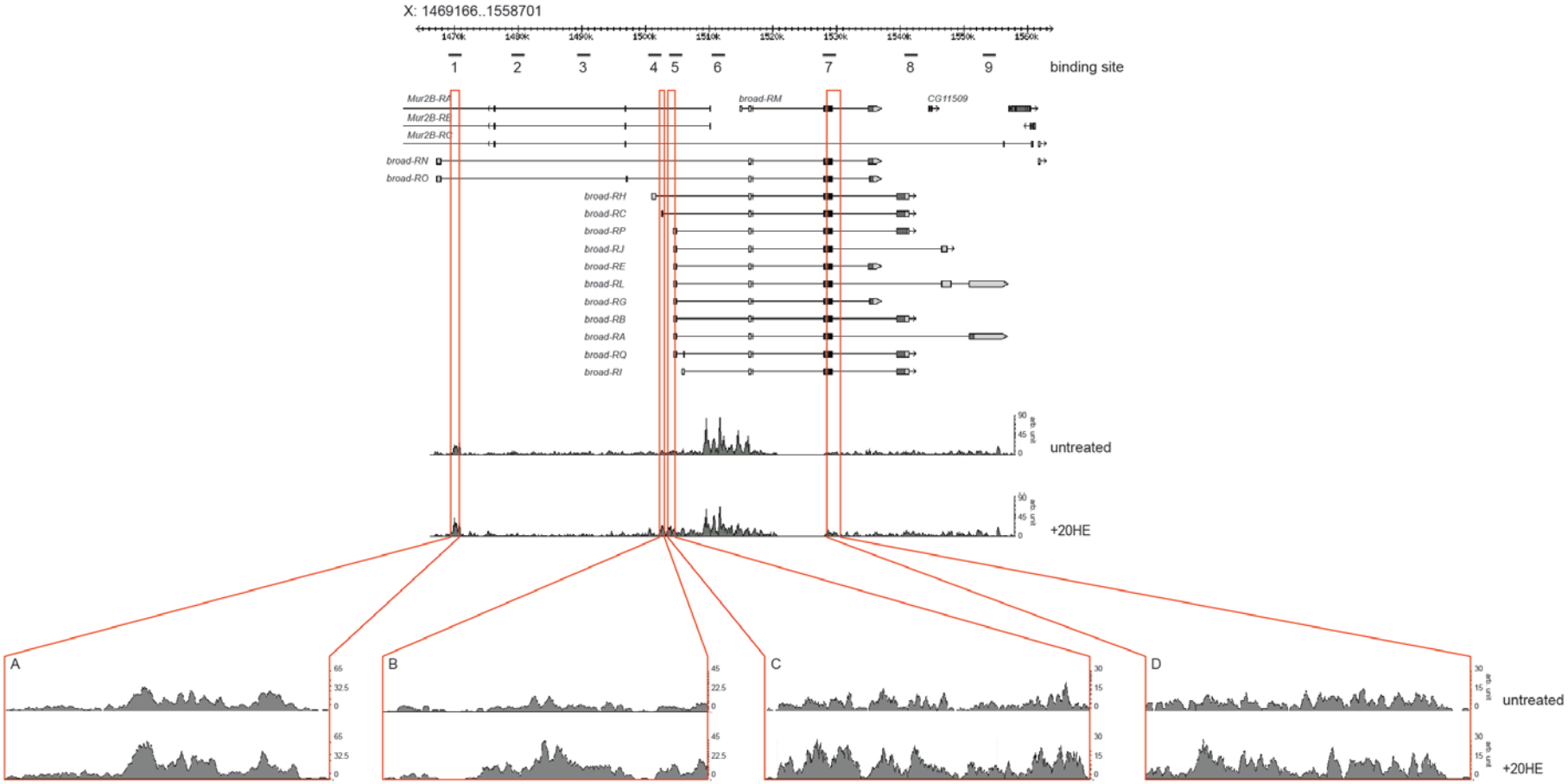

Figure 4.5: Mi-2 binding profile at the *broad* locus. (A) Detailed schematic representation of all transcripts at the *broad* locus. Numbers indicate the binding sites tested by ChIP qPCR (Figures 4.7, 4.8, 4.26 and 4.27). (B) Genome browser view showing Mi-2 sequencing reads obtained from ChIP with anti-Mi-2 antibody in untreated and 20HE treated cells. Zoom-in of regions A-D displaying increased Mi-2 binding upon 20HE stimulation are framed in red lines.

The second locus that was chosen for further analysis as that of the *vrille* gene. The locus is located on the second chromosome, spans about 20kb and codes for four alternative transcripts (Figure 4.6). The promoter region of the *vrille(RE)* transcript overlaps with two annotated non-coding RNAs *CR44743* and *CR44742* that are transcribed in opposite direction from each other. Inspection of the binding pattern of Mi-2 in untreated cells at the *vrille* locus identified several peaks across the gene (Figure 4.6). Mi-2 peaks were mainly located in the extended first intron of the *vrille(RE)* transcript, but also in the intron region that is shared by all transcripts. In accordance with the observation at the *broad* gene, much less Mi-2 binding was detected in the exon and 3' UTR region of *vrille*. Upon 20HE treatment of S2 cells, two Mi-2 binding sites showed significant enrichment (Figure 4.6, red boxes). The first gained peak spanned about 500 bp and was located in the region preceding the *vrille(RE)* transcript that also contained the two non-coding RNA genes (Figure 4.6, region X). The second peak spanned approximately 800 bp and was located within the intron of the *vrille(RE)* and (*RD)* transcripts (Figure 4.6, region Y). All other peaks across the gene were not significantly changed upon ecdysone induction. Therefore, I concluded that similar to what had been observed at the *broad* locus, Mi-2 was bound across the *vrille* gene and further recruited to two regions in response to 20HE treatment.

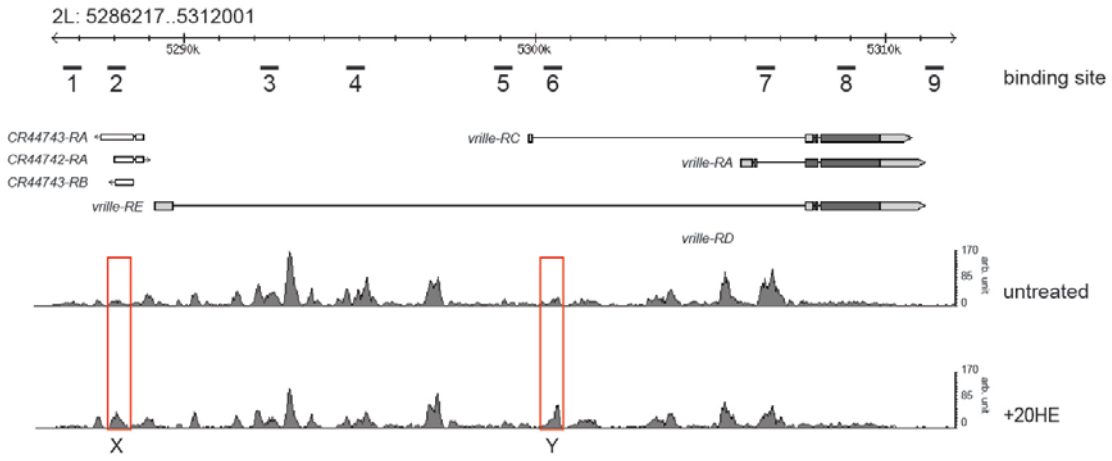

Figure 4.6: Mi-2 binding profile at the *vrille* locus. (A) Schematic representation of the *vrille* locus. Numbers indicate the binding sites tested by ChIP qPCR (Figures 4.7, 4.8, 4.22, 4.26 and 4.27). (B) Genome browser view showing Mi-2 sequencing reads obtained from ChIP with anti-Mi-2 antibody in untreated and 20HE treated cells. Regions with increased Mi-2 binding upon 20HE stimulation (X and Y) are framed in red lines.

The identified Mi-2 binding sites at the *broad* an *vrille* loci were further investigated by ChIP followed by qPCR. Mi-2 binding at nine different locations was examined (depicted by the numbers 1-9 in Figure 4.5 and 4.6). These locations were chosen

because they either represent ecdysone induced Mi-2 binding sites (1, 4, 5 and 7 in *broad*, 2 and 6 in *vrille*) or neighbouring sites not responsive to hormone treatment as predicted by ChIPSeq (Figures 4.5 and 4.6). One ChIP sample for each condition was incubated with rabbit IgG that served as a negative control. All experiments were performed as biological triplicates and one representative experiment is depicted in Figure 4.7. Mi-2 ChIP from untreated S2 cells showed similar differences of Mi-2 ChIP-signal between the nine analysed binding regions in ChIPSeq and ChIP followed by qPCR. In comparison, ChIP with rabbit IgG antibody was below 0.01% of input. At the *broad* locus, Mi-2 was detected strongly at binding sites 1 and 6 as 0.08% and 0.12% of input chromatin were precipitated in untreated S2 cells. In contrast, less binding of Mi-2, about 0.02 to 0.06% of input, was seen at all other binding sites as expected from the ChIPSeq profile (Figure 4.7). ChIP of Mi-2 in 20HE induced cells, precipitated significantly more Mi-2 at binding sites 4 and 5. This increase in Mi-2 binding was approximately threefold (0.11% of input) at position 4 and twofold at position 5 (0.14% of input) (Figure 4.7). Therefore, these regions represent an increased binding of Mi-2 in the presence of hormone, a finding that is in agreement with the results from ChIPSeq. ChIPSeq for Mi-2 also identified binding sites 1 and 7 to be enriched upon 20HE induction (Figure 4.5). However, only a slight increase in Mi-2 binding was observed at binding sites 1 and 7 in qPCR (Figure 4.7). From this, I concluded that Mi-2 ChIP followed by qPCR could verify some, but not all 20HE induced Mi-2 binding sites at the *broad* locus identified by ChIPSeq.

Comparable results were observed at the *vrille* locus (Figure 4.7). In contrast to the *broad* gene, Mi-2 binding was detected across the whole locus with less pronounced binding in the exon and 3'UTR in untreated cells (0.04 to 0.1% of input). This was in agreement with the findings from ChIPSeq (Figure 4.6). Further, the 20HE induced binding of Mi-2 to two regions of the *vrille* gene identified by ChIPSeq could be verified. Binding sites 2 and 6 showed a twofold increase (0.09 and 0.14% of input) in Mi-2 binding. Surprisingly, binding sites 8 and 9 also showed twofold (0.06%) and threefold (0.045% of input) increase in Mi-2 binding. As an additional control, a gene poor region (intergenic) was tested in qPCR. This region exhibited very low Mi-2 binding (0.01%) and showed no Mi-2 recruitment upon ecdysone induction. In conclusion, the Mi-2 binding pattern observed the *broad* and *vrille* locus in ChIPSeq was verified by qPCR and demonstrated ecdysone induced binding of Mi-2 to hormone regulated genes.

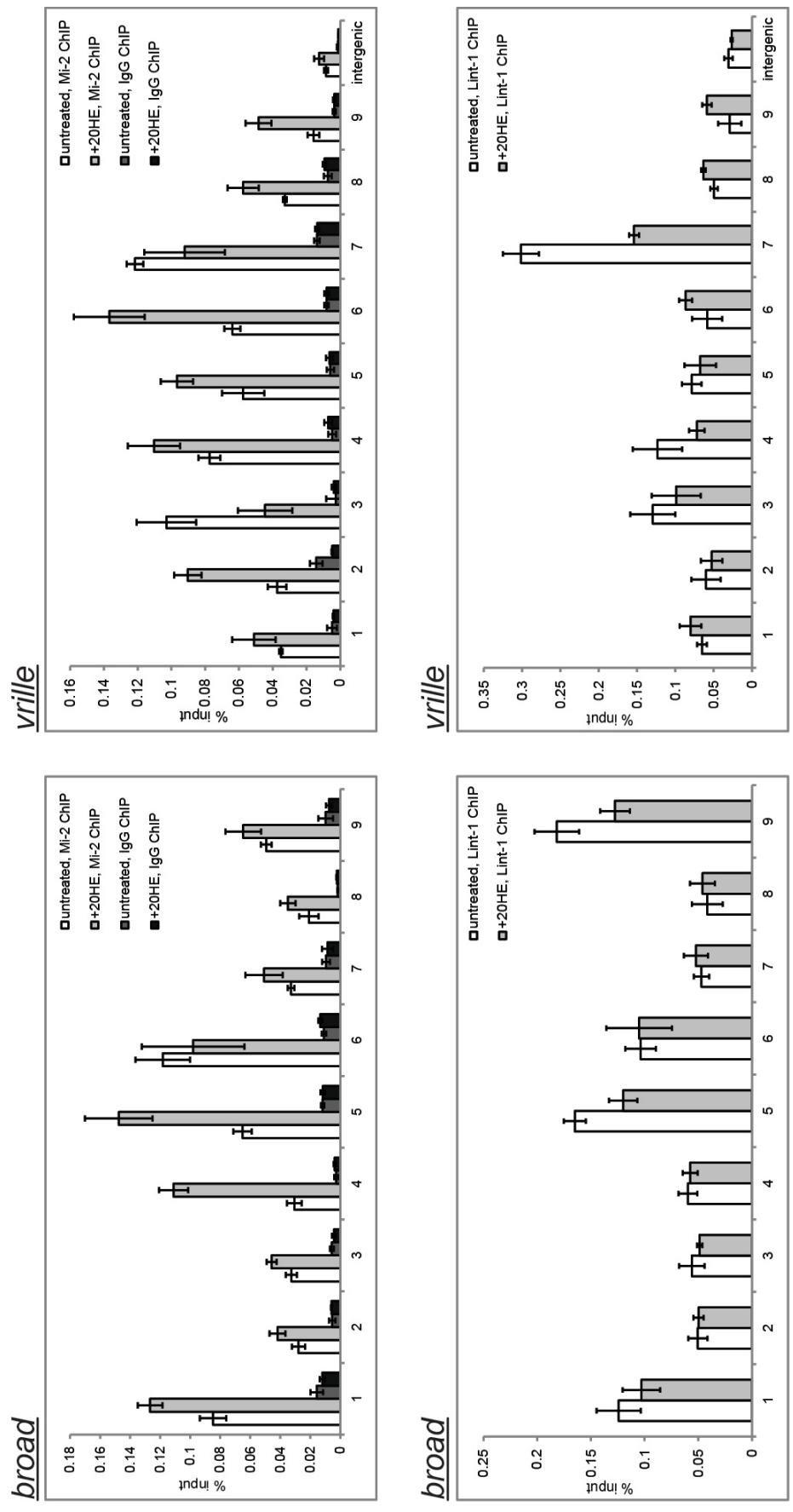

Figure 4.7: Validation of Mi-2 binding profile by ChIP qPCR. (A) ChIP was performed using an antibody against Mi-2 and rabbit polyclonal IgG as IP control. (B) ChIP was performed using an antibody against Lint-1. (A) and (B) Chromatin was prepared from untreated and 20HE treated S2 cells. Values are expressed as % input. Purified DNA was quantified by qPCR with oligos at the binding sites indicated in Figure 4.5 (*broad*) and Figure 4.6 (*vrille*). "intergenic" refers to an unrelated intergenic region on chromosome arm 2R (see Material and Methods). Experiments were performed as biological triplicates and one representative experiment is shown here.

4.1.6 Lint-1 is not recruited to ecdysone dependent genes upon 20HE treatment

To examine whether ecdysone dependent recruitment of Mi-2 to the *broad* and *vrille* loci is specific, ChIP was performed with an antibody against an unrelated protein, Lint-1. Lint-1 is a subunit of the LINT repressor complex that contributes to the repression of germline specific genes in the brain of Drosophila larvae (Meier et al., 2012). Further, Lint-1 is a protein that was not known to be involved in regulation of the ecdysone cascade and was not identified as an Mi-2 interacting protein. ChIP was performed as described previously in untreated and 20HE treated S2 cells (Figure 4.7). Lint-1 binding was detected across the *broad* and *vrille* locus at about 0.05% to 0.1% of input. However, the binding pattern did not resemble the profile of Mi-2 binding in untreated cells. Furthermore, none of the tested regions showed increased Lint-1 ChIP signal upon 20HE treatment. Therefore, binding of Mi-2 in untreated cells and the increase of Mi-2 ChIP signal at particular sites (4 and 5 in *broad*, 2 and 6 in *vrille*) appeared to be specific. This result further excluded the possibility that certain DNA sequences were more susceptible to precipitation by ChIP upon hormone induction.

4.1.7 Depletion of Mi-2 leads to a reduction of 20HE induced Mi-2 ChIP signals

In order to test if the ChIP signals observed with the anti-Mi-2 antibody are specific, and to exclude cross-reactivity of the antibody an additional specificity control was performed. Therefore, RNAi experiments followed by ChIP were conducted. Introduction of double-stranded RNA (dsRNA) that corresponds in sequence to a segment of the targeted mRNA has been shown to induce post-transcriptional gene silencing and to result in the degradation of the targeted mRNA (RNA interference)(Clemens et al., 2000). This application is a powerful tool to deplete Drosophila cells of specific proteins of interest. S2 cells were transfected with a dsRNA against GFP as a negative control and a dsRNA against Mi-2. To check for the efficiency of dsRNA mediated knockdown, Mi-2 protein levels were analysed by Western blot (Figure 4.8A). Efficient Mi-2 depletion was observed when comparing nuclear extracts from cells treated with Mi-2 dsRNA (lanes 3 and 4) compared to cells treated with GFP dsRNA (lanes 1 and 2). This effect was not altered upon treatment of cells with 20HE.

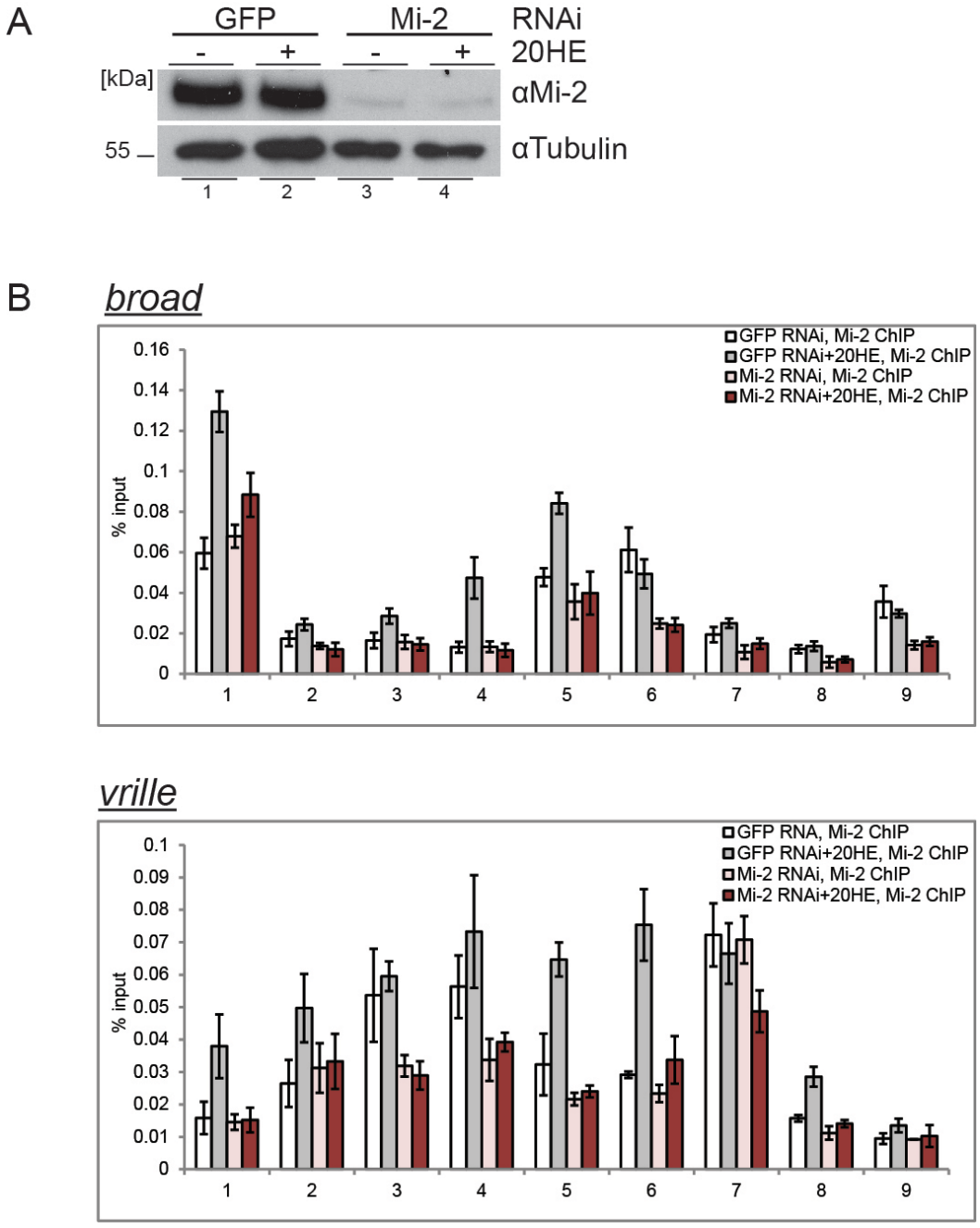

Figure 4.8: Validation of Mi-2 specific binding sites by ChIP qPCR by RNAi. (A) Nuclear extracts from S2 cells treated with dsRNA against GFP or Mi-2 and incubated with (+) or without (-) 20HE were subjected to Western blot using antibodies indicated on the right. Detection of tubulin served as a loading control. Molecular weight in kDa is depicted on the left. (B) ChIP was performed using an antibody against Mi-2. Chromatin was prepared from S2 cells incubated with dsRNA against GFP (white and grey bars) or Mi-2 (light and dark red bars) and incubated with (grey and dark red bars) or without 20HE (white and light red bars). Values are expressed as % input. Purified DNA was quantified by qPCR with oligos at the binding sites indicated in Figure 4.5 (*broad*) and Figure 4.6 (*vrille*). "Intergenic" refers to an unrelated intergenic region on chromosome arm 2R (see Material and Methods). Experiments were performed as biological triplicates and one representative experiment is shown here.

Cells treated with dsRNA were subjected to ChIP analysis followed by qPCR. The samples treated with GFP dsRNA showed an Mi-2 binding pattern for *broad* and *vrille*, in untreated and 20HE treated cells (Figure 4.8, white and grey bars) that was comparable to the profile described previously (Figure 4.7). However, the %input showed some variability in comparison to the experiment described in Fig. 4.7, which was probably due to biological variation. The Mi-2 binding profile in untreated S2 cells that were depleted of Mi-2 did not change considerably (Figure 4.7, light red bars). Only a small decrease at binding sites 6, 8 and 9 of the *broad* gene and binding sites 3 and 4 of the *vrille* gene were observed. This is a surprising result as the depletion of Mi-2 seemed to not have a significant effect on Mi-2 binding to chromatin. One reason for this observation could be that only the soluble nuclear fraction of Mi-2 was depleted by dsRNA, whereas a rather stable fraction of Mi-2 remained associated with chromatin over several cell cycles (Anna Ernst, data not shown). However, when analysing the binding pattern of Mi-2 upon ecdysone treatment in Mi-2 dsRNA treated cells, it was observed that Mi-2 recruitment at the expected binding sites was abolished (Figure 4.7, dark red bars). This was clear at binding sites 1, 4 and 5 of the *broad* and binding sites 2 and 6 of the *vrille* gene Therefore, I concluded that Mi-2 enrichment upon hormonal stimulation was abolished in Mi-2 depleted cells. Also, these results indicated that the observed Mi-2 binding was specific and not a result of cross-reactivity of the Mi-2 antibody.

4.2 Function of Mi-2 at ecdysone dependent genes

4.2.1 Mi-2 functions as a transcriptional repressor at ecdysone induced genes

Mi-2 had been previously shown to function as a co-repressor at developmental and proneural genes (Kunert et al., 2009; Murawsky et al., 2001). In contrast, Mi-2 acts as a co-activator to promote full transcriptional activation of heat shock genes (Murawska et al., 2011). The observation that Mi-2 was recruited to several ecdysone dependent genes prompted us to examine its role at the *broad* and *vrille* gene. In order to investigate the function of Mi-2, expression of *vrille* and *broad* in Mi-2 depleted cells was analysed.

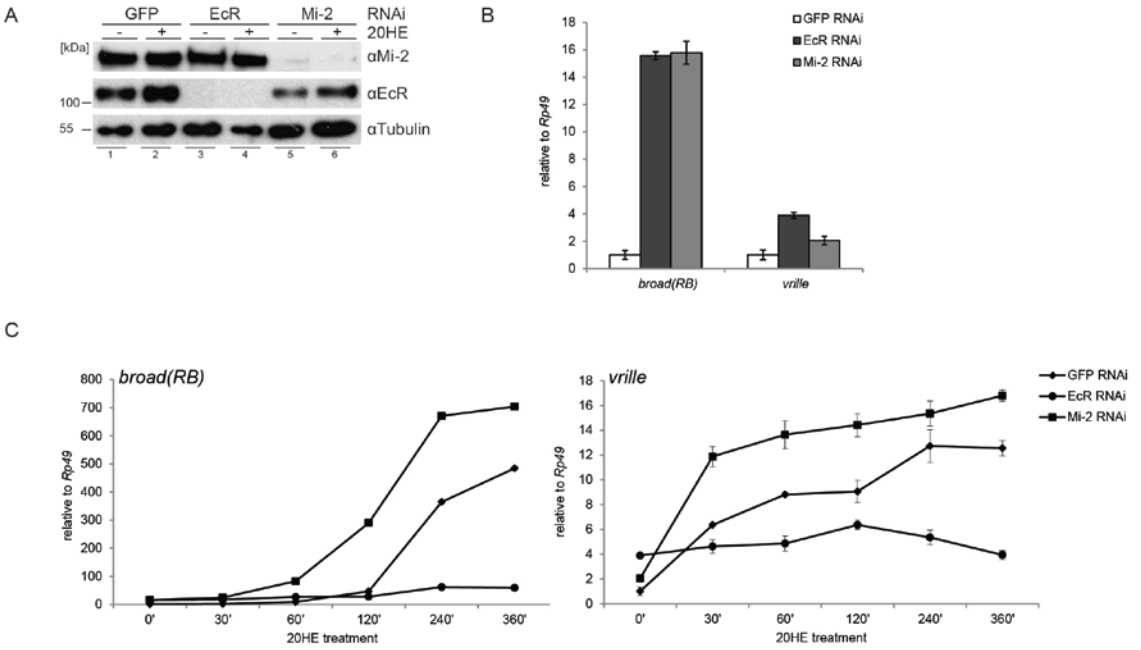

Figure 4.9: Expression of *broad* and *vrille* in Mi-2 depleted cells. (A) Nuclear extracts from S2 cells treated with dsRNA against GFP, EcR or Mi-2 and incubated with (+) or without (-) 20HE were subjected to Western blot using antibodies indicated on the right. Detection of tubulin served as a loading control. Molecular weight in kDa is depicted on the left. (B) Expression of mRNA of *broad* and *vrille* from untreated S2 cells incubated with dsRNA against GFP (white bars), EcR (dark grey bars) or Mi-2 (light grey bars) was determined by RTqPCR. mRNA levels were calculated relative to the housekeeping gene *Rp49* and mRNA levels in cells treated with GFP dsRNA were set to 1. (C) Timecourse of mRNA expression of *broad* and *vrille* upon 0, 30, 60, 120, 240 and 360 minutes of 20HE induction in S2 cells treated with dsRNA against GFP (rhombus), EcR (circle) or Mi-2 (square) was determined by RTqPCR. mRNA levels were calculated relative to the housekeeping gene *Rp49* and mRNA levels in untreated cells incubated with GFP dsRNA were set to 1. Error bars denote standard deviation of technical triplicates. Standard deviations for *broad* are not visible in the time course due to the scale of the y-axis. Experiments were performed as biological triplicates and one representative experiment is shown here.

Hence, S2 cells were subjected to dsRNA treatment as described above. In addition, a dsRNA specifically targeting EcR was introduced as a positive control since knockdown of EcR had been shown to efficiently abolish the activation of the ecdysone cascade (Beckstead et al., 2005). The depletion of EcR and Mi-2 was efficient as demonstrated by Western blot (Figure 4.9A, lanes 1-6). Additionally, it was observed that Mi-2 protein level was not affected upon EcR knockdown (lanes 3 and 4). However, upon Mi-2 depletion, EcR protein levels seemed to be slightly decreased (lanes 5 and 6). Expression analyses demonstrated that knockdown of Mi-2 as well as EcR lead to a 15-fold increase of *broad* transcript levels in cells that were not treated with 20HE (Figure 4.9B). Also, expression of *vrille* was fourfold upregulated in EcR and twofold upregulated in Mi-2 dsRNA treated cells. This demonstrated that depletion of Mi-2 and EcR lead to expression of ecdysone-regulated genes that are otherwise less transcribed in untreated S2 cells. Further, expression of *broad* and *vrille* was examined

at five different time points upon ecdysone induction in dsRNA treated cells (Figure 4.9C). Cells incubated with a dsRNA against GFP showed an eightfold increase of *broad* expression 60 min after 20HE induction. Expression of *broad* mRNA further increased with time, reaching about 480-fold increase compared to non-treated cells (t=0') after six hours. *Vrille* transcription was sixfold higher after 30 minutes and further increased up to 16-fold after six hours of 20HE treatment. As expected, in cells depleted of EcR, mRNA levels did not show a robust induction after six hours of ecdysone treatment. In contrast, depletion of Mi-2 from S2 cells, led to a significant increase of expression of *broad* at all measured time points compared to GFP treated samples (300-fold after 2 hours, 720-fold after six hours). Comparable results were found for the *vrille* gene, where expression in Mi-2 depleted cells was 18-fold upregulated after six hours as compared to a 12-fold increase in *vrille* mRNA in GFP dsRNA treated cells. From these results, I hypothesised that in untreated cells Mi-2 as well as EcR function as transcriptional repressors at the *broad* and *vrille* genes. Further, I confirmed that EcR is a crucial factor for efficient transcriptional activation upon 20HE treatment. By contrast, Mi-2 appears to retain its function as a co-repressor upon 20HE treatment, as its depletion resulted in superactivation of both genes.

4.2.2. Depletion of Iswi does not lead to superactivation of ecdysone dependent genes

To investigate whether the function of Mi-2 is specific for this particular ATP-dependent chromatin remodeler, we depleted a different ATP-dependent chromatin remodeler of the SNF2 family, namely Iswi, from S2 cells. Iswi was previously shown to function as a transcriptional activator of ecdysone regulated genes in Drosophila (Badenhorst et al., 2005). Efficient knockdown of *Iswi* by RNAi was verified by decreased levels of mRNA in RTqPCR as no antibody for detection of protein levels in Western blot was available (Figure 4.10A). In cells treated with a dsRNA against *Iswi*, expression of *Iswi* was 30-fold downregulated compared to GFP treated cells. Interestingly, *Iswi* expression was fivefold decreased in GFP dsRNA treated cell that were induced with 20HE. Therefore, I hypothesised, that *Iswi* mRNA expression was negatively influenced by ecdysone.

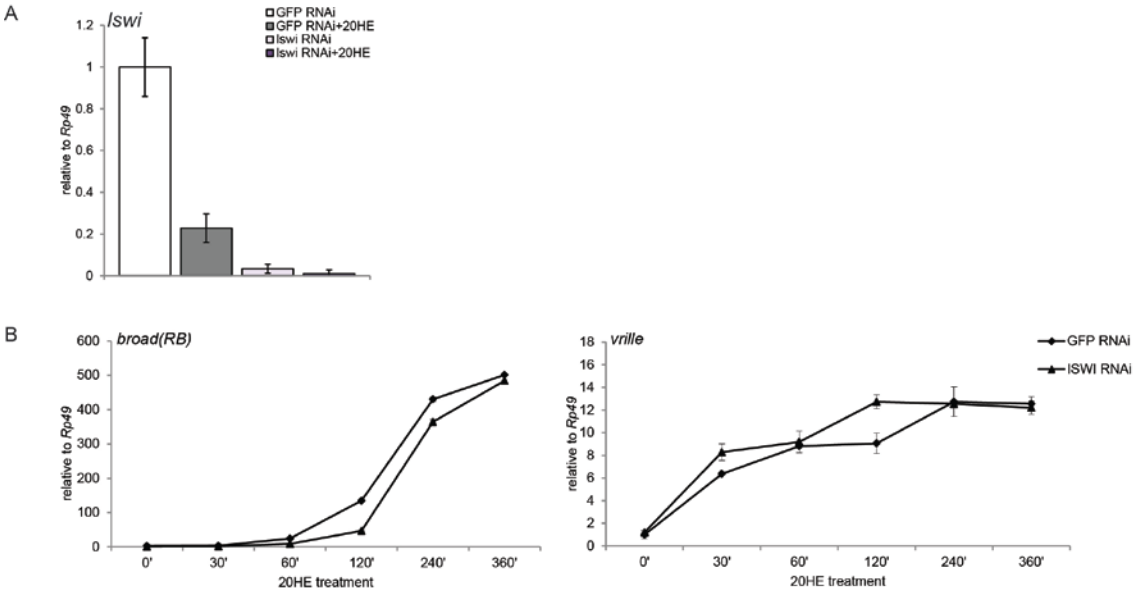

Figure 4.10: Expression of *broad* and *vrille* in Iswi depleted cells. (A) Expression of mRNA of *Iswi* incubated with dsRNA against GFP (white and grey bars) and Iswi (light and dark purple bars) in S2 cells incubated with (grey and dark purple bars) or without (white and light purple bars) 20HE was determined by RTqPCR. mRNA levels were calculated relative to the housekeeping gene *Rp49* and mRNA levels in untreated cells incubated with GFP dsRNA were set to 1. (B) Timecourse of mRNA expression of *broad* and *vrille* upon 0, 30, 60, 120, 240 and 360 minutes of 20HE induction in S2 cells treated with dsRNA against GFP (rhombus) and Iswi (triangle) was determined by RTqPCR. mRNA levels were calculated relative to the housekeeping gene *Rp49* and mRNA levels in untreated cells incubated with GFP dsRNA were set to 1. Error bars denote standard deviation of technical triplicates. Standard deviations for *broad* are not visible in the time course due to the scale of the y-axis. Experiments were performed as biological triplicates and one representative experiment is shown here.

In uninduced cells (t=0') *broad* was twofold upregulated when treated with Iswi dsRNA compared to GFP dsRNA treated cells, whereas no change was detected for *vrille* expression (Figure 4.10B and data not shown). Upon hormonal stimulation, expression of *broad* was decreased twofold in *Iswi* depleted cells as compared to GFP dsRNA after 60 and 120 minutes. This difference in expression levelled off four hours after induction when comparable amounts of mRNA in GFP and Iswi dsRNA treated cells were detected. No significant difference between GFP and Iswi dsRNA treated cells was observed for *vrille* expression. These experiments demonstrated that Iswi does not appear to function as a transcriptional repressor or activator of *broad* and *vrille*. Further, I hypothesised that Mi-2 functions as a major repressive ATP-dependent chromatin remodeler at the ecdysone induced genes *broad* and *vrille.*

4.2.3 Mi-2 regulates transcription of two non-coding RNAs

Mi-2 binding upon 20HE treatment occurred in a genomic region that does not only contain promoter sequences of the *vrille* gene, but also codes for two non-coding

RNAs *CR44742* and *CR44743*. Thus, I proposed that Mi-2 may not only contribute to the regulation of *vrille* expression but could also influence expression of these ncRNAs. Both RNAs were expressed to a low extent in S2 cells, but were upregulated about 20-fold upon 20HE treatment (Figure 4.11). Interestingly, changes in expression of both RNAs in EcR and Mi-2 depleted cells were comparable with the findings for the *vrille* gene (Figure 4.9C). In uninduced cells treated with a dsRNA against Mi-2 *CR44742* and *CR44743* transcripts were upregulated about fivefold compared to GFP treated cells. In the presence of hormone, noncoding transcript levels were fourfold higher in Mi-2 depleted cells than in GFP dsRNA treated cells. In agreement with the findings above (Figure 4.9B), depletion of EcR resulted in derepression of both ncRNAs in uninduced S2 cells by about twofold. Induction of the ecdysone cascade resulted in an increase in both transcripts in EcR depleted cells, however this transcriptional activation was not as strong as the effect seen in GFP dsRNA treated cells. I concluded that Mi-2 and EcR contributed to the regulation of the two ncRNAs *CR44742* and *CR44743*, in a manner comparable to what was observed for *broad* and *vrille* expression.

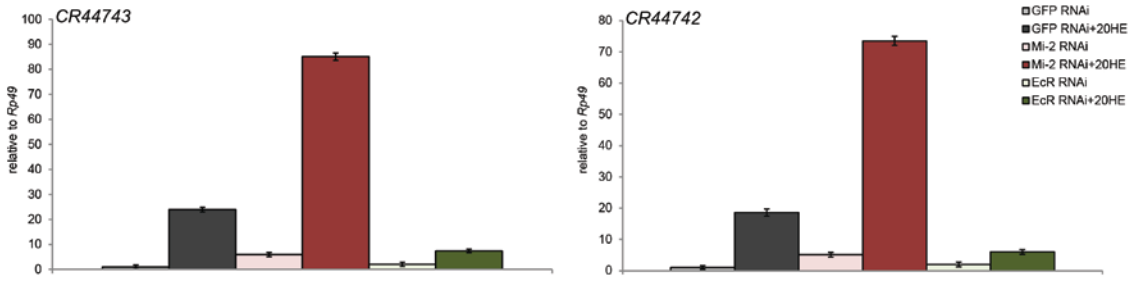

Figure 4.11: Expression of non-coding RNAs in Mi-2 depleted cells. Expression of *CR44743* and *CR44742* incubated with dsRNA against GFP (light and dark grey bars), EcR (light and dark green bars) or Mi-2 (light and dark red bars) in untreated (light bars) and six hours 20HE treated (dark bars) S2 cells was determined by RTqPCR. mRNA levels were calculated relative to the housekeeping gene *Rp49* and mRNA levels in untreated cells incubated with GFP dsRNA were set to 1.Error bars denote standard deviation of technical triplicates. Experiments were performed as biological triplicates and one representative experiment is shown here.

4.3 Interaction studies on Mi-2 and EcR

4.3.1 Mi-2 and EcR interact *in vitro*

Mi-2 has been previously shown to interact with transcription factors such as tramtrack69 and hunchback (Kehle et al., 1998; Murawsky et al., 2001). Therefore, I hypothesised that recruitment to ecdysone dependent genes is mediated by an interaction with EcR. In order to test this hypothesis, the Baculovirus expression

system was used as it allows for overexpression and purification of large eukaryotic proteins such as Mi-2 (220kDa) and EcR (110kDa). Sf9 cells were infected with baculoviruses expressing Mi-2, EcR or, as a control, the unrelated Lint-1 protein. Mi-2 and Lint-1 were overexpressed as epitope-tagged fusion proteins with an N-terminal FLAG octapeptide (from here on referred to as FLAG). Proteins were expressed individually or in combination and their expression was analysed in Western blot (Figure 4.12, lanes 1-6). Due to differences in virus titer, expression of Lint-1-FLAG was stronger than Mi-2-FLAG expression. However, EcR protein levels were comparable in all samples. FLAG-tagged proteins were precipitated from whole cell extracts using anti-FLAG antibody immobilised on agarose beads (from here on referred to as FLAG-beads).

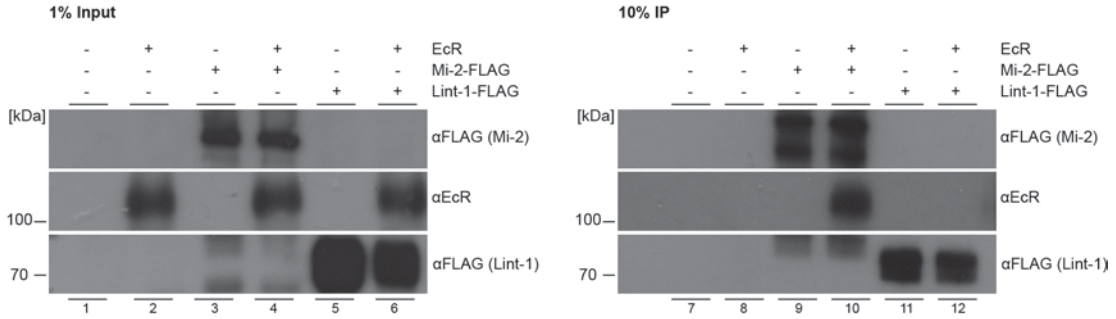

Figure 4.12: Mi-2 interacts with EcR *in vitro*. Sf9 cells were co-infected with baculoviruses expressing Mi-2-FLAG or Lint-1-FLAG and EcR as indicated on top. Extracts were immunoprecipitated with anti-FLAG antibody immobilised on agarose beads. Immunoprecipitates were subjected to Western blot using antibodies indicated on the right. Left panel shows 1% of the total input sample that was used for IP. Right panel shows 10% of the total immunoprecipitated sample. Molecular weight in kDa is depicted on the left.

In the extracts before immunoprecipitation (IP) Mi-2-FLAG runs as a single band (lanes 3 and 4), whereas after incubation with FLAG beads the electrophoretic mobility of Mi-2-FLAG changed and it runs as two bands (lanes 9 and 10). This was probably due to protein degradation of Mi-2-FLAG by proteases during the IP. Also, there was a Western blot signal visible in the panel where Lint-1-FLAG was detected, but in lanes where Lint-1-FLAG was not expressed (lanes 3,4, 9 and 10). These bands originate from degradation products of Mi-2-FLAG with a smaller molecular weight that ran faster in SDS-PAGE and were also detected by the anti-FLAG antibody. When Mi-2-FLAG and EcR were co-expressed in Sf9 cells, IP of Mi-2-FLAG showed clear co-immunoprecipitation (co-IP) of EcR (lane 10). Precipitation of Lint1-FLAG did not show co-IP of EcR (lane 12), indicating the interaction between Mi-2 and EcR was specific. This demonstrated that Mi-2 and EcR can interact physically when overexpressed in Sf9 cells.

4.3.2 Interaction of Mi-2 and EcR is independent of 20HE

Interaction studies have demonstrated that interaction of the EcR complex with other proteins can depend on the presence of ecdysone (Badenhorst et al., 2005; Tsai et al., 1999). To investigate whether the interaction between Mi-2 and EcR may also be influenced by the hormone, a FLAG-IP experiment was performed. Sf9 cells were cultured under three different conditions. Generally, Sf9 cells were grown in fetal bovine serum (FBS) supplemented medium. However, FBS contains a mixture of bioactive substances including mammalian steroid hormones. These hormones are capable to function as hormone analogues, thereby changing the nuclear receptor (NR) conformation to a "hormone-bound" state (Samuels et al., 1973). In order to remove these hormones, FBS was treated with dextran-coated charcoal (Chen, 1967). Sf9 cells grown in charcoal-depleted, normal or 20HE supplemented medium and were co-infected with a virus expressing Mi-2 and FLAG-EcR. Western blot analysis showed that expression of Mi-2 and FLAG-EcR was not altered under different culture conditions (Figure 4.13, lanes 1-6). In accordance with the results described above, IP of FLAG-EcR enriched Mi-2 on FLAG beads (lanes 10-12). Interestingly, there was no change in the amount of precipitated Mi-2 under the three different culture conditions. Therefore, I concluded that the interaction between Mi-2 and EcR did not depend on ecdysone in this *in vitro* assay system.

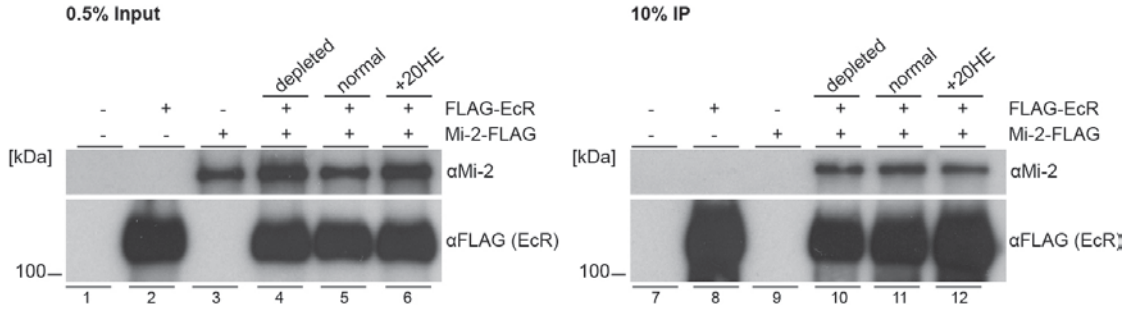

Figure 4.13: Interaction of Mi-2 with EcR is independent of 20HE. Sf9 cells were co-infected with baculoviruses expressing FLAG-EcR and untagged Mi-2 as indicated on top in hormone depleted, normal or 20HE supplemented medium.. Extracts were immunoprecipitated with anti-FLAG antibody immobilised on agarose beads. Immunoprecipitates were subjected to Western blot using antibodies indicated on the right. Left panel shows 0.5% of the total input sample that was used for IP. Right panel shows 10% of the total immunoprecipitated sample. Molecular weight in kDa is depicted on the left.

4.3.3 Mi-2 and EcR form a stable complex *in vitro*

In order to investigate if Mi-2 and EcR interact in a stoichiometric manner, Sf9 cells were co-infected with viruses expressing FLAG-EcR and untagged Mi-2 protein. To purify sufficient amounts for visualisation of both proteins on Coomassie stained SDS-

PAGE gels, large scale FLAG purifications were conducted. Additionally, FLAG-bound proteins were washed several times with high salt washing buffer of up to 1M. Coomassie staining revealed the purified proteins with almost no enrichment of unspecific contaminants (Figure 4.14). Precipitation of FLAG-Mi-2 resulted in strong enrichment of Mi-2 with a high purity (lanes 1 and 2). Only a small amount of degradation product below the full-length Mi-2 at 220kDa was detected. Purification of FLAG-EcR showed also strong enrichment of the protein at an expected molecular weight of 110kDa (lanes 3 and 4). However, several additional bands were detected in Coomassie stained SDS PAGE. These bands could either be degradation products of FLAG-EcR or endogenous Sf9 proteins that were co-immunoprecipitated together with FLAG-EcR. When co-expressing FLAG-EcR and Mi-2, purification of FLAG-EcR showed co-purification of Mi-2 at apparent stoichiometric quantities (lanes 5 and 6). This demonstrated that the interaction between EcR and Mi-2 occurred in a stoichiometric manner and was stable even under high salt conditions.

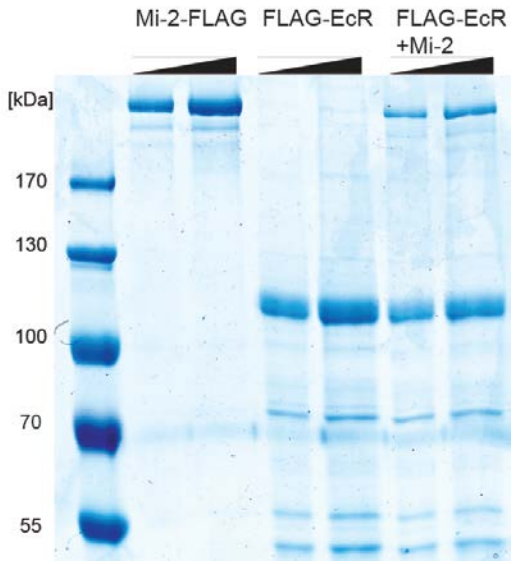

Figure 4.14: Mi-2 and EcR form a stable complex. Sf9 cells were infected with baculoviruses expressing Mi-2-FLAG, FLAG-EcR or FLAG-EcR and untagged Mi-2, respectively. Large scale extracts from infected cells were immunoprecipitated with anti-FLAG antibody immobilised on agarose beads and washed twice with buffer containing 1M NaCl. Proteins were eluted from the beads with FLAG peptide. Purified proteins were subjected to SDS-PAGE and subsequently stained with Coomassie. 500ng and 1µg of protein was loaded. Molecular weight in kDa is depicted on the left.

4.3.4 EcR and Mi-2 interact *in vivo*

The results obtained from Sf9 cell overexpression experiments demonstrated that Mi-2 and EcR can interact. In order to investigate if this interaction occurs under physiological conditions in S2 cells, co-IP of EcR and Mi-2 was performed. In addition,

a hormone dependency of the interaction was examined by comparing untreated and 20HE treated S2 cells. As negative controls, IP with rat IgG and anti-p53 (rat) antibody was performed. Drosophila p53 is not known to interact with EcR. Mi-2 was immunoprecipitated from nuclear extracts using a monoclonal rat anti-Mi-2 antibody (Figure 4.15, lanes 4 and 8). In accordance with previous results, EcR was co-immunoprecipitated in the Mi-2 IP sample. IP with control antibodies (p53: lanes 2 and 6; IgG: lanes 3 and 7) did not show enrichment of Mi-2 or EcR. Moreover, there was no significant difference of EcR co-IP between untreated and 20HE treated S2 cells. This experiment confirmed the findings from overexpressed recombinant proteins and demonstrated that Mi-2 and EcR interact under physiological conditions in S2 cells. Further, it verified that this interaction is independent of the hormone 20HE.

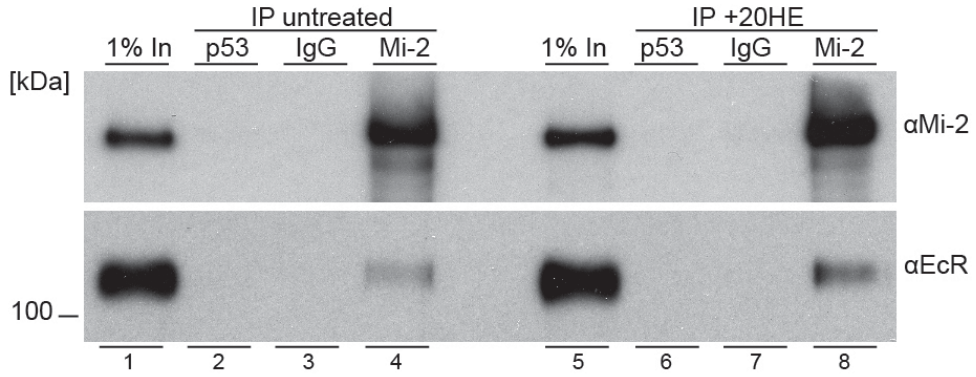

Figure 4.15: Mi-2 interacts with EcR *in vivo*. Nuclear extract from S2 cells were subjected to IP using monoclonal rat Mi-2 or rat p53 antibody or rat IgG, respectively. Immunoprecipitates were subjected to Western blot using antibodies indicated on the right. “1% In” refers to 1% of the total input sample that was used for IP. Molecular weight in kDa is depicted on the left.

4.3.5 The ATPase domain of Mi-2 directly interacts with EcR

Mi-2 and EcR were shown to interact when overexpressed in Sf9 cells. This system maximises proper folding and posttranslational modification of large proteins which is often a limitation in bacterial expression systems. However, as it is based on eukaryotic insect cells, it was possible that the interaction of Mi-2 and EcR was mediated by one or several endogenous proteins. In order to investigate whether Mi-2 and EcR bind directly, a bacterial expression system was used. In addition, the Mi-2 domain that is involved in interaction with EcR was mapped. For this purpose, several Mi-2 deletion mutants were designed (Figure 4.16A). The first fragment contained 690 amino acids of the N-terminus including the PHD fingers and chromodomains, whereas the second fragment spanned the entire ATPase domain from amino acid 691 to 1270. A third fragment contained the complete C-terminal domain until amino acid 1982. All

fragments were expressed and purified via an N-terminal glutathione S-transferase (form here on referred to as GST) tag in *E.coli* (Figure 4.16B). GST and the C-terminus of Lint-1 were also expressed and purified to serve as negative controls in the GST pull-down. Both, the N-terminal and C-terminal fragment of Mi-2 as well as the Lint-1 fragment ran as a double band, which was possibly due to protein degradation during the purification process. The purified proteins were used in an interaction study with *in vitro* translated, ^{35}S-methionine labelled EcR that allows for easy detection (Figure 4.16C). Interestingly, EcR was significantly enriched on beads containing the ATPase domain of Mi-2 (Figure 4.16, lane 4), whereas GST as well as the N-terminus and C-terminus of Mi-2 and Lint-1 displayed only weak binding to EcR (lanes 2, 3, 5 and 9). As a negative control, all beads were incubated with *in vitro* translated, radioactively labelled luciferase. Luciferase was not detected to bind any of the GST-tagged proteins, demonstrating the specificity of the interaction assay. This result demonstrated that the EcR interaction surface within Mi-2 seems to reside in the ATPase domain and that this domain is sufficient for an interaction with EcR. This interaction is likely to be direct although it is formally possible that it is mediated by a factor present in the rabbit reticulocyte lysate used to *in vitro* translate EcR.

Several studies have shown that certain NR interacting proteins bind to the NR upon hormonal induction and contribute to transcriptional activation of NR target genes. The interaction surface with which these co-activators bind to NRs has been shown to accommodate the highly conserved amino acid sequence “LXXLL” where “L” is leucine and “X” is any amino acid (Heery et al., 1997). Analysing the amino acid sequence within the ATPase domain of Mi-2, this motif was found to be present once in the first ATPase lobe (aa 913-917; Figure 4.16A yellow star). In order to test whether this motif mediates the interaction with the EcR the amino acid sequence “LFHLL” was mutated to “LFHAA”. Introduction of this mutation has been shown previously to disrupt the interaction surface between NRs and interacting proteins (McInerney et al., 1998). Expression and purification of the GST-tagged mutant ATPase domain demonstrated that the mutant protein was expressed to a comparable extent as the wildtype protein (Figure 4.16D). Subsequently, both proteins as well as the C-terminus of Mi-2 and GST (Figure 4.16D) as negative controls, were incubated with radioactively labelled EcR in a GST pull-down assay (Figure 4.16E).

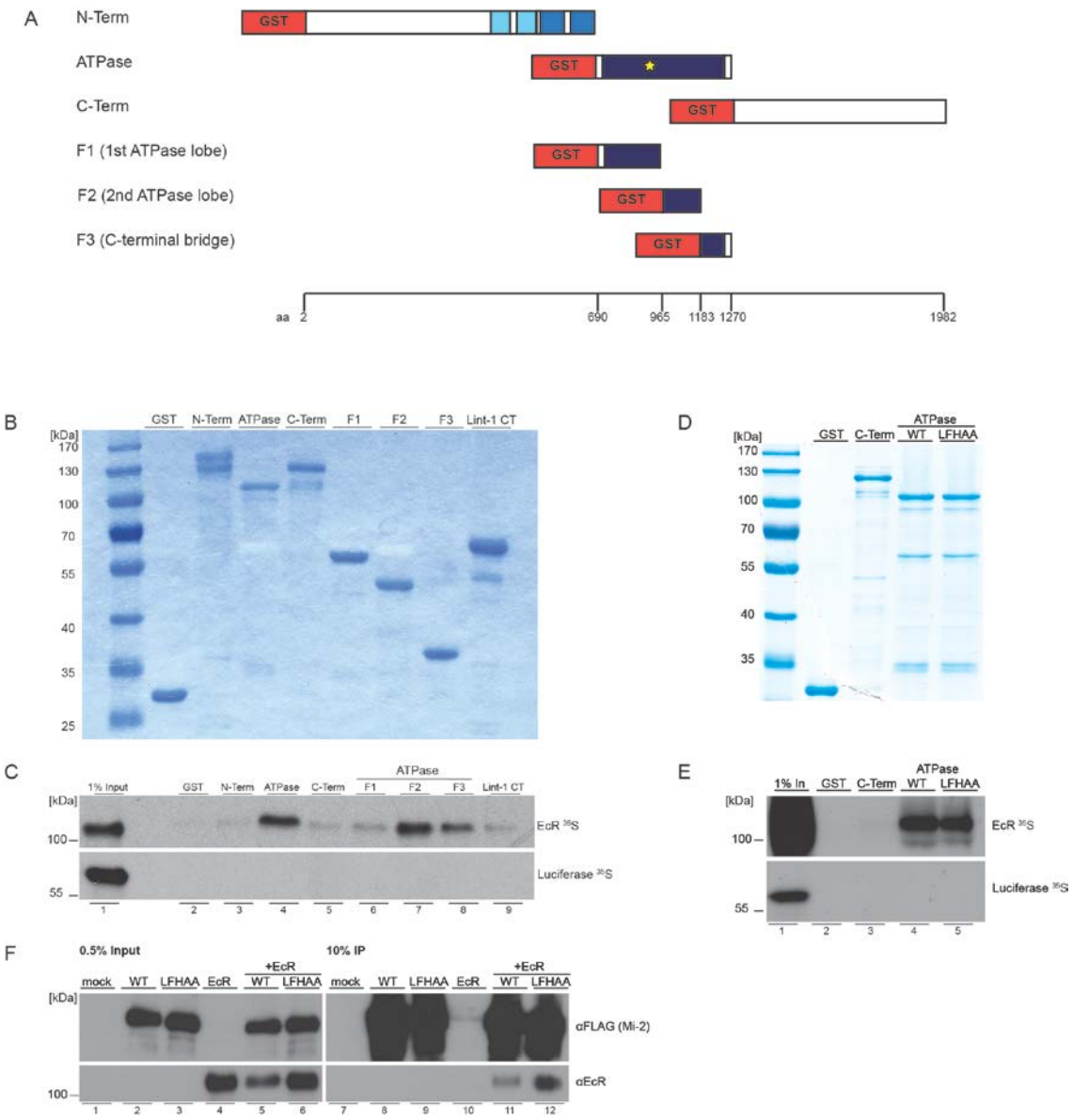

Figure 4.16: ATPase domain of Mi-2 interacts with EcR. (A) Schematic representation of designed Mi-2 GST fragments. C-terminal GST-tag is indicated in red. Blue boxes depict domains within Mi-2: light blue - PHD domain, medium blue - Chromodomain, dark blue - ATPase domain. Yellow star indicates position of the LFHLL motif within the ATPase domain. Guide below depicts position of amino acids (aa) within the protein. (B) Coomassie stained SDS-PAGE of GST proteins depicted in (A) as well as GST and GST-Lint-1 C-terminus (Lint-1 CT). 500ng of purified protein was loaded. (C) *In vitro* translated, ^{35}S-labelled EcR (upper panel) or Luciferase (lower panel) were incubated with 2µg of proteins on Glutathione beads. Lint-1 C-Terminus (Lint-1 CT) and GST served as a negative control. Bound proteins were separated by SDS-PAGE and detected by autoradiography. Input: 1% of *in vitro* translations. (D) Coomassie stained SDS-PAGE of GST-Mi-2 C-terminus (C-Term), wildtype ATPase and ATPase mutant (LFHAA) as well as GST. 500ng of purified protein was loaded. (E) *In vitro* translated, ^{35}S-labelled EcR (upper panel) or Luciferase (lower panel) were incubated with 2µg of proteins on Glutathione beads. Mi-2 C-Terminus (C-Term) and GST served as a negative control. Bound proteins were separated by SDS-PAGE and detected by autoradiography. Input (1%In): 1% of *in vitro* translations. (F) Sf9 cells were co-infected with baculoviruses expressing Mi-2-FLAG WT or LFHAA mutant and EcR as indicated on top. Extracts were immunoprecipitated with anti-FLAG antibody immobilised on agarose beads. Immunoprecipitates were subjected to Western blot using antibodies indicated on the right. Left panel shows 0.5% of the total input sample that was used for IP. Right panel shows 10% of the total immunoprecipitated sample. Molecular weight in kDa is depicted on the left.

Similarly to the results observed before, the wildtype ATPase domain bound EcR whereas no binding to the C-terminal domain and the GST sample was observed (Figure 4.16E lanes 2-4). Notably, pull-down of EcR with the mutant ATPase domain was as efficient as with the wildtype protein (lanes 4 and 5). Also, specificity of the GST pull-down was confirmed by incubation of all proteins with radioactively labelled luciferase as a negative control (Figure 4.16F, lower panel). As expected, none of the GST-tagged proteins bound to luciferase (lanes 2-5). Therefore, I concluded that the LFHLL motif is not the crucial amino acid sequence that mediates the interaction with EcR in this *in vitr*o assay.

In the GST pull-down assay, the isolated ATPase domain was used to precipitate EcR. However, a difference in interaction may depend on the presence of full-length proteins *in vivo*. Hence, the same changes in amino acid sequence were introduced by site-directed mutagenesis into the full-length Mi-2 protein for expression in the Baculovirus system. Western blot illustrates that the wildtype as well as the mutant proteins were expressed to a similar extent (Figure 4.16F, lanes 2-3 and 5-6). As shown previously, IP of wildtype Mi-2-FLAG co-purified EcR (lane 11). Co-expression of the FLAG-tagged LFHAA mutant and EcR did show stronger enrichment of EcR after co-IP (lane 12). However, EcR expression in the cells co-expressing EcR and the LFHAA mutant (lane 6) was stronger than in the co-expression of Mi-2 WT and EcR (lane 5). Therefore, I concluded that both, the WT and LFHAA Mi-2 can interact with EcR to a similar extent. In summary, the LFHAA motif in the ATPase domain of Mi-2 did also not contribute to the interaction with EcR in the context of the full-length protein.

Since the LFHLL motif within the first ATPase lobe of Mi-2 was shown to not be relevant for an interaction with EcR, I wanted to further map the binding domain within the Mi-2 ATPase that contributes to this interaction. In order to accomplish this, smaller fragments of the Mi-2 ATPase domain were designed. A recent publication by Hauk *et al.* addressed the structure of the ATPase domain of yeast Chd1 by crystallography (Hauk et al., 2010). Since the ATPase domain is highly conserved between different ATP-dependent chromatin remodelers of the SNF2 superfamily, this crystal structure was used to identify three subdomains within the ATPase domain of Mi-2. Therefore, the ATPase domain was split into three fragments, containing the first ATPase lobe (F1, aa 690 to 965), the second ATPase lobe (F2, aa 966 to 1183) and the C-terminal bridge (F3, aa 1184 to 1270) (Figure 4.16A). All three fragments were expressed, purified as GST fusion proteins (Figure 4.16B) and subjected to incubation with radioactively labelled EcR (Figure 4.16C lanes 6-8). The fragment F2, containing the

second ATPase lobe showed strongest interaction with EcR. However, also the C-terminal bridge (F3) enriched EcR in the *in vitro* pull-down assay. Fragment F1 that contained the first ATPase lobe, showed no enrichment of EcR. In conclusion, the GST pull-down assay demonstrated that the interaction between Mi-2 and EcR is most likely direct. Interestingly, this interaction was mapped to the ATPase domain of Mi-2, more specifically to the second ATPase lobe as well as the C-terminal bridge.

4.3.6 ATPase domains of several chromatin remodelers interact with EcR

The ATPase domain is highly conserved between several ATP-dependent chromatin remodeler of the SNF2 superfamily in different species. Previous results demonstrated that the interaction between EcR and Mi-2 was dependent on the ATPase domain of Mi-2. To investigate whether other chromatin remodelers can bind via their ATPase domain to EcR, the ATPase domains of ISWI, Chd1 and Chd3 were expressed and purified as GST-tagged proteins. Detection of the purified samples on Coomassie showed enriched proteins at the expected molecular weights, yet in all protein samples few additional bands were detected, indicating protein degradation (Figure 4.17A). The GST-tagged ATPase domains of the different chromatin remodelers were incubated with *in vitro* translated, ^{35}S-labelled EcR. Surprisingly, all tested ATPase domains showed binding to EcR (Figure 4.17B lanes 4-7). Mi-2, ISWI and Chd1 enriched comparable amounts of EcR, whereas Chd3 pulled down more EcR compared to the other ATPase domains. As demonstrated before, GST and Lint-1 C-terminus, that served as negative controls, showed only weak interaction with EcR (lanes 2 and 3). Also, incubation of GST-bound proteins with *in vitro* translated luciferase did not result in binding to any of the tested proteins, demonstrating the specificity of the experiment. From these results I concluded that the isolated ATPase domains of Mi-2, Iswi, Chd1 and Chd3 can interact with EcR *in vitro*.

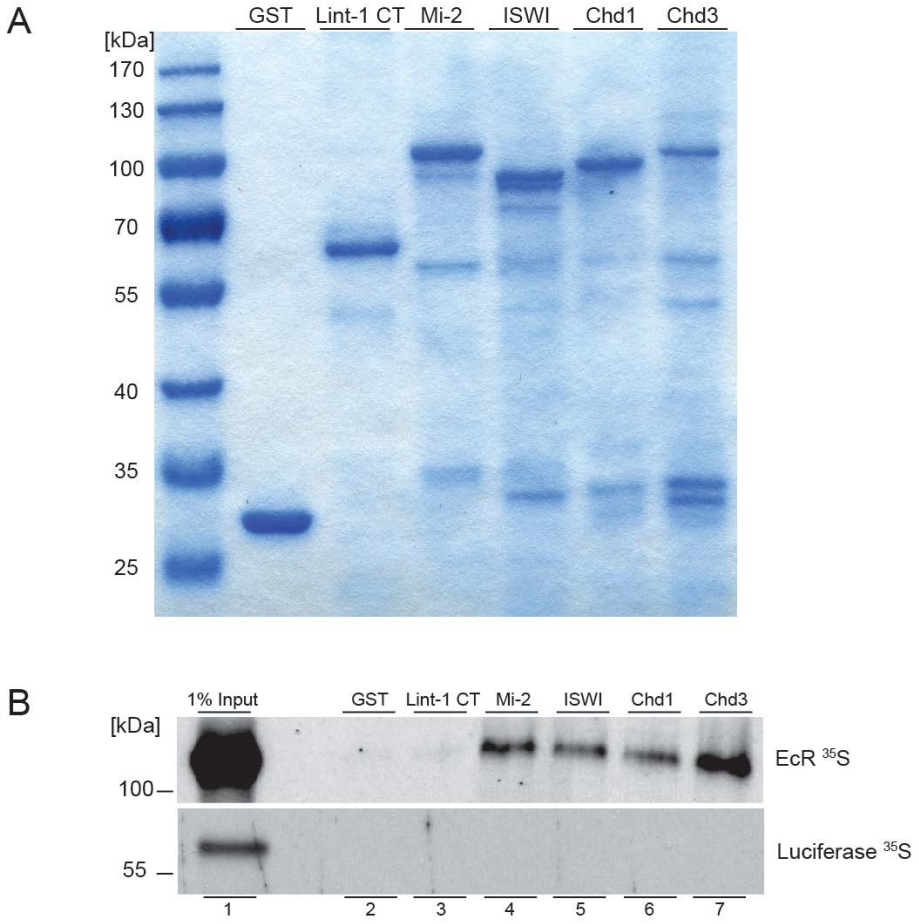

Figure 4.17: ATPase domains of several ATP-dependent chromatin remodelers interact with EcR. (A) Coomassie stained SDS-PAGE of GST-ATPases as well as GST and GST-Lint-1 C-terminus (Lint-1 CT). 500ng of purified protein was loaded. (B) *In vitro* translated, ^{35}S-labelled EcR (upper panel) or Luciferase (lower panel) were incubated with 2µg of proteins on Glutathione beads. Lint-1 C-Terminus (Lint-1 CT) and GST served as a negative control. Bound proteins were separated by SDS-PAGE and detected by autoradiography. Input: 1% of *in vitro* translations. Molecular weight in kDa is depicted on the left. Experiment was designed by me and performed by Anna Ernst under my supervision.

4.3.7 The activation function 2 (AF2) of EcR interacts with Mi-2

In order to identify the domain within EcR that mediates the interaction with Mi-2, mapping studies with isolated EcR domains were conducted. EcR contains four conserved domains that have been studied in detail in several NRs (Figure 4.18A) (Hill et al., 2013). The N-terminus contains a domain that has been shown to contribute to transcriptional activation independent of the presence on hormone and is therefore called activation function 1 (AF1). Located adjacent to the AF1 is the DNA binding domain (DBD) that has been shown to directly mediate DNA contacts. Further, the activation function 2 (AF2) that contains the ligand binding domain, and a rather unstructured C-terminal domain (CT) make up the full-length EcR protein. All four fragments were produced and radioactively labelled with ^{35}S-methionine by *in vitro*

translation (Figure 4.18B, lanes 4, 7, 10 and 13). These fragments were then used in a GST pull-down assay with GST-Mi-2-ATPase domain and GST (as a negative control). As expected, incubation of the ATPase domain and full-length EcR showed clear enrichment of EcR in comparison to GST (lanes 2 and 3). Interestingly, also incubation with AF1, DBD and AF2 showed interaction with the ATPase domain (lanes 6, 9 and 12). In comparison, no protein was enriched when beads were exposed to *in vitro* translated C-terminus of EcR or luciferase (lanes 15 and 18). This observation was made in the presence of 150mM (data not shown) as well as under more stringent conditions with 250mM salt (Figure 4.18). This result showed that the AF1, DBD and AF2 domains of EcR can interact with the ATPase domain of Mi-2 in a GST pull-down.

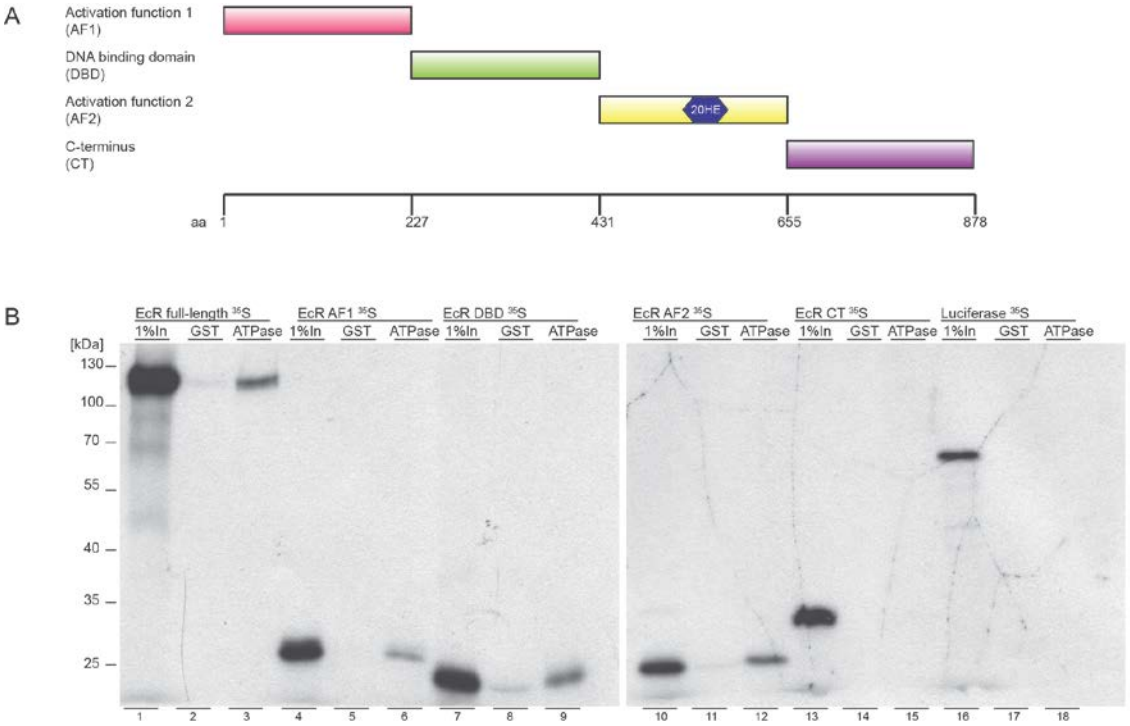

Figure 4.18: Multiple EcR fragments can interact with Mi-2 ATPase domain in GST pull-down assays. (A) Schematic representation of EcR domains produced by *in vitro* translation in (B). Ecdysone (20HE) binding site is indicated in blue. Guide below depicts position of amino acids (aa) within the protein. (B) *In vitro* translated, ^{35}S-labelled EcR domains or Luciferase were incubated with 2µg of GST or Mi-2 ATPase domain on Glutathione beads. Bound proteins were separated by SDS-PAGE and detected by autoradiography. Input (1%In): 1% of *in vitro* translations. Molecular weight in kDa is depicted on the left.

Mapping of the interaction domain of EcR was also performed using an independent interaction assay. Therefore, FLAG-tagged versions of AF1, DBD, AF2 and the C-terminal domain of EcR were expressed in Sf9 cells in the presence of untagged full-length Mi-2. Three of the four viruses were expressed to a similar extent (Figure 4.19 lanes 3,4 and 6), FLAG-AF2 however, was expressed less (lane 5). In order to get an idea which of the fragments interacts with Mi-2, FLAG-IP was performed (lanes 11-20).

Co-expression of the FLAG-AF2 and Mi-2 resulted in strong co-IP of Mi-2 (lane 19). All other FLAG-EcR fragments did not co-immunoprecipitate Mi-2 (lanes 17, 18 and 20). This result demonstrated that the AF2 domain of EcR can interact with full-length Mi-2 when overexpressed in the Baculovirus system. In conclusion, the AF2 domain was identified in two independent assays as the domain that bound to Mi-2. Therefore, it is most likely that this domain plays an important role in mediating the interaction between Mi-2 and EcR.

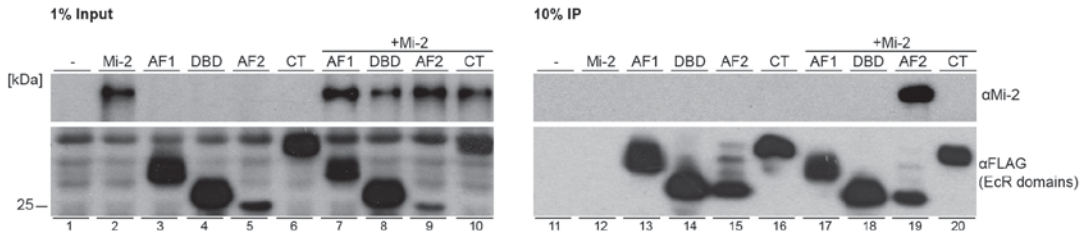

Figure 4.19: AF2 domain of EcR interacts with Mi-2. Sf9 cells were co-infected with baculoviruses expressing FLAG-tagged EcR domains as indicated in Figure 4.19A and Mi-2 as indicated on top. Extracts were immunoprecipitated with anti-FLAG antibody immobilised on agarose beads. Immunoprecipitates were subjected to Western blot using antibodies indicated on the right. Left panel shows 1% of the total input sample that was used for IP. Right panel shows 10% of the total immunoprecipitated sample. Molecular weight in kDa is depicted on the left.

4.3.8 Mi-2 ATPase domain and AF2 domain of EcR are sufficient for interaction

Previous results showed that the ATPase domain was able to interact with full-length EcR and that the AF2 domain bound to full-length Mi-2. In order to demonstrate that both domains are sufficient for this interaction, FLAG-tagged ATPase domain of Mi-2 and HA-tagged AF2 domain of EcR were co-expressed in Sf9 cells (Figure 4.20, lane 6). In addition, cells were infected with HA-AF1 as a negative control (lane 5). As observed earlier, expression of AF2 was much less efficient than expression of AF1. FLAG-IP of the Mi-2 ATPase domain showed co-IP of the EcR AF2 domain (lane 12). Also, co-IP of FLAG-Mi-2 in the presence of the AF1 domain showed enrichment of the AF1 in IP (lane 11). However, this interaction was much weaker compared to the interaction with the AF2 domain. Hence, it was confirmed that the ATPase domain of Mi-2 and the AF2 fragment of EcR were sufficient for an interaction between the two proteins.

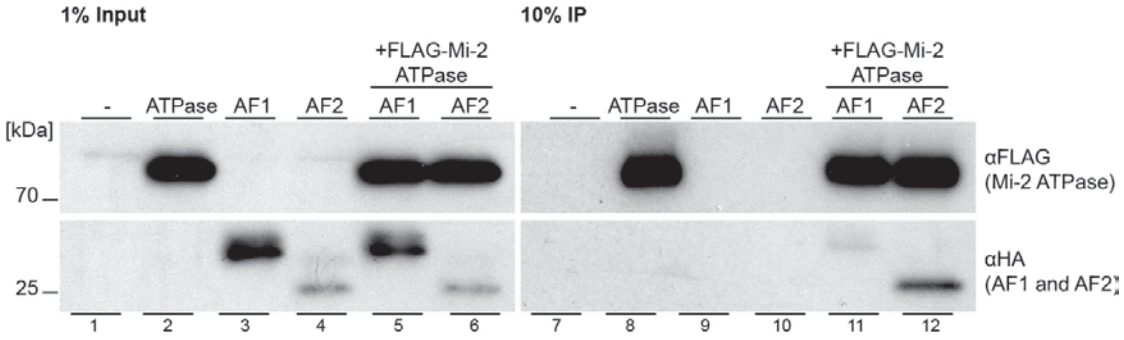

Figure 4.20: AF2 domain of EcR and ATPase domain of Mi-2 are sufficient for interaction. Sf9 cells were co-infected with baculoviruses expressing HA-tagged AF1 or AF2 fragments and FLAG- Mi-2 ATPase as indicated on top. Extracts were immunoprecipitated with anti-FLAG antibody immobilised on agarose beads. Immunoprecipitates were subjected to Western blot using antibodies indicated on the right. Left panel shows 1% of the total input sample that was used for IP. Right panel shows 10% of the total immunoprecipitated sample. Molecular weight in kDa is depicted on the left.

4.4 Recruitment of Mi-2 to ecdysone dependent genes

4.4.1 Inhibition of transcription elongation does not affect Mi-2 recruitment

Previous studies demonstrated various recruitment mechanisms for Mi-2 to chromatin. For example, Mi-2 can be recruited by poly-ADP-ribose (PAR) and binds to the nascent *hsp70* transcript upon activation of gene expression by heat shock (Murawska et al., 2011). Therefore, it was proposed that Mi-2 follows the elongating RNA PolII by association with the nascent transcript. 5,6-dichloro-1-beta-D-ribofuranosylbenzimidazole (DRB) blocks transcription at the early stages of RNA Pol II elongation by inhibiting CDK7 kinase (Dubois et al., 1994). To test the effect of inhibition of transcription elongation at the *vrille* gene, Mi-2 ChIP was performed in the presence of DRB. Efficient DRB treatment was demonstrated by a fivefold decrease of *vrille* transcript in 20HE stimulated cells in the presence of DRB as compared to 20HE induced cells without inhibitor. However, transcription elongation was not completely inhibited, since some increase in *vrille* transcript was detected compared to untreated S2 cells (Figure 4.21A). Mi-2 binding analysed by ChIP did not show any changes in untreated cells upon incubation with DRB (Figure 4.21B). Furthermore, recruitment of Mi-2 to the previously identified regions was not impaired in the presence of the inhibitor. In conclusion, reduction of nascent *vrille* RNA levels did not disturb Mi-2 binding to the gene. This indicates that an interaction with the nascent RNA transcript does not make a significant contribution to binding of Mi-2 to the *vrille* locus.

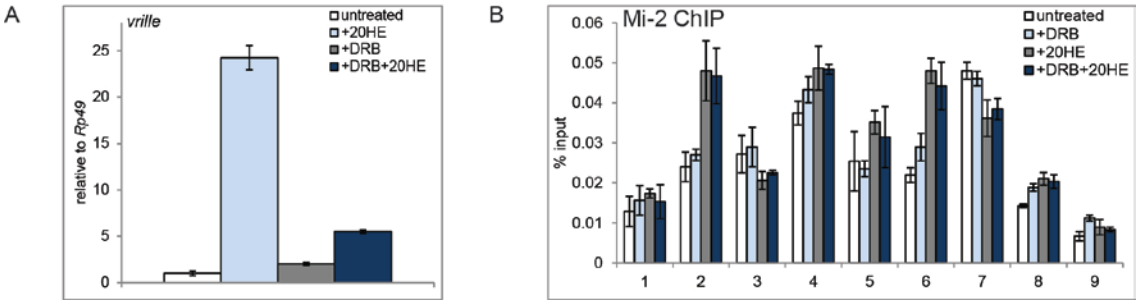

Figure 4.21: Mi-2 binding to *vrille* is not altered upon 5,6-dichloro-1-bold beta-D-ribofuranosylbenzimidazole (DRB) treatment. (A) Expression of mRNA of *vrille* in cells incubated with (white and grey bars) or without (light and dark blue bars) 20HE and additionally stimulated with DRB (grey and dark blue bar) was determined by RTqPCR. mRNA levels were calculated relative to the housekeeping gene *Rp49* and mRNA levels in untreated cells were set to 1. (B) ChIP was performed using an antibody against Mi-2. Chromatin was prepared from S2 cells incubated with (white and grey bars) or without (light and dark blue bars) 20HE and additionally stimulated with DRB (grey and dark blue bars). Purified DNA was quantified by qPCR with oligos at the binding sites indicated in Figure 4.6. Values are expressed as % input. Error bars denote standard deviation of technical triplicates. Experiments were performed as biological triplicates and one representative experiment is shown here.

4.4.2 Mi-2 binding on chromatin correlates with EcR binding sites

Since an interaction with the nascent RNA transcript appeared not to play an important role in dMi-2 recruitment I investigated the potential involvement of EcR in Mi-2 recruitment to chromatin. NRs have been demonstrated to function by recruiting co-regulatory proteins to chromatin. Since Mi-2 and EcR interact physically, I hypothesised that EcR can recruit Mi-2 to specific binding sites in the genome. EcR binding sites were mapped genome-wide in Drosophila in two studies to date. A publication by Gauhar and colleagues identified EcR/USP binding upon six hours of 20HE treatment in Kc167 cells using DamID (Gauhar et al., 2009). This study identified 502 binding sites for the EcR/USP complex. Due to technical reasons, the binding regions identified by DamID are rather broad with an average size of 4 to 5kb. A recent study by the Stark lab mapped EcR binding sites by ChIPSeq in S2 cells (Shlyueva et al., 2014). This technique identified 9148 EcR binding sites in untreated and 9305 EcR binding sites in cells that were treated for 24 hours with 20HE.

In order to test if Mi-2 and EcR reside in close proximity on chromatin, the overlap between Mi-2 and EcR binding sites was analysed on a genome-wide level. Therefore, Mi-2 binding sites from ChIPSeq were compared to ChIPSeq data for EcR published by the Stark lab. To determine the correlation between Mi-2 and EcR binding sites, the strongest 10% Mi-2 peaks (in terms of tag counts) were selected and used to calculate the overlap with all EcR binding sites (Figure 4.22A). I selected the strongest 10% Mi-2 peaks since these obtained the most reads from sequencing and were therefore the

most confident. Mi-2 and EcR peaks had to overlap by at least one base in order to be defined as “overlapping”. In case two or more Mi-2 binding sites overlapped with the same EcR peak, this co-occupancy was only counted once. In untreated S2 cells, 215 out of 1643 Mi-2 binding sites overlapped with EcR binding sites. This overlap was comparable in 20HE treated cells, where 198 out of 1499 Mi-2 peaks coincided with EcR binding sites. In both conditions, approximately 13% of Mi-2 binding sites overlapped with EcR peaks. This overlap was significantly higher than expected if the binding sites were randomly distributed across the genome (Monte-Carlo-method, personal communication R. Pahl and F. Finkernagel). These results were further supported by a comparison between 20HE induced Mi-2 binding sites (103 peaks, Table 7.1) and all EcR binding sites in the presence of 20HE from the Stark data. Here, 35 of 103 induced Mi-2 peaks overlapped with EcR binding sites in the presence of hormone (Figure 4.22B). Even though this comparison considered only a small subset of Mi-2 binding sites that are more than 2.3fold induced upon 20HE treatment, 33.7% of these binding sites show an overlap with EcR binding sites. In summary, genome-wide analysis identified a significant overlap between Mi-2 and EcR binding sites in both untreated and 20HE treated S2 cells.

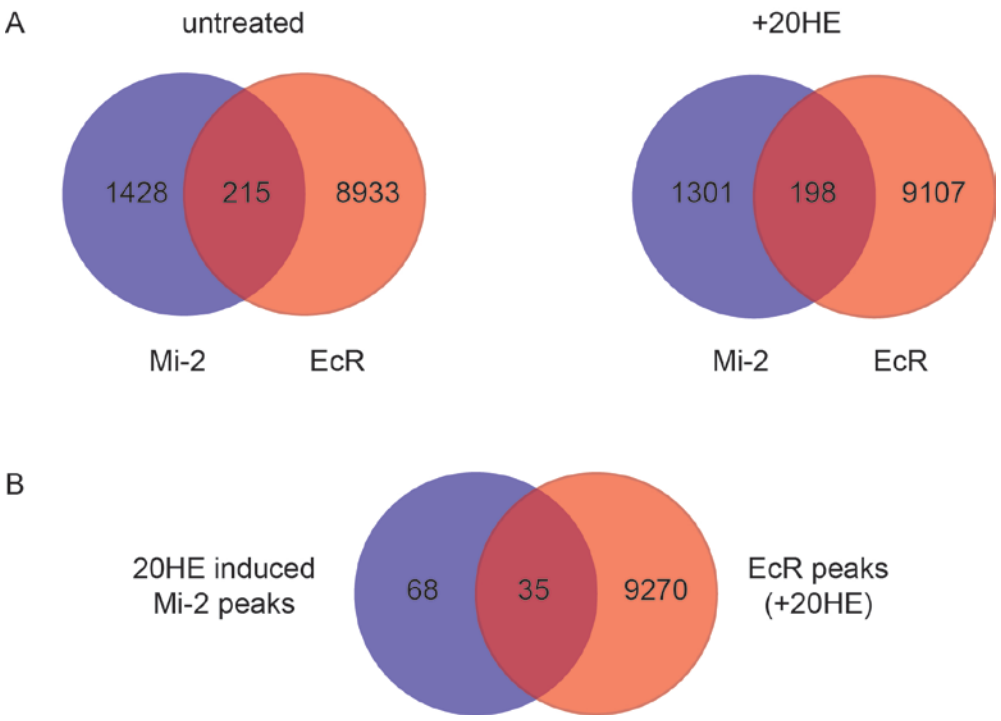

Figure 4.22: Genome-wide overlap of Mi-2 and EcR binding sites. (A) Overlap between Mi-2 and EcR binding sites in untreated and +20HE treated S2 cells is depicted in a Venn diagram. The 10% Mi-2 bindings sites with the highest tag count in ChIPSeq were considered. (B) Overlap between 20HE induced Mi-2 binding sites (Appendix, Table 7.1) and EcR binding sites in 20HE treated S2 cells is depicted in a Venn diagram. (A) and (B) EcR binding sites were taken from (Shlyueva et al., 2014). Overlap is defined as a co-occupancy of Mi-2 and EcR binding sites of at least 1bp at the same genomic region.

For detailed investigation of the co-occupancy of Mi-2 and EcR at the *broad* and *vrille* loci, the EcR binding profile, identified by the two studies described above, was analysed (Figures 4.23 and 4.24). Gauhar and colleagues identified several EcR/USP binding sites upon 20HE treatment at the *broad* locus (Figure 4.23, grey boxes). The Mi-2 peak in the 5' UTR (Figure 4.5, region A) as well as the region within the first intron (Figure 4.5, region B and C) showed an overlap with 20HE induced EcR/USP binding mapped by DamID. However, no overlap between 20HE induced EcR/USP binding at region D within the exon of the *broad* (Figure 4.5) gene was identified. With respect to *vrille* the study found two broader regions of 20HE induced EcR/USP binding both of which overlap with either one of the regions where Mi-2 is recruited upon 20HE induction (Figure 4.24, grey boxes).

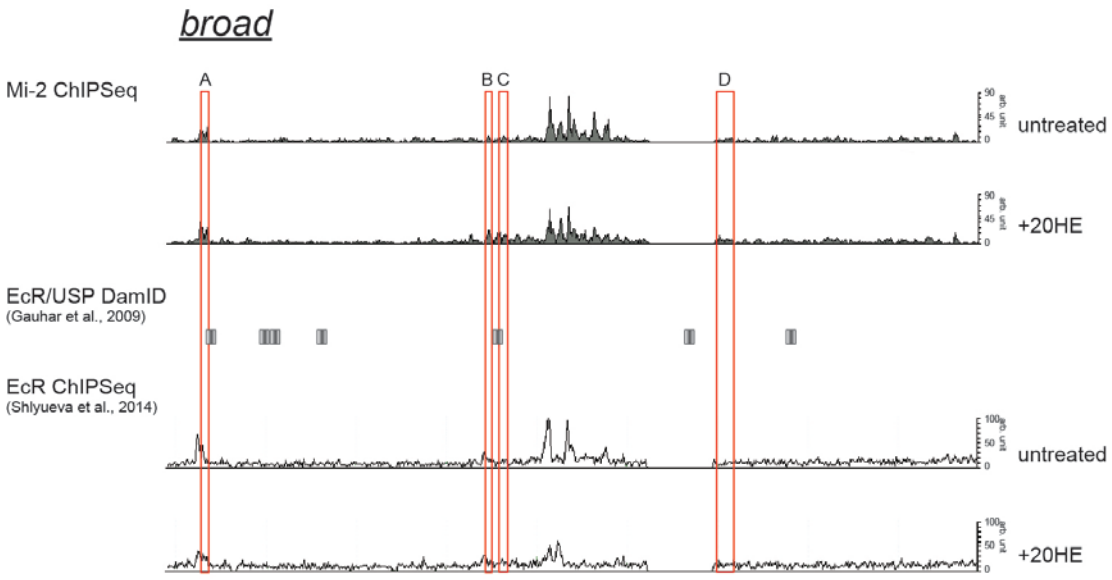

Figure 4.23: Comparison of Mi-2 and EcR binding sites at the *broad* locus. Mi-2 binding profile at the *broad* locus as demonstrated in Figure 4.5. Regions A-D (red boxes) depict sites of increased Mi-2 binding upon 20HE treatment as calculated from ChIPSeq (Zoom-in Figure 4.5). EcR/USP binding sites identified by DamID upon six hours of 20HE treatment taken from (Gauhar et al., 2009) are depicted as grey boxes. EcR ChIPSeq tracks from (Shlyueva et al., 2014) in untreated and 20HE treated cells are illustrated.

The identification of EcR binding sites by ChIPSeq from the Stark lab allowed to directly compare binding profiles of Mi-2 and EcR with a better resolution than the EcR/USP binding sites identified by DamID. Interestingly, at the *broad* locus, EcR displayed a similar binding pattern as Mi-2 in untreated cells (Figure 4.23). Both proteins showed enriched binding at the 5' UTR and a broad binding region within the first intron (see Figure 4.5). EcR binding in 20HE treated cells was not altered significantly in the study from the Stark lab. No clear enrichment of EcR upon hormonal stimulation was detected across the *broad* gene and at the 20HE induced Mi-2 binding

sites A to D. This difference may be due to the fact that the Stark lab identified EcR binding sites by ChIPSeq after 24 hours of 20HE treatment. However, *broad* is an early induced gene that is transcribed shortly after 20HE treatment (Figure 4.9C). Therefore, I hypothesised that 20HE induced EcR binding at the *broad* locus can be detected shortly after hormonal treatment, but can not be seen after 24 hours, the time point analysed by the Stark lab. This may explain why no overlap between 20HE induced Mi-2 and EcR binding at the *broad* gene could be detected. Also, EcR and Mi-2 ChIPSeq tracks were compared for the *vrille* gene (Figure 4.24). In contrast to the observations at the *broad* gene, the binding of Mi-2 and EcR identified by ChIPSeq in untreated cells did not display a comparable pattern. Interestingly, when comparing the EcR and Mi-2 binding profile in 20HE treated cells, EcR binding as determined by the Stark study was clearly enriched at the second 20HE induced Mi-2 binding site (region Y) at the *vrille* locus. No such overlap was observed for the first Mi-2 peak (region X) within the *vrille* gene. In conclusion, a comparison of the Stark ChIPSeq data set has revealed that Mi-2 and EcR coincide at several binding sites at the *broad* and *vrille* genes in the absence of hormone. Additionally, 20HE induced Mi-2 binding identified in this thesis and EcR binding upon hormonal treatment determined by the Stark lab were shown to coincide at one binding site within the *vrille* gene.

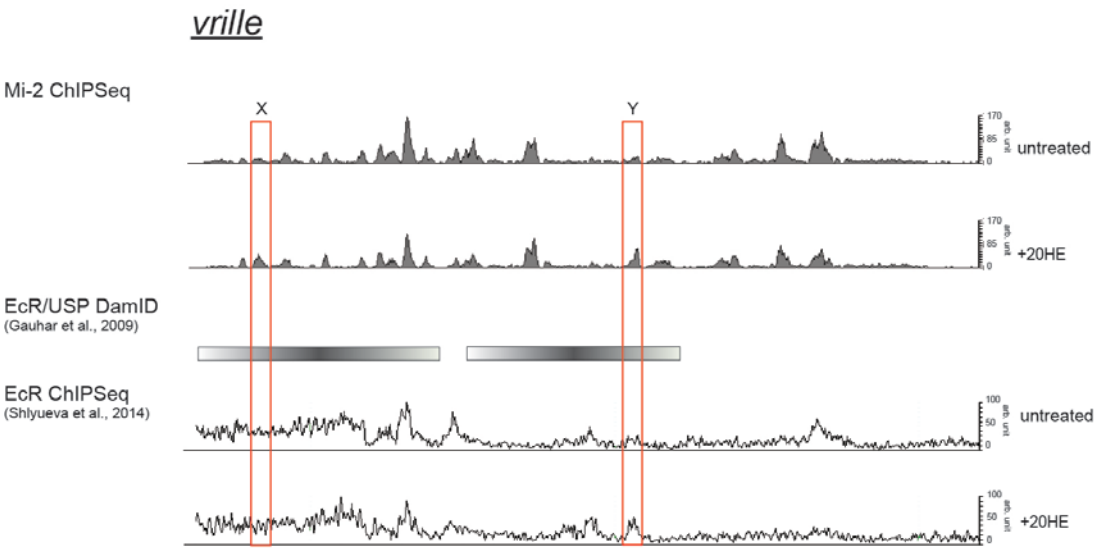

Figure 4.24: Comparison of Mi-2 and EcR binding sites at the *vrille* locus. Mi-2 binding profile at the *vrille* locus as demonstrated in Figure 4.5. Regions X and Y (red boxes) depict sites of increased Mi-2 binding upon 20HE treatment as calculated from ChIPSeq. EcR/USP binding sites identified by DamID upon six hours of 20HE treatment taken from (Gauhar et al., 2009) are depicted as grey boxes. EcR ChIPSeq tracks from (Shlyueva et al., 2014) in untreated and 20HE treated cells are illustrated.

In order to verify binding of EcR/USP within the *broad* and *vrille* genes at the binding sites identified above, EcR ChIP followed by qPCR was performed. However, anti-EcR

antibody did not precipitate EcR efficiently in ChIP (data not shown). To circumvent this problem, binding sites were analysed by ChIP with an anti-USP antibody since EcR is recruited to ecdysone responsive genes in complex with its heterodimerisation partner USP (Figure 4.25) (Thomas et al., 1993).

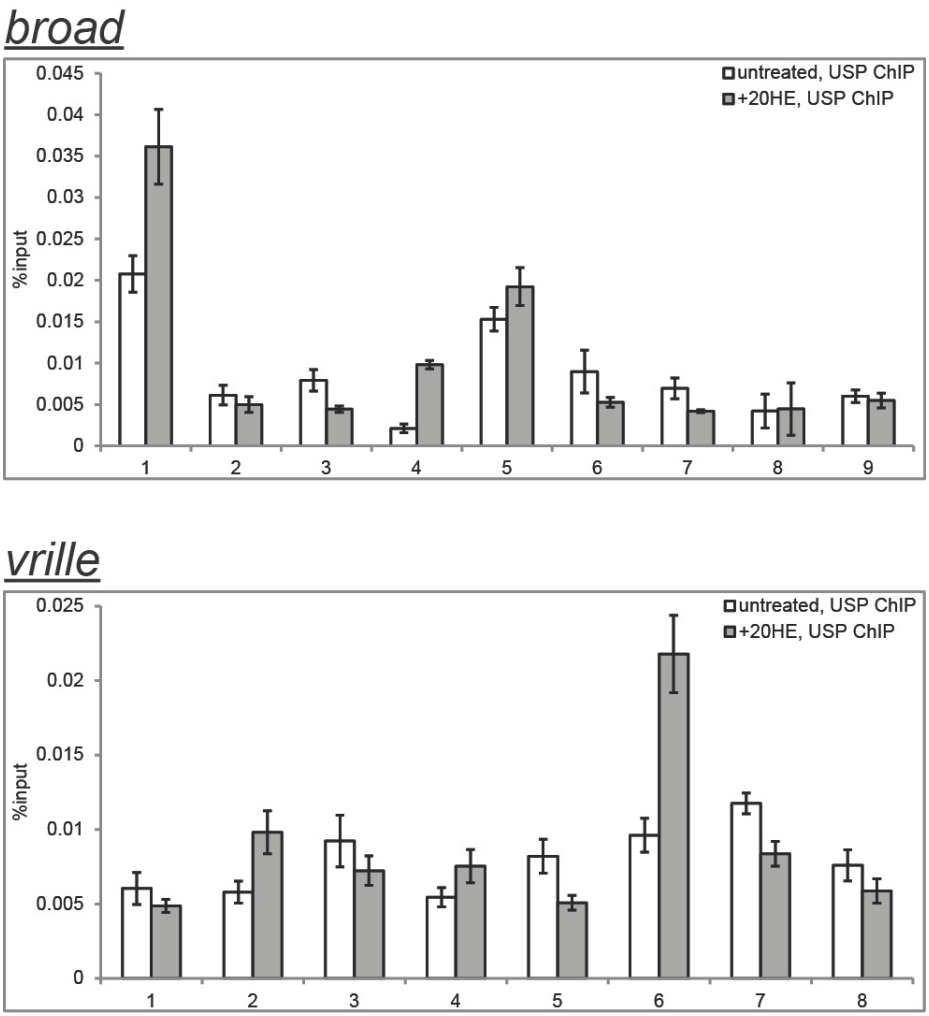

Figure 4.25: Identification of USP binding sites at *vrille* and *broad* by ChIP qPCR. (A) ChIP was performed using an antibody ag41ainst USP. Chromatin was prepared from untreated (white bars) and 20HE treated (grey bars) S2 cells. Values are expressed as % input. Purified DNA was quantified by qPCR with oligos at binding sites indicated in Figure 4.5 (*broad*) and Figure 4.6 (*vrille*). “Intergenic” refers to an unrelated intergenic region on chromosome arm 2R (see Material and Methods). Error bars denote standard deviation of technical triplicates. Experiment was performed as biological duplicate and one representative experiment is shown here.

Unfortunately, precipitation of USP was also inefficient as only 0.01% input was precipitated at most of the sites tested in untreated and 20HE treated cells. However, a few binding sites showed higher enrichment of USP upon 20HE treatment. For the *broad* gene, binding site 1 and 4 showed two- to threefold increased USP signal upon hormonal stimulation. Both of these regions overlapped with sites of Mi-2 recruitment upon ecdysone induction (Figure 4.23). However, binding site 5 that overlapped with a

predicted EcR/USP region, did not show enrichment of USP in ChIP (Gauhar et al., 2009). At the *vrille* gene two binding sites (2 and 6) showed twofold increased recruitment of USP upon 20HE stimulation. In fact, these two sites also showed enrichment of Mi-2 in ecdysone treated cells (Figure 4.6 and Figure 4.7, regions X and Y), and overlapped with the predicted EcR/USP binding sites in the study by Gauhar and colleagues (Figure 4.24). In summary, USP binding sites at the *broad* and *vrille* locus were identified by ChIP. These are likely to be also bound by EcR since EcR and USP heterodimerise in the presence of ecdysone. This may further confirm the correlation between Mi-2 and EcR/USP binding on chromatin. The co-occupancy of Mi-2 and EcR at ecdysone dependent genes together with the ability of both proteins to interact physically (Figure 4.12 and 4.15) may indicate a functional interaction of both proteins in the regulation of hormone regulated genes.

4.4.3 Depletion of EcR decreases recruitment of Mi-2 to *broad* and *vrille* in 20HE treated cells

As described above, Mi-2 and EcR co-occupy several binding sites on chromatin. Further it was shown that both proteins can interact in S2 cells. EcR contains a DNA binding domain that can interact with DNA in a sequence specific manner (Hill et al., 2013) whereas Mi-2 does not contain such a domain. Therefore, I hypothesised that EcR recruits Mi-2 to the *broad* and *vrille* genes in S2 cells. In order to test this hypothesis, EcR was depleted by RNAi and subsequently Mi-2 ChIP was performed for the *broad* and *vrille* genes. The depletion of EcR was efficient as demonstrated by Western blot (Figure 4.9A and data not shown). The binding of Mi-2 across both the *broad* and *vrille* genes did not decrease significantly in untreated, EcR depleted S2 cells as compared to cells treated with GFP dsRNA. (Figure 4.26, bright green bars). However, when EcR depleted S2 cells were stimulated with 20HE, no further recruitment of Mi-2 to the expected sites was detected (dark green bars *broad*: 1, 4 and 5; *vrille*: 2 and 6). I concluded that EcR was not required to maintain Mi-2 binding at ecdysone dependent genes in untreated S2 cells. However, EcR was required for recruitment of Mi-2 to the *broad* and *vrille* genes upon 20HE induction.

broad

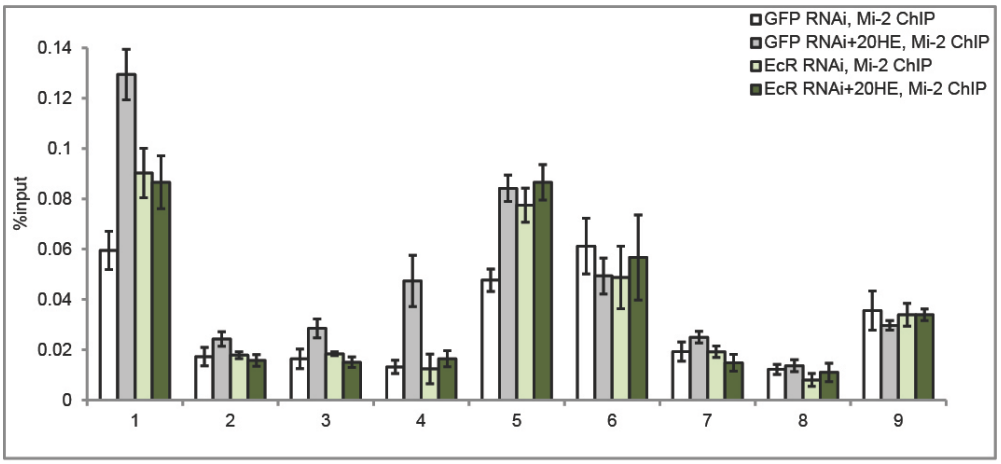

vrille

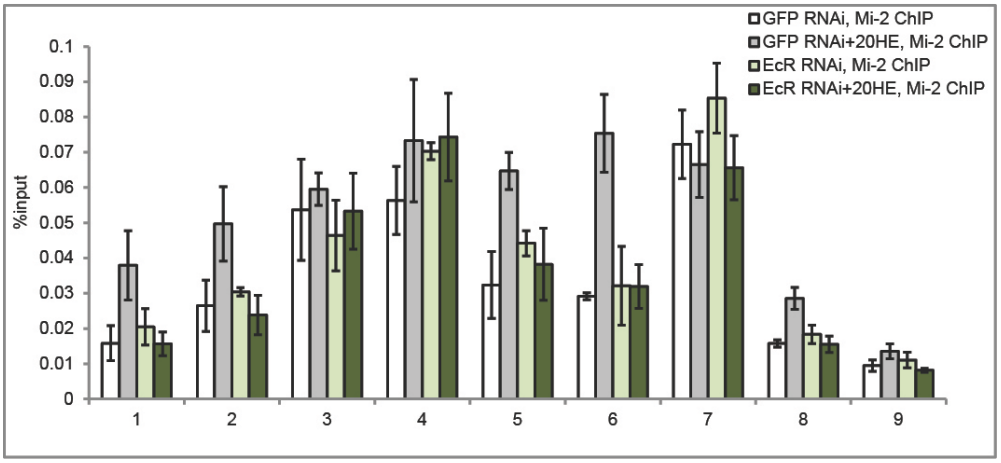

Figure 4.26: Mi-2 recruitment to *broad* and *vrille* upon depletion of EcR. Chromatin was prepared from S2 cells incubated with dsRNA against GFP (white and grey bars) or EcR (light and dark green bars) and incubated with (grey and dark green bars) or without 20HE (white and light green bars). Values are expressed as % input. Purified DNA was quantified by qPCR with oligos at binding regions indicated in Figure 4.5 (*broad*) and Figure 4.6 (*vrille*). Error bars denote standard deviation of technical triplicates. Experiment was performed as biological triplicates and one representative experiment is shown here.

4.5 Regulation of chromatin structure by Mi-2 at the *vrille* gene

4.5.1 Mi-2 maintains chromatin structure at the *vrille* gene

Mi-2 is a nucleosome stimulated, ATP-dependent chromatin remodeler that functions by altering DNA-nucleosome contacts. Therefore, I hypothesised that Mi-2 may contribute to repression of ecdysone dependent genes by changing the DNA accessibility at these loci. In order to establish sites of less DNA accessibility at the *vrille* gene, MNase mapping was performed. MNase is a nuclease that preferentially cleaves internucleosomal DNA. However, DNA that is wrapped within a nucleosome is

relatively protected from digestion by MNase (Heins et al., 1967). I designed three overlapping oligo pairs for every region of interest, such that each oligo pair covered approximately 147 bps, the size of a DNA fragment that is protected from MNase digest by a nucleosome. Seven regions across the *vrille* gene were tested for their sensitivity to MNase (Figure 4.27A, regions A-G). Only when the DNA fragment including both binding sites of an oligo pair were not digested by MNase, a PCR fragment could be generated (Figure 4.27B). Thereby, I determined one oligo pair for each of the seven tested regions that showed the least MNase sensitivity (highest relative MNase protection, Figure 4.27B).

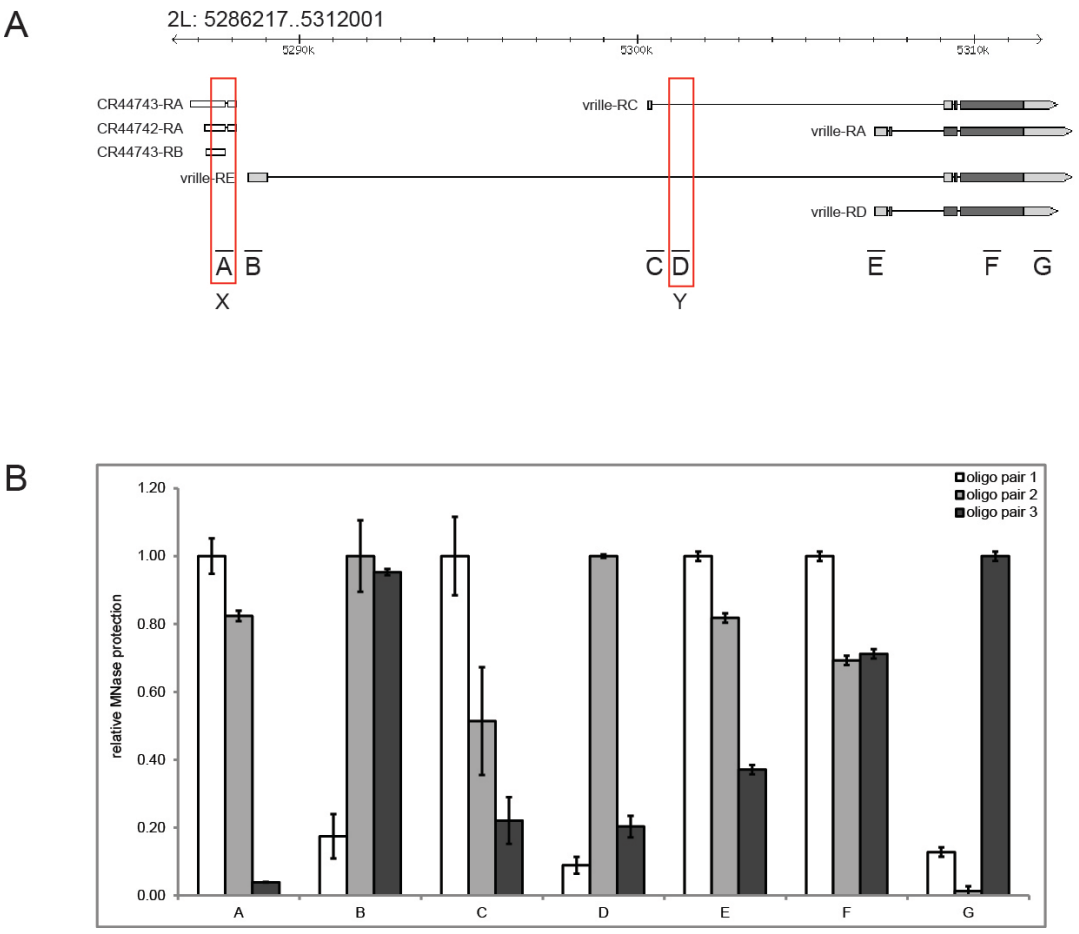

Figure 4.27: Identification of regions in the *vrille* locus that are less sensitive to MNase digest. (A) Schematic representation of the *vrill*e locus. Identified regions with less MNase sensitivity are indicated (A-G). Regions X and Y depict binding sites with increased Mi-2 binding upon 20HE treatment as identified from ChIPSeq (Figure 4.6). (B) MNase mapping was performed in untreated S2 cells. DNA protected from MNase digest was detected by qPCR with three different oligo pairs (1-3) for each tested genomic region (A-G). Relative MNase digest was calculated as $\Delta Ct = 2^{-(Ct_{digested} - Ct_{undigested})}$ (see Material and Methods). Best protected sample for each genomic region was set to 1. Error bars denote standard deviation of technical triplicates. Experiment was performed as biological triplicates and one representative experiment is shown here.

The protection of these regions from MNase is likely due to the presence of nucleosomes. Therefore, these regions are referred to as nucleosomes from here on. However, important to note is that this experiment can not exclude that the observed MNase protection of these regions was due to the binding of other proteins such as transcription factors (Henikoff et al., 2011).

In order to analyse the effect of 20HE treatment on the MNase sensitivity of these seven potential nucleosomes, MNase mapping in untreated and 20HE treated S2 cells was performed (Figure 4.28, white and grey bars). No significant change in MNase sensitivity was observed at most of the tested nucleosomes (A, B, C, F and G). However, at nucleosomes D and E a twofold increase in MNase sensitivity (less relative MNase protection) was detected. Nucleosome D is located within the transcribed region of *vrille(RE)* and *(RC)*, whereas nucleosome E resides at the TSS of the *vrille(RA)* and *(RD)* transcripts. This showed that two regions within the *vrille* gene displayed higher sensitivity to MNase digestion upon 20HE stimulation, whereas the majority of regions tested did not change significantly.

Further, I wanted to investigate the role of Mi-2 in the maintenance of the chromatin structure at the *vrille* gene. Therefore, S2 cells were treated with a dsRNA against Mi-2 and efficient depletion of Mi-2 was verified by Western blot (Figure 4.8 and data not shown). Depletion of Mi-2 showed no significant effect on the MNase sensitivity of most tested nucleosomes compared to GFP dsRNA treated cells (light red bars, B, E, F and G). A small increase (25%) in MNase sensitivity (less relative MNase protection) was detected for nucleosome D, whereas nucleosome C showed decreased (22%) MNase sensitivity (more relative MNase protection). The strongest effect was observed for nucleosome A. Here, depletion of Mi-2 resulted in an 80% increase in sensitivity to MNase digestion as compared to GFP dsRNA treated cells. Nucleosome A overlaps with the region where 20HE induced Mi-2 binding was detected (Figure 4.6, region X). Further, this region is in close proximity to the TSS of *vrille(RE)* and located within the transcribed regions of the two non-coding RNAs *CR44742* and *CR44743.* Both, the *vrille* gene and the non-coding RNAs showed higher expression levels in Mi-2 depleted, untreated cells as compared to GFP dsRNA treated cells (Figure 4.9B and 4.11). Therefore, I concluded that the loss in MNase sensitivity at region A upon Mi-2 depletion correlated with the derepression of *vrille* and the non-coding RNAs.

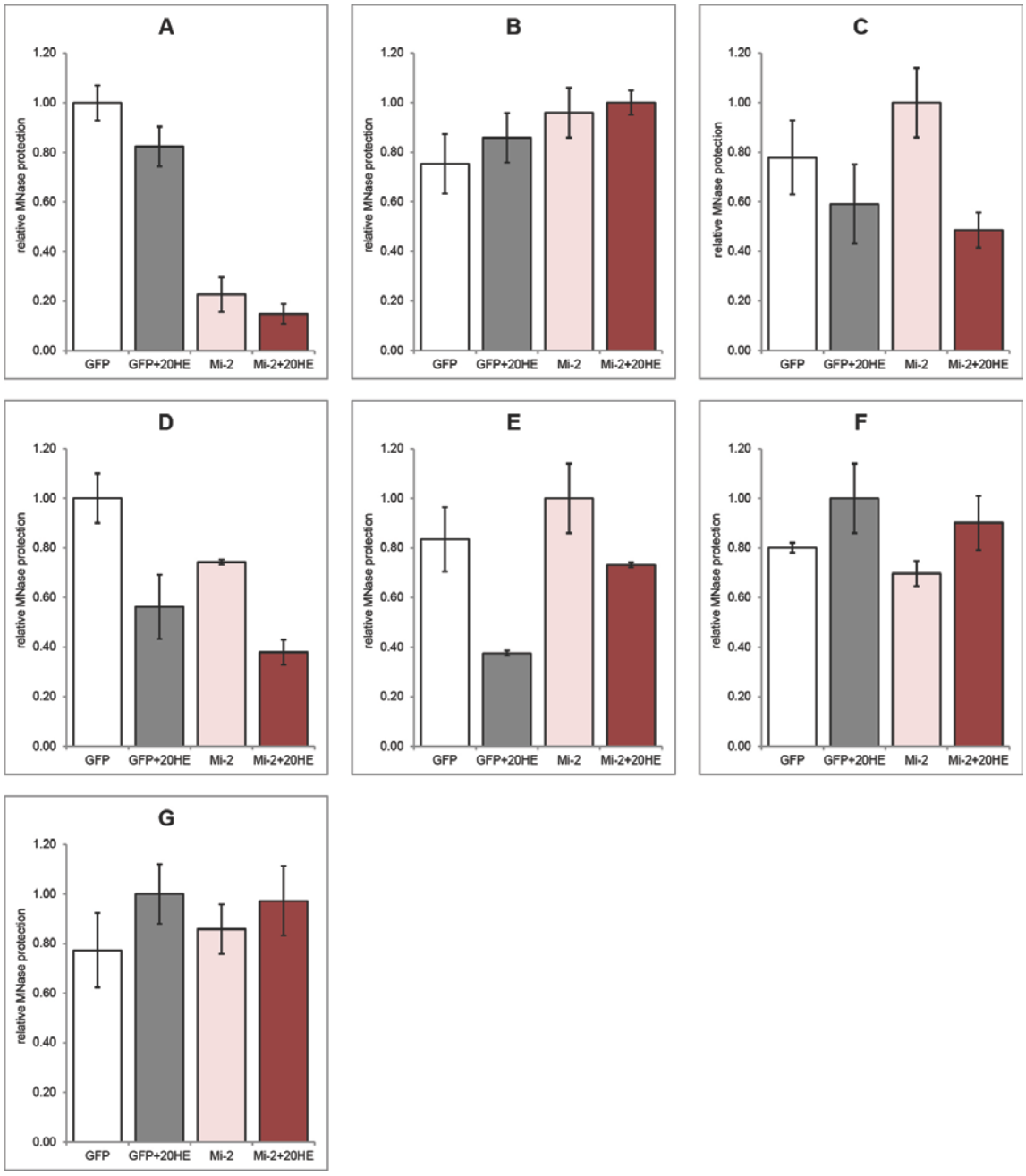

Figure 4.28: Depletion of Mi-2 results in increased MNase sensitivity at the *vrille* gene. MNase mapping was performed in cells treated with dsRNA against GFP (white and grey bars) or Mi-2 (light and dark red bars) in the absence (white and light red bars) or presence (grey and dark red bars) of 20HE. MNase digest was detected by qPCR with one oligo pairs for each tested genomic region (A-G) as determined in Figure 4.27.Relative MNase digest was calculated as $\Delta Ct = 2^{-(Ct_{digested} - Ct_{undigested})}$ (see Material and Methods). Best protected sample for each genomic region was set to 1. Error bars denote standard deviation of technical triplicates. Experiment was performed as biological triplicates and one representative experiment is shown here.

In addition, I wanted to examine the effect of 20HE treatment on MNase sensitivity in Mi-2 depleted cells. Similar to the previous experiment, no strong effect was observed at nucleosomes B, E,F and G and an increase in MNase sensitivity was detected for

nucleosome D. However, nucleosome E showed less increase in MNase sensitivity upon 20HE treatment in Mi-2 depleted cells (25% less relative MNase protection) compared to GFP dsRNA treated cells (50% less relative MNase protection). The increase in MNase sensitivity at nucleosome A upon 20HE treatment was comparable to the findings in untreated, Mi-2 depleted cells. Mi-2 depletion resulted again in a strong increase in MNase sensitivity as compared to GFP dsRNA treated cells (81% less relative MNase protection). From these findings I concluded, that the MNase sensitivity at the *vrille* gene is changed upon 20HE treatment. Further, Mi-2 potentially maintains the chromatin structure at a certain position in the *vrille* gene and the two non-coding RNAs both in untreated and 20HE treated cells. This function of Mi-2 may correlate with its role in the regulation of transcription of *vrille* and the non-coding RNAs in untreated and 20HE treated cells.

5 Discussion

The results described in this thesis demonstrate a function of the ATP dependent chromatin remodeler Mi-2 in the transcriptional regulation of ecdysone dependent genes. Mi-2 was shown to be recruited to several ecdysone dependent genes upon induction of the ecdysone cascade where it functioned as a transcriptional co-repressor. The recruitment of Mi-2 was mediated by a physical interaction with EcR. More specifically, this interaction was found to take place between the ATPase domain of Mi-2 and the activation function 2 (AF2) of EcR. Finally, Mi-2 was shown to maintain a closed chromatin structure at the *vrille* gene. Depletion of Mi-2 resulted in an increased DNA accessibility which correlated with the expression of the *vrille* gene.

5.1 Mi-2 is recruited to ecdysone dependent loci

Initially, it was demonstrated by immunofluorescence experiments that Mi-2 binds to the ecdysone induced puff of the *broad* gene on 3rd instar larvae polytene chromosomes (Magdalena Murawska, Figure 2.10). Previously, *broad* gene expression has been shown to be strongly induced upon ecdysone release and to directly contribute to the expression of late induced genes (Guay and Guild, 1991). Since Mi-2 bound to the *broad* locus on polytene chromosomes, I hypothesized that it is recruited to several other ecdysone inducible genes. In order to test this hypothesis, I aimed to identify genome-wide chromatin binding sites of Mi-2 in response to the hormone ecdysone (20HE). However, immunofluorescence on polytene chromosomes is very limited in its resolution. In order to get a detailed idea of ecdysone induced Mi-2 binding sites, Mi-2 ChIPSeq in untreated and 20HE treated S2 cells was performed.

Bioinformatic analysis identified 103 binding sites where Mi-2 recruitment was increased upon 20HE treatment (Supplementary table 4.1). One region that was highly occupied by Mi-2 upon 20HE treatment, was the *broad* gene (Figure 4.5). This finding verified the observation made on salivary gland polytene chromosomes (Figure 2.10). Several of the 103 identified Mi-2 binding sites were found to be in close proximity or within ecdysone regulated genes. From a selection of 12 Mi-2 binding sites that were strongly increased upon 20HE treatment, 10 were found to be associated with genes that are upregulated upon hormonal stimulation (Figure 4.4). These findings strongly indicate that Mi-2 is involved in the transcriptional regulation of ecdysone dependent genes. Further, the results demonstrate that, in addition to heat shock genes, Mi-2

functions as a regulator of a second group of environmentally regulated genes, namely ecdysone dependent genes (Murawska et al., 2011). This suggests that Mi-2 is involved in the coordinated regulation of related gene sets in Drosophila.

Bioinformatic analysis also identified Mi-2 binding sites upon 20HE induction that were not in the close proximity of an ecdysone inducible gene (Figure 4.4, Table 4.1). It has been shown that transcription of developmental genes is controlled by proteins that bind to enhancers. Enhancers are DNA sequences that can regulate gene transcription independent of the distance, orientation or location with respect to the promoter they control (Ong and Corces, 2011). In order to function, enhancers establish long-distance interactions with the promoter by looping of the intervening sequences (Levine et al., 2014). Therefore, I hypothesised that Mi-2 binding sites, that were not found in close proximity to a ecdysone regulated gene, may be located at ecdysone inducible enhancers with a greater distance from the gene they regulate. However, further experiments need to be conducted in order to confirm this hypothesis.

Mi-2 binding to chromatin was tested in the presence of hormone six hours after addition of 20HE to the medium. Therefore, ChIPSeq analysis visualised Mi-2 binding only at this particular stage of the ecdysone cascade. The gene regulatory processes initiated upon hormonal treatment were shown to occur in a cascade with numerous interrelated steps that activate or inhibit each other (Thummel, 1995). Gene expression analysis of different Drosophila tissues demonstrated that 2268 genes are differentially regulated during the larva to pupa transition (Li and White, 2003). Therefore, it is important to note that Mi-2 may occupy many more binding sites during the course of the ecdysone cascade, which were not identified in this experimental set up.

The binding determined by ChIPSeq was validated at two paradigmatic ecdysone-regulated genes, namely the *broad* and *vrille* loci (Figure 4.7). Here, the Mi-2 binding profile in untreated cells as well as in 20HE treated cell was verified by ChIP followed by qPCR. Recent studies found that highly expressed genes can produce an artefact in ChIPSeq (Teytelman et al., 2013). These so called “hyper-ChIPable” regions show a high enrichment of all kinds of unrelated proteins due to an open chromatin structure. In order to exclude misinterpretation of ChIP results, a ChIP experiment against a heterologous protein was suggested. Since ecdysone induced genes are highly induced upon 20HE treatment, I performed ChIPs with two different control antibodies (Figure 4.7). Control IP with an IgG rabbit antibody demonstrated the specificity of the Mi-2 antibody. Further, ChIP with an antibody against an unrelated protein Lint-1

showed a different distribution at the *broad* and *vrille* gene. Additional confidence about the ChIPSeq profile was gained by knockdown of Mi-2. Here, 20HE induced recruitment of Mi-2 was lost in Mi-2 depleted cells (Figure 4.8). This verified that Mi-2 binding was specific and that the identified DNA sequences were not precipitated due to an open, “hyper-ChIPable” chromatin structure at the loci.

Interestingly, the relative binding pattern of Mi-2 across the two analysed loci, *broad* and *vrille* upon ecdysone treatment was different from the relative pattern observed upon induction of heat shock genes in S2 cells. At the heat shock loci *hsp70* and *hsp22*, Mi-2 was shown to spread over the entire transcribed region upon induction by heat shock (Mathieu et al., 2012). Here, Mi-2 binding is strongest at the polyadenylation site of the heat shock genes and decreases further downstream where transcription termination takes place. However, Mi-2 is not recruited to the promoter of heat shock induced *hsp* genes. Therefore, it was hypothesised that Mi-2 associates with the nascent transcript and that this mechanism contributes to Mi-2 recruitment to heat shock genes. In comparison, at *broad* and *vrille*, Mi-2 is recruited to promoter regions (*vrille*, Figure 4.6 region X) as well as the first intron (*broad*, Figure 4.5 regions A-C and *vrille*, Figure 4.6 region Y). Mi-2 did neither associate with the entire gene body nor did it bind downstream of the polyadenylation site of the *broad* and *vrille* genes. These observations imply that the mechanism by which Mi-2 influences the transcription of heat shock loci and ecdysone inducible loci may differ between these genes.

Ecdysone induced Mi-2 binding was found in close proximity of the TSSs and within the introns of *broad* (Figure 4.6) and *vrille* (Figure 4.5). Genome-wide analysis of Mi-2 binding demonstrated that Mi-2 is globally enriched at intragenic regions (Mathieu, 2013). Within intragenic binding sites, Mi-2 has been found to preferentially bind close to the TSS and in introns. According to the classification by Kharchenko and colleagues, Mi-2 is enriched within chromatin state 1 (promoter and TSS marked by H3K4me3 and H3K9ac) and chromatin state 3 (intronic regulatory regions marked by H3K4me1, H3K18ac and H3K27ac) (Kharchenko et al., 2011). These findings are in line with results from Mi-2 ChIPSeq at the *broad* and *vrille* genes described in this thesis.

5.2 Mi-2 is a regulator of ecdysone dependent transcription

Mi-2 has been shown to be part of two repressive complexes in Drosophila. First, Mi-2 is a subunit of the NuRD complex that contributes to transcriptional repression by its histone deacetylase subunit (Kunert et al., 2009; Tong et al., 1998; Wade et al., 1998; Zhang et al., 1998). Second, Mi-2 interacts with Mep-1 in the Mec complex (Kunert et al., 2009). However, Mi-2 is also recruited to active heat shock loci upon heat shock where it promotes full transcriptional activation of *hsp* genes as detected by polytene chromosome staining and ChIP. (Mathieu et al., 2012; Murawska et al., 2011). Additionally, it binds to ecdysone regulated genes upon hormonal induction as described in this thesis. Therefore, Mi-2 can function as both, transcriptional activator and repressor, depending on the specific gene and the chromatin environment that it is recruited to.

RNASeq (Whole Transcriptome Shotgun Sequencing) analysis in Mi-2 depleted S2 cells showed changes in transcript levels of 1083 genes (E. Wagner, personal communication). 79% (857 genes) were upregulated upon depletion of Mi-2 whereas 21% (226 genes) were downregulated. Interestingly, RNASeq also identified several ecdysone dependent genes that were differentially expressed in Mi-2 knockdown cells. Most of these identified ecdysone dependent genes were upregulated (Hsp27, Eip71CD, Eip63, Eip78, E23 and Cpr49Ac) and only two were downregulated (ImpL2 and 3) upon Mi-2 depletion. These results are in line with the finding that Mi-2 contributes to repression of ecdysone dependent genes in the absence of hormone (Figure 4.9B).

Upon induction of the ecdysone cascade in S2 cells, Mi-2 depletion resulted in stronger transcriptional activation of *vrille*, *broad* and two non-coding RNAs as compared to GFP dsRNA treated cells (Figure 4.9C and D, Figure 4.11). This indicates that the presence of Mi-2 at these genes limits their expression. Hence, Mi-2 functions as a repressive modulator of transcription in the regulation of ecdysone dependent genes. The finding, that Mi-2 regulated transcription of an early induced gene (*broad*) in the ecdysone cascade as well as a late induced gene (*vrille*), demonstrates that Mi-2 influences gene expression at several time points of the ecdysone cascade.

The specificity of Mi-2 function in the transcriptional regulation of *broad* and *vrille* was further demonstrated by depletion of Iswi from S2 cells. Like Mi-2, Iswi belongs to the family of SNF2 type ATP-dependent chromatin remodelers and has been demonstrated to reside in three different complexes (ACF, CHRAC and NURF) in Drosophila. The NURF complex has been linked to activation of the ecdysone

cascade, since *Nurf* mutants display pupariation defects and fail to express ecdysone target genes (Badenhorst et al., 2005). Thus, it was expected that depletion of Iswi leads to a decrease in *vrille* and *broad* RNA levels. Surprisingly, neither *broad* nor *vrille* showed reduced expression as compared to GFP dsRNA treated cells (Figure 4.10B). The expected function of Iswi as an activator of ecdysone dependent genes could not be demonstrated. The absence of an effect on *broad* and *vrille* expression in Iswi depleted cells showed that not all ATP-dependent chromatin remodelers regulate the two analysed genes in the same way. However, due to the lack of an anti-Iswi antibody, knockdown efficiency on Iswi protein level could not be analysed and was only demonstrated on RNA level in RTqPCR (Figure 4.10A). It is possible that depletion of Iswi protein was insufficient and that therefore no effect on gene expression of *broad* and *vrille* was detected. However, this experiment demonstrated that the increased expression of *broad* and *vrille* was not a general feature of knockdown of an ATP-dependent chromatin remodeler, but that the effect seen in Mi-2 depleted cells was specific.

A study of the ATP dependent chromatin remodeler brahma demonstrated that it functions in the repression of a specific set of ecdysone induced genes (Zraly et al., 2006). Overexpression of a dominant negative *brahma* mutant in Drosophila resulted in strong derepression of the *Eig71* genes. The *Eig71* genes are a cluster on chromosome 3L that is coordinately transcribed from common intergenic promoter elements (Wright et al., 1996). Brahma was shown to be bound to these promoter elements in the absence of ecdysone, but dissociates upon transcriptional activation by 20HE treatment. In comparison to the results obtained for Mi-2 that functions in the regulation of *broad*, *vrille* and two non-coding RNAs, brahma functions as a repressor at a different set of genes, the *Eig71* cluster. Further, brahma is absent from the promoter upon transcriptional activation whereas Mi-2 binding is increased at several binding sites upon hormonal stimulation. In addition to the studies described for brahma and Iswi, an RNAi screen for EcR co-regulators in different Drosophila cell lines identified the CHD family member kismet as a strong activator of ecdysone dependent gene transcription (Davis et al., 2011). These studies show that several ATP-dependent chromatin remodelers have different functions in the regulation of ecdysone dependent genes. This thesis demonstrates for the first time a link between the ATP-dependent chromatin remodeler Mi-2 and the ecdysone cascade.

As mentioned above, Mi-2 resides in two different protein complexes in Drosophila. An open question is, which complex is responsible for the regulation of ecdysone

dependent genes. In general, the Mec complex, in which Mi-2 heterodimerises with Mep1, is the most abundant Mi-2 complex in Drosophila (Kunert et al., 2009). However, the p66 subunit of the NuRD complex has been demonstrated to be involved in the regulation of ecdysone inducible genes. In *p66* mutants, induction of *E74* and *DHR3* at the onset of metamorphosis was shown to be abolished (Kon et al., 2005). This thesis demonstrates that Mi-2 depletion results in activation of the ecdysone inducible genes *broad* and *vrille*. From the studies conducted so far, it is unclear which Mi-2 containing complex is more likely to be responsible for the regulation of 20HE genes. In order to answer this question, ChIP for overexpressed, FLAG-tagged NuRD and Mec subunits is currently being established in the Brehm lab. This strategy was chosen, since no suitable ChIP antibodies for NuRD and Mec subunits are available. FLAG-ChIPs for other complex subunits will be able to demonstrate which complex contributes to the modulation of ecdysone dependent genes by Mi-2. These experiments will lead to a better understanding of the mechanism by which Mi-2 contributes to repression of 20HE dependent genes.

The results described above demonstrating that Mi-2 represses ecdysone dependent genes were obtained in S2 cells (Figure 4.9). However, it will be interesting to analyse the function of Mi-2 in different tissues and time points of the ecdysone cascade in Drosophila larva. Initial experiments in this direction turned out problematic, since RNAi mediated knockdown of Mi-2 in larva resulted in developmental delay (data not shown). In order to circumvent these technical difficulties, UAS/Gal4 inducible expression system and overexpression of dominant negative Mi-2 mutants should be considered for future experiments.

5.3 Mi-2 interacts with EcR *in vivo*

The interaction of Mi-2 with EcR was demonstrated with the use of several experimental systems. First and foremost, Mi-2 was shown to interact with EcR *in vivo* in S2 cells by co-immunoprecipitation (co-IP) (Figure 4.15). This result was supported by the finding that Mi-2 binds to EcR when overexpressed in Sf9 cells (Figure 4.12 and 4.13). These experiments also demonstrated that Mi-2 and EcR form a stoichiometric complex (Figure 4.14).

Several interactions between nuclear receptors and their co-regulatory proteins have been demonstrated to occur in a hormone dependent manner. Classical co-activators,

such as the H3K4 methyltransferase TRR (trithorax related), interact with EcR in the presence of ecdysone (Sedkov et al., 2003). In contrast, transcriptional co-repressors, such as Smrter, associate with EcR in the absence of ligand (Tsai et al., 1999). However, interaction between Mi-2 and EcR has been demonstrated to be independent of 20HE (Figure 4.13 and 4.15). This finding suggests, that Mi-2 functions as a more general EcR co-regulator in uninduced and 20HE treated S2 cells. Further it implies that the increased binding of Mi-2 upon 20HE treatment to chromatin is not a consequence of an increased affinity to EcR. Instead, 20HE induced Mi-2 binding may be due to an increase in EcR binding to specific chromatin regions.

In addition, the interaction between EcR and Mi-2 did not require the classical “LXXLL” motif to be present in Mi-2 (Figure 4.16). This amino acid sequence is present in co-activators that interact with NRs in a hormone-dependent fashion (Heery et al., 1997). Accordingly, a motif “L/I-XX-I/V-I” had been identified to mediate the interaction between NRs and their co-repressors (Hu and Lazar, 1999). However, none such motif could be identified in Mi-2. These findings strengthen the hypothesis that Mi-2 is likely to function as a modulator of EcR in the presence and absence of 20HE.

Another aspect that has to be considered, is the role of ultraspiracle (USP). USP is the heterodimerisation partner of EcR and binds to the NR in the presence of hormone (Yao et al., 1992). The interaction studies conducted upon overexpression in Sf9 cell, addressed the binding of Mi-2 in the absence of USP (Figures 4.12 and 4.13). It is possible that the presence of USP could enhance or diminish Mi-2 binding to EcR. However, the interaction studies were also performed in S2 cells (Figure 4.25). Here, USP is expressed as judged by Western blot (data not shown) and ChIP analysis (Figure 4.25). No difference in Mi-2 binding to EcR was observed in the presence of 20HE, when USP potentially binds to EcR, as compared to untreated cells. Therefore, it is less likely that USP has an influence on the interaction between Mi-2 and EcR but further experiments have to be conducted to analyse the role of USP in detail.

5.4 The ATPase domain of Mi-2 interacts with the AF2 domain of EcR

Previous studies identified the C-terminus of Mi-2 to interact with sequence specific transcription factors like hunchback and Ttk69 (Kehle et al., 1998; Murawsky et al., 2001). Further, several K/R rich regions in the N-terminus of Mi-2 have been shown to

be critical for PAR-mediated recruitment of Mi-2 to active heat shock loci on polytene chromosomes (Murawska et al., 2011). In this thesis, mapping studies using Mi-2 and EcR fragments revealed that the Mi-2 ATPase domain interacts with the AF2 domain of EcR (Figures 4.16 – 4.21).This is the first time an interaction between an ATPase domain of a chromatin remodeler and a sequence specific transcription factor has been established. It also suggests a new possible regulatory mechanism for the catalytic activity of Mi-2 that may apply to other ATP-dependent chromatin remodelers.

The ATPase domain is the catalytic core of the ATP-dependent chromatin remodeler and makes direct contacts with the nucleosome in order to reposition it. Therefore, the interaction between EcR and Mi-2 via the ATPase could have an effect on the catalytic activity of the remodeler. Interestingly, the Bowman laboratory published a crystal structure of the highly related remodeler Chd1 (Hauk et al., 2010). The double chromodomains of Chd1 lay across the central cleft of the ATPase and contact both ATPase lobes. This conformation locks the ATPase in a catalytically inactive state and interferes with DNA binding to the ATPase. Interaction with a nucleosome relieves this inhibition and puts the ATPase domain in a catalytically active conformation. Therefore, this study established the principle that the ATPase activity can be regulated by direct contacts between the ATPase domain and an adjacent domain of the same protein. This principle may also apply to the findings described in this study, such that the regulation of the ATPase domain might be exerted by intermolecular interactions e.g. with EcR.

The auto-inhibitory mechanism provided by the Bowman laboratory allows Chd1 to discriminate between naked DNA and nucleosomes, thereby increasing the specificity of the remodeler. Substrate discrimination has also been observed for Mi-2, which is highly stimulated by nucleosomes, but shows almost no ATPase activity in the presence of DNA only (Brehm et al., 2000). As demonstrated in this thesis, EcR interacts mainly with a fragment containing the second ATPase lobe (Figure 4.16). In addition the C-terminal bridge of the Mi-2 ATPase domains was shown to bind to EcR. According to the Chd1 crystal structure this domain interacts with both ATPase lobes. Thereby the C-terminal bridge potentially influences domain motions of the ATPase domain. A possible effect of the interaction between EcR and the first ATPase lobe as well as the C-terminal bridge of the ATPase domain on the catalytic activity of Mi-2 is subject to current investigation in the Brehm lab. ATPase experiments are conducted to demonstrate if purified Mi-2 alone as well as Mi-2 bound to EcR (Figure 4.14) can hydrolyse ATP to the same extent in the presence of nucleosomes. These experiments

will further show whether the substrate discrimination between naked DNA and nucleosomes by the ATPase can be influenced by the presence of EcR.

As mentioned above, Mi-2 interacts with the AF2 domain of EcR. Upon ligand binding, the AF2 domain has been demonstrated to change its structural conformation (Billas et al., 2003) thereby allowing EcR to interact with various co-activator proteins. Suprisingly, the interaction between Mi-2 and the AF2 of EcR is ecdysone independent. Therefore, I hypothesised that this interaction occurs in a subdomain of the AF2 domain that retains its structural features upon ligand binding. As mentioned above the binding of Mi-2 to the AF2 domain of EcR may further be influenced by the heterodimerisation partner USP. This may be the case since the interaction between USP and EcR in presence of hormone is partially mediated by the AF2 (Germain and Bourguet, 2013)

5.5 Recruitment of Mi-2 is mediated by EcR

The finding that Mi-2 and EcR can interact in S2 cells, led to the hypothesis that EcR can recruit Mi-2 to specific chromatin regions. Therefore, the Mi-2 binding sites identified by ChIPSeq in this thesis were compared to EcR binding sites identified by two different studies (Figures 4.23 and 4.24). On a genome-wide level, EcR ChIPSeq data form the Stark lab allows for a valid comparison with the Mi-2 dataset. Genome-wide comparison of Mi-2 and EcR ChIPSeq showed a significant overlap (13%) between the top 10% Mi-2 peaks and EcR binding sites (Figure 4.22A) in both, untreated and 20HE treated cells. This overlap was even stronger (34%) when comparing 20HE induced Mi-2 binding sites and EcR binding sites in 20HE treated cells (Figure 4.22B). Further, comparison of ChIPSeq tracks at the *vrille* and *broad* gene dataset demonstrated a co-occupancy of genomic sites by EcR and Mi-2 (Figures 4.23 and 4.24). Moreover, these regions were also identified as EcR/USP binding sites by the DamID study (Gauhar et al., 2009). These findings strongly suggest, that Mi-2 and EcR co-occupy a subset of target genes. However, not all Mi-2 binding sites at both loci showed a clear correlation, which may be due to variations in the experimental setup. The EcR ChIPSeq dataset published by the Stark lab was prepared from S2 cells that were treated for 24 hours with 20HE, whereas Mi-2 binding sites in this thesis were analysed after six hours of hormonal treatment. Since the ecdysone response is a complex cascade, different genes might be regulated at the two time points tested. Therefore, I hypothesized that Mi-2 and EcR binding sites may

also differ between six and 24 hours after ecdysone induction. However, the finding that a significant proportion of Mi-2 binding sites overlap with EcR binding strengthened the hypothesis of EcR mediated Mi-2 recruitment to chromatin.

This hypothesis was further verified by experiments where EcR was depleted from S2 cells (Figure 4.26). As predicted, loss of EcR led to a decrease in 20HE induced Mi-2 binding to *vrille* and *broad*. Surprisingly, no strong effect on Mi-2 binding to chromatin was observed in untreated S2 cells. As mentioned before, Mi-2 depletion experiments demonstrated that RNAi treatment of S2 cells results in reduction of the soluble Mi-2 fraction (Anna Ernst, personal communication). However, some Mi-2 protein was not depleted by RNAi and remained associated with chromatin over several cell cycles. In that case, depletion of EcR would also not result in reduction of the stable, chromatin-bound fraction of Mi-2, as was observed. Also, EcR may be required for recruitment of Mi-2 to chromatin in untreated cells, but may not be essential for the maintenance of Mi-2 binding to chromatin. This could further explain, why depletion of EcR did not result in decreased Mi-2 binding to chromatin in untreated S2 cells. In addition, it is possible that other mechanisms contribute to Mi-2 binding at these two genes and therefore recruitment of Mi-2 mediated by EcR is not the only factor important for Mi-2 binding to chromatin (discussed below).

Previous genome-wide analysis of Mi-2 binding sites determined DNA binding motifs that were significantly enriched within the genomic regions bound by Mi-2 (DREME tool; Discriminative Regular Expression Motif Elicitation) (Mathieu, 2013). This identified the DNA binding motif for the transcription factor Gaf (GAGA transcription factor), however no robust, direct interaction between Gaf and Mi-2 could be demonstrated (Mathieu, 2013). The DNA motif search did not identify ecdysone response elements (EcRE) to co-occur with Mi-2 binding sites on chromatin. These elements are a pseudopalindromic sequence containing G(G/A)(T/A)CA half-sites separated by a variable spacer and are recognized by the EcR/USP heterodimer (Riddihough and Pelham, 1987). A possible reason why these elements were not picked up by the DNA motif search within Mi-2 binding sites is that EcRE motifs are not well defined and highly degenerated within the Drosophila genome (Maletta et al., 2014; Vogtli et al., 1998). Also, EcR may only be responsible for Mi-2 recruitment to chromatin of a small subset of all Mi-2 binding sites. This could further explain, why the EcRE motif was not identified as a significantly enriched DNA binding motif within genome-wide Mi-2 binding sites.

Since Mi-2 containing complexes lack subunits with sequence specific DNA binding activity, several recruitment mechanisms were proposed. First, the NuRD complex contains the subunits MBD2/3, which have been shown to bind to methylated CpG residues (Le Guezennec et al., 2006; Zhang et al., 1999). However, since methylation of CpG is confined to a short time window during embryonic development in Drosophila, MBD2/3 mediated recruitment of NuRD to methylated DNA seems to play a less general role in Drosophila than in mammals (Lyko et al., 2000).

Second, Mi-2 has been shown to interact with specific transcription factors in a SUMO-dependent manner (Stielow et al., 2008). The small ubiquitin-related modifier (SUMO) is reversibly attached to lysine residues of many transcription regulators and has been linked to repression of transcription (Hay, 2005). Interestingly, bioinformatic analysis predicted strong SUMOylation acceptor sites in the DBD and AF2 of EcR that could be verified experimentally (Seliga et al., 2013). In Western blot, SUMOylation of proteins results in a shift in mobility due to an increase of the molecular weight of about 15-17kDa for each SUMO added to the protein (Tatham et al., 2009). No such mobility shift was observed for EcR in Western blot from nuclear extracts of S2 cells (Figure 4.8, 4.9 and 4.15). However, the nuclear extracts subjected to Western blot did not include a SUMO protease inhibitor. It has been shown previously, that SUMOylation only occurs on a small proportion of a given transcription factor and that this modification is transient (Flotho and Melchior, 2013). Therefore, a possible SUMOylation of EcR in S2 cells may not have been detected in Western blot. In conclusion, SUMOylation could play a role in the interaction between Mi-2 and EcR, but further experiments have to be conducted in order to analyse the impact of EcR SUMOylation on Mi-2 interaction.

Third, Mi-2 recruitment to chromatin may be facilitated by domains present in the N-terminus of Mi-2. The PHD fingers are characterised by a Cys^4-His-Cys^3 motif that coordinates two zinc ions. Within the human homolog of Mi-2, CHD4, the PHD fingers have been shown to interact with the unmodified H3 tail and H3K9me3 (Mansfield et al., 2011). Further, Mi-2 contains two tandemly arranged chromodomains in its N-terminus. Chromodomains have mainly been studied as methyl-lysine binding domains (Flanagan et al., 2005; Jacobs and Khorasanizadeh, 2002). However, the chromodomains of Mi-2 do not possess specificity towards a certain methylation status of the histone (Murawska, 2011). Interestingly, the chromodomains of Mi-2 have been shown to bind DNA *in vitro* (Bouazoune et al., 2002). The mechanisms discussed here

may further contribute to Mi-2 binding to chromatin at the *vrille* and *broad* locus in addition to EcR mediated recruitment in untreated cells.

20HE induced Mi-2 binding is markedly reduced upon EcR depletion in S2 cells. Therefore, recruitment of Mi-2 by EcR occurs to be the major recruitment mechanism upon hormonal stimulation. However, other aspects of recruitment upon hormonal stimulation have to be taken in to consideration. Interaction of Mi-2 with poly-ADP-ribose (PAR) was demonstrated to be important for Mi-2 recruitment to active heat shock loci (Murawska et al., 2011). Interestingly, also ecdysone inducible genes have been shown to be a target of strong PARylation upon activation by hormonal treatment (Tulin and Spradling, 2003). Therefore, PAR may also contribute to Mi-2 recruitment to ecdysone induced genes. Recently Mi-2 was shown to bind the nascent mRNA at heat shock induced genes (Murawska et al., 2011). Further, Mi-2 recruitment seems to follow the binding pattern of the RNA PolII at the *hsp70* (Mathieu et al., 2012). In contrast to the Mi-2 binding pattern observed at heat shock genes, Mi-2 does not cover the entire transcribed region of the ecdysone inducible genes *broad* and *vrille*. At both, *hsp* genes and the *vrille* gene, inhibition of transcription elongation by 5,6-dichloro-1-bold beta-D-ribofuranosylbenzimidazole (DRB) did not result in decreased Mi-2 recruitment ((Murawska et al., 2011) (Figure 4.27B). However, the inhibition of transcription by DRB at the *vrille* gene was not complete (Figure 4.27A). In conclusion, recruitment of Mi-2 by transcription elongation or the nascent mRNA molecule to the *vrille* gene is less likely, but can not be fully excluded. The majority of EcREs are located within a transcribed region and as a consequence can not be tested in isolation from transcription. To test whether Mi-2 recruitment to EcREs is dependent on transcription, Mi-2 ChIP experiments at a reporter gene, that contains an isolated EcRE upstream of the promoter, are being established in the Brehm lab. In summary, the research described in this thesis established a new model for the recruitment of Mi-2 to chromatin by demonstrating that an interaction between Mi-2 and EcR is important for binding of Mi-2 to ecdysone dependent genes (Figure 5.1).

5.6 Several ATP-dependent chromatin remodeler can interact with EcR

Since the ATPase domain is highly conserved between different families of ATP-dependent chromatin remodelers, ATPase domains of selected chromatin remodelers were tested for an interaction with EcR (Figure 4.17). Interestingly, all tested ATPase

domains bound EcR *in vitro*. As described above, multiple studies have linked ATP-dependent chromatin remodelers to the regulation of ecdysone dependent genes in Drosophila. It is therefore possible, that the interaction between EcR and the ATPase domain is a highly conserved mechanism. However, since different ATP-dependent chromatin remodelers have different effects on transcription, this hypothesis lacks an explanation for the specificity of each remodeler. Specificity to the mode of action could be added by differences in complex composition of the particular ATP-dependent chromatin remodeler. Further, specificity in EcR interaction might be added by the presence of additional domains in the N-terminal and C-terminal regions of the chromatin remodeler (Figure 2.4). Also, expression levels of ATP-dependent chromatin remodeler may differ between developmental time points and different tissues.

As discussed above, the ATPase domains of several ATP dependent chromatin remodeler have been shown to interact with EcR. Therefore, I hypothesised that all chromatin remodeler have the potential to be recruited to chromatin by EcR. Notably, the Hager lab mapped the binding profile of three different ATP dependent chromatin remodeler by ChIPSeq in mouse cells (Morris et al., 2014). Comparing CHD4, the mammalian Mi-2 homolog, Brg1 and Snf2h they demonstrated that a large proportion of binding sites are shared by these three remodelers. This co-occupancy was not due to an interaction of these proteins, but due to a transient, sequential interaction of each remodeler with the same binding site. Although a study in Drosophila demonstrates that different chromatin remodeler are mutually exclusive at genomic regions (Moshkin et al., 2012), growing evidence indicates that different remodeler influence each other in an antagonistic manner. For example, this was shown on LPS stimulated immune responsive genes (Ramirez-Carrozzi et al., 2006). Here, SWI/SNF complex is recruited to enable activation of immune responsive genes. Along with recruitment of SWI/SNF, Mi-2/NuRD is binding to immune response genes where it functions to limit transcription of these genes in response to microbial infection. In conclusion, several ATP-dependent chromatin remodeler may be recruited to the same chromatin regions where they positively and negatively regulate transcription, thereby allowing a quick adaptation to extrinsic signals.

The result discussed above also indicated that the ATPase domain of Iswi can bind EcR *in vitro* (Figure 4.17). Depletion of Iswi in S2 cells did not show the same effect as depletion of Mi-2 on expression of *broad* and *vrille* (Figures 4.9 and 4.10). These findings suggest, that even though several ATP-dependent chromatin remodeler of the SNF2 family can bind to EcR *in vitro*, their function *in vivo* differs. Therefore, the

interaction between EcR and ATP-dependent chromatin remodelers may be conserved, but the effect of this interaction on recruitment to chromatin and transcriptional regulation depends on several other aspects. Additional aspects that influence the outcome of this interaction include adjacent domains within the remodeler, additional proteins that modulate interaction between EcR and the remodeler as well as the spatio-temporal expression of a remodeler protein.

5.7 Mi-2 maintains a closed chromatin structure at ecdysone regulated genes

MNase mapping studies conducted in this thesis demonstrated that Mi-2 maintains a closed chromatin structure at the *vrille* gene (Figure 4.28). Regions of DNA accessibility at the *vrille* gene were mapped by MNase digestion. MNase preferentially cleaves internucleosomal DNA, whereas DNA within a nucleosome is relatively protected from digestion. However, also transcription factors (TFs) that make direct contacts with a specific DNA sequence can protect DNA from digestion by MNase. Even though TFs can influence the pattern of the MNase digest, it is most likely that the regions of less DNA accessibility identified at the *vrille* gene (Figure 4.27) are due to the presence of nucleosomes at these positions. This hypothesis is further strengthened by the observation that depletion of the ATP-dependent chromatin remodeler Mi-2 results in changes of DNA accessibility (Figure 4.28). *In vitro* studies on ATP-dependent chromatin remodelers have shown that these enzymes can move the histone octamer along a DNA substrate, a process which is referred to as nucleosome sliding. Studies on mononucleosomes showed that different remodeler can lead to different nucleosome sliding products. For example, Iswi preferentially slides a central located nucleosome towards the end of the DNA fragment, whereas Mi-2 has been shown to mobilise end-positioned nucleosomes (Brehm et al., 2000; Langst et al., 1999). These *in vitro* studies demonstrated that ATP-dependent chromatin remodelers can affect the position of a nucleosome on a DNA substrate. However, these mechanisms may be completely different *in vivo*, where no mononucleosomes exist.

In vivo nucleosome positioning refers to the position a nucleosome favours with respect to the underlying DNA sequence. This positioning can be influenced by chromatin remodelers, transcription factors and RNA PolII. The proper positioning of nucleosomes over regulatory sequences allows the silencing of gene expression,

namely repression. The region that shows higher DNA accessibility upon Mi-2 depletion at the *vrille* gene, is located in close vicinity to a regulatory region. The potential nucleosome A is in the promoter of the *vrille(RE)* transcript and also within the transcribed region of the two non-coding RNAs *CR44743* and *CR44742*. Tissue-specific, developmentally regulated genes often have a TSS covered with a nucleosome and less well positioned nucleosomes in the transcribed region (Bai and Morozov, 2010). Recruitment of chromatin remodeler by NRs results in remodeling of the chromatin structure, thereby revealing critical regulatory regions for the binding of the transcription machinery. In contrast, remodeling enzymes with a repressive function position nucleosomes such that they cover regulatory regions (Radman-Livaja and Rando, 2010). In line with this, the presence of Mi-2 most likely contributes to DNA accessibility by positioning potential nucleosomes over these regulatory regions. This establishes a balance between co-activator and co-repressor proteins thereby limiting expression of the *vrille* gene.

The region that shows higher DNA accessibility upon Mi-2 depletion did overlap with an Mi-2 binding site that is increased upon 20HE treatment (Figure 4.6, regions X). Further, the increase in DNA accessibility upon Mi-2 depletion correlated with the expression status of the *vrille* gene as reduced levels of Mi-2 resulted in superactivation of the *vrille* gene upon 20HE treatment (Figure 4.9). This correlation may explain a mechanism by which Mi-2 contributes to the repression of ecdysone dependent genes by maintaining a closed chromatin structure at these loci. However, the MNase experiment only analysed one time point of the ecdysone cascade and few potential nucleosomes at the *vrille* gene. In order to gain a more detailed insight, it would be of interest to test the behaviour of all potential nucleosomes across the *vrille* gene in a time course experiment. In general, I concluded that the maintenance of a closed chromatin structure is the repressive mechanism by which Mi-2 contributes to transcriptional regulation of the *vrille* gene. Since Mi-2 is recruited to several ecdysone dependent genes, this mechanism may be general for the regulation of hormone regulated gene expression in Drosophila.

5.8 A recruitment model for Mi-2

The results obtained in this thesis, lead to the following model for the function of Mi-2 at ecdysone regulated genes (Figure 5.1). In untreated cells Mi-2 interacts with EcR and contributes to repression of 20HE dependent genes by maintaining a closed

chromatin structure (A). Upon addition of ecdysone, EcR interacts with co-activator complexes in a ligand dependent manner (B). These co-activators establish an open chromatin environment by modification of histones and remodeling of nucleosomes, resulting in recruitment of the transcription machinery to the TSS. Elongation of RNA PolII along the transcribed region results in production of the mRNA molecule upon ecdysone treatment. At the same time, EcR recruits co-repressor complexes, such as Mi-2, to binding sites close to the TSS and additional genomic sites. Mi-2 maintains a closed chromatin structure, thereby counteracting the function of co-activator complexes. This establishes a balance of events on chromatin structure that activate and repress transcription, thereby limiting transcriptional activation of ecdysone dependent genes. When Mi-2 is depleted from S2 cells, the balance of transcription activating and repressing events is shifted towards transcriptional activation (C). This results in a more open chromatin and increased recruitment of RNA PolII. As a consequence, transcription is not limited and mRNA levels are markedly increased compared to cells with Mi-2. This model illustrates the function of Mi-2 as a repressive modulator of transcription at ecdysone dependent genes.

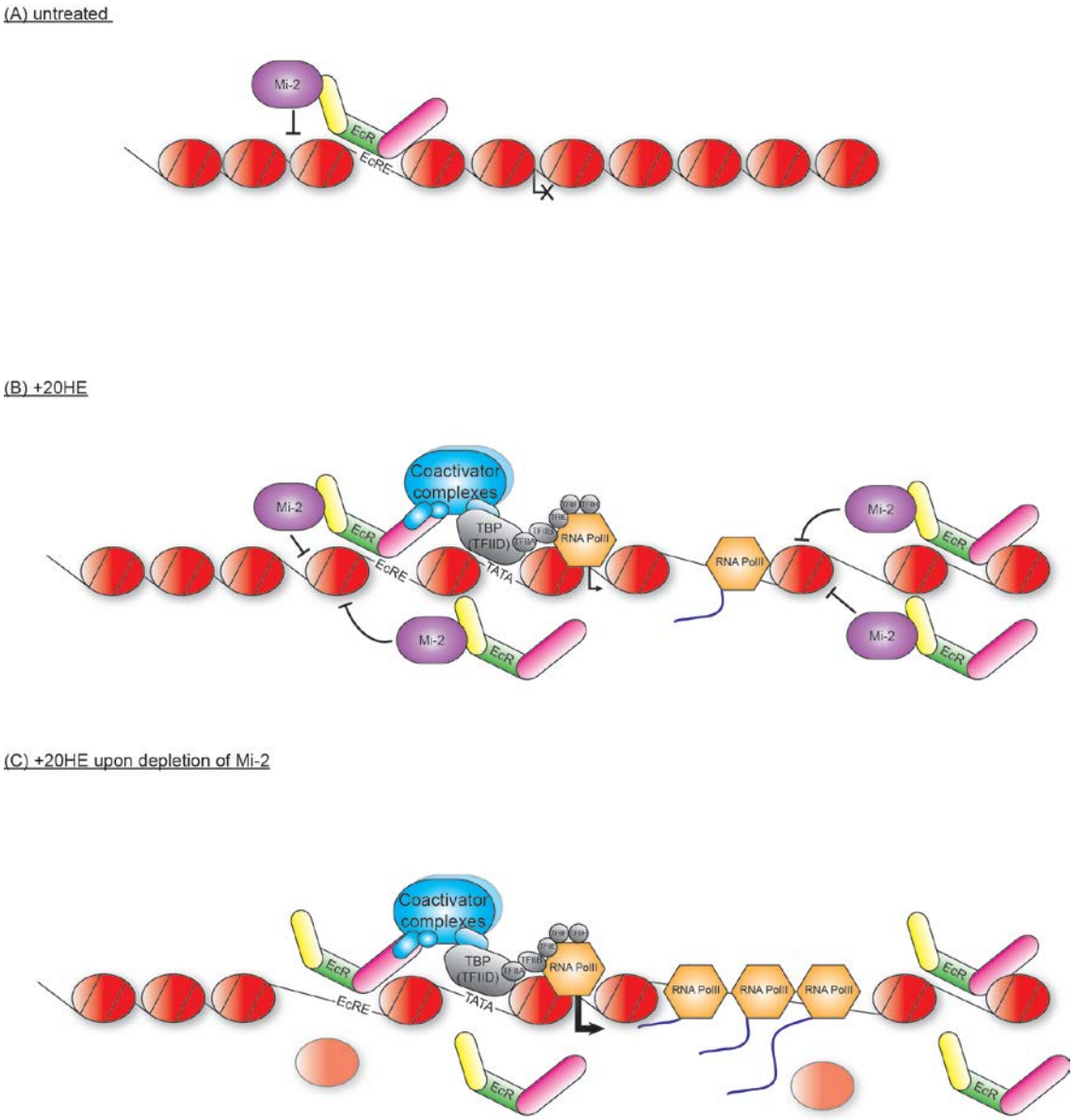

Figure 5.1: Model for function of Mi-2 at ecdysone regulated genes. (A) Chromatin environment of an ecdysone inducible gene in untreated cells. (B) 20HE treatment leads to transcription initiation and increased Mi-2 recruitment by EcR. (A) and (B) Mi-2 maintains a repressive chromatin structure at the gene. (C) Depletion of Mi-2 results in superactivation of ecdysone dependent genes due to a more open chromatin structure.

5.9 Conservation of cooperation between Mi-2 and NRs

The EcR/USP heterodimer is a conserved complex that resembles various vertebrate nuclear receptors. In line with this, the general mechanisms for co-activator and co-repressor complexes are highly conserved between multicellular organisms. This leads to the assumption that the recruitment mechanism for Mi-2 by EcR is evolutionary conserved in other species.

The *pS2* gene is an estrogen dependent gene that is regulated by the recruitment of co-activator and co-repressor complexes via the estrogen receptor (ER). Recruitment of these complexes has been shown to appear in a cyclical manner (Metivier et al., 2003). The *pS2* promoter contains two nucleosomes, NucE that covers the estrogen responsive element (ERE) and nucT that covers the TATA box (Figure 2.7). The nucleosome positions fluctuate in cycles together with the expression of the *pS2* gene. Interestingly, when CHD4, the mammalian homolog of Mi-2, is present at the promoter, the NucT is stabilised in a position covering the TATA box at the end of a transcriptional cycle. This mechanism for Mi-2 compares well to the model described in this thesis for ecdysone dependent genes. Also, a role for the Mi-2/NuRD complex in ER regulation has been established via the MTA subunit of NuRD. MTA is overexpressed in metastatic and aggressive breast cancer tumours (Jang et al., 2006). Interestingly, MTA was shown to interact with the AF2 domain of ER. This interaction recruits the NuRD complex to the estrogen inducible genes *pS2* and *c-Myc* in an estrogen dependent manner (Mazumdar et al., 2001). Here, a subunit of the NuRD complex other than Mi-2 has been identified to interact with the AF2 domain of a NR and is recruited to a gene promoter upon hormonal induction. This demonstrates that the interaction of a repressive complex with NRs via the AF2 domain can also be mediated by a different subunit within the complex. Thereby, these findings add further complexity to the mechanisms of coordinated recruitment of co-activator and co-repressor complexes to chromatin.

Another example is the association of CHD4 with the thyroid hormone receptor (TR) (Xue et al., 1998). TR functions in a wide variety of cellular processes thereby contributing to organ development, metabolism and heart rate. Antibody interference experiments with anti-CHD4 antibody demonstrated that the chromatin remodeler functions as a co-repressor of TR in the absence of thyroid hormone. This repressive activity was further linked to the NuRD complex, since incubation with the HDAC inhibitor TSA interfered with transcriptional repression by TR. These examples show, that Mi-2 is a conserved factor in regulation of hormone inducible genes and that the findings of this thesis could apply to other model systems.

In conclusion, this thesis established a new model for the function of the ATP-dependent chromatin remodeler Mi-2 in the regulation of a set of developmentally regulated genes in Drosophila. Mi-2 recruitment to ecdysone dependent genes is mediated by a physical interaction with EcR. Here, Mi-2 functions as a repressive modulator of ecdysone dependent gene transcription by maintaining a closed

chromatin structure at these loci. The finding that the ATPase domain of Mi-2 interacts with EcR implies a new regulatory mechanism for the catalytic domain of Mi-2 by intermolecular interactions. Future experiments will address this regulatory mechanism and the influence of EcR binding to the catalytic activity of Mi-2. Analysis of Mi-2 binding sites at different time points of the ecdysone cascade as well as the identification of the complex in which Mi-2 resides at ecdysone target genes will give further insight in the mechanism that contributes to the transcriptional repression of ecdysone dependent genes. Finally, the evolutionary conservation of the mechanism described here has to be addressed by similar experiments in different species.

6 References

Ables, E.T. and Drummond-Barbosa, D. The steroid hormone ecdysone functions with intrinsic chromatin remodeling factors to control female germline stem cells in Drosophila. *Cell Stem Cell* 7, 581-92 (2010).

Aguinaldo, A.M., Turbeville, J.M., Linford, L.S., Rivera, M.C., Garey, J.R., Raff, R.A. and Lake, J.A. Evidence for a clade of nematodes, arthropods and other moulting animals. *Nature* 387, 489-93 (1997).

Ahmad, K. and Henikoff, S. The histone variant H3.3 marks active chromatin by replication-independent nucleosome assembly. *Mol Cell* 9, 1191-200 (2002).

Amrhein, F. A biochemical analysis of transcription factor - coregulator interactions in Drosophila, Philipps-University Marburg (2012).

Arents, G., Burlingame, R.W., Wang, B.C., Love, W.E. and Moudrianakis, E.N. The nucleosomal core histone octamer at 3.1 A resolution: a tripartite protein assembly and a left-handed superhelix. *Proc Natl Acad Sci U S A* 88, 10148-52 (1991).

Armstrong, J.A., Papoulas, O., Daubresse, G., Sperling, A.S., Lis, J.T., Scott, M.P. and Tamkun, J.W. The Drosophila BRM complex facilitates global transcription by RNA polymerase II. *EMBO J* 21, 5245-54 (2002).

Ashburner, M. Ecdysone induction of puffing in polytene chromosomes of Drosophila melanogaster. Effects of inhibitors of RNA synthesis. *Exp Cell Res* 71, 433-40 (1972a).

Ashburner, M. Patterns of puffing activity in the salivary gland chromosomes of Drosophila. VI. Induction by ecdysone in salivary glands of D. melanogaster cultured in vitro. *Chromosoma* 38, 255-81 (1972b).

Ashburner, M. Puffs, genes, and hormones revisited. *Cell* 61, 1-3 (1990).

Ashburner, M. Sequential gene activation by ecdysone in polytene chromosomes of Drosophila melanogaster. I. Dependence upon ecdysone concentration. *Dev Biol* 35, 47-61 (1973).

Ashburner, M. Sequential gene activation by ecdysone in polytene chromosomes of Drosophila melanogaster. II. The effects of inhibitors of protein synthesis. *Dev Biol* 39, 141-57 (1974).

Badenhorst, P., Xiao, H., Cherbas, L., Kwon, S.Y., Voas, M., Rebay, I., Cherbas, P. and Wu, C. The Drosophila nucleosome remodeling factor NURF is required for Ecdysteroid signaling and metamorphosis. *Genes & Development* 19, 2540-2545 (2005).

Bai, L. and Morozov, A.V. Gene regulation by nucleosome positioning. *Trends in Genetics* 26, 476-483 (2010).

Bain, D.L., Heneghan, A.F., Connaghan-Jones, K.D. and Miura, M.T. Nuclear receptor structure: implications for function. *Annu Rev Physiol* 69, 201-20 (2007).

Bannister, A.J., Zegerman, P., Partridge, J.F., Miska, E.A., Thomas, J.O., Allshire, R.C. and Kouzarides, T. Selective recognition of methylated lysine 9 on histone H3 by the HP1 chromo domain. *Nature* 410, 120-4 (2001).

Bartkuhn, M., Straub, T., Herold, M., Herrmann, M., Rathke, C., Saumweber, H., Gilfillan, G.D., Becker, P.B. and Renkawitz, R. Active promoters and insulators are marked by the centrosomal protein 190. *EMBO J* 28, 877-88 (2009).

Bate, M. and Martinez Arias, A. The Development of Drosophila melanogaster, (*Cold Spring Harbor Laboratory Press*, *Plainview, N.Y.*) (1993).

Bauer, U.M., Daujat, S., Nielsen, S.J., Nightingale, K. and Kouzarides, T. Methylation at arginine 17 of histone H3 is linked to gene activation. *EMBO Rep* 3, 39-44 (2002).

Beato, M., Herrlich, P. and Schutz, G. Steroid hormone receptors: many actors in search of a plot. *Cell* 83, 851-7 (1995).

Beckendorf, S.K. and Kafatos, F.C. Differentiation in the salivary glands of Drosophila melanogaster: characterization of the glue proteins and their developmental appearance. *Cell* 9, 365-73 (1976).

Beckstead, R.B., Lam, G. and Thummel, C.S. The genomic response to 20-hydroxyecdysone at the onset of Drosophila metamorphosis. *Genome Biol* 6, R99 (2005).

Bender, M., Imam, F.B., Talbot, W.S., Ganetzky, B. and Hogness, D.S. Drosophila ecdysone receptor mutations reveal functional differences among receptor isoforms. *Cell* 91, 777-88 (1997).

Bernstein, B.E., Humphrey, E.L., Erlich, R.L., Schneider, R., Bouman, P., Liu, J.S., Kouzarides, T. and Schreiber, S.L. Methylation of histone H3 Lys 4 in coding regions of active genes. *Proc Natl Acad Sci U S A* 99, 8695-700 (2002).

Bhatia, S., Pawar, H., Dasari, V., Mishra, R.K., Chandrashekaran, S. and Brahmachari, V. Chromatin remodeling protein INO80 has a role in regulation of homeotic gene expression in Drosophila. *Genes Cells* 15, 725-35 (2010).

Bhaumik, S.R., Smith, E. and Shilatifard, A. Covalent modifications of histones during development and disease pathogenesis. *Nat Struct Mol Biol* 14, 1008-16 (2007).

Billas, I.M., Iwema, T., Garnier, J.M., Mitschler, A., Rochel, N. and Moras, D. Structural adaptability in the ligand-binding pocket of the ecdysone hormone receptor. *Nature* 426, 91-6 (2003).

Billas, I.M., Moulinier, L., Rochel, N. and Moras, D. Crystal structure of the ligand-binding domain of the ultraspiracle protein USP, the ortholog of retinoid X receptors in insects. *J Biol Chem* 276, 7465-74 (2001).

Biterge, B. and Schneider, R. Histone variants: key players of chromatin. *Cell Tissue Res* 356, 457-66 (2014).

Black, J.C., Van Rechem, C. and Whetstine, J.R. Histone lysine methylation dynamics: establishment, regulation, and biological impact. *Mol Cell* 48, 491-507 (2012).

Bouazoune, K., Mitterweger, A., Langst, G., Imhof, A., Akhtar, A., Becker, P.B. and Brehm, A. The dMi-2 chromodomains are DNA binding modules important for ATP-dependent nucleosome mobilization. *EMBO J* 21, 2430-40 (2002).

Bradford, M.M. A rapid and sensitive method for the quantitation of microgram quantities of protein utilizing the principle of protein-dye binding. *Anal Biochem* 72, 248-54 (1976).

Brehm, A., Langst, G., Kehle, J., Clapier, C.R., Imhof, A., Eberharter, A., Muller, J. and Becker, P.B. dMi-2 and ISWI chromatin remodelling factors have distinct nucleosome binding and mobilization properties. *EMBO J* 19, 4332-41 (2000).

Broadus, J., McCabe, J.R., Endrizzi, B., Thummel, C.S. and Woodard, C.T. The Drosophila beta FTZ-F1 orphan nuclear receptor provides competence for

stage-specific responses to the steroid hormone ecdysone. *Mol Cell* 3, 143-9 (1999).

Burakov, D., Crofts, L.A., Chang, C.P. and Freedman, L.P. Reciprocal recruitment of DRIP/mediator and p160 coactivator complexes in vivo by estrogen receptor. *J Biol Chem* 277, 14359-62 (2002).

Burd, C.J., Kinyamu, H.K., Miller, F.W. and Archer, T.K. UV radiation regulates Mi-2 through protein translation and stability. *J Biol Chem* 283, 34976-82 (2008).

Buszczak, M., Freeman, M.R., Carlson, J.R., Bender, M., Cooley, L. and Segraves, W.A. Ecdysone response genes govern egg chamber development during mid-oogenesis in Drosophila. *Development* 126, 4581-9 (1999).

Carbonell, A., Mazo, A., Serras, F. and Corominas, M. Ash2 acts as an ecdysone receptor coactivator by stabilizing the histone methyltransferase Trr. *Mol Biol Cell* 24, 361-72 (2013).

Carney, G.E. and Bender, M. The Drosophila ecdysone receptor (EcR) gene is required maternally for normal oogenesis. *Genetics* 154, 1203-11 (2000).

Carroll, J.S. *et al.* Genome-wide analysis of estrogen receptor binding sites. *Nat Genet* 38, 1289-97 (2006).

Celeste, A. *et al.* Genomic instability in mice lacking histone H2AX. *Science* 296, 922-927 (2002).

Chadwick, B.P. and Willard, H.F. A novel chromatin protein, distantly related to histone H2A, is largely excluded from the inactive X chromosome. *J Cell Biol* 152, 375-84 (2001).

Chalepakis, G., Postma, J.P. and Beato, M. A model for hormone receptor binding to the mouse mammary tumour virus regulatory element based on hydroxyl radical footprinting. *Nucleic Acids Res* 16, 10237-47 (1988).

Chandler, V.L., Maler, B.A. and Yamamoto, K.R. DNA sequences bound specifically by glucocorticoid receptor in vitro render a heterologous promoter hormone responsive in vivo. *Cell* 33, 489-99 (1983).

Chauhan, C., Zraly, C.B., Parilla, M., Diaz, M.O. and Dingwall, A.K. Histone recognition and nuclear receptor co-activator functions of Drosophila cara mitad, a homolog of the N-terminal portion of mammalian MLL2 and MLL3. *Development* 139, 1997-2008 (2012).

Chen, H., Lin, R.J., Xie, W., Wilpitz, D. and Evans, R.M. Regulation of hormone-induced histone hyperacetylation and gene activation via acetylation of an acetylase. *Cell* 98, 675-86 (1999).

Chen, J.D., Umesono, K. and Evans, R.M. SMRT isoforms mediate repression and anti-repression of nuclear receptor heterodimers. *Proc Natl Acad Sci U S A* 93, 7567-71 (1996).

Chen, R.F. Removal of Fatty Acids from Serum Albumin by Charcoal Treatment. *Journal of Biological Chemistry* 242, 173-& (1967).

Clapier, C.R., Langst, G., Corona, D.F., Becker, P.B. and Nightingale, K.P. Critical role for the histone H4 N terminus in nucleosome remodeling by ISWI. *Mol Cell Biol* 21, 875-83 (2001).

Clemens, J.C., Worby, C.A., Simonson-Leff, N., Muda, M., Maehama, T., Hemmings, B.A. and Dixon, J.E. Use of double-stranded RNA interference in Drosophila cell lines to dissect signal transduction pathways. *Proc Natl Acad Sci U S A* 97, 6499-503 (2000).

Clever, U. Actinomycin and Puromycin: Effects on Sequential Gene Activation by Ecdysone. *Science* 146, 794-5 (1964).

Costanzi, C. and Pehrson, J.R. Histone macroH2A1 is concentrated in the inactive X chromosome of female mammals. *Nature* 393, 599-601 (1998).

Cropley, J.E., Suter, C.M., Beckman, K.B. and Martin, D.I. Germ-line epigenetic modification of the murine A vy allele by nutritional supplementation. *Proc Natl Acad Sci U S A* 103, 17308-12 (2006).

Daubresse, G., Deuring, R., Moore, L., Papoulas, O., Zakrajsek, I., Waldrip, W.R., Scott, M.P., Kennison, J.A. and Tamkun, J.W. The Drosophila kismet gene is related to chromatin-remodeling factors and is required for both segmentation and segment identity. *Development* 126, 1175-87 (1999).

Davey, C.A., Sargent, D.F., Luger, K., Maeder, A.W. and Richmond, T.J. Solvent mediated interactions in the structure of the nucleosome core particle at 1.9 a resolution. *J Mol Biol* 319, 1097-113 (2002).

Davis, M.B., Carney, G.E., Robertson, A.E. and Bender, M. Phenotypic analysis of EcR-A mutants suggests that EcR isoforms have unique functions during Drosophila development. *Dev Biol* 282, 385-96 (2005).

Davis, M.B., SanGil, I., Berry, G., Olayokun, R. and Neves, L.H. Identification of common and cell type specific LXXLL motif EcR cofactors using a bioinformatics refined candidate RNAi screen in Drosophila melanogaster cell lines. *BMC Dev Biol* 11, 66 (2011).

De Vos, P., Claessens, F., Peeters, B., Rombauts, W., Heyns, W. and Verhoeven, G. Interaction of androgen and glucocorticoid receptor DNA-binding domains with their response elements. *Mol Cell Endocrinol* 90, R11-6 (1993).

Delacroix, L., Moutier, E., Altobelli, G., Legras, S., Poch, O., Choukrallah, M.A., Bertin, I., Jost, B. and Davidson, I. Cell-specific interaction of retinoic acid receptors with target genes in mouse embryonic fibroblasts and embryonic stem cells. *Mol Cell Biol* 30, 231-44 (2010).

DeLisle, A.J., Graves, R.A., Marzluff, W.F. and Johnson, L.F. Regulation of histone mRNA production and stability in serum-stimulated mouse 3T6 fibroblasts. *Mol Cell Biol* 3, 1920-9 (1983).

Denton, D., Aung-Htut, M.T. and Kumar, S. Developmentally programmed cell death in Drosophila. *Biochim Biophys Acta* 1833, 3499-506 (2013a).

Denton, D., Aung-Htut, M.T., Lorensuhewa, N., Nicolson, S., Zhu, W., Mills, K., Cakouros, D., Bergmann, A. and Kumar, S. UTX coordinates steroid hormone-mediated autophagy and cell death. *Nat Commun* 4, 2916 (2013b).

Devarakonda, S., Harp, J.M., Kim, Y., Ozyhar, A. and Rastinejad, F. Structure of the heterodimeric ecdysone receptor DNA-binding complex. *EMBO J* 22, 5827-40 (2003).

Dhalluin, C., Carlson, J.E., Zeng, L., He, C., Aggarwal, A.K. and Zhou, M.M. Structure and ligand of a histone acetyltransferase bromodomain. *Nature* 399, 491-6 (1999).

DiRenzo, J., Shang, Y., Phelan, M., Sif, S., Myers, M., Kingston, R. and Brown, M. BRG-1 is recruited to estrogen-responsive promoters and cooperates with factors involved in histone acetylation. *Mol Cell Biol* 20, 7541-9 (2000).

Dorighi, K.M. and Tamkun, J.W. The trithorax group proteins Kismet and ASH1 promote H3K36 dimethylation to counteract Polycomb group repression in Drosophila. *Development* 140, 4182-92 (2013).

Dou, Y., Milne, T.A., Ruthenburg, A.J., Lee, S., Lee, J.W., Verdine, G.L., Allis, C.D. and Roeder, R.G. Regulation of MLL1 H3K4 methyltransferase activity by its core components. *Nat Struct Mol Biol* 13, 713-9 (2006).

Dubois, M.F., Nguyen, V.T., Bellier, S. and Bensaude, O. Inhibitors of transcription such as 5,6-dichloro-1-beta-D-ribofuranosylbenzimidazole and isoquinoline sulfonamide derivatives (H-8 and H-7) promote dephosphorylation of the carboxyl-terminal domain of RNA polymerase II largest subunit. *J Biol Chem* 269, 13331-6 (1994).

Durr, H., Flaus, A., Owen-Hughes, T. and Hopfner, K.P. Snf2 family ATPases and DExx box helicases: differences and unifying concepts from high-resolution crystal structures. *Nucleic Acids Res* 34, 4160-7 (2006).

Ebbert, R., Birkmann, A. and Schuller, H.J. The product of the SNF2/SWI2 paralogue INO80 of Saccharomyces cerevisiae required for efficient expression of various yeast structural genes is part of a high-molecular-weight protein complex. *Mol Microbiol* 32, 741-51 (1999).

Ebert, A., Lein, S., Schotta, G. and Reuter, G. Histone modification and the control of heterochromatic gene silencing in Drosophila. *Chromosome Res* 14, 377-92 (2006).

Elfring, L.K. *et al.* Genetic analysis of brahma: the Drosophila homolog of the yeast chromatin remodeling factor SWI2/SNF2. *Genetics* 148, 251-65 (1998).

Elfring, L.K., Deuring, R., McCallum, C.M., Peterson, C.L. and Tamkun, J.W. Identification and characterization of Drosophila relatives of the yeast transcriptional activator SNF2/SWI2. *Mol Cell Biol* 14, 2225-34 (1994).

Elgin, S.C. and Reuter, G. Position-effect variegation, heterochromatin formation, and gene silencing in Drosophila. *Cold Spring Harb Perspect Biol* 5, a017780 (2013).

Ernst, J. *et al.* Mapping and analysis of chromatin state dynamics in nine human cell types. *Nature* 473, 43-9 (2011).

Feigl, G., Gram, M. and Pongs, O. A member of the steroid hormone receptor gene family is expressed in the 20-OH-ecdysone inducible puff 75B in Drosophila melanogaster. *Nucleic Acids Res* 17, 7167-78 (1989).

Ferreira, T.R., W.S. ImageJ User Guide — IJ 1.46. (2010 - 2012).

Filion, G.J. *et al.* Systematic protein location mapping reveals five principal chromatin types in Drosophila cells. *Cell* 143, 212-24 (2010).

Finch, J.T. and Klug, A. Solenoidal model for superstructure in chromatin. *Proc Natl Acad Sci U S A* 73, 1897-901 (1976).

Flanagan, J.F., Mi, L.Z., Chruszcz, M., Cymborowski, M., Clines, K.L., Kim, Y., Minor, W., Rastinejad, F. and Khorasanizadeh, S. Double chromodomains cooperate to recognize the methylated histone H3 tail. *Nature* 438, 1181-5 (2005).

Flemming, W. Zellsubstanz, Kern und Zelltheilung, 424 S. (*Verlag von F.C.W. Vogel*, *Leipzig*) (1882).

Flotho, A. and Melchior, F. Sumoylation: a regulatory protein modification in health and disease. *Annu Rev Biochem* 82, 357-85 (2013).

Forneris, F., Binda, C., Vanoni, M.A., Battaglioli, E. and Mattevi, A. Human histone demethylase LSD1 reads the histone code. *J Biol Chem* 280, 41360-5 (2005).

Fullwood, M.J. *et al.* An oestrogen-receptor-alpha-bound human chromatin interactome. *Nature* 462, 58-64 (2009).

Gamble, M.J. and Kraus, W.L. Multiple facets of the unique histone variant macroH2A: from genomics to cell biology. *Cell Cycle* 9, 2568-74 (2010).

Gangaraju, V.K., Prasad, P., Srour, A., Kagalwala, M.N. and Bartholomew, B. Conformational changes associated with template commitment in ATP-dependent chromatin remodeling by ISW2. *Mol Cell* 35, 58-69 (2009).

Gauhar, Z., Sun, L.V., Hua, S., Mason, C.E., Fuchs, F., Li, T.R., Boutros, M. and White, K.P. Genomic mapping of binding regions for the Ecdysone receptor protein complex. *Genome Res* 19, 1006-13 (2009).

Germain, P. and Bourguet, W. Dimerization of nuclear receptors. *Methods Cell Biol* 117, 21-41 (2013).

Godowski, P.J., Rusconi, S., Miesfeld, R. and Yamamoto, K.R. Glucocorticoid receptor mutants that are constitutive activators of transcriptional enhancement. *Nature* 325, 365-8 (1987).

Goldberg, A.D. *et al.* Distinct factors control histone variant H3.3 localization at specific genomic regions. *Cell* 140, 678-91 (2010).

Gonsalves, S.E., Neal, S.J., Kehoe, A.S. and Westwood, J.T. Genome-wide examination of the transcriptional response to ecdysteroids 20-hydroxyecdysone and ponasterone A in Drosophila melanogaster. *BMC Genomics* 12, 475 (2011).

Goodwin, G.H. Isolation of cDNAs encoding chicken homologues of the yeast SNF2 and Drosophila Brahma proteins. *Gene* 184, 27-32 (1997).

Green, G.R., Collas, P., Burrell, A. and Poccia, D.L. Histone phosphorylation during sea urchin development. *Semin Cell Biol* 6, 219-27 (1995).

Gronemeyer, H. and Moras, D. Nuclear receptors. How to finger DNA. *Nature* 375, 190-1 (1995).

Guay, P.S. and Guild, G.M. The ecdysone-induced puffing cascade in Drosophila salivary glands: a Broad-Complex early gene regulates intermolt and late gene transcription. *Genetics* 129, 169-75 (1991).

Guccione, E., Bassi, C., Casadio, F., Martinato, F., Cesaroni, M., Schuchlautz, H., Luscher, B. and Amati, B. Methylation of histone H3R2 by PRMT6 and H3K4 by an MLL complex are mutually exclusive. *Nature* 449, 933-7 (2007).

Guiochon-Mantel, A., Loosfelt, H., Lescop, P., Christin-Maitre, S., Perrot-Applanat, M. and Milgrom, E. Mechanisms of nuclear localization of the progesterone receptor. *J Steroid Biochem Mol Biol* 41, 209-15 (1992).

Hagemeier, C., Cook, A. and Kouzarides, T. The retinoblastoma protein binds E2F residues required for activation in vivo and TBP binding in vitro. *Nucleic Acids Res* 21, 4998-5004 (1993).

Handler, A.M. Ecdysteroid titers during pupal and adult development in Drosophila melanogaster. *Dev Biol* 93, 73-82 (1982).

Hans, F. and Dimitrov, S. Histone H3 phosphorylation and cell division. *Oncogene* 20, 3021-7 (2001).

Hargreaves, D.C. and Crabtree, G.R. ATP-dependent chromatin remodeling: genetics, genomics and mechanisms. *Cell Res* 21, 396-420 (2011).

Hauk, G., McKnight, J.N., Nodelman, I.M. and Bowman, G.D. The chromodomains of the Chd1 chromatin remodeler regulate DNA access to the ATPase motor. *Mol Cell* 39, 711-23 (2010).

Hay, R.T. SUMO: a history of modification. *Mol Cell* 18, 1-12 (2005).

Heery, D.M., Kalkhoven, E., Hoare, S. and Parker, M.G. A signature motif in transcriptional co-activators mediates binding to nuclear receptors. *Nature* 387, 733-6 (1997).

Heins, J.N., Suriano, J.R., Taniuchi, H. and Anfinsen, C.B. Characterization of a nuclease produced by Staphylococcus aureus. *J Biol Chem* 242, 1016-20 (1967).

Heintzman, N.D. *et al.* Distinct and predictive chromatin signatures of transcriptional promoters and enhancers in the human genome. *Nat Genet* 39, 311-8 (2007).

Helsen, C., Kerkhofs, S., Clinckemalie, L., Spans, L., Laurent, M., Boonen, S., Vanderschueren, D. and Claessens, F. Structural basis for nuclear hormone receptor DNA binding. *Mol Cell Endocrinol* 348, 411-7 (2012).

Heming, B.S. Insect development and evolution, 444 S. (*Cornell University Press*, *Ithaca, New York*) (2003).

Henikoff, J.G., Belsky, J.A., Krassovsky, K., MacAlpine, D.M. and Henikoff, S. Epigenome characterization at single base-pair resolution. *Proc Natl Acad Sci U S A* 108, 18318-23 (2011).

Hill, R.J., Billas, I.M., Bonneton, F., Graham, L.D. and Lawrence, M.C. Ecdysone receptors: from the Ashburner model to structural biology. *Annu Rev Entomol* 58, 251-71 (2013).

Ho, L. and Crabtree, G.R. Chromatin remodelling during development. *Nature* 463, 474-84 (2010).

Hollenberg, S.M., Giguere, V., Segui, P. and Evans, R.M. Colocalization of DNA-binding and transcriptional activation functions in the human glucocorticoid receptor. *Cell* 49, 39-46 (1987).

Horn, P.J. and Peterson, C.L. Molecular biology. Chromatin higher order folding--wrapping up transcription. *Science* 297, 1824-7 (2002).

Hoskins, R.A. *et al.* Sequence finishing and mapping of Drosophila melanogaster heterochromatin. *Science* 316, 1625-8 (2007).

Hsu, J.Y. *et al.* Mitotic phosphorylation of histone H3 is governed by Ipl1/aurora kinase and Glc7/PP1 phosphatase in budding yeast and nematodes. *Cell* 102, 279-91 (2000).

Hu, X. and Lazar, M.A. The CoRNR motif controls the recruitment of corepressors by nuclear hormone receptors. *Nature* 402, 93-6 (1999).

Hyllus, D., Stein, C., Schnabel, K., Schiltz, E., Imhof, A., Dou, Y., Hsieh, J. and Bauer, U.M. PRMT6-mediated methylation of R2 in histone H3 antagonizes H3 K4 trimethylation. *Genes Dev* 21, 3369-80 (2007).

Ito, T., Bulger, M., Pazin, M.J., Kobayashi, R. and Kadonaga, J.T. ACF, an ISWI-containing and ATP-utilizing chromatin assembly and remodeling factor. *Cell* 90, 145-55 (1997).

Jackson, T.A., Richer, J.K., Bain, D.L., Takimoto, G.S., Tung, L. and Horwitz, K.B. The Partial Agonist Activity of Antagonist-Occupied Steroid Receptors Is Controlled by a Novel Hinge Domain-Binding Coactivator L7/SPA and the Corepressors N-CoR or SMRT. *Molecular Endocrinology* 11, 693-705 (1997).

Jackson, V., Shires, A., Tanphaichitr, N. and Chalkley, R. Modifications to histones immediately after synthesis. *J Mol Biol* 104, 471-83 (1976).

Jacobs, S.A. and Khorasanizadeh, S. Structure of HP1 chromodomain bound to a lysine 9-methylated histone H3 tail. *Science* 295, 2080-3 (2002).

Jakob, M. *et al.* Novel DNA-binding element within the C-terminal extension of the nuclear receptor DNA-binding domain. *Nucleic Acids Res* 35, 2705-18 (2007).

Jang, A.C., Chang, Y.C., Bai, J. and Montell, D. Border-cell migration requires integration of spatial and temporal signals by the BTB protein Abrupt. *Nat Cell Biol* 11, 569-79 (2009).

Jang, K.S., Paik, S.S., Chung, H., Oh, Y.H. and Kong, G. MTA1 overexpression correlates significantly with tumor grade and angiogenesis in human breast cancers. *Cancer Sci* 97, 374-9 (2006).

Jiang, C., Baehrecke, E.H. and Thummel, C.S. Steroid regulated programmed cell death during Drosophila metamorphosis. *Development* 124, 4673-83 (1997).

Johnston, D.M., Sedkov, Y., Petruk, S., Riley, K.M., Fujioka, M., Jaynes, J.B. and Mazo, A. Ecdysone- and NO-mediated gene regulation by competing EcR/Usp and E75A nuclear receptors during Drosophila development. *Mol Cell* 44, 51-61 (2011).

Kangaspeska, S., Stride, B., Metivier, R., Polycarpou-Schwarz, M., Ibberson, D., Carmouche, R.P., Benes, V., Gannon, F. and Reid, G. Transient cyclical methylation of promoter DNA. *Nature* 452, 112-5 (2008).

Karim, F.D. and Thummel, C.S. Temporal coordination of regulatory gene expression by the steroid hormone ecdysone. *EMBO J* 11, 4083-93 (1992).

Kehle, J., Beuchle, D., Treuheit, S., Christen, B., Kennison, J.A., Bienz, M. and Muller, J. dMi-2, a hunchback-interacting protein that functions in polycomb repression. *Science* 282, 1897-900 (1998).

Kharchenko, P.V. *et al.* Comprehensive analysis of the chromatin landscape in Drosophila melanogaster. *Nature* 471, 480-5 (2011).

Kilpatrick, Z.E., Cakouros, D. and Kumar, S. Ecdysone-mediated up-regulation of the effector caspase DRICE is required for hormone-dependent apoptosis in Drosophila cells. *J Biol Chem* 280, 11981-6 (2005).

Kimura, S. *et al.* Drosophila arginine methyltransferase 1 (DART1) is an ecdysone receptor co-repressor. *Biochem Biophys Res Commun* 371, 889-93 (2008).

King-Jones, K., Charles, J.P., Lam, G. and Thummel, C.S. The ecdysone-induced DHR4 orphan nuclear receptor coordinates growth and maturation in Drosophila. *Cell* 121, 773-84 (2005).

Kiss, I., Beaton, A.H., Tardiff, J., Fristrom, D. and Fristrom, J.W. Interactions and developmental effects of mutations in the Broad-Complex of Drosophila melanogaster. *Genetics* 118, 247-59 (1988).

Klymenko, T., Papp, B., Fischle, W., Kocher, T., Schelder, M., Fritsch, C., Wild, B., Wilm, M. and Muller, J. A Polycomb group protein complex with sequence-specific DNA-binding and selective methyl-lysine-binding activities. *Genes Dev* 20, 1110-22 (2006).

Kobor, M.S., Venkatasubrahmanyam, S., Meneghini, M.D., Gin, J.W., Jennings, J.L., Link, A.J., Madhani, H.D. and Rine, J. A protein complex containing the conserved Swi2/Snf2-related ATPase Swr1p deposits histone variant H2A.Z into euchromatin. *PLoS Biol* 2, E131 (2004).

Kodani, M. The Protein of the Salivary Gland Secretion in Drosophila. *Proc Natl Acad Sci U S A* 34, 131-5 (1948).

Koelle, M.R., Talbot, W.S., Segraves, W.A., Bender, M.T., Cherbas, P. and Hogness, D.S. The Drosophila EcR gene encodes an ecdysone receptor, a new member of the steroid receptor superfamily. *Cell* 67, 59-77 (1991).

Kon, C., Cadigan, K.M., da Silva, S.L. and Nusse, R. Developmental roles of the Mi-2/NURD-associated protein p66 in Drosophila. *Genetics* 169, 2087-100 (2005).

Konev, A.Y. *et al.* CHD1 motor protein is required for deposition of histone variant H3.3 into chromatin in vivo. *Science* 317, 1087-90 (2007).

Kopeć, S. Studies on the Necessity of the Brain for the Inception of Insect Metamorphosis. *Biological Bulletin* 42, 323-342 (1922).

Kouzarides, T. Chromatin modifications and their function. *Cell* 128, 693-705 (2007).

Kozlova, T. and Thummel, C.S. Essential roles for ecdysone signaling during Drosophila mid-embryonic development. *Science* 301, 1911-4 (2003).

Krogan, N.J. *et al.* The Paf1 complex is required for histone H3 methylation by COMPASS and Dot1p: linking transcriptional elongation to histone methylation. *Mol Cell* 11, 721-9 (2003).

Kunert, N., Wagner, E., Murawska, M., Klinker, H., Kremmer, E. and Brehm, A. dMec: a novel Mi-2 chromatin remodelling complex involved in transcriptional repression. *EMBO J* 28, 533-44 (2009).

Kusch, T., Florens, L., Macdonald, W.H., Swanson, S.K., Glaser, R.L., Yates, J.R., 3rd, Abmayr, S.M., Washburn, M.P. and Workman, J.L. Acetylation by Tip60 is required for selective histone variant exchange at DNA lesions. *Science* 306, 2084-7 (2004).

Kwon, S.Y., Xiao, H., Glover, B.P., Tjian, R., Wu, C. and Badenhorst, P. The nucleosome remodeling factor (NURF) regulates genes involved in Drosophila innate immunity. *Dev Biol* 316, 538-47 (2008).

Kwon, S.Y., Xiao, H., Wu, C. and Badenhorst, P. Alternative splicing of NURF301 generates distinct NURF chromatin remodeling complexes with altered modified histone binding specificities. *PLoS Genet* 5, e1000574 (2009).

Laemmli, U.K. Cleavage of structural proteins during the assembly of the head of bacteriophage T4. *Nature* 227, 680-5 (1970).

Lamond, A.I. and Earnshaw, W.C. Structure and function in the nucleus. *Science* 280, 547-53 (1998).

Langst, G., Bonte, E.J., Corona, D.F. and Becker, P.B. Nucleosome movement by CHRAC and ISWI without disruption or trans-displacement of the histone octamer. *Cell* 97, 843-52 (1999).

Lavorgna, G., Karim, F.D., Thummel, C.S. and Wu, C. Potential role for a FTZ-F1 steroid receptor superfamily member in the control of Drosophila metamorphosis. *Proc Natl Acad Sci U S A* 90, 3004-8 (1993).

Le Guezennec, X., Vermeulen, M., Brinkman, A.B., Hoeijmakers, W.A., Cohen, A., Lasonder, E. and Stunnenberg, H.G. MBD2/NuRD and MBD3/NuRD, two distinct complexes with different biochemical and functional properties. *Mol Cell Biol* 26, 843-51 (2006).

Levine, M., Cattoglio, C. and Tjian, R. Looping back to leap forward: transcription enters a new era. *Cell* 157, 13-25 (2014).

Lewin, B. Genes V, xxiv, 1272 p. (*Oxford University Press*, *Oxford ; New York*) (1994).

Li, G. and Reinberg, D. Chromatin higher-order structures and gene regulation. *Curr Opin Genet Dev* 21, 175-86 (2011).

Li, T.R. and White, K.P. Tissue-specific gene expression and ecdysone-regulated genomic networks in Drosophila. *Dev Cell* 5, 59-72 (2003).

Lo, W.S., Trievel, R.C., Rojas, J.R., Duggan, L., Hsu, J.Y., Allis, C.D., Marmorstein, R. and Berger, S.L. Phosphorylation of serine 10 in histone H3 is functionally linked in vitro and in vivo to Gcn5-mediated acetylation at lysine 14. *Mol Cell* 5, 917-26 (2000).

Luger, K., Dechassa, M.L. and Tremethick, D.J. New insights into nucleosome and chromatin structure: an ordered state or a disordered affair? *Nat Rev Mol Cell Biol* 13, 436-47 (2012).

Luger, K., Mader, A.W., Richmond, R.K., Sargent, D.F. and Richmond, T.J. Crystal structure of the nucleosome core particle at 2.8 A resolution. *Nature* 389, 251-60 (1997).

Luijsterburg, M.S. *et al.* A new non-catalytic role for ubiquitin ligase RNF8 in unfolding higher-order chromatin structure. *EMBO J* 31, 2511-27 (2012).

Lusser, A., Urwin, D.L. and Kadonaga, J.T. Distinct activities of CHD1 and ACF in ATP-dependent chromatin assembly. *Nat Struct Mol Biol* 12, 160-6 (2005).

Lyko, F., Ramsahoye, B.H. and Jaenisch, R. DNA methylation in Drosophila melanogaster. *Nature* 408, 538-40 (2000).

Maletta, M., Orlov, I., Roblin, P., Beck, Y., Moras, D., Billas, I.M. and Klaholz, B.P. The palindromic DNA-bound USP/EcR nuclear receptor adopts an asymmetric organization with allosteric domain positioning. *Nat Commun* 5, 4139 (2014).

Malik, H.S. and Henikoff, S. Phylogenomics of the nucleosome. *Nat Struct Biol* 10, 882-91 (2003).

Manelyte, L. and Längst, G. Chromatin Remodelers and Their Way of Action. in *Chromatin Remodeling* (ed. Radzioch, D.) (*InTech*, 2013).

Mangelsdorf, D.J. *et al.* The nuclear receptor superfamily: the second decade. *Cell* 83, 835-9 (1995).

Mansfield, R.E., Musselman, C.A., Kwan, A.H., Oliver, S.S., Garske, A.L., Davrazou, F., Denu, J.M., Kutateladze, T.G. and Mackay, J.P. Plant homeodomain (PHD) fingers of CHD4 are histone H3-binding modules with preference for unmodified H3K4 and methylated H3K9. *J Biol Chem* 286, 11779-91 (2011).

Marhold, J., Brehm, A. and Kramer, K. The Drosophila methyl-DNA binding protein MBD2/3 interacts with the NuRD complex via p55 and MI-2. *BMC Mol Biol* 5, 20 (2004).

Marmorstein, R. and Zhou, M.M. Writers and Readers of Histone Acetylation: Structure, Mechanism, and Inhibition. *Cold Spring Harb Perspect Biol* 6(2014).

Marygold, S.J. *et al.* The ribosomal protein genes and Minute loci of Drosophila melanogaster. *Genome Biol* 8, R216 (2007).

Mathieu, E.-L. Genome-wide analysis of dMi-2 binding sites, Philipps-University Marburg (2013).

Mathieu, E.L., Finkernagel, F., Murawska, M., Scharfe, M., Jarek, M. and Brehm, A. Recruitment of the ATP-dependent chromatin remodeler dMi-2 to the transcribed region of active heat shock genes. *Nucleic Acids Res* 40, 4879-91 (2012).

Matsuoka, S. *et al.* ATM and ATR substrate analysis reveals extensive protein networks responsive to DNA damage. *Science* 316, 1160-6 (2007).

Maurer-Stroh, S., Dickens, N.J., Hughes-Davies, L., Kouzarides, T., Eisenhaber, F. and Ponting, C.P. The Tudor domain 'Royal Family': Tudor, plant Agenet, Chromo, PWWP and MBT domains. *Trends Biochem Sci* 28, 69-74 (2003).

Mazumdar, A., Wang, R.A., Mishra, S.K., Adam, L., Bagheri-Yarmand, R., Mandal, M., Vadlamudi, R.K. and Kumar, R. Transcriptional repression of oestrogen receptor by metastasis-associated protein 1 corepressor. *Nat Cell Biol* 3, 30-7 (2001).

McInerney, E.M. *et al.* Determinants of coactivator LXXLL motif specificity in nuclear receptor transcriptional activation. *Genes Dev* 12, 3357-68 (1998).

Meier, K. Identification and functional characterisation of dL(3)mbt-containing complexes in *Drosophila melanogaster*, Philipps-University Marburg (2012).

Meier, K., Mathieu, E.L., Finkernagel, F., Reuter, L.M., Scharfe, M., Doehlemann, G., Jarek, M. and Brehm, A. LINT, a novel dL(3)mbt-containing complex, represses malignant brain tumour signature genes. *PLoS Genet* 8, e1002676 (2012).

Mendel, G.J. and Tschermak, E. Versuche über Pflanzenhybriden zwei Abhandlungen (1865 und 1869), 62 S. (*Engelmann*, *Leipzig*) (1901).

Mendiburo, M.J., Padeken, J., Fulop, S., Schepers, A. and Heun, P. Drosophila CENH3 is sufficient for centromere formation. *Science* 334, 686-90 (2011).

Mendoza-Parra, M.A. and Gronemeyer, H. Genome-wide studies of nuclear receptors in cell fate decisions. *Semin Cell Dev Biol* 24, 706-15 (2013).

Meneghini, M.D., Wu, M. and Madhani, H.D. Conserved histone variant H2A.Z protects euchromatin from the ectopic spread of silent heterochromatin. *Cell* 112, 725-36 (2003).

Metivier, R. *et al.* Cyclical DNA methylation of a transcriptionally active promoter. *Nature* 452, 45-50 (2008).

Metivier, R., Penot, G., Hubner, M.R., Reid, G., Brand, H., Kos, M. and Gannon, F. Estrogen receptor-alpha directs ordered, cyclical, and combinatorial recruitment of cofactors on a natural target promoter. *Cell* 115, 751-63 (2003).

Mohrmann, L., Langenberg, K., Krijgsveld, J., Kal, A.J., Heck, A.J. and Verrijzer, C.P. Differential targeting of two distinct SWI/SNF-related Drosophila chromatin-remodeling complexes. *Mol Cell Biol* 24, 3077-88 (2004).

Morettini, S. *et al.* The chromodomains of CHD1 are critical for enzymatic activity but less important for chromatin localization. *Nucleic Acids Res* 39, 3103-15 (2011).

Morgan, T.H. The mechanism of Mendelian heredity, xiii, 262 p. (*Holt*, *New York*) (1915).

Morris, S.A., Baek, S., Sung, M.H., John, S., Wiench, M., Johnson, T.A., Schiltz, R.L. and Hager, G.L. Overlapping chromatin-remodeling systems collaborate genome wide at dynamic chromatin transitions. *Nat Struct Mol Biol* 21, 73-81 (2014).

Mosallanejad, H., Soin, T. and Smagghe, G. Selection for resistance to methoxyfenozide and 20-hydroxyecdysone in cells of the beet armyworm, Spodoptera exigua. *Arch Insect Biochem Physiol* 67, 36-49 (2008).

Moshkin, Y.M. *et al.* Remodelers organize cellular chromatin by counteracting intrinsic histone-DNA sequence preferences in a class-specific manner. *Mol Cell Biol* 32, 675-88 (2012).

Mu, J.J., Wang, Y., Luo, H., Leng, M., Zhang, J., Yang, T., Besusso, D., Jung, S.Y. and Qin, J. A proteomic analysis of ataxia telangiectasia-mutated (ATM)/ATM-Rad3-related (ATR) substrates identifies the ubiquitin-proteasome system as a regulator for DNA damage checkpoints. *J Biol Chem* 282, 17330-4 (2007).

Mujtaba, S. *et al.* Structural mechanism of the bromodomain of the coactivator CBP in p53 transcriptional activation. *Mol Cell* 13, 251-63 (2004).

Murawska, M. Functional characterization of ATP-dependent chromatin remodelers of the CHD family of Drosophila, Philipps-University Marburg (2011).

Murawska, M., Hassler, M., Renkawitz-Pohl, R., Ladurner, A. and Brehm, A. Stress-induced PARP activation mediates recruitment of Drosophila Mi-2 to promote heat shock gene expression. *PLoS Genet* 7, e1002206 (2011).

Murawska, M., Kunert, N., van Vugt, J., Langst, G., Kremmer, E., Logie, C. and Brehm, A. dCHD3, a novel ATP-dependent chromatin remodeler associated with sites of active transcription. *Mol Cell Biol* 28, 2745-57 (2008).

Murawsky, C.M., Brehm, A., Badenhorst, P., Lowe, N., Becker, P.B. and Travers, A.A. Tramtrack69 interacts with the dMi-2 subunit of the Drosophila NuRD chromatin remodelling complex. *EMBO Rep* 2, 1089-94 (2001).

Nagy, L., Kao, H.Y., Chakravarti, D., Lin, R.J., Hassig, C.A., Ayer, D.E., Schreiber, S.L. and Evans, R.M. Nuclear receptor repression mediated by a complex containing SMRT, mSin3A, and histone deacetylase. *Cell* 89, 373-80 (1997).

Narlikar, G.J., Sundaramoorthy, R. and Owen-Hughes, T. Mechanisms and functions of ATP-dependent chromatin-remodeling enzymes. *Cell* 154, 490-503 (2013).

Neigeborn, L. and Carlson, M. Genes affecting the regulation of SUC2 gene expression by glucose repression in Saccharomyces cerevisiae. *Genetics* 108, 845-58 (1984).

Nettles, K.W. and Greene, G.L. Ligand control of coregulator recruitment to nuclear receptors. *Annu Rev Physiol* 67, 309-33 (2005).

Ng, H.H., Robert, F., Young, R.A. and Struhl, K. Targeted recruitment of Set1 histone methylase by elongating Pol II provides a localized mark and memory of recent transcriptional activity. *Mol Cell* 11, 709-19 (2003).

Nishino, Y. *et al.* Human mitotic chromosomes consist predominantly of irregularly folded nucleosome fibres without a 30-nm chromatin structure. *EMBO J* 31, 1644-53 (2012).

Nuclear Receptors Nomenclature, C. A unified nomenclature system for the nuclear receptor superfamily. *Cell* 97, 161-3 (1999).

O'Shaughnessy, A. and Hendrich, B. CHD4 in the DNA-damage response and cell cycle progression: not so NuRDy now. *Biochem Soc Trans* 41, 777-82 (2013).

Olefsky, J.M. Nuclear receptor minireview series. *J Biol Chem* 276, 36863-4 (2001).

Ong, C.T. and Corces, V.G. Enhancer function: new insights into the regulation of tissue-specific gene expression. *Nat Rev Genet* 12, 283-93 (2011).

Ornaghi, P., Ballario, P., Lena, A.M., Gonzalez, A. and Filetici, P. The bromodomain of Gcn5p interacts in vitro with specific residues in the N terminus of histone H4. *J Mol Biol* 287, 1-7 (1999).

Oro, A.E., McKeown, M. and Evans, R.M. Relationship between the product of the Drosophila ultraspiracle locus and the vertebrate retinoid X receptor. *Nature* 347, 298-301 (1990).

Osborne, C.S. *et al.* Active genes dynamically colocalize to shared sites of ongoing transcription. *Nat Genet* 36, 1065-71 (2004).

Papoulas, O., Beek, S.J., Moseley, S.L., McCallum, C.M., Sarte, M., Shearn, A. and Tamkun, J.W. The Drosophila trithorax group proteins BRM, ASH1 and ASH2 are subunits of distinct protein complexes. *Development* 125, 3955-66 (1998).

Pauli, A., van Bemmel, J.G., Oliveira, R.A., Itoh, T., Shirahige, K., van Steensel, B. and Nasmyth, K. A direct role for cohesin in gene regulation and ecdysone response in Drosophila salivary glands. *Curr Biol* 20, 1787-98 (2010).

Pepke, S., Wold, B. and Mortazavi, A. Computation for ChIP-seq and RNA-seq studies. *Nat Methods* 6, S22-32 (2009).

Peters, A.H. *et al.* Partitioning and plasticity of repressive histone methylation states in mammalian chromatin. *Mol Cell* 12, 1577-89 (2003).

Petesch, S.J. and Lis, J.T. Rapid, transcription-independent loss of nucleosomes over a large chromatin domain at Hsp70 loci. *Cell* 134, 74-84 (2008).

Petryk, A. *et al.* Shade is the Drosophila P450 enzyme that mediates the hydroxylation of ecdysone to the steroid insect molting hormone 20-hydroxyecdysone. *Proc Natl Acad Sci U S A* 100, 13773-8 (2003).

Pokholok, D.K. *et al.* Genome-wide map of nucleosome acetylation and methylation in yeast. *Cell* 122, 517-27 (2005).

Polo, S.E., Kaidi, A., Baskcomb, L., Galanty, Y. and Jackson, S.P. Regulation of DNA-damage responses and cell-cycle progression by the chromatin remodelling factor CHD4. *EMBO J* 29, 3130-9 (2010).

Radman-Livaja, M. and Rando, O.J. Nucleosome positioning: how is it established, and why does it matter? *Dev Biol* 339, 258-66 (2010).

Raisner, R.M., Hartley, P.D., Meneghini, M.D., Bao, M.Z., Liu, C.L., Schreiber, S.L., Rando, O.J. and Madhani, H.D. Histone variant H2A.Z marks the 5' ends of both active and inactive genes in euchromatin. *Cell* 123, 233-48 (2005).

Ramirez-Carrozzi, V.R., Nazarian, A.A., Li, C.C., Gore, S.L., Sridharan, R., Imbalzano, A.N. and Smale, S.T. Selective and antagonistic functions of SWI/SNF and Mi-2beta nucleosome remodeling complexes during an inflammatory response. *Genes Dev* 20, 282-96 (2006).

Reddy, B.A., Bajpe, P.K., Bassett, A., Moshkin, Y.M., Kozhevnikova, E., Bezstarosti, K., Demmers, J.A., Travers, A.A. and Verrijzer, C.P. Drosophila transcription factor Tramtrack69 binds MEP1 to recruit the chromatin remodeler NuRD. *Mol Cell Biol* 30, 5234-44 (2010).

Reid, G., Hubner, M.R., Metivier, R., Brand, H., Denger, S., Manu, D., Beaudouin, J., Ellenberg, J. and Gannon, F. Cyclic, proteasome-mediated turnover of unliganded and liganded ERalpha on responsive promoters is an integral feature of estrogen signaling. *Mol Cell* 11, 695-707 (2003).

Rewitz, K.F., Yamanaka, N. and O'Connor, M.B. Developmental checkpoints and feedback circuits time insect maturation. *Curr Top Dev Biol* 103, 1-33 (2013).

Richards, G. The radioimmune assay of ecdysteroid titres in Drosophila melanogaster. *Mol Cell Endocrinol* 21, 181-97 (1981).

Richards, G. Sequential gene activation by ecdysone in polytene chromosomes of Drosophila melanogaster. IV. The mid prepupal period. *Dev Biol* 54, 256-63 (1976).

Riddihough, G. and Pelham, H.R. An ecdysone response element in the Drosophila hsp27 promoter. *EMBO J* 6, 3729-34 (1987).

Rinn, J.L. and Chang, H.Y. Genome regulation by long noncoding RNAs. *Annu Rev Biochem* 81, 145-66 (2012).

Robins, D.M., Paek, I., Seeburg, P.H. and Axel, R. Regulated expression of human growth hormone genes in mouse cells. *Cell* 29, 623-31 (1982).

Roder, K., Hung, M.S., Lee, T.L., Lin, T.Y., Xiao, H., Isobe, K.I., Juang, J.L. and Shen, C.J. Transcriptional repression by Drosophila methyl-CpG-binding proteins. *Mol Cell Biol* 20, 7401-9 (2000).

Rosenfeld, C.S. Animal models to study environmental epigenetics. *Biol Reprod* 82, 473-88 (2010).

Rossetto, D., Avvakumov, N. and Cote, J. Histone phosphorylation: a chromatin modification involved in diverse nuclear events. *Epigenetics* 7, 1098-108 (2012).

Ruiz-Carrillo, A., Wangh, L.J. and Allfrey, V.G. Processing of newly synthesized histone molecules. *Science* 190, 117-28 (1975).

Ruthenburg, A.J., Allis, C.D. and Wysocka, J. Methylation of lysine 4 on histone H3: intricacy of writing and reading a single epigenetic mark. *Mol Cell* 25, 15-30 (2007).

Saiki, R.K., Scharf, S., Faloona, F., Mullis, K.B., Horn, G.T., Erlich, H.A. and Arnheim, N. Enzymatic amplification of beta-globin genomic sequences and restriction site analysis for diagnosis of sickle cell anemia. *Science* 230, 1350-4 (1985).

Sakabe, K., Wang, Z. and Hart, G.W. Beta-N-acetylglucosamine (O-GlcNAc) is part of the histone code. *Proc Natl Acad Sci U S A* 107, 19915-20 (2010).

Sambrook, J. and Russell, D.W. Molecular cloning a laboratory manual, 3 vols. (*Cold Spring Harbor Laboratory Press*, *Cold Spring Harbor, New York*) (2001).

Samuels, H.H., Tsai, J.S. and Cintron, R. Thyroid hormone action: a cell-culture system responsive to physiological concentrations of thyroid hormones. *Science* 181, 1253-6 (1973).

Sanchez, R. and Zhou, M.M. The PHD finger: a versatile epigenome reader. *Trends Biochem Sci* 36, 364-72 (2011).

Santos-Rosa, H., Schneider, R., Bannister, A.J., Sherriff, J., Bernstein, B.E., Emre, N.C., Schreiber, S.L., Mellor, J. and Kouzarides, T. Active genes are tri-methylated at K4 of histone H3. *Nature* 419, 407-11 (2002).

Sawatsubashi, S. *et al.* Ecdysone receptor-dependent gene regulation mediates histone poly(ADP-ribosyl)ation. *Biochem Biophys Res Commun* 320, 268-72 (2004).

Sawatsubashi, S. *et al.* A histone chaperone, DEK, transcriptionally coactivates a nuclear receptor. *Genes Dev* 24, 159-70 (2010).

Schneider, I. Cell lines derived from late embryonic stages of Drosophila melanogaster. *J Embryol Exp Morphol* 27, 353-65 (1972).

Schneider, R., Bannister, A.J., Myers, F.A., Thorne, A.W., Crane-Robinson, C. and Kouzarides, T. Histone H3 lysine 4 methylation patterns in higher eukaryotic genes. *Nat Cell Biol* 6, 73-7 (2004).

Schubiger, M., Wade, A.A., Carney, G.E., Truman, J.W. and Bender, M. Drosophila EcR-B ecdysone receptor isoforms are required for larval molting and for neuron remodeling during metamorphosis. *Development* 125, 2053-62 (1998).

Scully, R. and Xie, A. Double strand break repair functions of histone H2AX. *Mutat Res* 750, 5-14 (2013).

Sedkov, Y. *et al.* Methylation at lysine 4 of histone H3 in ecdysone-dependent development of Drosophila. *Nature* 426, 78-83 (2003).

Seelig, H.P., Moosbrugger, I., Ehrfeld, H., Fink, T., Renz, M. and Genth, E. The major dermatomyositis-specific Mi-2 autoantigen is a presumed helicase involved in transcriptional activation. *Arthritis Rheum* 38, 1389-99 (1995).

Segraves, W.A. and Hogness, D.S. The E75 ecdysone-inducible gene responsible for the 75B early puff in Drosophila encodes two new members of the steroid receptor superfamily. *Genes Dev* 4, 204-19 (1990).

Seliga, J., Bielska, K., Wieczorek, E., Orlowski, M., Niedenthal, R. and Ozyhar, A. Multidomain sumoylation of the ecdysone receptor (EcR) from Drosophila melanogaster. *J Steroid Biochem Mol Biol* 138, 162-73 (2013).

Sewack, G.F. and Hansen, U. Nucleosome positioning and transcription-associated chromatin alterations on the human estrogen-responsive pS2 promoter. *J Biol Chem* 272, 31118-29 (1997).

Shahbazian, M.D. and Grunstein, M. Functions of site-specific histone acetylation and deacetylation. *Annu Rev Biochem* 76, 75-100 (2007).

Shang, Y., Hu, X., DiRenzo, J., Lazar, M.A. and Brown, M. Cofactor dynamics and sufficiency in estrogen receptor-regulated transcription. *Cell* 103, 843-52 (2000).

Shi, Y., Lan, F., Matson, C., Mulligan, P., Whetstine, J.R., Cole, P.A., Casero, R.A. and Shi, Y. Histone demethylation mediated by the nuclear amine oxidase homolog LSD1. *Cell* 119, 941-53 (2004).

Shlyueva, D., Stelzer, C., Gerlach, D., Yanez-Cuna, J.O., Rath, M., Boryn, L.M., Arnold, C.D. and Stark, A. Hormone-responsive enhancer-activity maps reveal predictive motifs, indirect repression, and targeting of closed chromatin. *Mol Cell* 54, 180-92 (2014).

Skene, P.J. and Henikoff, S. Histone variants in pluripotency and disease. *Development* 140, 2513-24 (2013).

Sliter, T.J. and Gilbert, L.I. Developmental arrest and ecdysteroid deficiency resulting from mutations at the dre4 locus of Drosophila. *Genetics* 130, 555-68 (1992).

Smagghe, G. Ecdysone, structures and functions. xlii, 583 p. (2009).

Smagghe, G., Goodman, C.L. and Stanley, D. Insect cell culture and applications to research and pest management. *In Vitro Cell Dev Biol Anim* 45, 93-105 (2009).

Smeenk, G., Wiegant, W.W., Vrolijk, H., Solari, A.P., Pastink, A. and van Attikum, H. The NuRD chromatin-remodeling complex regulates signaling and repair of DNA damage. *J Cell Biol* 190, 741-9 (2010).

Sobel, R.E., Cook, R.G., Perry, C.A., Annunziato, A.T. and Allis, C.D. Conservation of deposition-related acetylation sites in newly synthesized histones H3 and H4. *Proc Natl Acad Sci U S A* 92, 1237-41 (1995).

Soshnikova, N.V., Vorob'eva, N.E., Krasnov, A.N., Georgieva, S.G., Nabirochkina, E.N. and Shidlovskii Iu, V. [Novel complex, formed by transcription coactivator SAYP]. *Mol Biol (Mosk)* 43, 1055-62 (2009).

Srinivasan, S., Armstrong, J.A., Deuring, R., Dahlsveen, I.K., McNeill, H. and Tamkun, J.W. The Drosophila trithorax group protein Kismet facilitates an early step in transcriptional elongation by RNA Polymerase II. *Development* 132, 1623-35 (2005).

Srinivasan, S., Dorighi, K.M. and Tamkun, J.W. Drosophila Kismet regulates histone H3 lysine 27 methylation and early elongation by RNA polymerase II. *PLoS Genet* 4, e1000217 (2008).

Stielow, B., Sapetschnig, A., Kruger, I., Kunert, N., Brehm, A., Boutros, M. and Suske, G. Identification of SUMO-dependent chromatin-associated transcriptional repression components by a genome-wide RNAi screen. *Mol Cell* 29, 742-54 (2008).

Stokes, D.G., Tartof, K.D. and Perry, R.P. CHD1 is concentrated in interbands and puffed regions of Drosophila polytene chromosomes. *Proc Natl Acad Sci U S A* 93, 7137-42 (1996).

Stunnenberg, H.G. Mechanisms of transactivation by retinoic acid receptors. *Bioessays* 15, 309-15 (1993).

Szerlong, H.J. and Hansen, J.C. Nucleosome distribution and linker DNA: connecting nuclear function to dynamic chromatin structure. *Biochem Cell Biol* 89, 24-34 (2011).

Talbot, W.S., Swyryd, E.A. and Hogness, D.S. Drosophila tissues with different metamorphic responses to ecdysone express different ecdysone receptor isoforms. *Cell* 73, 1323-37 (1993).

Tamkun, J.W., Deuring, R., Scott, M.P., Kissinger, M., Pattatucci, A.M., Kaufman, T.C. and Kennison, J.A. brahma: a regulator of Drosophila homeotic genes structurally related to the yeast transcriptional activator SNF2/SWI2. *Cell* 68, 561-72 (1992).

Tatham, M.H., Rodriguez, M.S., Xirodimas, D.P. and Hay, R.T. Detection of protein SUMOylation in vivo. *Nat Protoc* 4, 1363-71 (2009).

Teytelman, L., Thurtle, D.M., Rine, J. and van Oudenaarden, A. Highly expressed loci are vulnerable to misleading ChIP localization of multiple unrelated proteins. *Proc Natl Acad Sci U S A* 110, 18602-7 (2013).

Thomas, H.E., Stunnenberg, H.G. and Stewart, A.F. Heterodimerization of the Drosophila ecdysone receptor with retinoid X receptor and ultraspiracle. *Nature* 362, 471-5 (1993).

Thummel, C.S. From embryogenesis to metamorphosis: the regulation and function of Drosophila nuclear receptor superfamily members. *Cell* 83, 871-7 (1995).

Tolstorukov, M.Y., Goldman, J.A., Gilbert, C., Ogryzko, V., Kingston, R.E. and Park, P.J. Histone variant H2A.Bbd is associated with active transcription and mRNA processing in human cells. *Mol Cell* 47, 596-607 (2012).

Tong, J.K., Hassig, C.A., Schnitzler, G.R., Kingston, R.E. and Schreiber, S.L. Chromatin deacetylation by an ATP-dependent nucleosome remodelling complex. *Nature* 395, 917-21 (1998).

Trievel, R.C., Beach, B.M., Dirk, L.M., Houtz, R.L. and Hurley, J.H. Structure and catalytic mechanism of a SET domain protein methyltransferase. *Cell* 111, 91-103 (2002).

Truman, J.W. Hormonal control of insect ecdysis: endocrine cascades for coordinating behavior with physiology. *Vitam Horm* 73, 1-30 (2005).

Tsai, C.C., Kao, H.Y., Yao, T.P., McKeown, M. and Evans, R.M. SMRTER, a Drosophila nuclear receptor coregulator, reveals that EcR-mediated repression is critical for development. *Mol Cell* 4, 175-86 (1999).

Tsukada, Y., Fang, J., Erdjument-Bromage, H., Warren, M.E., Borchers, C.H., Tempst, P. and Zhang, Y. Histone demethylation by a family of JmjC domain-containing proteins. *Nature* 439, 811-6 (2006).

Tsukiyama, T., Daniel, C., Tamkun, J. and Wu, C. ISWI, a member of the SWI2/SNF2 ATPase family, encodes the 140 kDa subunit of the nucleosome remodeling factor. *Cell* 83, 1021-6 (1995).

Tsukiyama, T. and Wu, C. Purification and properties of an ATP-dependent nucleosome remodeling factor. *Cell* 83, 1011-20 (1995).

Tulin, A. and Spradling, A. Chromatin loosening by poly(ADP)-ribose polymerase (PARP) at Drosophila puff loci. *Science* 299, 560-2 (2003).

Tulin, A., Stewart, D. and Spradling, A.C. The Drosophila heterochromatic gene encoding poly(ADP-ribose) polymerase (PARP) is required to modulate chromatin structure during development. *Genes Dev* 16, 2108-19 (2002).

Van Hooser, A.A. *et al.* Specification of kinetochore-forming chromatin by the histone H3 variant CENP-A. *J Cell Sci* 114, 3529-42 (2001).

Varga-Weisz, P.D., Wilm, M., Bonte, E., Dumas, K., Mann, M. and Becker, P.B. Chromatin-remodelling factor CHRAC contains the ATPases ISWI and topoisomerase II. *Nature* 388, 598-602 (1997).

Vaughn, J.L., Goodwin, R.H., Tompkins, G.J. and McCawley, P. The establishment of two cell lines from the insect Spodoptera frugiperda (Lepidoptera; Noctuidae). *In Vitro* 13, 213-7 (1977).

Verdaasdonk, J.S. and Bloom, K. Centromeres: unique chromatin structures that drive chromosome segregation. *Nat Rev Mol Cell Biol* 12, 320-32 (2011).

Vogtli, M., Elke, C., Imhof, M.O. and Lezzi, M. High level transactivation by the ecdysone receptor complex at the core recognition motif. *Nucleic Acids Res* 26, 2407-14 (1998).

Vorobyeva, N.E., Nikolenko, J.V., Krasnov, A.N., Kuzmina, J.L., Panov, V.V., Nabirochkina, E.N., Georgieva, S.G. and Shidlovskii, Y.V. SAYP interacts with DHR3 nuclear receptor and participates in ecdysone-dependent transcription regulation. *Cell Cycle* 10, 1821-7 (2011).

Wade, P.A., Jones, P.L., Vermaak, D. and Wolffe, A.P. A multiple subunit Mi-2 histone deacetylase from Xenopus laevis cofractionates with an associated Snf2 superfamily ATPase. *Curr Biol* 8, 843-6 (1998).

Wang, Q., Li, W., Liu, X.S., Carroll, J.S., Janne, O.A., Keeton, E.K., Chinnaiyan, A.M., Pienta, K.J. and Brown, M. A hierarchical network of transcription factors governs androgen receptor-dependent prostate cancer growth. *Mol Cell* 27, 380-92 (2007).

White, K.P., Rifkin, S.A., Hurban, P. and Hogness, D.S. Microarray analysis of Drosophila development during metamorphosis. *Science* 286, 2179-84 (1999).

Wood, A.M., Van Bortle, K., Ramos, E., Takenaka, N., Rohrbaugh, M., Jones, B.C., Jones, K.C. and Corces, V.G. Regulation of chromatin organization and inducible gene expression by a Drosophila insulator. *Mol Cell* 44, 29-38 (2011).

Woodard, C.T., Baehrecke, E.H. and Thummel, C.S. A molecular mechanism for the stage specificity of the Drosophila prepupal genetic response to ecdysone. *Cell* 79, 607-15 (1994).

Wright, L.G., Chen, T., Thummel, C.S. and Guild, G.M. Molecular characterization of the 71E late puff in Drosophila melanogaster reveals a family of novel genes. *J Mol Biol* 255, 387-400 (1996).

Wu, L. and Winston, F. Evidence that Snf-Swi controls chromatin structure over both the TATA and UAS regions of the SUC2 promoter in Saccharomyces cerevisiae. *Nucleic Acids Res* 25, 4230-4 (1997).

Wu, W.H., Alami, S., Luk, E., Wu, C.H., Sen, S., Mizuguchi, G., Wei, D. and Wu, C. Swc2 is a widely conserved H2AZ-binding module essential for ATP-dependent histone exchange. *Nat Struct Mol Biol* 12, 1064-71 (2005).

Wysocka, J. *et al.* A PHD finger of NURF couples histone H3 lysine 4 trimethylation with chromatin remodelling. *Nature* 442, 86-90 (2006).

Xue, Y., Wong, J., Moreno, G.T., Young, M.K., Cote, J. and Wang, W. NURD, a novel complex with both ATP-dependent chromatin-remodeling and histone deacetylase activities. *Mol Cell* 2, 851-61 (1998).

Yamanaka, N., Rewitz, K.F. and O'Connor, M.B. Ecdysone control of developmental transitions: lessons from Drosophila research. *Annu Rev Entomol* 58, 497-516 (2013).

Yao, T.P., Forman, B.M., Jiang, Z., Cherbas, L., Chen, J.D., McKeown, M., Cherbas, P. and Evans, R.M. Functional ecdysone receptor is the product of EcR and Ultraspiracle genes. *Nature* 366, 476-9 (1993).

Yao, T.P., Segraves, W.A., Oro, A.E., McKeown, M. and Evans, R.M. Drosophila ultraspiracle modulates ecdysone receptor function via heterodimer formation. *Cell* 71, 63-72 (1992).

Yin, V.P. and Thummel, C.S. Mechanisms of steroid-triggered programmed cell death in Drosophila. *Semin Cell Dev Biol* 16, 237-43 (2005).

Zentner, G.E. and Henikoff, S. Regulation of nucleosome dynamics by histone modifications. *Nat Struct Mol Biol* 20, 259-66 (2013).

Zhang, H., Roberts, D.N. and Cairns, B.R. Genome-wide dynamics of Htz1, a histone H2A variant that poises repressed/basal promoters for activation through histone loss. *Cell* 123, 219-31 (2005).

Zhang, K., Chen, Y., Zhang, Z. and Zhao, Y. Identification and verification of lysine propionylation and butyrylation in yeast core histones using PTMap software. *J Proteome Res* 8, 900-6 (2009).

Zhang, Y., LeRoy, G., Seelig, H.P., Lane, W.S. and Reinberg, D. The dermatomyositis-specific autoantigen Mi2 is a component of a complex containing histone deacetylase and nucleosome remodeling activities. *Cell* 95, 279-89 (1998).

Zhang, Y., Ng, H.H., Erdjument-Bromage, H., Tempst, P., Bird, A. and Reinberg, D. Analysis of the NuRD subunits reveals a histone deacetylase core complex and a connection with DNA methylation. *Genes Dev* 13, 1924-35 (1999).

Zraly, C.B., Middleton, F.A. and Dingwall, A.K. Hormone-response genes are direct in vivo regulatory targets of Brahma (SWI/SNF) complex function. *J Biol Chem* 281, 35305-15 (2006).

7 Appendix

ChIPSeq results: Mi-2 binding sites that are increased and decreased upon 20HE treatment

Table 7.1: List of >2.3-fold induced Mi-2 binding sites in 20HE treated cell. Depicted is the exact chromosomal location within the Drosophila genome and the next transcript as well as the primary and secondary gene associated with a binding site. Ratio +20HE/ untreated represents the enrichment of tag counts of Mi-2 ChIPSeq in 20HE versus untreated S2 cells.

chromosomal location	Next transcript	Primary gene	Secondary gene	Ratio +20HE/ untreated
3L: 24462060..24462693	*mRpS5*	*CR12460*	*mRpS5*	13.8652
3L: 24458030..24458555	*mRpS5*	*CR12460*	*mRpS5*	12.2824
Uextra: 28768380..28768617		*mir-5613*		7.9206
X: 3302484..3302942	*CG14269*	*tRNA: CR32493*	*CG14269*	5.4690
X: 1843508..1846640	*Hr4*	*Hr4*	*CG3587*	4.5522
X: 1503765..1504886	*br*	*Mur2B*	*br*	4.4419
Uextra: 28123664..28124271		*mir-5613*		4.2924
X: 14721782..14722082	*rut*	*rut*	*CG14408*	4.2157
3R: 5789105..5790032	*Art4*	*Art4*	*Gr85a*	4.0372
Uextra: 28815421..28815618		*mir-5613*		3.8867
Uextra: 8455330..8455668		*mir-5613*		3.8001
X: 2231851..2232522	*phl*	*Ilp6*	*mRpL14*	3.7960
2L: 5300104..5300770	*vri*	*vri*	*CG14024*	3.6915
X: 1504917..1507842	*br*	*Mur2B*	*br*	3.4217
2L: 5287818..5288374	*Bub1*	*Bub1*	*Bsg25D*	3.4067
2L: 12013199..12014424	*Rh5*	*Rh5*	*CG6734*	3.2974
X: 11324806..11325412	*Gs2*	*Gs2*	*Sk1*	3.2943
2L: 3338014..3339943	*E23*	*CG15408*	*CG3285*	3.2753
X: 10103534..10103976	*CG15309*	*CR43899*	*CG15309*	3.2687
3L: 9874400..9874823	*CG34382*	*CG34382*	*Taf2*	3.2616
2L: 20775940..20776358	*cad*	*cad*	*Pomp*	3.2516
2R: 8276716..8277539	*Cpr49Ad*	*Cpr49Ad*	*Cpr49Ac*	3.2398

Uextra: 28630820..28631122		*mir-5613*		3.2330
2R: 8274002..8275419	*Cpr49Ac*	*Cpr49Ac*	*CG8501*	3.2058
2L: 18466593..18467235	*Ntf-2r*	*mir-100*	*let-7*	3.1695
Uextra: 22409842..22410060		*mir-5613*		3.1143
X: 20426782..20427264	*RunxB*	*CG42580*	*RunxB*	3.0964
X: 8750894..8751585	*CG12075*	*CG12075*	*Moe*	3.0604
3R: 5794832..5795928	*Art4*	*Art4*	*Gr85a*	2.9624
3L: 14259140..14259394	*fz*	*fz*	*CG7906*	2.9244
2R: 8275543..8276672	*Cpr49Ac*	*Cpr49Ac*	*Cpr49Ad*	2.9186
3L: 18001599..18002423	*Eip75B*	*snoRNA:Me28S-A30*	*CG32192*	2.8970
3L: 3513769..3514084	*ImpE2*	*ImpE2*	*Eip63E*	2.8835
X: 713260..713516	*CG13358*	*CG13358*	*Sec22*	2.8544
3L: 18070756..18071312	*CG34252*	*CG34252*	*CG43253*	2.8519
2L: 19143606..19144699	*l(2)37Cg*	*l(2)37Cg*	*brat*	2.8389
X: 10451120..10451663	*spri*	*CG15296*	*spri*	2.8358
3R: 8473077..8475218	*CG6234*	*CG6234*	*CG6753*	2.8092
2L: 2201183..2203697	*CG31668*	*CG31668*	*CG34172*	2.8044
3L: 21246306..21248087	*CG43218*	*CG43218*	*CG9391*	2.8027
3R: 17716304..17717273	*dnd*	*CR43844*	*dnd*	2.7873
X: 7615961..7616355	*Hira*	*Hira*	*CG15478*	2.7649
2L: 14133181..14134541	*CG17341*	*CG17341*	*CG31769*	2.7601
Uextra: 3142533..3143070		*mir-5613*		2.7504
2R: 8272367..8273672	*Cpr49Ac*	*Cpr49Ac*	*CG8501*	2.7439
X: 3301687..3302416	*CG14269*	*tRNA:CR32493*	*CG14269*	2.7324
3L: 18030730..18031379	*CG32192*	*CG32192*	*CG42393*	2.7290
2R: 16292917..16293375	*CG12484*	*CG12484*	*CG11192*	2.6889
X: 9933174..9934572	*Yp2*	*Yp2*	*Yp1*	2.6677

X: 2641292..2641682	*Syx4*	*Syx4*	*CR43494*	2.6585
3R: 5790070..5791294	*Art4*	*Art4*	*Gr85a*	2.6272
3R: 8696512..8696792	*CG10126*	*CG10126*	*d-cup*	2.6102
2L: 19144962..19145706	*l(2)37Cg*	*l(2)37Cg*	*brat*	2.6092
3L: 18014925..18015483	*CG32192*	*CG32192*	*Me28S-A30*	2.5867
3L: 22584847..22585187	*CG6914*	*CG6914*	*Trxr-2*	2.5852
3L: 16188172..16189205	*CG33687*	*CG33687*	*CG33688*	2.5820
2R: 14461756..14462609	*Rgk2*	*Rgk2*	*GEFmeso*	2.5480
3L: 10394910..10395184	*CG12362*	*CR43990*	*CG12362*	2.5377
2L: 8194971..8195442	*CG8475*	*CG8475*	*CG8460*	2.5314
2L: 18464765..18465594	*Ntf-2r*	*mir-100*	*let-7*	2.5236
X: 17774457..17774986	*CG12985*	*CG12985*	*mnb*	2.4949
3L: 17999364..17999887	*Eip75B*	*snoRNA:Me28S-A30*	*CG32192*	2.4878
2L: 6553184..6553919	*osm-6*	*osm-6*	*CoVb*	2.4813
2R: 1250846..1251037	*CG10417*	*CR42646*	*CG10417*	2.4813
3R: 9615984..9617028	*Dip-B*	*tRNA:CR31588*	*tRNA:CR31331*	2.4813
3L: 20901170..20901495	*CG11458*	*CG11458*	*CR43930*	2.4813
3L: 15505120..15506229	*Eip71CD*	*Eip71CD*	*gdl-ORF39*	2.4754
2R: 5643448..5643852	*CG1690*	*CG1690*	*trpl*	2.4699
3R: 27237979..27238436	*CG11337*	*CG11337*	*Gprk2*	2.4620
2L: 6058316..6059133	*CG34180*	*CG34180*	*CG9140*	2.4415
3L: 16357029..16357942	*Cpr72Eb*	*Cpr72Eb*	*Cpr72Ea*	2.4299
X: 1529697..1531480	*br*	*CG11509*	*Mur2B*	2.4295
3R: 18151526..18152007	*CG34377*	*CG34377*	*CG7080*	2.4259
2L: 3342851..3343810	*E23*	*CG15408*	*E23*	2.4243
X: 1875314..1876057	*Hr4*	*CG4406*	*mir-2496*	2.4230
3L: 10374649..10375147	*CG12362*	*mir-276a*	*CR43990*	2.4228

Uextra: 9037036..9037469		*mir-5613*		2.4160
2L: 19138491..19139316	*l(2)37Cg*	*l(2)37Cg*	*brat*	2.4141
3L: 17920866..17921664	*CG43173*	*CG43173*	*CG43174*	2.4005
3L: 18029337..18029832	*CG32192*	*CG32192*	*CG42393*	2.3927
3L: 7985616..7986433	*nmo*	*nmo*	*CG8038*	2.3849
2R: 17359656..17360228	*Sdc*	*Sdc*	*Sara*	2.3843
X: 5864642..5865166	*Grip*	*Grip*	*fs(1)M3*	2.3808
2R: 14469701..14471433	*GEFmeso*	*GEFmeso*	*CG42697*	2.3737
Uextra: 19603848..19604095		*mir-5613*		2.3637
X: 1537028..1537665	*CG11509*	*CG11509*	*dor*	2.3538
X: 1533867..1534613	*CG11509*	*CG11509*	*Mur2B*	2.3458
2L: 7949371..7949722	*Snoo*	*CG7231*	*Snoo*	2.3428
X: 11892213..11892525	*fw*	*CG18130*	*fw*	2.3395
X: 9226269..9226871	*CG34450*	*CG34450*	*c12.2*	2.3365
2R: 14462841..14463419	*Rgk2*	*Rgk2*	*GEFmeso*	2.3322
3L: 21886645..21887430	*mub*	*CR43878*	*tRNA: CR32449*	2.3313
X: 2668112..2668569	*CG32795*	*CG32795*	*w*	2.3230
3L: 24463611..24464073	*mRpS5*	*CR12460*	*mRpS5*	2.3202
3L: 17774121..17774458	*CG42815*	*CG42815*	*CG42816*	2.3155
3R: 16311985..16312319	*mun*	*mun*	*Dic2*	2.3155
2L: 685066..685263	*ds*	*ds*	*Hsp60B*	2.3129
2L: 9013602..9014028	*Rcd-1r*	*Rcd-1r*	*CG13102*	2.3129
X: 1471465..1473414	*br*	*br*	*snmRNA:400*	2.3081
Uextra: 17026012..17026285		*mir-5613*		2.3047
X: 61849..62242	*CG17168*	*CG17168*	*CG17163*	2.3041
2L: 21243780..21244644	*Hr39*	*Hr39*	*CG31626*	2.3028
3R: 7747786..17748477	*CG17843*	*CG17843*	*CG6690*	2.3020

Table 7.2: List of >2.3-fold reduced Mi-2 binding sites in 20HE treated cell. Depicted is the exact chromosomal location within the Drosophila genome and the next transcript as well as the primary and secondary gene associated with a binding site. Tag-count ratio untreated/ +20HE represents the enrichment of tag counts of Mi-2 ChIPSeq in untreated versus 20HE S2 cells.

chromosomal location	Next transcript	Primary gene	Secondary gene	Ratio untreated/20HE
Uextra: 27400817..27400998		*mir-5613*		15.8296
X: 5236532..5236939	*SK*	*SK*	*CanB*	8.8053
2R: 109336..109515	*CG40498*	*CG40498*	*CR41510*	8.6932
Uextra: 13391307..13391485		*mir-5613*		8.3380
3R: 22570923..22571440	*CG14247*	*CG14247*	*CG6403*	7.2095
3R: 8888795..8889060	*sim*	*sim*	*pic*	7.0215
X: 10190575..10190924	*alpha-Man-I*	*alpha-Man-I*	*CG2909*	6.6932
2L: 11786961..11787359	*CG14931*	*CG14931*	*CG14932*	6.0110
X: 4230247..4230784	*CG12693*	*CG12693*	*norpA*	5.7990
2L: 5417933..5418411	*H15*	*CR43713*	*H15*	5.5308
2L: 7969397..7969762	*Snoo*	*CG7231*	*Snoo*	5.3915
3R: 2722209..2722499	*CG43252*	*CG43252*	*ftz*	4.6670
2L: 6134668..6135176	*CG9222*	*CG9222*	*tectonic*	4.6084
3L: 11270134..11270638	*CG6175*	*CG6175*	*scyl*	4.4649
Uextra: 28804580..28804810		*mir-5613*		4.4622
3L: 19108530..19109016	*Spn75F*	*Spn75F*	*Gem2*	4.3457
X: 9384900..9385274	*mgl*	*mgl*	*CR43497*	4.0420
X: 12453252..12453494	*Cpr11B*	*Cpr11B*	*CG43921*	3.9795
Uextra: 28167248..28167427		*mir-5613*		3.9406
3L: 8362622..8362912	*ImpE1*	*ImpE1*	*Idh*	3.8399
Uextra: 2642373..2642607		*mir-5613*		3.7615
2R: 12734855..12735215	*Ugt37c1*	*Ugt37c1*	*IntS8*	3.6241
X: 17673342..17673732	*unc-4*	*unc-4*	*OdsH*	3.5118
Uextra: 28829111..28829429		*mir-5613*		3.4407

2L: 13331861..13332546	*CG43778*	*CG43778*	*CG16826*	3.4150
2L: 11470160..11470631	*CG43355*	*sala*	*CG43355*	3.3799
Uextra: 28220103..28220410		*mir-5613*		3.3639
X: 4171661..4172132	*CG15578*	*CG15578*	*CG15577*	3.1346
2R: 1266981..1267166	*CG10417*	*CR42646*	*CG10417*	3.0659
2L: 4914413..4914808	*hoe1*	*CG2837*	*hoe1*	3.0002
2R: 15454304..15454799	*sm*	*tRNA:CR33535*	*CG43111*	2.9778
3R: 6332978..6333331	*hth*	*mir-4944*	*Cyp12e1*	2.9555
X: 10452041..10452481	*spri*	*CG15296*	*spri*	2.9083
2L: 15487734..15488164	*Tim17b2*	*Tim17b2*	*sna*	2.8211
X: 6507477..6508039	*pigs*	*pigs*	*Apc7*	2.7943
3L: 10541371..10541787	*CG6527*	*CG6527*	*S-Lap4*	2.7819
3R: 10661706..10662371	*CG3610*	*CG3610*	*btsz*	2.7099
3R: 2343166..2343492	*CG15185*	*CG15185*	*tRNA:M2:83F*	2.7006
3L: 14682302..14682704	*CG13477*	*CG13477*	*CG5048*	2.6920
Uextra: 26582216..26582436		*mir-5613*		2.6818
X: 16004851..16005387	*CG42353*	*CG42353*	*CG42354*	2.6705
3R: 12367826..12368189	*CG14891*	*CG14891*	*CG14903*	2.6644
3L: 1263286..1263732	*CG9134*	*CG9134*	*CG9133*	2.6396
X: 3211203..3211736	*CG10793*	*CG10793*	*dm*	2.6350
X: 20326668..20327162	*CG32506*	*CG32506*	*CG42578*	2.6330
3L: 10023755..10024167	*dpr6*	*dpr6*	*CG14160*	2.6252
X: 4019863..4020204	*GlcAT-I*	*GlcAT-I*	*Tip60*	2.6252
3L: 1396356..1396650	*CG40178*	*CG40178*	*CG41320*	2.6183
X: 15146322..15146619	*PPYR1*	*PPYR1*	*CG9106*	2.6144
X: 3428489..3428843	*CG32791*	*CR34335*	*CG13021*	2.5495
2L: 22476847..22477185	*CG17494*	*CG17494*	*CG17493*	2.5468
3L:	*Eip74EF*	*Eip74EF*	*CG6259*	2.5464

17596817..17597587				
Uextra: 28551649..28551832		*mir-5613*		2.5425
X: 18794163..18794556	*CG7378*	*CG7378*	*CG7349*	2.5390
3L: 2513457..2513863	*Dbp80*	*Dbp80*	*Me18S-C419*	2.5375
3L: 16451635..16452177	*dsx-c73A*	*dsx-c73A*	*aos*	2.5258
2L: 2399822..2400233	*VGlut*	*VGlut*	*CG43750*	2.5077
2L: 16845121..16845590	*CG13284*	*CG13284*	*CG31810*	2.4778
3R: 24109232..24109692	*CG34437*	*CG34437*	*CG34436*	2.4531
2R: 10785671..10786004	*Cyp317a1*	*Cyp317a1*	*Cyp6a8*	2.4450
3L: 19011488..19011984	*CG18136*	*CG18136*	*CG3808*	2.4428
X: 1495924..1496288	*br*	*Mur2B*	*br*	2.4380
2R: 15800029..15800365	*CG13872*	*CR43421*	*CG13872*	2.4293
3R: 13416301..13416786	*CG7587*	*CG7587*	*Sgs5*	2.4222
2L: 16361491..16361775	*jhamt*	*jhamt*	*CaBP1*	2.4181
3R: 9449234..9449624	*CG9269*	*CG9269*	*CG10841*	2.4087
Uextra: 8511041..8511394		*mir-5613*		2.4087
3L: 15530614..15531136	*CrebA*	*CrebA*	*CG43248*	2.3882
2R: 5427890..5428266	*CG1888*	*CG1888*	*CR43651*	2.3847
2R: 12496005..12496488	*CG5065*	*CG5065*	*CG8303*	2.3714
2L: 7181374..7181857	*CG4495*	*CG4495*	*CG4496*	2.3652
2L: 4237378..4237977	*RpL40*	*RpL40*	*CG3702*	2.3347
2R: 5350963..5351303	*Camta*	*CG33757*	*CG33758*	2.3196
3R: 26458740..26459222	*CG2267*	*CG2267*	*CG31013*	2.3169
2L: 16874931..16875414	*CG32832*	*CG32832*	*CG31743*	2.3131
3L: 13349125..13349986	*Nplp2*	*Nplp2*	*CG17687*	2.3126

List of abbreviations and acronyms

20HE	20-hydroxyecdysone
α	anti
A	alanine
aa	amino acid
ac	acetyl/ acetylated
ADP	adenosine diphosphate
AF	activation function
Ash	absent, small, or homeotic discs 1
ATP	adenosine triphosphate
ATPase	ATP hydrolysing domain
BAP	Brahma-associated proteins
BLAST	basic local alignment search tool
bp	base pair
BRK	brahma and kismet domain
BSA	bovine serum albumin
C-	carboxy-
CBP	CREB-binding protein
cDNA	complementary DNA
CG	computed protein-coding gene
CHD	chromodomain-helicase-DNA binding
ChIP	chromatin immunoprecipitation
CoA	CoenzymeA
CP190	centrosomal protein 190
CpG	cytosine-phospatidyl-guanosine
CR	computed non-protein-coding-gene
Ct	cycle threshold
CT	C-terminus
CTCF	CCCCTC-binding factor
Da	Dalton
DAPI	4',6-diamidino-2-phenylindole
DBD	DNA-binding domain
dd	double distilled
dMec	Drosophila MEP-1-containing complex
DMSO	dimethyl sulfoxide
DNA	desoxyribonucleic acid

dNTP	desoxyribonucleotide triphosphate
DRB	5,6-dichloro-1-beta-D-ribofuranosylbenzimidazole
dsRNA	double stranded RNA
DTT	dithiotreithol
E.coli	*Escherichia coli*
EcR	ecdysone receptor
EcRE	ecdysone response element
EDTA	ethylenedioxy-diethylene-dinitrilo-tetraacetic acid
EGTA	ethylene glycol-bis-(2-aminoethyl)-N,N,N', N'-tetraacetic acid
ER	estrogen receptor
EtBr	ethidiumbromide
F	phenylalanin
FAD	flavin adenine dinucleotide
FBS	fetal bovine serum
FTZ-F1	fushi tarazu transcription factor 1
fw/ fwd	forward
g	gram
Gaf	GAGA transcription factor
Gcn5	General control of amino acid synthesis protein 5
GFP	green fluorescent protein
GR	glucocorticoid receptor
GST	glutathione-S-transferase
H	histone
HAS	helicase-sant domain
HAT	histone acetyltransferase
HDAC	histone deacetylase
HEPES	N-(2-Hydroxyethyl)piperazine-N′-(2-ethanesulfonic acid)
HMG	high mobility group
HP1	heterochromatin protein 1
HRP	horseradish peroxidase
hr(s)	hour(s)
HRE	hormone response element
HS	heat shock
hsp	heat shock protein
Ig	immunoglobuline
In	input
INO80	inositol requiring 80

IP	immunoprecipitation
IPTG	isopropyl β-D-1-thiogalactopyranoside
ISWI	imitation switch
*iv*T	*in vitro* translation
K	lysine
k	kilo
L	leucine
LB	Luria-Bertani
LBD	ligand-binding domain
LSD1	lysine-specific demethylase 1
M	molar
MCF-7	Michigan Cancer Foundation - 7
MBP	methyl-CpG-binding protein
me	methyl
Mec	Mep1-containing complex
Mep1	mog interacting ectopic P granulocytes 1
min	minutes(s)
MMTV	mouse mammary tumour virus
MNase	micrococcal nuclease
mRNA	messenger ribonucleic acid
MTA	metastasis associated protein
N-	amino-
N-CoR	nuclear receptor co-repressor
NF-1	nuclear factor 1
NR	nuclear receptor
nuc	nucleosome
NuRD	nucleosome remodeling and histone deacetylation
NURF	nucleosome remodeling factor
OD	optical density
PAA	polyacrylamide
PAGE	polyacrylamide gel electrophoresis
PAR	poly(ADP-ribose)
PARP	poly(ADP-robose) polymerase
PBAP	Polybromo-associated BAP
PEV	position-effect variegation
PBS	phosphate buffered saline
PCR	polymerase chain reaction

Ph	polyhomeotic
PHD	plant homeo domain
PMSF	phenylmethane sulfonyl fluoride
PRMT	protein arginine methyltransferase
PTM	post-translational modification
PVDF	polyvinylidine difluoride
qPCR	quantitative PCR
R	arginine
rDNA	ribosomal DNA
re/rev	reverse
RNA	ribonucleic acid
RNAi	RNA interference
RNAPolII	RNA polymerase II
Rp49	ribosomal protein 49
Rpd3	reduced potassium dependency 3
rpm	revolutions per minute
RT	reverse transcriptase/ room temperature
S	serine
S. cerevisiae	*Saccharomyces cerevisiae*
SDS	sodium dodecyl sulphate
sec	second
seq	sequencing
SMRT	silencing mediator for retinoid or thyroid-hormone receptor
Snf2	sucrose non-fermenting protein 2 homolog
SUMO	small ubiquitin-like modifier
SWI/SNF	switch/sucrose non-fermenting
T	threonine
TBP	TATA-binding protein
Temed	N,N,N′,N′-Tetramethylethylenediamine
TF	transcription factor
TR	thyroid hormone receptor
Tris	tris(hydroxymethyl)aminomethane
TRR	trithorax related
TSS	transcriptional start site
Ttk69	tramtrack69
USP	ultraspiracle
UTX	ubiquitously transcribed tetratricopeptide repeat on X

UTR	untranslated region
v/v	volume per volume
w/v	weight per volume
WT	wild type
Zn	Zinc

Curriculum vitae

List of academic teachers

My academic teachers at the Martin-Luther-University Halle Wittenberg were:

Acknowledgements

Foremost, I would like to express my sincere gratitude to my supervisor Alexander. I am most thankful for the fact that you gave me all the freedom and time I needed to develop as a scientist. Your constant guidance, enthusiasm and motivation helped me every single day in the lab. Thanks to you, I now feel confident to tackle whatever difficulties I may face in my professional future.

Also, I would like to thank Prof. Dr. Rainer Renkawitz for helpful experimental suggestions as my co-supervisor. Furthermore, I appreciate that you took your time to review my PhD thesis.
I am indebted to the support from the IRTG1384 and the TRR81. The possibilities to enhance my skills in various seminars and workshops was very helpful during my thesis. On top of this, the opportunity to attend several national and international meetings allowed me to develop my ideas and get into contact with many great scientists.

In my daily work I have been blessed with a friendly and cheerful group of fellow students. I thank all the past and present lab mates that contributed in one way or the other to this thesis: Magdalena, Karin, Judith, Evelyne, Jonathan, Stephan, Kristina Corina and Karim. A big thank you also goes to Florian and Roman, who helped me with the bioinformatics.

A special remark goes to all the students I supervised during my time in the Brehm lab. Most of you definitely challenged my patience, but more importantly, you lightened up my day and made sure there was always something to laugh about. Here's to you: Matthias, Olga, Felix, Julia, Kathleen, Lisa and Anna.

I give my gratitude to my colleague and friend Steffi. Your honest words and warm hugs made me put things into perspective more than once. All I wish for, is that you remain the humble and caring person you are. You have a good heart and I am thankful to have you in my life.

I highly appreciate the constant support from my family. Ma and Pa, thank you for believing in me and bringing me back to my roots whenever I needed it. Further I'd like to thank my sister for being the best role model when it comes to life beyond the lab. You are doing a truly awesome job with raising these kids and caring for your family!

Finally, I would like to thank that one special person. Maybe life is just a brief crack of light between two eternities of darkness. If so, then you are the one that makes my light shine brighter than I could have ever imagined. I am looking forward to nurture and grow our connection with every day of my life and I know that whatever obstacles we may face, we can overcome them. Thank you, Erik!

Ehrenwörtliche Erklärung

Ich erkläre ehrenwörtlich, dass ich die dem Fachbereich Medizin Marburg zur Promotionsprüfung eingereichte Arbeit mit dem Titel „Function of the ATP-dependent chromatin remodeler Mi-2 in the regulation of ecdysone depdendent genes in *Drosophila melanogaster*“ im Institut für Molekularbiologie und Tumorforschung unter Leitung von Prof. Dr. Rolf Müller mit Unterstützung durch Prof. Dr. Alexander Brehm ohne sonstige Hilfe selbst durchgeführt und bei der Abfassung der Arbeit keine anderen als die in der Dissertation aufgeführten Hilfsmittel benutzt habe. Ich habe bisher an keinem in- oder ausländischen Medizinischen Fachbereich ein Gesuch um Zulassung zur Promotion eingereicht, noch die vorliegende oder eine andere Arbeit als Dissertation vorgelegt.

Judith Kreher, Marburg, den 04.08.2014